G.J. van den Bogerd

The Impact of Clutch Operation in Propulsion Mode Transitions

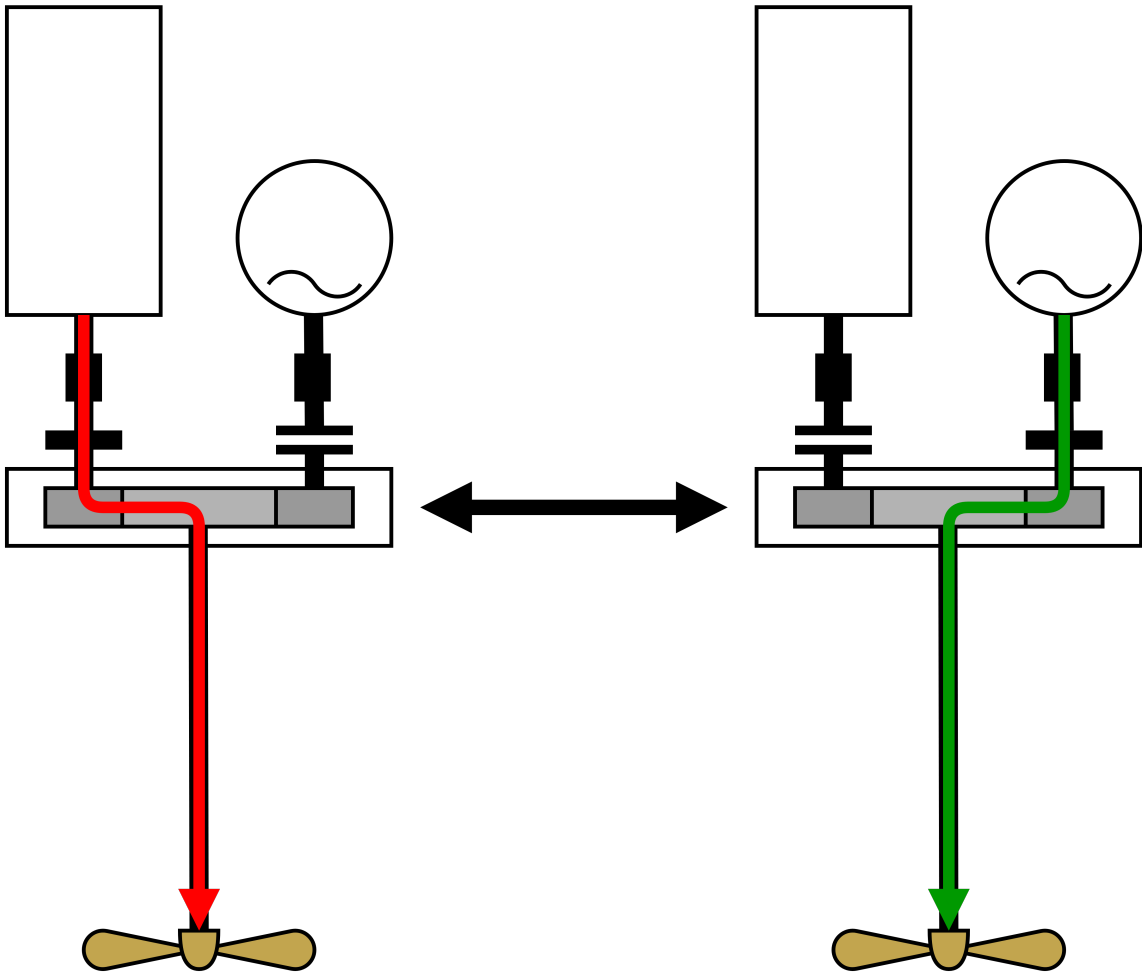

TU Delft

The Impact of Clutch Operation in Propulsion Mode Transitions

By

G.J. van den Bogerd

Master Thesis

in partial fulfilment of the requirements for the degree of

Master of Science
in Mechanical Engineering

at the Department Maritime and Transport Technology of Faculty Mechanical, Maritime and Materials Engineering of Delft University of Technology
to be defended publicly on Friday August 19, 2022 at 15:00

Student number:	4348133	
MSc track:	Multi-Machine Engineering	
Report number:	2022.MME.8686	
Thesis committee:	Dr. ir. H. Polinder,	TU Delft committee chair & supervisor, 3mE
	Dr. ir. S. Nasiri,	TU Delft committee member, 3mE
	Dr. ir. A. Coraddu,	TU Delft committee member, 3mE
	Dr. ir. U. Shipurkar,	company supervisor, MARIN
Date:	August 14, 2022	

TU Delft

Preface

This thesis is the result of a graduation project conducted at MARIN on the subject of propulsion system modelling. This project is the last part of the masters degree program for Mechanical Engineering with a specialisation in Multi-Machine Engineering at the Delft University of Technology. This thesis is written for readers with a background in engineering. In the appendix a research paper is included that summarises the conducted research.

This project has been a valuable learning experience where virtually all of the courses in the TU Delft Mechanical Engineering study programme have been proven useful in some sense. I had the desire to learn more on how to build a model for a complex system and was guided by Henk Polinder towards the zero-emissions lab at MARIN which has ultimately resulted in the writing of this thesis.

First I want to thank my supervisors Udai Shipurkar from MARIN and Henk Polinder from the TU Delft for their guidance over the course of this project. I appreciate the freedom that I have been given in conducting the research and will miss our bi-weekly meetings. All good things must come to an end, eventually.

I want to thank Douwe Stapersma for the valuable feedback and suggestions that he has provided me with in his role as advisor. It has been a privilege to have had such an authority on the subject of propulsion system modelling to learn from and discuss the project with. I want to thank Rinze Geertsma for so kindly providing the diesel engine model from his doctoral thesis that was easy to integrate in the propulsion system model as a result of his neatly structured implementation. I want to thank Moritz Krijgsman for the opportunity to conduct this graduation project in the context of the development of the virtual zero-emissions laboratory at MARIN. Furthermore I want to thank all the people at MARIN who have helped me over the course of this project and wish them the best on their mission towards better ships and blue oceans.

I am grateful for my family that has supported me over the course of my study at the TU Delft and have provided me with the opportunities to develop myself. Also I would like to thank my friends for enduring the wanderings of my technical mind in our conversations and for distracting me with sometimes much needed reliefs from studying. Finally I would like to thank my wife Annewendy, for always being there for me.

Gerrit van den Bogerd
Hengelo(Gld), August 2022

Abstract

Over the coming decades the worldwide fleet of ships will have to change to reduce emissions. Hybridisation of the propulsion system is a stepping stone to full electrification, which is required to reduce emissions of the maritime sector to zero. In hybrid propulsion systems, clutches are used to switch between drive engines when transitioning between operational modes. The operation of clutches is indicated to generate significant disturbances in propulsion systems, however, this impact is overlooked in hybrid propulsion simulation studies in the scientific literature. The identified research gap is addressed in this thesis by simulating propulsion mode transition in a hybrid propulsion system and analysing the impact of clutch operation, using of a model developed for this purpose.

A hybrid propulsion is defined by introducing multi disk wet friction clutches in a reference propulsion system consisting of a 9.1 MW diesel engine in parallel with a 3 MW electric motor. A broad scope of impact measures, that includes the electric load on the power system and the temperature development of the clutch, is defined and the system is thoroughly modelled to enable evaluation of these measures. The Transmission system is modelled with a higher fidelity than typically applied in propulsion system simulation studies to enable assessment of the basic vibratory behaviour of the transmission system. The considered propulsion modes transitions are between diesel and electric propulsion. To enable these transitions, three transition control approaches with an increasing degree of sophistication are implemented.

The developed model is used to perform simulations, from which it is concluded that torsional vibrations, gear hammer and a drop in propeller speed characterise the significant impact of clutch operation on hybrid propulsion systems in propulsion mode transitions. It is also concluded that the impact of clutch operation can be limited by implementing an appropriate propulsion control approach for the transition. A torque controlled handover of drive torque between engines is identified as a suitable approach. However, the induction machine switching from torque to speed control introduces power peaks in the load profile that have the potential to severely disrupt the stability of the ships power system. It is finally concluded that the temperature development of the clutch during the propulsion mode transitions is not significant.

It is shown in this thesis that there can be a significant impact on the propulsion system as a result of the operation of clutches in propulsion mode transitions. Therefore, this impact has to be taken into consideration when designing hybrid propulsion systems. The model described in this thesis can be used to predict the impact of clutch operation in the early stages of the design process. Furthermore, the model can be used to develop and evaluate propulsion mode transition control approaches.

List of Figures

1.1 MARIN Zero Emissions Lab. *Source [2]* . . . 2
1.2 Typical hybrid propulsion architecture. *Source [4]* . . . 3
1.3 System boundary depicting the scope of the research in this thesis. . . . 8

2.1 Hybrid propulsion architecture with multi plate wet friction clutches to enable dynamic switching between the electric and diesel engine in propulsion mode transitions. . . . 12
2.2 Hybrid propulsion system operational modes, power flow is represented by red(Diesel engine power) and yellow (Electric motor power) arrows. . . . 13
2.3 Brake Specific Fuel Consumption of the reference diesel engine. This figure has been generated using the model for this diesel engine described in [36]. . . . 13
2.4 Schematic representation and model coupling of the propulsion system model. . . . 15
2.5 Schematic of a lumped inertia i, where x and y are the connected submodels. . . . 16
2.6 Typical wet friction clutch engagement. *Source [51]* . . . 21
2.7 Schematic of the Stribeck behaviour. *Source [51]* . . . 22
2.8 Schematic of the clutch variables in the context of the connected lumped inertias J_i and J_j. . 23
2.9 Clutch state definitions and transition conditions. . . . 24
2.10 Clutch actuation pressure curve $P(t)$ . . . 26
2.11 Schematic presentation of the diesel engine model and the interaction between its subsystems, consisting of Algebraic Equations (AE) or Differential and Algebraic Equations (DAE). *Source: [60]* . . . 28
2.12 Matching diagram for the selected wageningen B5-75 propeller. . . . 33

3.1 Diesel and Electric Propulsion at 600 rpm, steady state operation with ship speed of 10 kn . 41
3.2 Clutch torque for the transition from electric to diesel mode using the instant transition approach in sea state 3. . . . 43
3.3 Clutch temperature for the transition from electric to diesel mode using the instant transition approach in sea state 3. . . . 44
3.4 Rotational speed in the engine speed reference frame for the transition from electric to diesel mode using the instant transition approach in sea state 3. . . . 44
3.5 Torques in the engine torque reference frame for the transition from electric to diesel mode using the instant transition approach in sea state 3. . . . 45
3.6 Gear mesh force for the transition from electric to diesel mode using the instant transition approach in sea state 3. . . . 45
3.7 Shaft line stress for the transition from electric to diesel mode using the instant transition approach in sea state 3. . . . 45
3.8 Clutch torque for the transition from diesel to electric mode using the instant transition approach in sea state 3. . . . 46
3.9 Clutch temperature for the transition from diesel to electric mode using the instant transition approach in sea state 3. . . . 47
3.10 Rotational speed in the engine speed reference frame for the transition from diesel to electric mode using the instant transition approach in sea state 3. . . . 47
3.11 Torques in the engine torque reference frame for the transition from electric to diesel mode using the instant transition approach in sea state 3. . . . 48

3.12 Gear mesh force for the transition from electric to diesel mode using the instant transition approach in sea state 3. . . . 48
3.13 Shaftline stress for the transition from electric to diesel mode using the instant transition approach in sea state 3. . . . 48
3.14 Clutch torque for the transition from electric to diesel mode using the staged transition approach in sea state 3. . . . 50
3.15 Rotational speed in the engine speed reference frame for the transition from electric to diesel mode using the staged transition approach in sea state 3. . . . 51
3.16 Diesel Engine fuel rack setpoint for the transition from electric to diesel mode using the staged transition approach in sea state 3. . . . 51
3.17 Gear mesh force for the transition from electric to diesel mode using the staged transition approach in sea state 3. . . . 51
3.18 Torques in the engine torque reference frame for the transition from electric to diesel mode using the staged transition approach in sea state 3. . . . 52
3.19 Clutch torque for the transition from diesel to electric mode using the staged transition approach in sea state 3. . . . 53
3.20 Diesel Engine fuel rack setpoint for the transition from diesel to electric mode using the staged transition approach in sea state 3. . . . 53
3.21 Induction machine drive power for the transition from diesel to electric mode using the staged transition approach in sea state 3. . . . 53
3.22 Rotational speed in the engine speed reference frame for the transition from diesel to electric mode using the staged transition approach in sea state 3. . . . 53
3.23 Torques in the engine torque reference frame for the transition from diesel to electric mode using the staged transition approach in sea state 3. . . . 54
3.24 Gear mesh force for the transition from diesel to electric mode using the staged transition approach in sea state 3. . . . 54
3.25 Clutch torque for the transition from electric to diesel mode using the torque controlled transition approach in sea state 3. . . . 56
3.26 Rotational speed in the engine speed reference frame for the transition from electric to diesel mode using the torque controlled transition approach in sea state 3. . . . 57
3.27 Diesel Engine fuel rack setpoint for the transition from electric to diesel mode using the torque controlled transition approach in sea state 3. . . . 57
3.28 Gear mesh force for the transition from electric to diesel mode using the torque controlled transition approach in sea state 3. . . . 57
3.29 Torques in the engine torque reference frame for the transition from electric to diesel mode using the torque controlled transition approach in sea state 3. . . . 57
3.30 Clutch torque for the transition from diesel to electric mode using the torque controlled transition approach in sea state 3. . . . 59
3.31 Diesel Engine fuel rack setpoint for the transition from diesel to electric mode using the torque controlled transition approach in sea state 3. . . . 59
3.32 Induction machine drive power for the transition from diesel to electric mode using the torque controlled transition approach in sea state 3. . . . 59
3.33 Rotational speed in the engine speed reference frame for the transition from diesel to electric mode using the torque controlled transition approach in sea state 3. . . . 59
3.34 Torques in the engine torque reference frame for the transition from diesel to electric mode using the torque controlled transition approach in sea state 3. . . . 60
3.35 Gear mesh force for the transition from diesel to electric mode using the torque controlled transition approach in sea state 3. . . . 60
3.36 Torques in the engine torque reference frame for the transition from electric to diesel mode using the torque controlled transition approach in sea state 5. . . . 61
3.37 Rotational speed in the engine speed reference frame for the transition from electric to diesel mode using the torque controlled transition approach in sea state 5. . . . 62

3.38 Operation of the diesel engine for the transition from electric to diesel mode using the torque controlled transition approach in sea state 5. 62
3.39 Operation of the induction machine for the transition from electric to diesel mode using the torque controlled transition approach in sea state 5. 62

List of Tables

1.1 Table summarising the reviewed literature on propulsion system simulation concerning the significant dynamics and model fidelity of the transmission system. 6

2.1 Inertia parameters. 17
2.2 Shaftline parameters. 18
2.3 Gearbox parameters 20
2.4 Elastic coupling parameters 20
2.5 Parameter shared by both the diesel engine and induction machine clutches 26
2.6 Parameters for the DE clutch 27
2.7 Parameters for the IM clutch 27
2.8 Validation of the calibrated lumped thermal model 27
2.9 Hull model parameters 32
2.10 Wave model parameters 32
2.11 Parameters for the propeller model 33

3.1 Table summarising the key results of the operational transitions between electric(E) and diesel(D) mode at a speed of 10 knots(18.5 km/h), corresponding with a engine speed set-point of 600 rpm, in sea state 3. 64

Contents

Preface i

Abstract ii

List of Figures iii

List of Tables v

1 Introduction 1
- 1.1 Problem Description . . . 2
- 1.2 Research Background . . . 2
  - 1.2.1 Maritime Propulsion Systems . . . 3
  - 1.2.2 Simulation of Maritime Transmission Systems . . . 5
  - 1.2.3 Research Gap . . . 7
- 1.3 Research Structure . . . 8
  - 1.3.1 Research Question . . . 8
  - 1.3.2 Scope . . . 8
  - 1.3.3 Methodology . . . 9
- 1.4 Thesis Outline . . . 9

2 System Modelling 10
- 2.1 System Description . . . 11
  - 2.1.1 Reference Ship and Propulsion System . . . 11
  - 2.1.2 Clutches . . . 11
  - 2.1.3 System Definition . . . 12
  - 2.1.4 Propulsion Modes and Transitions . . . 13
- 2.2 System Model Description . . . 14
  - 2.2.1 Impact Measures . . . 14
  - 2.2.2 Conceptual Model . . . 15
- 2.3 Transmission System Modelling . . . 16
  - 2.3.1 Rotational Dynamics . . . 16
  - 2.3.2 Shaftline Model . . . 17
  - 2.3.3 Gearbox Model . . . 19
  - 2.3.4 Elastic Coupling Model . . . 20
- 2.4 Clutch Modelling . . . 21
  - 2.4.1 Characteristics of Multi Disk Wet Friction Clutches . . . 21
  - 2.4.2 Clutch Model . . . 22
  - 2.4.3 Clutch Model Parameters . . . 26
  - 2.4.4 Clutch Thermal Model Calibration . . . 27
- 2.5 Drivers & Control Modelling . . . 28
  - 2.5.1 Diesel Engine & Governor Model . . . 28
  - 2.5.2 Induction Machine & Drive Model . . . 28
  - 2.5.3 Propulsion Control Model . . . 29
- 2.6 Propulsion Modelling . . . 31

2.6.1 Hull Model . . . 31
2.6.2 Wave Model . . . 32
2.6.3 Propeller Model . . . 32
2.7 Implementation & Validation . . . 34
2.7.1 Implementation . . . 34
2.7.2 Validation . . . 36
2.8 Conclusions . . . 37

3 Propulsion Mode Transition Simulations 40
3.1 Setup of the Simulations . . . 41
3.1.1 Propulsion Mode Transitions . . . 41
3.1.2 Impact Evaluation . . . 42
3.2 Propulsion Mode Transitions using the Instant Approach . . . 43
3.2.1 Results Instant Electric to Diesel Transition . . . 43
3.2.2 Results Instant Diesel to Electric Transition . . . 46
3.2.3 Impact of Clutch Operation in the Instant Transitions . . . 49
3.3 Propulsion Mode Transitions using the Staged Approach . . . 50
3.3.1 Results Staged Electric to Diesel Transition . . . 50
3.3.2 Results Staged Diesel to Electric Transition . . . 52
3.3.3 Impact of Clutch Operation in the Staged Transitions . . . 55
3.4 Propulsion Mode Transitions using the Torque Controlled Approach . . . 56
3.4.1 Results Torque Controlled Electric to Diesel Transition . . . 56
3.4.2 Results Torque Controlled Diesel to Electric Transition . . . 58
3.4.3 Results Torque Controlled Electric to Diesel Transition in a Rough Sea . . . 61
3.4.4 Impact of Clutch Operation in the Torque Controlled Transitions . . . 63
3.5 Comparison of the Impact of Clutch Operation in the Simulations . . . 64
3.5.1 Conclusions . . . 64
3.6 Discussion of the Propulsion Mode Transition Simulation Results . . . 65
3.6.1 Impact on the Hybrid Propulsion System . . . 65
3.6.2 Clutch Operation . . . 66
3.6.3 Influence of the Primary Controllers . . . 67
3.6.4 Propulsion Mode Transitions . . . 68
3.7 Conclusions . . . 69

4 Conclusions & Recommendations 71
4.1 Conclusions . . . 71
4.2 Recommendations for Further Research . . . 73

Bibliography 74

A Scientific Research Paper 79

B Complete Simulation Results 93
B.1 Simulation Output Description . . . 94
B.2 Steady State Propulsion Mode Simulation Results . . . 95
B.3 Propulsion Mode Transitions Simulation Results . . . 102

Chapter 1

Introduction

In this chapter first the problem is introduced in section 1.1. In section 1.2 the research background is discussed and a research gap is identified. In section 1.3 the research question and scope are defined, and the methodology is described. Finally the outline of this thesis is described in section 1.4.

1.1 Problem Description

Over the coming decades the worldwide fleet of ships will have to change radically to reduce emissions and comply with the Paris Agreements, that aims to keep the average increase in the earth's temperature below 2°C [1]. To aid this maritime energy transition, MARIN is developing a test environment, the Zero Emissions Lab (ZEL) [2]. This lab is shown in fig.1.1 and includes: a propeller in a cavitation tunnel driven by an electric drive system, batteries, fuel cells, a generator set, an AC bus and a DC bus, at a power level in the order of 75 kW.

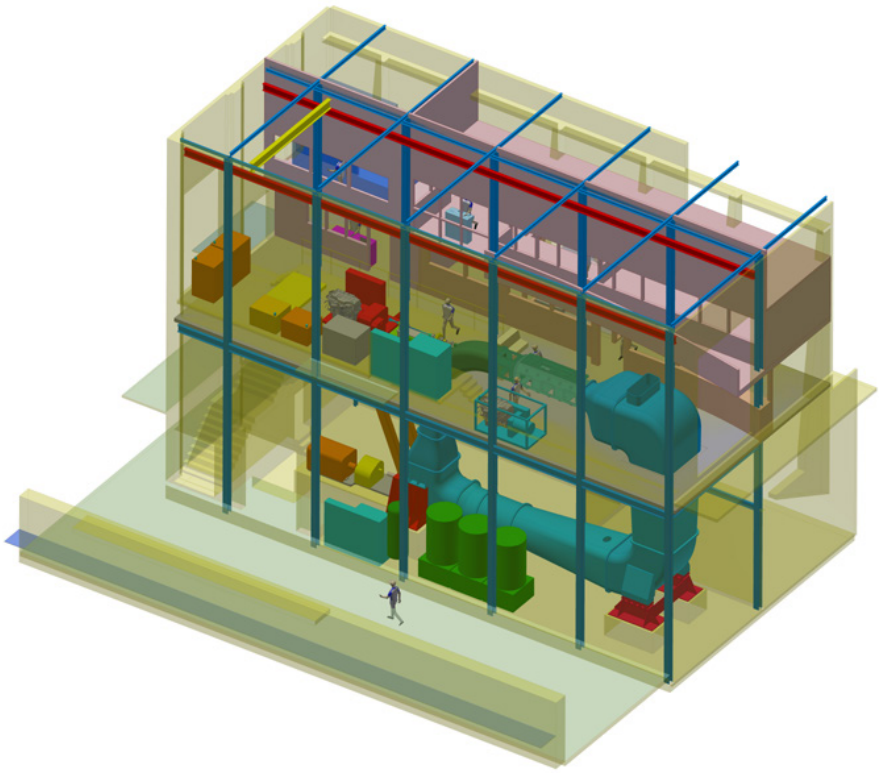

Figure 1.1: MARIN Zero Emissions Lab. *Source [2]*

Besides the physical lab, a digital version of this lab is being developed, the virtual-ZEL (v-ZEL). The v-ZEL can be used to investigate the performance of propulsion systems under a wider range of operating conditions than is possible in the lab, and simulates the behaviour of the propulsion system at full scale. To investigate propulsion system performance in the virtual-ZEL, models are needed to simulate the behaviour of maritime propulsion systems. Specifically in regards to the transmission system, which dynamics and components need to be modelled, is an area of research. Therefore it is the objective of this graduation project to contribute to the development of the transmission system of the v-ZEL and to address challenges in the scientific literature by researching the dynamics of the transmission system in maritime propulsion systems.

1.2 Research Background

It is the aim of this section to provide a background for the research in this thesis. Starting with maritime propulsion systems and their developments toward zero-emission in subsection 1.2.1. Followed by a review of the literature in regards to simulation of maritime transmission systems in subsection 1.2.2. Concluded with the identification of the research gap in subsection 1.2.3.

1.2.1 Maritime Propulsion Systems

A marine propulsion systems function is to generate thrust, enabling the ship to move at the desired speed. Thereby providing mobility, one of the most important operational functions, to support the mission of the ship. Examples of such missions are transporting cargo, installing offshore wind turbines or naval defence operations. A propulsion system can be divided in three main components: the driver that delivers mechanical power to the system, the propulsor that converts the mechanical power to thrust and the transmission system that transfers the mechanical power of the driver(s) to the propulsor [3]. Maritime Propulsion Systems can be classified in accordance with the nature of the driver(s) in three categories:

- **Mechanical propulsion** can either have a low speed diesel engine directly connected to the propeller with a separate generator setup to provide energy for the auxiliary loads [4]. Or a higher speed engine where a reduction gearbox has to be included. These configurations are characterised by high efficiencies in the design condition, but with limited efficiency in part-load conditions [3]. For naval applications, gas turbines can be used in place of, or combined with, diesel engines, as they provide high power in a relatively small form factor. However, this comes at the cost of efficiency [3].
- **Electrical propulsion** has electric motors as drivers that are powered by an expanded generator setup. This configurations allows for generator operation at the optimum efficiency over a wide operating range. However, total efficiency of electric propulsion systems power by generators is typically lower than mechanical propulsion, as the electric power conversion introduces additional losses in the system [3].
- **Hybrid propulsion** is defined in this thesis as a combination of mechanical and electrical propulsion. In a hybrid configuration, as in fig.1.2 the electric motor and ICE are both mechanically connected to the propeller. Propulsion can be provided by both engines combined or separately, resulting in the ability to operate at high total efficiency over a wide operating range. The electric motor can also act as generator and provide power for the ships electrical systems. The downside of hybrid architectures is the increased complexity of the propulsion system relative to both mechanical and electrical propulsion [3].

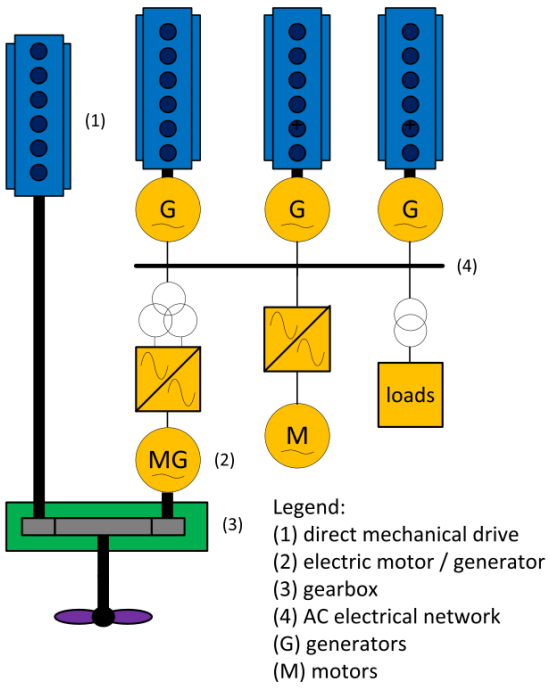

Figure 1.2: Typical hybrid propulsion architecture. *Source [4]*

1.2.1.1 Transition to Zero Emission Propulsion Systems

The International Maritime Organisation (IMO) drives the shipping industry to introduce more efficient and lower emission propulsion systems by mandating a maximum Energy Efficiency Design Index (EEDI) to obtain certification [5]. As EEDI requirements are increased over the years to further reduce emissions, developments such as the introduction of alternative fuels, slow steaming or predictive maintenance, will not be sufficient. Electrification has the potential to reduce emissions to the required level and this will increase the transition speed to hybrid and electrical systems [6]

Developments in Mechanical Propulsion To reduce the environmental impact of mechanical propulsion architectures, next to improving the systems efficiency, is the introduction of alternative fuels such as methanol [7] in dual fuel engines. To enable more efficient propulsion at various operating points, mechanical architectures with two combustion engines have been developed. Both engines cover part of the operating range and this configuration is adopted for example in naval ships that have variable mission profile. Combined diesel and diesel configurations (CODAD) have been developed for naval application, these configurations have an engine to provide high power for the main propulsion and an engine for lower speeds. The transmission system enables switching between engines by means of clutches, enabling the optimal engine for the required speed and thereby increasing the systems efficiency. To reduce the size, weight and emissions of the CODAD propulsion plant, the low speed diesel engine can be replaced with an electric motor[8], effectively transitioning to a hybrid propulsion system.

Developments in Electrical Propulsion For electric propulsion, the generators for the electric grid that power the electric machines can be partially or entirely replaced by lower or zero emission alternatives such as batteries or fuel cells [9], [4]. However, supply and storage of sufficient electric energy on the scale of a large ship over a long voyage, still needs further technological development [6]. A complementary path to reduce emissions is to increase the systems efficiency. For the typical rotational speeds of electric machines, reduction gearboxes are needed, leading to losses in the propulsion system. Direct drive electric machines are in active development in terms of size [10], [11], [12] and reliability [13], that reduce the need for a gearbox and the corresponding friction losses.

Hybridisation of the Propulsion System Hybrid propulsion in itself is an approach to reduce emissions. It combines the advantages of electric and mechanical propulsion. At design speed the diesel engine is able to operate at its peak efficiency. The electric motor enables efficient operation at part-load conditions and can be used to supplement the diesel engine in, for example, acceleration manoeuvres to reduce emissions [14] or adverse weather conditions [5]. In Inal, Charpentier, and Deniz [6] it is concluded that internal combustion engine (ICE) is still the best option for providing the required power given current technological maturity. To reduce emissions the ICE can be combined with various energy storage systems and an electric motor, depending on the ship's mission profile [6]. In a hybrid system, the problem of electric energy storage is reduced in magnitude compared to full electric propulsion, as the electric motor does not need to provide the main propulsion power. For hybrid propulsion an energy management strategy needs to be used to select the optimal propulsion mode and thus minimise fuel consumption and emissions [15], [16]. Considering the various possible propulsion modes in hybrid systems, dynamic switching between these modes is identified as a challenge [6]. Evaluating the developments to reduce emissions, hybridisation of the propulsion system is identified as a path that is both attainable given current energy storage technology and a stepping stone to full electric propulsion, that will be required to reduce emissions to zero.

1.2.1.2 Conclusion

In this subsection regarding maritime propulsion systems, the hybrid propulsion architecture and its corresponding challenges are identified as relevant cases for the MARIN ZEL and v-ZEL. Specifically dynamic switching between operational modes is a relevant problem arising in the transition to zero-emission propulsion systems that could be addressed by further development of transmission system simulation models.

1.2.2 Simulation of Maritime Transmission Systems

Corresponding with the identified dynamic propulsion mode transition challenge in hybrid propulsion systems, the relevant scientific literature concerning clutch simulation in maritime transmission systems is explored and discussed in sub-subsection 1.2.2.1. To gain insight into simulation of the transmission system, the propulsion system simulation literature is further investigated concerning the dynamics and model fidelity of the transmission system in sub-subsection 1.2.2.2. Sub-subsection 1.2.2.3 concludes this subsection on the simulation of maritime transmission systems.

1.2.2.1 Simulation of Clutch Operation in Maritime Transmission Systems

Typical applications for Clutches in maritime propulsion systems are: enabling a reverse gearing, engage a power-take-off (PTO), disconnect engines for free running or maintenance and finally, and most relevant for this research, selecting and combining main drive engines to enable dynamic switching between operational modes.

Work by Deleroi [17], includes a multi disk friction clutch model to engage the reverse gearing in a propulsion system crash stop simulation model. The maximum clutch torque was modelled on the basis of a lookup table based upon experimental fits from manufacturer data sheet. A parameter variation was performed to investigate the influence of the initial clutch gradient on the rotational speed curves of the propeller and diesel engine. It was concluded that the propulsion system behaviour is strongly dependent on the slope of the initial torque transfer of the clutch.

In Engja [18] the propulsion system model includes a friction type clutch. The clutch is used to start the ship's propulsion. A Torque peak is identified at the moment of lockup due to synchronisation being achieved followed by a low frequency torque oscillation. The influence of the pressure profile is investigated and a less steep pressure profile results in slower engagement and corresponding lower torque oscillation amplitude and frequency.

Montazeri-Gh and Miran Fashandi [19] includes a friction type clutch in a maritime propulsion simulation model to connect two gas turbines in a cross connect architecture. This publication is mainly focused on the bond graph modelling of the gas turbines and the clutch is modelled using the the Bond Graph approach as introduced in Engja [18]. It is concluded that "the engagement of clutches may generate large dynamic loads in the torsional mode" [19].

In a study on the mode switching process in a combined diesel or gas architecture (CODOG) [20] a Synchro-Self-Shifting(SSS) clutch is simulated. The effect of clutch geometry on the mesh time and induced torque pulse are investigated to enable model based design of the SSS clutch. An SSS clutch is typically only applied in naval propulsion architectures [3].

It is concluded that some research has been conducted regarding clutches in maritime transmission systems where generation of large dynamic torque loads is identified. However clutch operation to enable dynamic switching between operational modes in hybrid propulsion systems has seen little attention.

1.2.2.2 Dynamics in Maritime Transmission Systems and Corresponding Model Fidelity

Simulation of the transmission system is further investigated concerning the significant dynamics and model fidelity in the literature on propulsion system simulation. The reviewed literature is summarised in table 1.1 and is further discussed in this sub-subsection.

In typical maritime propulsion system simulations that only consider shaft speed and transmitted torque, the mechanical power transmission system is modelled as a single lumped inertia [21], [22], [23], [24], [14], [25]. For studies that consider torsional disturbances and resonance, the mechanical power transmission system is broken up into a varying number of flexibly connected lumped moments of inertia [26], [27], [28], [29]. The highest fidelity of the transmission system models is reached when using a finite element approach as in Gong, Liu, Liu, *et al.* [30]. This fidelity level is suitable to asses the transmission of steady state vibrations but computationally expensive for longer dynamic simulations.

Table 1.1: Table summarising the reviewed literature on propulsion system simulation concerning the significant dynamics and model fidelity of the transmission system.

Publication	**Propulsion System**		**Transmission System**		
	Architecture	**Sub-models**	**Dynamics**	**Framework**	**Model Fidelity**
Bartlett et al. 1999 [26]	Combined Diesel and Gas	Shaft, Propeller, Reduction gearbox, Prime movers	*Overtorquing of the driveshaft during rapid acceleration.*	Distributed and Single Lumped Inertia	Shaft speed, Transmitted torque, Torsional vibrations
Apsleyt et al. 2009 [21]	Full Electric	Power electronics, Induction Machine, Propeller, Ship	*Induced thrust disturbance is transmitted to the motortorque and supply current sensitivity to this disturbance has been demonstrated.*	Single Lumped Inertia	Shaft speed, Transmitted torque
Figari and Altosole 2007 [22]	Twin Gas Turbines	Hydrodynamics, Gas turbines, Propeller	*Transient behaviour of the ship is virtually unaffected by mass moment of inertia of the rotating parts.*	Single Lumped Inertia	Shaft speed, Transmitted torque
Viviani et al. 2008 [23]	Combined Diesel and Gas	Engine, Governor, Gears, Propeller, Rudder	*In ship turning unbalanced propeller loads lead to shaft overloads and unbalanced force on the reduction gears.*	Single Lumped Inertia	Shaft speed, Transmitted torque
Altosole et al. 2010 [24]	Combined Diesel-Electric and Gas	Ship, Propulsion plant, Control system	*Torque unbalances during fast turning of the ship*	Single Lumped Inertia	Shaft speed, Transmitted torque, Shaftline losses
Geertsma et al. 2017 [14]	Diesel Electric Parallel Hybrid	Diesel Engine, Induction Machine, Frequency converter, Gearbox, Shaft, CPP, Hull, Waves and Wind	*Load distribution between the induction machine and the diesel engine lead to a reduced thermal load on the diesel engine.*	Single Lumped Inertia, Linear Torque Loss model	Shaft speed, Transmitted torque, Gearbox losses, Shaftline losses
Dermentzoglou and Papadopoulos 2016 [31], 2018 [32]	Diesel Electric Parallel Hybrid	Engine, Propeller, Induction Machine, EM controllers, Planetary gearbox	*Rotating and Mesh frequencies of the gearbox could be detected in the electromagnetic torque and stator current.*	Detailed Gearbox EOM	Gearbox mesh stiffness, backlash, transmission error, translational and rotational modes
Godjevac et al. 2016 [33]	Dual Diesel	Engines, Gearbox	*10 Percent gearbox losses in low load operating regimes.*	Thermal Network	Gearbox losses, Gearbox thermals
Gong et al. 2021 [30]	Combined Diesel and Gas	Cross-connect gearbox	*Vibration transmission is present between gearboxes, higher coupling in at low operating speed.*	Generalised finite element	Vibration coupling
Skjong et al. 2016 [25]	Direct drive Mechanical with shaft generator	Electrical system, Diesel Engine, Shaft system, Vessel, Propeller, Battery system	*Transmitted disturbance from the wave action on the electric system voltage in the order of 1-2 percent.*	Single Lumped Inertia, Co-simulation	Shaft speed, Transmitted torque, Shaftline losses
Ayu et al. 2017 [27]	Electric Azimuth	Electric motor, Bevel gearboxes, Propeller, Shafts	*Response to ventilation condition of the propeller: small effect on rotational speed (5 percent deviation) and large effect on shaft torque (60 percent deviation).*	6 Lumped Inertias connected by spring-dampers	Shaft speed, Transmitted torque, Torsional vibrations
Guo et al. 2017 [28]	Diesel with shaft generator	Diesel engine Flywheel, Gearbox, Generator,Propeller	*Resonance, PID tuning to prevent torsional vibration problems.*	35 Lumped Inertias connected by spring-dampers	Shaft speed, Transmitted torque, Torsional vibrations
Xiao et al. 2018 [29]	Diesel Electric Parallel Hybrid	Diesel Engines, Flexible couplings, Electric motor, CPP	*Peak stresses in the shafting system due to ICE operating point at resonant frequency.*	5 Lumped Inertias connected by spring-dampers	Shaft speed, Transmitted torque, Torsional vibrations, non-linear stiffness
Montezeri and Fashandi 2019 [19]	Cross-connected Twin GT	Gas turbines, Prop, Couplings,Gears, Clutches,Generator,	*Engagement of clutches may generate large dynamic loads in the torsional mode.*	Multiple Lumped Inertias,	Shaft speed, Transmitted torque, Clutch operation
Engja 2000 [18]	Diesel with shaft generator	Diesel Engine, Gearbox, Clutch Elastic Couplings, Clutch Hydraulics	*When performing clutching operations, large transient loads may occur in the transmission system.*	Multiple Lumped Inertias connected by spring-dampers	Shaft speed, Transmitted torque, Clutch operation, Torsional vibrations
Deleroi 1995 [17]	Diesel with reversible gearbox	Diesel Engine, Governor, Clutch, Gearbox, Ship, Propeller	*Drop in engine speed due to clutch engagement, clutch operation limited by friction heat.*	Single Lumped Inertia	Shaft speed, Transmitted torque, Clutch operation

When the transmission of hydrodynamic disturbances from propeller to the engine are considered in simulation models, the fidelity of the transmission system is typically extended to include losses in the shaftline and gearbox [24], [14], [25]. The transmission system is then modelled as a single lumped inertia with a loss factor on the transmitted torque. A suitable torque loss model is evaluated in Godjevac, Drijver, Vries, *et al.* [33]. However, in Ayu, Kambrath, Yoon, *et al.* [27] the impact of hydrodynamic disturbances on the shaft torque and speed is investigated by using multiple lumped inertias, but the losses in the shaftline are not considered. In Dermentzoglou and Papadopoulos [31] and Dermentzoglou and Prousalidis [32] it is concluded that the gear mesh stiffness has a relevant impact on the electric motor currents in a hybrid architecture.

The multi-inertia approach is also applied when the torque disturbance generated in clutch operation is investigated in Montazeri-Gh and Miran Fashandi [19], Engja [18]. However, Deleroi [17] does not use this approach, as the only concern in this study is the speed drop of the diesel engine during clutch operation.

It is identified that for disturbances transmitted from the propeller to the engines, the system is typically modelled as a single lumped inertia, whereas when the impact on the transmission system components is evaluated the multi-inertia approach is applied. When investigating the operation of clutches, an impact on both the transmission system itself as well as an impact on the transmission of power from the engines to the propeller can be expected. Therefore a merging of the typical model fidelity for both these impacts is a suitable approach to investigate dynamic switching between operational modes.

It is concluded that the large torque loads from clutch operation can be evaluated by using a multi inertia transmission system model where the system's flexibility is taken into account. Considering that the switching between operational modes takes place in a dynamic operational condition, dynamics such as thrust disturbances and ship speed are also of relevance. A simulation model where a broad range of transmission system model fidelity's are merged, is therefore an appropriate approach to investigate dynamic switching between operational modes. The modelling frameworks in the reviewed literature cover the range of fidelity that is required for such a model.

1.2.2.3 Conclusion

In this subsection on the simulation of maritime transmission systems it is concluded that clutch operation to enable dynamic switching between operational modes in hybrid propulsion systems has seen little attention in the scientific literature. This lack of attention is unjustified as clutch operation is indicated to generate significant disturbances in propulsion systems. It is further concluded that a simulation model where a broad range of transmission and propulsion system model fidelities are merged, might be an appropriate approach to investigate this problem. The identified modelling frameworks in the reviewed literature should covers the range of fidelity that is required to develop such a simulation model.

1.2.3 Research Gap

Over the coming decades, the worldwide fleet of ships will have to change radically to reduce emissions and comply with the Paris Agreements which aims to keep the average increase in the earth's temperature below 2°C [1]. As EEDI requirements are increased over the years to reduce emissions, the transition speed to hybrid and electrical systems will increase [6]. Hybrid propulsion system enables optimum performance and efficiency over its operating range and is identified as an architecture that is both attainable given current energy storage technology and is a possible stepping stone to full electric propulsion. The hybrid propulsion system is thus highly relevant in the path toward zero emission propulsion systems and correspondingly the MARIN ZEL.

Dynamic switching between operational modes is identified as a challenge for hybrid propulsion architectures [6]. In hybrid propulsion systems the operation of clutches in the transmission system enables switching between drive engines when transitioning between operational modes. Clutch operation is indicated to generate significant disturbances in propulsion systems [18], [19], [17]. However, this impact is overlooked in hybrid propulsion simulation studies in the scientific literature. A simulation model where a broad range of transmission and propulsion system model fidelities are merged, is identified as an appropriate approach to investigate this problem. Therefore an apparent research gap concerning clutch operation in hybrid propulsion systems in the context of propulsion mode transitions is identified.

1.3 Research Structure

This section introduces the structure of the conducted research in this thesis. First the research question is established in subsection 1.3.1, then the scope is defined in subsection 1.3.2 and finally the applied methodology is described in subsection 1.3.3.

1.3.1 Research Question

In the previous section on the background of the research, an apparent research gap concerning clutch operation in hybrid propulsion systems in the context of propulsion mode transitions is identified. The relevance of this knowledge gap is further supported by an example known at MARIN related to the hybrid propulsion system of a naval vessel, consisting of a large main diesel engine and a relatively small electric motor (PTI). A mismatch between the energy stored in the propulsion systems (due to high rotational inertia and stiffness) and the (peak) power of the electric motor driving the PTI resulted in problems when engaging the clutch. It was indicated that while simulations were performed during the basic engineering phase of the vessel, these simulations focused on the mechanical side of the issue and the design of the high-level control philosophy. Using a more detailed model for clutch engagement and system dynamics could have provided insight into the response of the coupled mechanical-electrical system. The research in this thesis aims to address the identified knowledge gap by investigating the following main research question:

What is the impact of clutch operation in propulsion mode transitions on hybrid maritime propulsion systems?

1.3.2 Scope

Having established the main research question, the scope of the research is further defined here. In section 1.2 it is concluded that clutch operation is expected to have both an impact on the transmission system components themselves, as well as the operation of the engines. Moreover, the state of the sea is expected to be relevant when transitioning between propulsion modes. Consequently, the system boundary is drawn around the hybrid propulsion system as defined in fig. 1.3. As visualised in the figure, the state of the sea and selected propulsion mode are considered external signals to the system. The electric load is considered as an output signal, the ship's power systems are out of scope for this thesis. A form of propulsion control is included that translates a propulsion mode setpoint to the corresponding control signals for the diesel engine, electric motor and clutch.

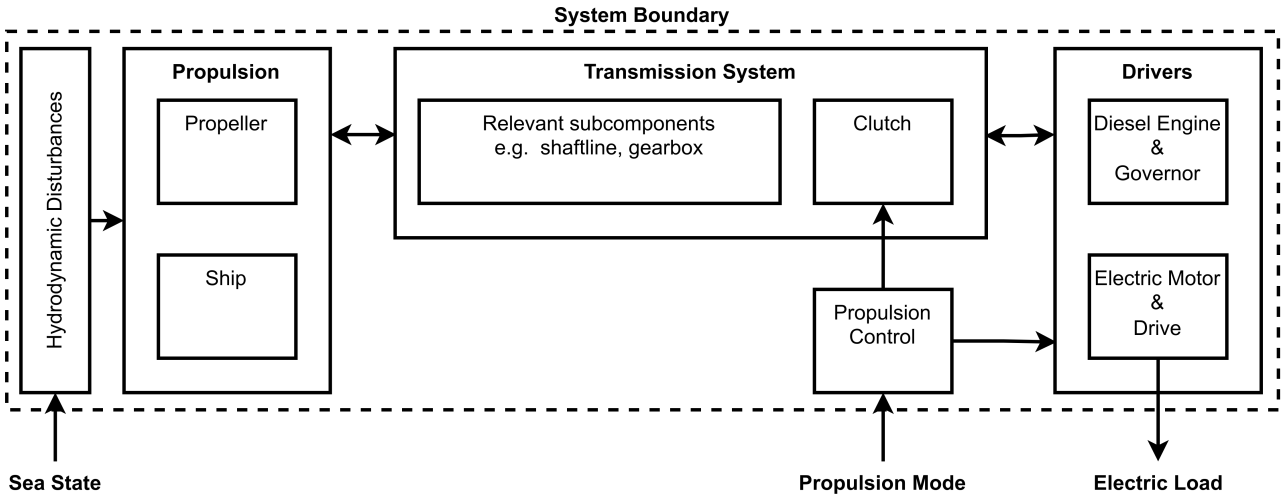

Figure 1.3: System boundary depicting the scope of the research in this thesis.

1.3.3 Methodology

To be able to address the main research question, a system is defined, characteristics and dynamics of maritime clutches are investigated and a propulsion system model is developed enabling the evaluation of the impact of clutch operation in propulsion mode transitions. The mathematical model is implemented in Matlab Simulink and the validity of the system model is assessed. The propulsion system model is then used to evaluate the impact of clutch operation in propulsion mode transitions by running simulations. Multiple propulsion control approaches for the mode transitions are applied and the results compared. In this methodology the following sub-research questions are addressed:

- *What is an appropriate hybrid maritime propulsion system case to investigate clutch operation in propulsion mode transitions?*
- *What are the characteristics and dynamics of a typical clutch in a maritime propulsion system?*
- *How to model the hybrid maritime propulsion system to enable evaluation of the impact of clutch operation in propulsion mode transitions?*
- *How to approach the propulsion mode transitions from a propulsion control point of view?*

1.4 Thesis Outline

This thesis is structured following the introduced methodology. In chapter 2 the system modelling is described. First a hybrid propulsion system case is defined in section 2.1. The modelling of the defined propulsion system is described in sections 2.2-2.6. In section 2.7 the implementation and validity of the system model is discussed. Section 2.8 concludes the chapter by summarising how the sub-research questions have been addressed.

The main research question is addressed in chapter 3 by performing simulations, using the hybrid propulsion system model described in chapter 2. In section 3.1 the setup of the simulation experiments is described. In sections 3.2 - 3.4 the results of the simulations are analysed. In section 3.5 the results of the propulsion mode transitions simulations are compared. In section 3.6 the simulation results are discussed. Section 3.7 concludes this chapter by summarising how the the main research question has been addressed in this chapter.

Finally the conclusions and recommendations of this thesis are presented in chapter 4.

Chapter 2

System Modelling

In this chapter first a hybrid propulsion system case is defined in section 2.1. The modelling of this system is described in sections 2.2-2.6. In section 2.7 the implementation and validity of the system model is discussed. Section 2.8 concludes this chapter by summarising how the sub-research questions have been addressed.

2.1 System Description

In this section, the system and its characteristics are described. First the reference ship and propulsion system are introduced in subsection 2.1.1. Then the clutches are discussed in subsection 2.1.2. By combining the reference systems and the clutches, the complete system is defined in subsection 2.1.3. Finally the propulsion modes and transitions for the hybrid propulsion system are addressed in subsection 2.1.4.

2.1.1 Reference Ship and Propulsion System

The hybrid propulsion system in this thesis is fitted to a feeder type container ship that can be regarded as a possible ship type for hybrid propulsion [4] (mean parameters for this ship type: 14 MW MCR, 1650 TEU, 20 knots [34]). The DAMEN Container Feeder 1700 is selected as a case study. The ship has a length of 172 m and is originally fitted with a 11.6 MW 2-stroke diesel engine which propels the ship at 18 kn when using 85% of its available engine power [35].

As a reference propulsion system, the hybrid propulsion system used in Geertsma, Negenborn, Visser, *et al.* [14] and further described in Geertsma [36] is selected. The internal combustion engine (ICE) is a 20 cylinder four stroke diesel engine with a nominal power of 9.1 MW at 16.7 rev/s (1000 rpm). The electric motor/generator (MG) is a 10 pole at 3.15 kV with a synchronous speed of 600 rpm and a nominal power of 3 MW. Both engines are coupled to the propeller with the same gear ratio. As a result, the electric motor can be used for low speed operation and the diesel engine is most suitable for the higher speed operation. To enable separate operation clutches have to be introduced in the propulsion system. Fitted with the new hybrid propulsion system the ship has a combined propulsion power of 12.1 MW available.

2.1.2 Clutches

The clutches in the hybrid propulsion system are used for selecting and combining main drive engines to enable dynamic switching between operational modes. From investigating the product range of highly regarded manufacturing companies in the maritime industry (ZF, Wartsila, Reintjes, Renk, SSS, Orthlinghaus) and consulting Woud and Stapersma [3], it is identified that the multi plate wet friction clutch is the primarily used clutch type for this operation. Multi Plate Wet Friction Clutch are typically integrated in dual engine gearboxes such as in the reference propulsion system.

An alternative clutch type is the double-cone dry friction clutch. However, double-cone dry friction clutches are typically shaft mounted and integrated with flexible couplings to engage PTO machines such as pumps. Another alternative is the hydraulic coupling, typically used to dampen torsional vibrations originating from the diesel engine, the fluid coupling is characterised by its relatively high power loss when engaged but virtually wear free operation [3]. A final alternative is the Synchro-Self-Shifting (SSS) clutch , although this clutch type is typically used in naval ships and application in commercial shipping is thus far limited. It is claimed by the manufacturer that the SSS clutch provides a great number of advantages over friction type clutches [37], smooth engagement, low wear and high reliability forming the main arguments. The advantages arise from this clutch type being fundamentally different during engagement (synchronous clutches vs friction slip clutches) [38]. It is thus concluded that there are some alternative clutch types that could be investigated in further research. Considering that the multi plate fiction clutch is typically applied to enable propulsion mode transitions, this clutch type is selected for the hybrid propulsion system case in this thesis.

2.1.3 System Definition

Introducing multi plate wet friction clutches in the selected hybrid propulsion system enables transitions between various modes for the reference ship's propulsion. Transmission system flexibility is relevant and therefore the flexible couplings between the gearbox and engines, that are typically present to deal with shaft misalignment and vibrations, are included in the system. The resulting system is depicted in fig.2.1 and contains the following components:

- Reference ship hull
- Wageningen-B series fixed pitch propeller
- Reference propulsion system diesel engine
- Reference propulsion system electric motor
- Ortlinghaus 202 series clutches
- Vulkan 2400 series elastic couplings
- Reference ship shaftline
- Reference propulsion system gearbox

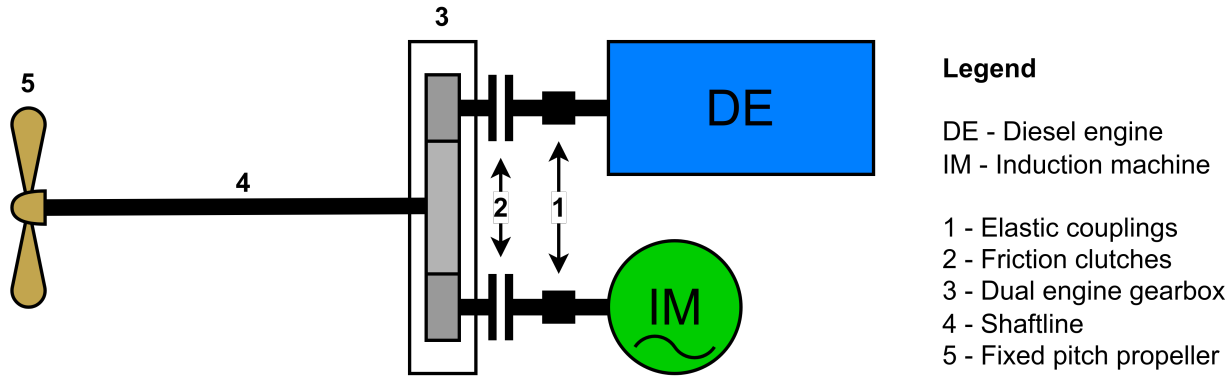

Figure 2.1: Hybrid propulsion architecture with multi plate wet friction clutches to enable dynamic switching between the electric and diesel engine in propulsion mode transitions.

The hybrid propulsion systems allows for operation in various operational modes, as will be discussed in the next subsection 2.1.4, therefore a new propeller will have to be matched. The Wageningen B-series [39] is publicly available and suitable for application on merchant vessels and is therefore selected for the system. The propeller is matched to enable the ship to propel itself at 15 knots using 85% of the available diesel engine power, following the developments in slow steaming and using the typical engine margin for merchant vessels [3]. It is the function of the electric motor in this architecture to propel the ship at lower speeds and assist the diesel engine in adverse weather conditions [5] or acceleration manoeuvres [14]. These assist modes are considered outside the scope of the current research, they are however relevant when determining the design parameters of the components, as the combined power of both engines has to be taken into consideration.

For the clutches and flexible couplings manufacturers are selected with a high reputation that have a wide range of publicly available reference data [40], [41] . The selection of specific components will be discussed when the model parameters are determined.

A clutch is included that couples the electric motor, this clutch could be excluded when the electric motor does not have permanent magnets in either the stator or rotor. In that case the electric motor can be disconnected electrically and put in a free spinning mode. As the electric motor in the system is an induction motor the clutch could thus be let out. In terms of redundancy, the ability to disconnect the electric motor when problems occur, is however desirable include this clutch. Moreover, this research is not focused on a specific electric motor type, therefore, it is elected to include a clutch to enable (de)coupling the electric motor.

2.1.4 Propulsion Modes and Transitions

The hybrid propulsion system defined in the preceding subsection 2.1.3 is able to operate in a number of modes. An overview of these modes is depicted in fig.2.2. The considered propulsion modes within the scope of this thesis are diesel engine propulsion and electric propulsion. Below 600 rpm and at low power the diesel engine operates at a relatively low fuel efficiency, as can be assessed from fig.2.3. The induction machine however, at 600 rpm, would operate at its design speed and corresponding high efficiency. Therefore the transitions between these modes can be expected at that operational point.

The assist, generator, reverse and off modes and corresponding transitions are not considered within the scope of this research. The simulation results of the transitions between the diesel and electric propulsion modes are expected to provide insight on the impact of propulsion mode transitions in general.

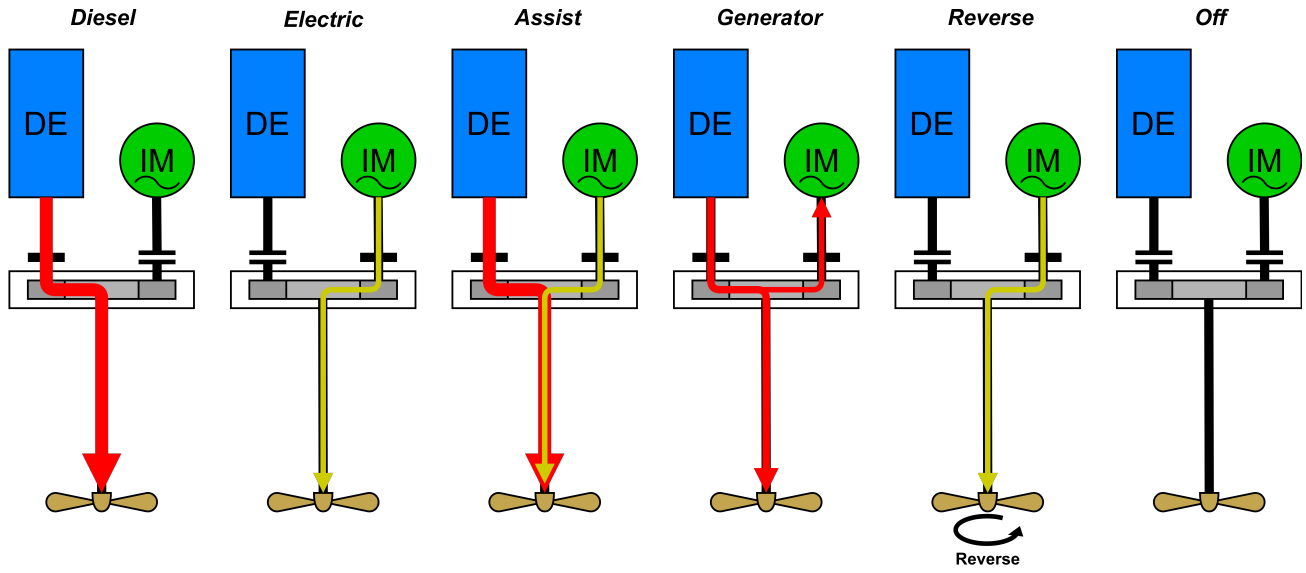

Figure 2.2: Hybrid propulsion system operational modes, power flow is represented by red(Diesel engine power) and yellow (Electric motor power) arrows.

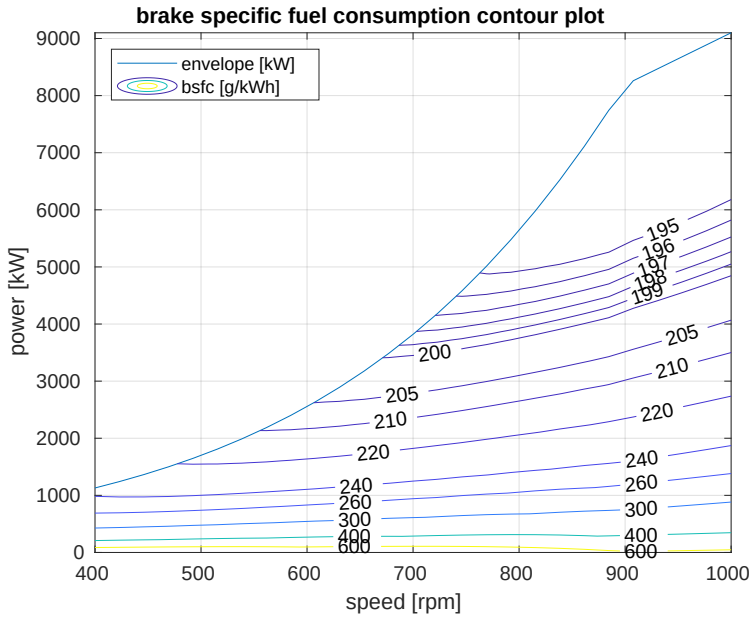

Figure 2.3: Brake Specific Fuel Consumption of the reference diesel engine. This figure has been generated using the model for this diesel engine described in [36].

2.2 System Model Description

It is the aim of this section to provide an overview of the system model. First the considered impact measures are defined in subsection 2.2.1. Then in subsection 2.2.2 the concept for the system model is described.

2.2.1 Impact Measures

Before the system can be modelled at an appropriate fidelity level, the impact measures have to be defined. In section 1.2 it is concluded that clutch operation is expected to have both an impact on the transmission system components themselves, as well as the operation of the engines. Therefore a broad spectrum of impact measures is defined, covering the expected impact on the various components of the hybrid propulsion system.

In Deleroi [17] the impact of clutch operation on the engines is identified. Therefore, the operation of the diesel engine and induction machine relative to their envelopes is selected as an impact measure. In the scope of this research it is determined that the electric load is considered as an output signal, and that the ship's power systems are out of scope for this thesis. However, given the relevance of the electric load on the power system for further developments in electrification, the impact of clutch operation in propulsion mode transitions on the electric load is evaluated. As a result the following impact measures are defined in regards to the impact on the driver side of the system:

- Operation of the induction machine relative to its torque-speed operating envelope
- Operation of the diesel engine relative to its torque-speed operating envelope
- Electric load profile of the induction machine

In Engja [18] it is concluded that large transient loads may occur in the transmission system when performing clutch operations. Therefore the low frequency torsional vibrations in the transmission system are evaluated as in Engja [18]. The large transient loads could also result in excessive stress in the shaftline, and therefore this should be evaluated. In Deleroi [17] the operation of the clutch is identified as being limited by the developed heat during clutch operation. This impact is therefore taken into consideration. From experience at MARIN it was identified that hammering of the gears in the gearbox could be a significant impact of the operation of clutches. When gears hammer back and forth, the tooth surface is work-hardened by the impact force making the surface both harder and more brittle, increasing the risk of damage to the gear teeth surface. This results in the following impact measures for evaluating the impact on the transmission system components:

- Low frequency torsional vibrations
- Stress in the shaftline
- Temperature of the clutch
- Gear hammer in the gearbox

The typical control goal for ship propulsion systems is maintaining the speed of the propeller at the desired setpoint [4]. As during the transition between propulsion modes this speed is expected to be impacted, a final impact measure is defined:

- Rotational speed of the propeller

2.2.2 Conceptual Model

Considering the defined scope in 1.3.2, system in 2.1 and the impact measures in 2.2.1 a conceptual model for the system is defined. This model enables the evaluation of the selected impact measures in the considered propulsion mode transitions for the selected hybrid propulsion system. In this subsection the overall concept for this model is described.

In the research background it is concluded that the large transient torque loads from clutch operation can be evaluated by using a multi-inertia transmission system model, where the systems flexibility is taken into account. The torsional vibration concepts are not typically applied for the dynamic evaluation of the transmission system, as they are used to calculate steady state torsional vibrations and resonance at fixed operating points. The low frequency torsional vibration behaviour of the system is taken into consideration, therefore the torsional vibration concepts are applied to the transmission system as previously done in [18]. In this concept the inertias connected by the clutch can be in two states: rigidly connected or uncoupled. This is further described in section 2.4.

The multi inertia concept is integrated in the model concept, resulting in fig.2.4 where a schematic representation and the coupling of the submodels is given. Also, in the conceptual model figure, the system subdivision as introduced in subsection 1.3.2, is further developed according to the definition of the system components in subsection 2.1.3. The multi-inertia rotational dynamics are the glue connecting the mechanical subsystems together. In sections 2.3 - 2.6 the submodels are further described.

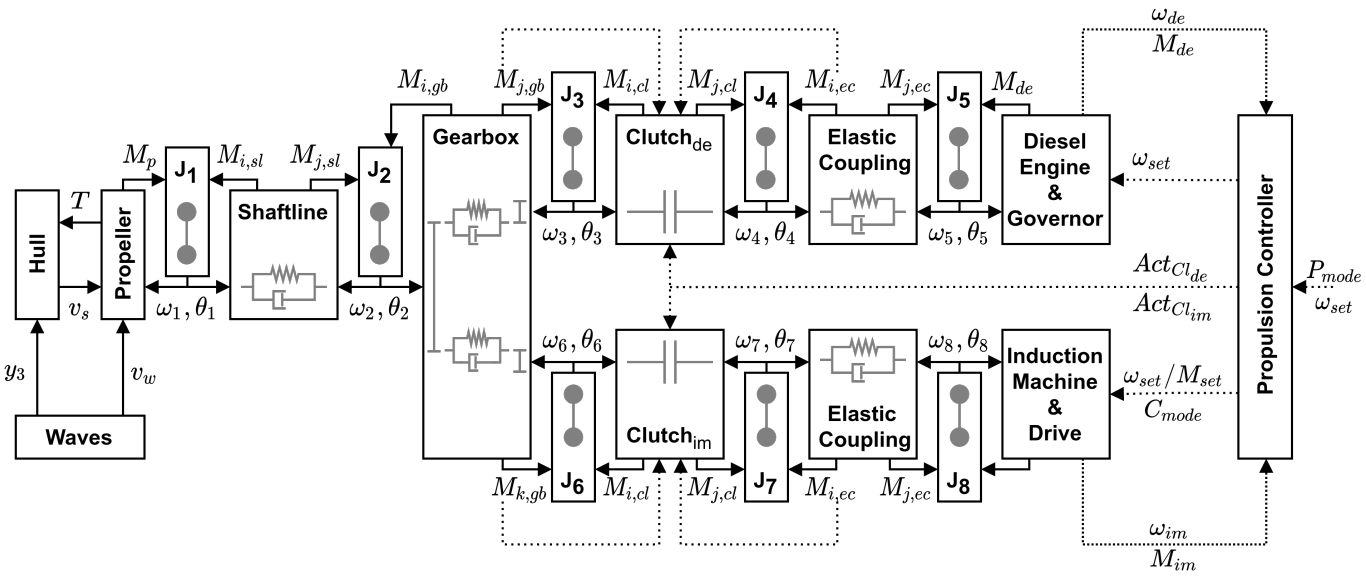

Figure 2.4: Schematic representation and model coupling of the propulsion system model.

2.3 Transmission System Modelling

In this section, the modelling of the transmission system is described. In subsection 2.3.1 the modelling of the rotational dynamics is discussed. In subsection 2.3.2 the shaftline modelling is described. In subsection 2.3.3 the model for the gearbox is presented. Finally in subsection 2.3.4 the model for the elastic couplings is described. The model for the clutch is part of the transmission system but discussed separately in section 2.4.

2.3.1 Rotational Dynamics

The multi-inertia rotational dynamics are the glue connecting the mechanical subsystems. To asses the basic vibratory behaviour of the transmission system, the system is divided in 8 lumped inertias connected by the nonrigid subsystems (shaftline, gearbox, elastic couplings). This structure can be identified in the schematic representation of the propulsion system model in fig.2.4. The lumped inertia element represents a section of the transmission system from which the inertias are lumped and regarded as rigidly coupled. The shafting and inertias are assumed to be perfectly aligned, the movement of the inertia can therefore be reduced to rotation only and whirling is neglected. Axial stiffness is assumed to be much larger than the torsional stiffness and axial dynamics are thus neglected.

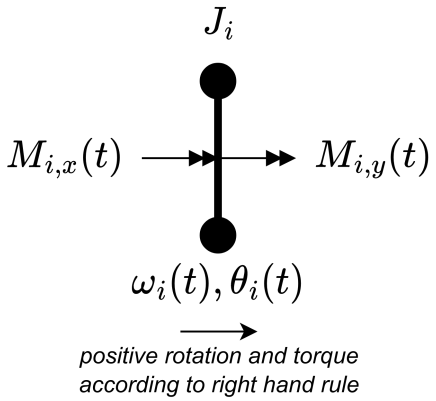

Figure 2.5: Schematic of a lumped inertia i, where x and y are the connected submodels.

The rotational dynamics are governed by (2.3.1 - 2.3.3) where $J_{i,x}$ and $J_{i,y}$ represent the inertia contributions of the connecting sub-system x and y respectively. $M_{i,x}$ and $M_{i,y}$ represent the applied torque from the connected sub-systems to the lumped inertia element. The state variables ω_i in rad/s and θ_i in rad describe the rotation of the inertia element. For the torque and speed, right hand side rotation of the propeller when viewed from the stern is defined as positive. The loads are then represented in the system by having a negative sign.

$$\dot{\omega_i}(t) = \ddot{\theta_i}(t) = \frac{J_i}{M_i(t)} \tag{2.3.1}$$

$$J_i = J_{i,x} + J_{i,y} \tag{2.3.2}$$

$$M_i(t) = M_{i,x}(t) + M_{i,y}(t) \tag{2.3.3}$$

2.3.1.1 Rotational Dynamics Model Parameters

The parameters for the lumped inertias of the complete model in fig.2.4 are presented in table 2.1 and have been obtained by combining the inertia contributions of the connecting submodels.

Table 2.1: Inertia parameters.

Inertia	
J_1	$22239\ kg \cdot m^2$
J_2	$3213\ kg \cdot m^2$
J_3	$16\ kg \cdot m^2$
J_4	$44\ kg \cdot m^2$
J_5	$663\ kg \cdot m^2$
J_6	$10\ kg \cdot m^2$
J_7	$16\ kg \cdot m^2$
J_8	$31\ kg \cdot m^2$
Total	$26232\ kg \cdot m^2$

2.3.2 Shaftline Model

To accurately simulate the dynamic behaviour of the transmission system the speed and torque dependent friction losses and flexibility of the components have to be taken into consideration. The shaftline friction is typically modelled employing a static efficiency coefficient [25]. For part load conditions this tends to underestimate the friction [33]. For this model a torque loss function with a dependence of rotational speed and transmitted torque is therefore selected. The shaftline model is divided into two submodels, the material model describing the shaft flexibility and the friction model that describes the losses from shaft bearings. For the material model the stress in the shaftline is considered as this has been selected as an impact measure. The torque contributions of both submodels are added (2.3.4) ,(2.3.5) and are applied to the respective lumped inertias on each side of the shaft line as visualised in the conceptual model fig.2.4.

$$M_{i,sl}(t) = M_{i,sl_f}(t) + M_{sl}(t) \tag{2.3.4}$$

$$M_{j,sl}(t) = M_{j,sl_f}(t) - M_{sl}(t) \tag{2.3.5}$$

2.3.2.1 Shaftline Material Model

As is common in the stationary torsional vibration analysis of maritime propulsion systems [42], a Kelvin-Voigt material model [43] is applied. In such a material model (2.3.6) the shaft flexibility is modelled as a parallel spring damper, represented in fig.2.4. The spring and damper are assumed to have no mass and the stiffness k_{ij} and damping c_{ij} are assumed linear.

$$M_{sl}(t) = k_{i,j}[\theta_j(t) - \theta_i(t)] + c_{i,j}[\omega_j(t) - \omega_i(t)] \tag{2.3.6}$$

$$\tau_{sl}(t) = r_{sl}\frac{G_{sl}[\theta_j(t) - \theta_i(t)]}{l_{sl}} \tag{2.3.7}$$

$$\sigma_{ax}(t) = \frac{T(t)}{\pi \cdot r_{sl}^2} \tag{2.3.8}$$

$$\sigma_{eq}(t) = \sqrt{\sigma_{ax}^2 + 3\tau_{sl}^2} \tag{2.3.9}$$

Shaft line stress is evaluated from the pure shear (2.3.7) and the axial load from the propeller thrust (2.3.8). It is assumed that the load on the shaft is a pure combination of the torsional shear and axial pressure and that the full thrust force is transferred through the shaft to the thrust bearing in the gearbox. This assumption is based on a perfectly aligned shafting system with zero axial friction. The Von Mises equivalent stress (2.3.9) can be evaluated relative to the yield limit of $275\ MPa$ for C45 steel [44]. To asses the effect of axial friction from the stern tube and shaft bearings, and whirling vibration from misalignment, more detailed design information and a higher fidelity model is needed. The selected approach can however be used to asses the general impact on shaftline stress.

2.3.2.2 Shaftline Friction Model

The friction in the shaft line $M_{i/j,sl_f}$ is modelled (2.3.10 - 2.3.11), using a torque loss model [33]. The torque loss model parameterisation is based on a division of the nominal shaft line losses between a dimensionless constant loss parameter a_{loss}, velocity dependent loss parameter b_{loss} and torque dependent loss parameter c_{loss}. All for normalised values of the torque $\frac{|M_{sl}(t)|}{M_{sl_{nom}}}$ and rotational speed $\frac{|\omega_{i/j}(t)|}{\omega_{sl_{nom}}}$. The nominal shaft line torque loss is derived from the nominal shaft line torque $M_{sl_{nom}}$ and efficiency η_{sl}. The values for the efficiency and loss parameters can either be fitted to manufacturer data or estimated. Finally the torque losses are calculated and applied separately to the lumped inertias on both sides of the shaft line. The losses are divided equally between both inertias (2.3.4) ,(2.3.5) and $sign[-\omega_i(t)]$ ensures that the direction of the applied friction counters the direction of rotation. In the separated velocity dependence of the torque loss on both sides of the shaft, absolute damping can be identified.

$$M_{i,sl_f}(t) = sign[-\omega_i(t)] \cdot \frac{1}{2} \cdot M_{sl_{nom}}[1-\eta_{sl}] \cdot [a_{loss} + b_{loss}\frac{|\omega_i(t)|}{\omega_{sl_{nom}}} + c_{loss}\frac{|M_{sl}(t)|}{M_{sl_{nom}}}] \tag{2.3.10}$$

$$M_{j,sl_f}(t) = sign[-\omega_j(t)] \cdot \frac{1}{2} \cdot M_{sl_{nom}}[1-\eta_{sl}] \cdot [a_{loss} + b_{loss}\frac{|\omega_j(t)|}{\omega_{sl_{nom}}} + c_{loss}\frac{|M_{sl}(t)|}{M_{sl_{nom}}}] \tag{2.3.11}$$

2.3.2.3 Shaftline Model Parameters

The parameters for the shaftline model are presented in table 2.2. The length of the shaftline l has been taken from the reference ship product sheet [35]. The shaftline radius is calculated using (2.3.12) from Lloyd's Register [45]. With configuration dependent parameters $k = 1$ for shaft's with integral couplings and $F = 95$ for engine installations with slip type clutches. P is the shaft power in kW and R is the rotational speed of the shaft in rpm these result from the propulsion system case $P = 12100\ kW$ and $R = 129\ rpm$ [14] and $\sigma_u = 560\ MPa$ for C45 steel [44]. The mass moment of inertia J_{sl} is calculated using (2.3.13) where $\rho_{sl} = 8740\ kg/m^3$ for C45 steel.

Table 2.2: Shaftline parameters.

length of the shaftline l_{sl}	$20\ m$
radius of the solid shaftline r_{sl}	$0.199\ m$
shear modulus of the shaft material G_{sl}	$8.3 \cdot 10^{10}\ Pa$
material damping coefficient $c_{i,j}$	$2.158 \cdot 10^3\ Nm \cdot s/rad$
material stiffness coefficient $k_{i,j}$	$1.022 \cdot 10^7\ Nm/rad$
shaft line mass moment of inertia $J_{i,sl}$ and $J_{j,sl}$	$215\ kg \cdot m^2$
shaft line efficiency η_{sl} at nominal torque and speed	0.99
nominal shaftline torque $M_{sl_{nom}}$	$896 \cdot 10^3\ Nm$
nominal shaftline speed $\omega_{sl_{nom}}$	$13.51\ rad/s$
shaft line constant loss parameter a_{loss}	0.1
shaft line velocity dependent loss parameter b_{loss}	0.4
shaft line torque dependent loss parameter c_{loss}	0.5

$$r_{sl} = \frac{1}{2} \cdot F \cdot k \sqrt[3]{\frac{P}{R}[\frac{560}{\sigma_u + 160}]} mm \tag{2.3.12}$$

$$J_{sl} = \frac{\pi}{2} l_{sl} \cdot \rho_{sl} \cdot r_{sl}^4 \tag{2.3.13}$$

The stiffness is derived using (2.3.14) and (2.3.15) where $G_{sl} = 83\ GPa$ for the shafting material[3]. The damping coefficient $c_{i,j}$ can be estimated using (2.3.16) [46] where $\Psi = 0.05$ is the relative power

dissipation of a hysteresis cycle and $f_{damp} = 6\ Hz$ is the approximate frequency of the hysteresis cycle. This frequency is dependent on the forced vibration of the shaft and an average value for this frequency over a number of simulations is taken as the constant value for this parameter.

$$k_{i,j} = \frac{G_{sl} \cdot J_{sl_{polar}}}{l_{sl}} \tag{2.3.14}$$

$$J_{sl_{polar}} = \frac{\pi}{2} r_{sl}^4 \tag{2.3.15}$$

$$c_{i,j} = \Psi \cdot \frac{k_{i,j}}{(2\pi)^2 \cdot f_{damp}} \tag{2.3.16}$$

$M_{sl_{nom}}$ and $\omega_{sl_{nom}}$ result from the reference propulsion system. $\eta_{sl} = 0.99$ is a common estimation for the nominal shaft line efficiency as in Geertsma, Negenborn, Visser, *et al.* [14]. a_{loss}, b_{loss} and c_{loss} are values proposed for a load following the propeller law in Godjevac, Drijver, Vries, *et al.* [33].

2.3.3 Gearbox Model

The gearbox model should representatively transmit low frequency torsional vibrations in the transmission system and is to include the friction losses. Vibrations from time varying gear meshing stiffness are of a high frequency and out of scope for the current investigation. The gears have to be modelled separately to be able to asses the occurrence of gear hammer, indicated by zero crossing force at the gear mesh. The gearbox model is split into two submodels, one describing gear mesh and the other the friction losses. The contributions of these models are combined as in (2.3.17-2.3.20) and visualised in fig.2.2.2. Where r_i, r_j and r_k are the radius's of the respective gears and the friction is applied at the main drive gear i.

$$M_{i,gb}(t) = M_{i,gb_{loss}}(t) + M_{gb}(t) \tag{2.3.17}$$

$$M_{gb}(t) = r_i \cdot F_{i,j}(t) + r_i \cdot F_{i,k}(t) \tag{2.3.18}$$

$$M_{j,gb}(t) = r_j \cdot -F_{i,j}(t) \tag{2.3.19}$$

$$M_{k,gb}(t) = r_k \cdot -F_{i,k}(t) \tag{2.3.20}$$

2.3.3.1 Gear Mesh model

The gear meshes $F_{i,j}(t)$ and $F_{i,k}(t)$ that transfer force between gears i, j, k are modelled as a parallel spring damper acting along the gear line of action. Modelled with a constant damping $c_{i,j}$, $c_{i,k}$ and stiffness coefficients $k_{i,j}$, $k_{i,k}$ as in Xu and Zhou [47]. A higher fidelity model would include the time varying mesh stiffness and transmission error such as in Wang and Zhu [48]. This step in model fidelity is deemed excessive for the evaluation of both gear hammer and the transmission of large, low frequency torque vibrations. The spring and damper displacements can be described using the small angle approximation $rtan(\theta) \approx r\theta$. The effect of point contact elasto-hydrodynamic lubrication is not taken into consideration.

$$F_{i,j}(t) = k_{i,j}[r_j\theta_j(t) - r_i\theta_i(t)] + c_{i,j}[r_j\omega_j(t) - r_i\omega_i(t)] \tag{2.3.21}$$

$$F_{i,k}(t) = k_{i,k}[r_k\theta_k(t) - r_i\theta_i(t)] + c_{i,k}[r_k\omega_k(t) - r_i\omega_i(t)] \tag{2.3.22}$$

2.3.3.2 Gearbox Friction Model

Gearbox friction $M_{i,gb_{loss}}(t)$ is modelled (2.3.23) the same as the shaftline friction as a torque loss model that is proposed in Godjevac, Drijver, Vries, *et al.* [33] and applied in Geertsma, Negenborn, Visser, *et al.* [14]. The friction torque is applied at the propeller side gear i of the gearbox.

$$M_{i,gb_{loss}}(t) = sign[-\omega_i(t)] \cdot M_{gb,loss_{nom}}[a_{gb} + b_{gb}\frac{|\omega_i(t)|}{\omega_{gb_{nom}}} + c_{gb}\frac{|M_{gb}(t)|}{M_{gb_{nom}}}] \tag{2.3.23}$$

2.3.3.3 Gearbox Model Parameters

The parameters for the gearbox model are presented in table 2.3. Gear mesh stiffness and damping parameters are determined as in Xu and Zhou [47]. Friction parameters are defined for the reference propulsion system case in Geertsma [36] and gear geometry is based on estimations.

Table 2.3: Gearbox parameters

gear ratio i	7.75
gear radius r_i	$0.944\ m$
gear radius r_j and r_k	$0.122\ m$
gear mesh damping coefficient $c_{i,j}$ and $c_{i,k}$ in $Nm \cdot s/rad$	$1.06 \cdot 10^4\ Nm \cdot s/rad$
gear mesh stiffness coefficient $k_{i,j}$ and $k_{i,k}$ in Nm/rad	$1.48 \cdot 10^8\ Nm/rad$
gear mass moment of inertia J_i, gb	$3.00 \cdot 10^3\ kg \cdot m^2$
gear mass moment of inertia $J_{j,gb}$ and $J_{k,gb}$	$0.831\ kg \cdot m^2$
nominal gearbox torque loss $M_{gb,loss_{nom}}$	$3.58 \cdot 10^4\ Nm$
nominal propeller shaft torque $M_{gb_{nom}}$	$8.96 \cdot 10^5\ Nm$
nominal propeller shaft speed $\omega_{gb_{nom}}$	$13.51\ rad/s$
dimensionless gearbox constant loss parameter a_{gb}	0.0269
dimensionless gearbox velocity dependent loss parameter b_{gb}	0.7254
dimensionless gearbox torque dependent loss parameter c_{gb}	0.2454

2.3.4 Elastic Coupling Model

Included between the engines and gearbox is an elastic coupling, used to prevent problems in regarding to misalignment and transmission of vibrations to and from the gearbox and engines. The flexible coupling is the component in the transmission system with the lowest stiffness and thus contributes significantly to the rotational dynamics. The torques $M_{i,ec}(t)$ and $M_{j,ec}(t)$ are defined by (2.3.24), (2.3.25) and connect to the lumped inertias as visualised in fig.2.4. The flexible coupling is modelled as a parallel spring damper (2.3.26) with constant stiffness $k_{i,j}$ and damping $c_{i,j}$ coefficients. Frequency dependent material characteristics are not taken into consideration.

$$M_{i,ec}(t) = M_{ec}(t) \tag{2.3.24}$$
$$M_{j,ec}(t) = -M_{ec}(t) \tag{2.3.25}$$
$$M_{ec}(t) = k_{i,j}[\theta_j(t) - \theta_i(t)] + c_{i,j}[\omega_j(t) - \omega_i(t)] \tag{2.3.26}$$

2.3.4.1 Elastic Coupling Model Parameters

The parameters for the elastic couplings are presented in table 2.4. The flexible coupling parameters have been obtained from the manufacturer data [41]. The specific types in the Vulkan 2400 series have been selected based on their torque and rotational speed capacities. The damping coefficient has been determined using the same methodology as for the shaftline.

Table 2.4: Elastic coupling parameters

	DE elastic coupling	IM elastic coupling
damping coefficient $c_{i,j}$	$2.297 \cdot 10^3\ Nm \cdot s/rad$	$2.232 \cdot 10^3\ Nm \cdot s/rad$
stiffness coefficient $k_{i,j}$	$6.40 \cdot 10^5\ Nm/rad$	$3.90 \cdot 10^5\ Nm/rad$
mass moment of inertia $J_{i,ec}$	$29.1\ kg \cdot m^2$	$7.2\ kg \cdot m^2$
mass moment of inertia $J_{j_{ec}}$	$42.9\ kg \cdot m^2$	$13.6\ kg \cdot m^2$

2.4 Clutch Modelling

In this section, the modelling of the clutch is described. First the characteristics of multi disk wet friction clutches are described in subsection 2.4.1. Then in subsection 2.4.2 the development of the clutch model is described. In subsection 2.4.3 the model parameters for the clutches are defined. Finally in subsection 2.4.4 the calibration of the clutch thermal model is described.

2.4.1 Characteristics of Multi Disk Wet Friction Clutches

In a multi disk wet friction clutch, half the plates are typically steel with a sintered bronze lining [40] and have teeth that engage with the housing. The other half of the plates, typically steel, engage with a central hub. To engage the clutch, the oil lubricated stack of plates is pressed together ,increasing the friction between the plates and resulting in a transfer of torque.

The friction torque is a function of the actuation pressure, relative rotational speed and the temperature of the oil. Due to the coupling between the fluid dynamic and mechanical regimes in wet friction, the friction model is difficult to approach analytically [49]. Maximum transmittable torque through the clutch is a function of the static coefficient of friction and the applied pressure. A multi disk friction clutch has an increased torque capacity for each additional plate due to spline friction [50], this effect is not considered significant for the engagement dynamics.

In fig.2.6 the behaviour of a typical wet friction clutch during engagement is presented. First the hydraulic cylinder fills without exerting a pressure high enough to move the friction plates, $t_f - t_e$ in fig.2.6. The plates are typically force segregated by a spring to prevent excessive friction during free rotation. At t_e in fig.2.6 the plates start being pressed together and as the pressure ramps up, the friction torque increases correspondingly. The friction torque reduces the relative velocity of the two sides of the clutch eventually, leading to the state of synchronisation, or lockup, indicated by t_L in fig.2.6. At this point the two sides of the clutch are coupled and the pressure keeps building to increase the maximum transferable torque through the clutch.

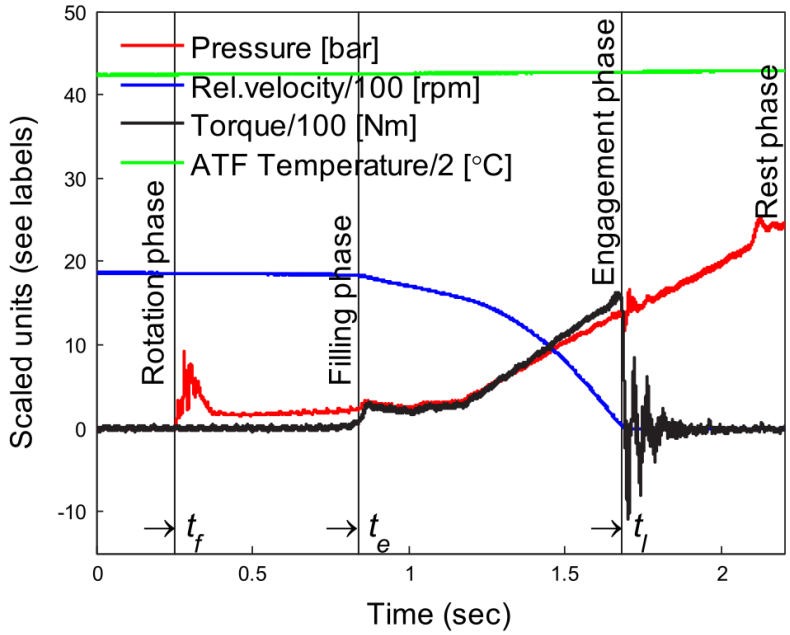

Figure 2.6: Typical wet friction clutch engagement. *Source [51]*

2.4.1.1 Characteristics of Wet Friction

Torque transfer in wet friction clutches during the engagement process can be divided into three phases [52], were separate lubrication regimes can be identified [44]:

- Hydrodynamic Lubrication, shear stresses in the thin film transfer the torque.
- Mixed Lubrication, film shear and contact torque transfer.
- Boundary Lubrication, mechanical contact dominated torque transfer.

The lubricating and cooling oil between the the friction disks results in a strong dependence of the instantaneous coefficient of friction on the relative velocity of the disks. The nonlinear effect due to friction dependence on oil viscosity, pressure and relative velocity is called the stribeck behaviour and is visualised in fig. 2.7. Initially the hydrodynamic friction dominates the torque transfer resulting in a relatively high coefficient of friction. The coefficient of friction drops as the film thickness reduces in the mixed lubrication phase. As the relative velocity approaches zero, the coefficient of frictions decreases rapidly, resulting form the fact that the static coefficient of friction is typically lower than the boundary lubrication coefficient of friction.

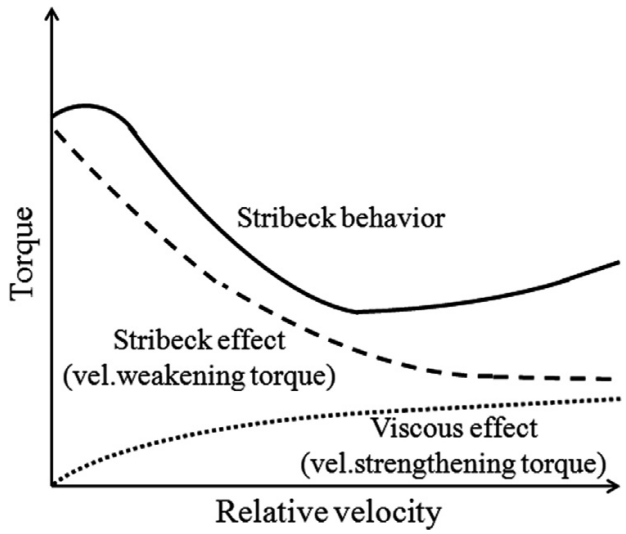

Figure 2.7: Schematic of the Stribeck behaviour. *Source [51]*

Lin, Tan, He, *et al.* [53] Analyses the friction plate temperature for multi plate wet friction clutches in maritime gearboxes. The biggest contribution to peak plate temperature is the selected engagement pressure curve. For the friction model, a constant sliding friction coefficient and uniformly distributed plate pressure are assumed. The experiment includes a full scale test using a multi plate wet friction clutch and dummy loads.

Davis, Sadeghi, and Krousgrill [52] Simulates thermal effects in wet clutch engagement by extending an isothermal wet clutch engagement model. The experimental results indicate that including fluid thermal effects is critical in predicting wet clutch engagement. As the oil heats up during the clutch engagement, the effective coefficient of friction drops drastically as a result of a reduced oil viscosity.

It is concluded that the critical dependencies of wet friction in the engagement of wet friction clutches are: the applied pressure on the disks, the relative velocity of the clutch halves and the temperature of the oil between the friction interfaces.

2.4.2 Clutch Model

It is the function of the clutches in the hybrid propulsion system model to select and combine main drive engines to enable dynamic switching between operational modes. If the clutch is locked, the relative velocities of the clutch halves should be zero and the system should behave as if rigidly coupled. When the

clutch is open, both halves of the clutch must be able to rotate independently. The engagement procedure should reflect the energy losses and conservation of momentum. A thermal model should be implemented to identify the operation of the clutch relative to its operational limits. In Deleroi [17] a strong dependence on the initial torque gradient on the impact of clutch engagement is identified. The literature on multi plate wet friction shows that this initial torque gradient is a result of the hydrodynamic torque transfer in wet friction and is strongly dependent on the oil temperature and relative rotational speed at engagement. These dependencies are therefore to be taken into account in the clutch model.

The model of the clutch is divided in three submodels that each cover part of the requirements. The state model defines the behaviour of the clutch in the open and closed condition, the wet friction model describes the friction between the clutch plates and the thermal model describes the temperature of the clutch plates. These submodels are further described in the sub-subsections 2.4.2.1-2.4.2.3.

In fig.2.8 the variables connecting the clutch submodel with the propulsion system are visualised. Where $M_{i,x}(t)$ is the torque of a subsystem x connected on the left of lumped inertia J_i and $M_{j,y}(t)$ is the torque of a subsystem y connected on the right of lumped inertia J_j. Resulting from the rotational dynamics ω_i and ω_j are the rotational speeds of the lumped inertias. The clutch model defines torque $M_{cl}(t)$ that is applied to both connected inertias, but with a reversed sign.

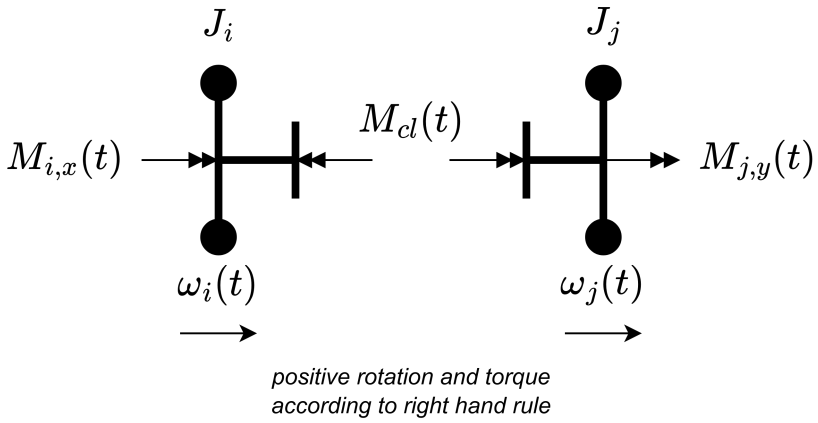

Figure 2.8: Schematic of the clutch variables in the context of the connected lumped inertias J_i and J_j.

2.4.2.1 Clutch State Submodel

When clutches are actuated in a system, then at a certain time instant denoted as lockup-time, a state change occurs as the system changes from a decoupled to a coupled state as the slip approaches zero. There are multiple approaches to this problem: a change in model structure can be made [17] where a switch is made from two to one differential equations for the rotational dynamics at lock-up, secondly the friction law can be replaced by a stiffness at lock-up [51] to investigate post lock-up torsional vibrations, finally the change can be achieved by switching the definition of the clutch torque at lock-up to ensure that the relative rotational velocity remains constant [18].

Switching the definition of the clutch torque $M_{cl}(t)$ in fig.2.8, at lock-up is selected for the clutch state model. The transition from the locked state to the slipping state is defined in fig.2.9. In the slipping state the torque through the clutch $M_{cl}(t)$ is defined by the friction torque $M_f(t)$ that acts opposite to the direction of the relative velocity $sign(\omega_r(t))$. The magnitude of the friction is determined by the wet friction submodel. In the locked state, the torque through the clutch is as defined in 2.4.6. The state transitions from slipping to locked when the holding torque exceeds or equals the torque to be transmitted $|M_{lock}(t)| \leq M_f(t)$ and the relative velocity is zero $\omega_r(t) = 0$. The state transitions from locked to slipping when the torque to keep both sides synchronised exceeds the holding torque $|M_{lock}(t)| > M_f(t)$.

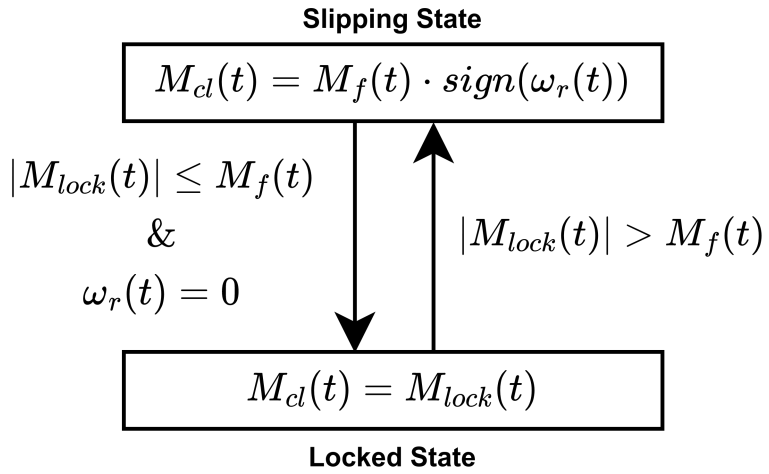

Figure 2.9: Clutch state definitions and transition conditions.

In the locked state the torque through the clutch is defined by (2.4.6) to keep both inertias synchronised. This results from considering the governing equations for the two inertias to be coupled, (2.4.2) and (2.4.3), visualised in fig.2.8. In the locked condition both inertias should behave as if rigidly coupled, this means that the relative velocity (2.4.1) should be constant. This condition leads to both inertias having to experience the same acceleration (2.4.5). Substituting (2.4.2), (2.4.3) and (2.4.4) into (2.4.5) and rearranging the terms results in (2.4.6) which defines the clutch torque in the locked state.

$$\omega_r(t) = \omega_j(t) - \omega_i(t) \tag{2.4.1}$$
$$J_i\dot{\omega}_i(t) = M_{i,x}(t) + M_{cl}(t) \tag{2.4.2}$$
$$J_j\dot{\omega}_i(t) = M_{j,y}(t) - M_{cl}(t) \tag{2.4.3}$$
$$M_{cl}(t) = M_{lock}(t) \tag{2.4.4}$$
$$\omega_r(t) = constant \rightarrow \dot{\omega}_r(t) = 0 \rightarrow \dot{\omega}_i(t) = \dot{\omega}_j(t) \tag{2.4.5}$$
$$M_{lock}(t) = \frac{J_i M_{j,y}(t) - J_j M_{i,x}(t)}{J_i + J_j} \tag{2.4.6}$$

2.4.2.2 Wet Friction Submodel

The friction in the clutch is assumed to only be a result of the friction between the plates. For detailed design analysis, the friction of the disk splines with the housing and hub should be considered to better asses the holding torque of the clutch [50]. The friction in the clutch can be described by the stribeck curve from fig.2.7. This curve can be divided in three parts: the initial stage where the torque transfer is dominated by hydrodynamic shear forces, the middle part where the friction torque is a mix of the contact friction and hydrodynamic shear, and finally the phase where contact torque dominates the friction. To approximate the stribeck behaviour, the load sharing approach is selected such as applied in Davis, Sadeghi, and Krousgrill [52]. The load sharing approach (2.4.7) entails that the friction is split in a hydrodynamic part $M_{visc}(t)$ and contact friction part $M_{cont}(t)$. The friction is a function of the pressure on the disk stack $P(t)$, when there is no pressure applied the friction is considered zero (2.4.8).

$$P(t) > 0 \rightarrow M_f(t) = M_{cont}(t) + M_{visc}(t) \tag{2.4.7}$$
$$P(t) = 0 \rightarrow M_f(t) = 0 \tag{2.4.8}$$

Regarding the clutch geometry, the effective torque radius of the friction at the interface r_e is described by (2.4.9) assuming a constant pressure distribution between the disks, where r_o and r_i are the outside and inside radius of the friction disks. The area of a friction interface A_{fi} is defined by (2.4.10).

$$r_e = \frac{2}{3}\frac{r_o^3 - r_i^3}{r_o^2 - r_i^2} \tag{2.4.9}$$

$$A_{fi} = \pi[r_o^2 - r_i^2] \tag{2.4.10}$$

The contact friction is simplified to a constant friction coefficient μ as in [53]. The resulting friction torque $M_{cont}(t)$ is a function (2.4.11) of applied pressure $P(t)$, the number of friction interfaces N, the effective torque radius r_e and the area of a friction interface A_{fi}.

An alternative approach would be to use experimental data obtained from clutch engagements or a pin on disk test [54] to fit a curve describing the contact friction as a function of $\omega_r(t)$ [51]. However, the hydrodynamic friction part of the load sharing concept makes sure the overall friction behaviour during the engagement represents the stribeck behaviour. The dependence of the friction coefficient μ on the relative velocity is thus covered by this approach. Therefore the contact friction can be modelled using a constant coefficient of friction.

$$M_{cont}(t) = N \cdot \mu \cdot r_e \cdot A_{fi} \cdot P(t) \tag{2.4.11}$$

The hydrodynamic shear torque $M_{visc}(t)$ is modelled [51] as a function (2.4.12) of the relative velocity $\omega_r(t)$, the number of friction interfaces N, the effective torque radius r_e, the area of a friction interface A_{fi}, oil film viscosity $\eta(t)$ and thickness $h(t)$. The equation for hydrodynamic shear (2.4.12) is based on Newton's law of viscosity assuming laminar flow between parallel plates [55]. The film thickness $h(t)$ is assumed to be dependent on the applied pressure $P(t)$ and rapidly decreases from the initial thickness h_0 to the final thickness h_c corresponding with asperity contact governed by (2.4.13). Film thickness h_t can be assumed independent of temperature, as the temperature development in the oil film results in a reduced viscosity that overwhelms the effect of decreasing film thickness due to temperature [52]. The oil viscosity $\eta(t)$ is dependent (2.4.14) on the temperature $T_{oil}(t)$, dynamic viscosity shape function parameter κ and the base viscosity η_0.

$$M_{visc}(t) = \frac{N \cdot \eta(t) \cdot A_{fi} \cdot r_e^2}{h(t)} \cdot |\omega_r| \tag{2.4.12}$$

$$h(t) = \frac{h_0}{P(t) + 1} + h_c \tag{2.4.13}$$

$$\eta(t) = \eta_0 \cdot e^{-\kappa T_{oil}(t)} \tag{2.4.14}$$

2.4.2.3 Clutch Thermal model

Heat $\dot{Q}_f(t)$ generated in the clutch results (2.4.15) from the relative sliding velocity $\omega_r(t)$ and friction force $M_f(t)$ [53]. It can be assumed that all the heat is absorbed by the friction plates as the oil film is thin, also the temperature of the oil at the friction interface can be assumed equal to the temperature of the friction plate surface [52]. The friction interface is modelled as a homogeneous thermal mass m_{fi} of which the temperature is determined by (2.4.16). T_{oil_0} is the initial oil temperature in the clutch, c_{fi} is the specific heat of the thermal mass. The thermal mass m_{fi} is described by (2.4.17) where N is the number of friction interfaces, A_{fi} is the area of a friction interface, d_{fi} is the thickness and finally ρ_{fi} the density.

The next step in fidelity for the thermal model would be the implementation of a thermal finite element (FE) model as in [53], [52], [56]. FE thermal models require detailed information on the clutch geometry and material and are computationally expensive. The lumped thermal mass thickness d_{fi} is correspondingly calibrated using the thermal FE results in Lin, Tan, He, *et al.* [53]. This is described in subsection 2.4.4.

$$\dot{Q}_f(t) = |\omega_r(t)| \cdot M_f(t) \tag{2.4.15}$$

$$T_{fi}(t) = T_{oil}(t) = \frac{Q_f(t)}{m_{fi} \cdot c_{fi}} + T_{oil_0} \tag{2.4.16}$$

$$m_{fi} = N \cdot A_{fi} \cdot d_{fi} \cdot \rho_{fi} \tag{2.4.17}$$

2.4.3 Clutch Model Parameters

There are two clutches in the propulsion system. First the shared parameters in table 2.5 will be discussed followed by a specification of the parameters specific to the diesel engine and induction machine clutches.

The engagement pressure map in fig.2.10 defines $P(t)$. The pressure map is adapted from profiles in Lin, Tan, He, *et al.* [53] and Deleroi [17] and matches the two stage engagement approach that is cited by manufacturers of marine clutches [57], [58]. The peak pressure is taken from the specification of the clutches [40] that serve as a reference.

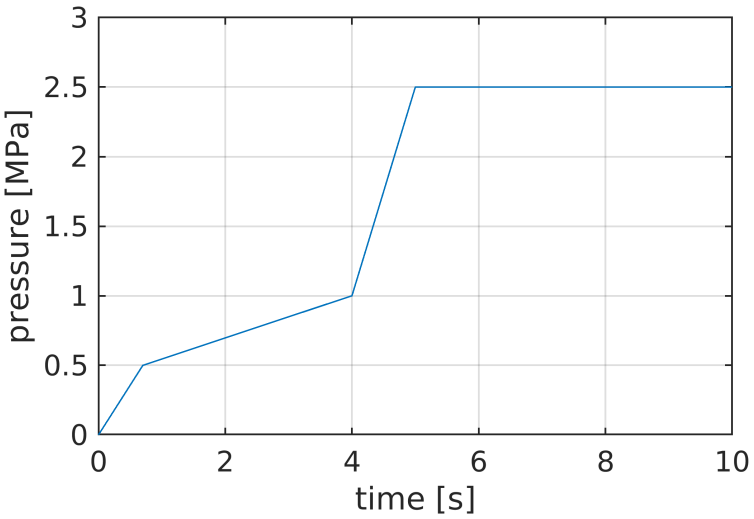

Figure 2.10: Clutch actuation pressure curve $P(t)$

The coefficient of friction μ has been selected in the centre of the typically cited range for oil lubricated steel on sintered bronze contact [44], [53]. The contact oil film thickness is selected to be equal to the surface roughness of the clutch plates for sintered bronze, that also coincides with the cited values in Davis, Sadeghi, and Krousgrill [52]. The initial film thickness is estimated at $2\ mm$. Oil viscosity parameters are taken for the oil [59] as also used in Iqbal, Al-Bender, Ompusunggu, *et al.* [51]. The initial oil temperature is set at $50\ ^{\circ}C$ corresponding with typical gearbox operating temperatures. The specific heat and density of the thermal mass are mean values for steel and the thickness of the lumped thermal mass has been obtained from the calibration of the thermal model as discussed in subsection 2.4.4.

Table 2.5: Parameter shared by both the diesel engine and induction machine clutches

coefficient of friction μ	0.10
contact oil film thickness at the friction interface h_c	$6 \cdot 10^{-6}\ m$
initial oil film thickness at the friction interface h_0	$2.0 \cdot 10^{-3}\ m$
base viscosity η_0	$0.0703\ Pa \cdot s$
dynamic viscosity shape function parameter κ	0.0203
initial oil temperature T_{oil_0}	$50\ ^{\circ}C$
specific heat of the thermal mass c_{fi}	$450\ J/kg \cdot K$
thickness of the lumped thermal mass d_{fi}	$0.020\ m$
density of the thermal mass material ρ_{fi}	$8000\ kg/m^3$

For the diesel engine clutch the size 80 Ortlinghaus 202 clutch is selected [40]. The geometric parameters are derived from the product sheet and presented in tab.2.6. Using (2.4.11) and inserting the $2.5\ MPa$ operating pressure along with the clutch specific geometric parameters, the holding torque of the selected clutch can be determined. As the relative velocity is zero in the locked condition only the contact friction

has to be considered. The holding torque is calculated to be $103.5\ kNm$ which translates to a margin of 19% relative to the $86.9\ kNm$ nominal diesel engine torque at $1000\ rpm$.

Table 2.6: Parameters for the DE clutch

mass moment of inertia $J_{i,cl}$ and J_{j_cl}	$15\ kg \cdot m^2$
outer radius of the clutch disks r_o	$0.232\ m$
inner radius of the clutch disks r_i	$0.162\ m$
number of friction interfaces N	24

Table 2.7: Parameters for the IM clutch

mass moment of inertia $J_{i,cl}$ and J_{j_cl}	$9\ kg \cdot m^2$
outer radius of the clutch disks r_o	$0.206\ m$
inner radius of the clutch disks r_i	$0.144\ m$
number of friction interfaces N	20

For the induction machine clutch the size 78 Ortlinghaus 202 clutch is selected [40]. The geometric parameters are derived from the product sheet and presented in table 2.7. Similar as for the diesel engine clutch the holding torque can be calculated at the operating pressure and is found to be $60.3\ kNm$ which translates to a margin of 26% relative to the $47.7\ kNm$ nominal induction machine torque at $600\ rpm$.

2.4.4 Clutch Thermal Model Calibration

The Clutch Thermal model is calibrated against a thermal FE of a clutch plate in and can thus be used to evaluate the operation of the clutch relative to its thermal limits. The oil temperature is limited by the temperature at which the oil starts burning. The flame temperature is $200℃$ for the considered oil [59].

The thermal model for the clutch has been calibrated using the data from maritime clutch engagement thermal characteristics validated against test bench experiments in Lin, Tan, He, *et al.* [53]. The studied clutch in Lin, Tan, He, *et al.* [53] has similar parameters to the clutches used in this thesis. A Simulink framework has been set up where the propeller and diesel engine torque-speed characteristic as used in Lin, Tan, He, *et al.* [53] are implemented. As [53] uses a similar friction model for the contact friction, the parameters can be applied directly. The driving and driven torque are used to match the thermal input to the clutch plates. The difference being that in Lin, Tan, He, *et al.* [53] this flux is fed into a thermal FE model and in this thesis it is fed into a lumped thermal mass model.

The lumped thermal mass model has been calibrated by selecting the value for the effective friction interface depth d_{fi}. The value for d_{fi} is fitted to match the surface temperature for the 400 rpm engagement and found to be $d_{fi} = 0.020\ m$. The found value for the effective depth of the thermal model is of the same order as the thickness of the clutch plates, which is considered a realistic outcome. Having determined that the found value for the calibrated model is realistic, the thermal calibration is further validated using the data for a range of engagement revolving speeds from Lin, Tan, He, *et al.* [53]. Table 2.8 presents the result of this process and confirms that the calibrated thermal model closely matches the lumped thermal model over the range of the experiments.

Engagement revolving speed	300 rpm	350 rpm	400 rpm	450 rpm
Surface Temperature from FEA [53]	67.3 °C	78 °C	92.5 °C	106.0 °C
Calibrated Lumped Thermal Model ($d_{fi} = 0.020\ m$)	70.5 °C	80.3 °C	92.7 °C	105.9 °C

Table 2.8: Validation of the calibrated lumped thermal model

As the geometric parameters for the clutches used in this thesis closely match the values in [53] ($r_o = 0.245$ and $r_i = 0.165$ in [53], $r_o = [0.232\ 0.206]$ and $r_i = [0.162\ 0.144]$ in this thesis) it is concluded that the $d_{fi} = 0.020\ m$ value can be applied to the clutches in this thesis and result in a realistic representation of the clutch surface temperature.

2.5 Drivers & Control Modelling

In this section, the models for the drivers and propulsion control are described. In subsection 2.5.1 the model for the diesel engine and governor is described. In subsection 2.5.2 the model for the induction machine and drive is described. Finally in subsection 2.5.3 the propulsion control model is discussed.

2.5.1 Diesel Engine & Governor Model

The model for the diesel engine and governor dynamics is provided by dr.ir. R.D.Geertsma and further described in Geertsma [36]. The mean value first principle model describes the dynamic performance and includes the thermal loading of the engine. The thermal loading is described by the air excess ratio, turbocharger entry temperature and exhaust valve temperature. Fig.2.11 provides an overview of the diesel engine model structure. The diesel engine fuel pump is controlled by the governor. The governor contains a PI speed controller with an anti windup loop, also charge air inlet pressure and speed dependent fuel limiters are implemented. Parameters for the diesel engine, PI controller and fuel limiters are obtained from the reference for the hybrid propulsion system (table 3.3, 3.4, 5.1 and 5.2 in Geertsma [36]). The parameters for a 20 cylinder four stroke diesel engine are selected. The engine operates at a nominal power of 9.1 MW at 16.7 rev/s (1000 rpm).

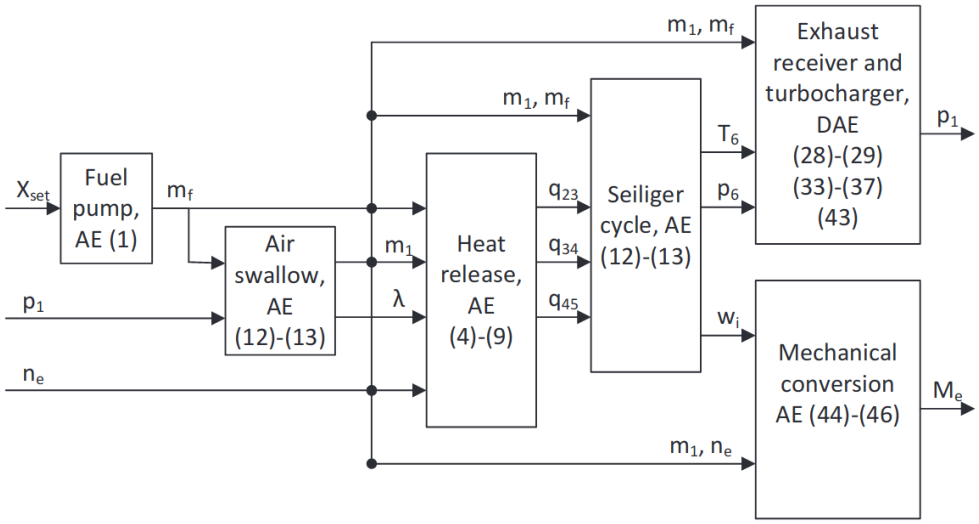

Figure 2.11: Schematic presentation of the diesel engine model and the interaction between its subsystems, consisting of Algebraic Equations (AE) or Differential and Algebraic Equations (DAE). *Source: [60]*

2.5.2 Induction Machine & Drive Model

The induction machine and drive models are part of the v-ZEL and are provided by dr.ir. U.Shipurkar from MARIN. The model captures the dynamics of the electric machine using standard dynamic models [61], where non-linear effects are not included. The dynamic model of the induction machine is implemented in the dq-reference frame, based on the inverse-y equivalent circuit and ignores transient reactances and saturation effects. Induction machine parameters are obtained from the reference for the hybrid propulsion system (table 5.3 in Geertsma [36]). The electric motor/generator (MG) is a 10 pole at 3.15 kV with synchronous speed of 600 rpm and a nominal power of 3 MW.

The electric machine is driven using direct torque control with an outer speed control loop. The torque PI control loop parameters are determined using Internal Mode Control [62]. The outer speed PI control loop is tuned using the symmetric optimum criteria [63] considering the entire propulsion system inertia as a rigidly coupled system. From the propulsion controller the control approach can be selected to either be speed or torque control. The tuned response of the electric machine results in a strict implementation of the control goal of matching the shaft speed set point. This approach can be considered a worst case scenario

in terms of torque loads on the propulsion system components, the effect of this has to be evaluated in the simulation experiments. Selecting the optimal control objective is considered out of scope for this thesis.

2.5.3 Propulsion Control Model

For the control architecture two control levels are defined. The primary control level containing the torque and speed control loops of the engines and the clutch activation. The primary control level is integrated in the diesel and electric motor models that have already been discussed. The second control level is implemented in the propulsion controller that regulates the propulsion modes and mode transitions and feeds control set points and control modes to the primary control level. The propulsion controller functions by selecting a state for the propulsion control outputs based on the propulsion mode setpoint P_{mode} in fig.2.4. These states are further described in the following sub-subsections regarding propulsion modes and propulsion mode transitions.

2.5.3.1 Propulsion Modes

The electric and diesel propulsion modes are considered within the scope of this research. The control signals are defined in fig.2.4. For these propulsion modes the following propulsion controller states are defined:

Diesel Propulsion Mode

- Diesel engine clutch closed $Act_{Cl,de} = 1$
- Induction machine clutch open $Act_{Cl,im} = 0$
- Diesel engine speed setpoint matches system setpoint $\omega_{set,de} = \omega_{set}$
- Induction machine in torque control mode $C_{mode} = 2$
- Induction machine torque setpoint at zero $M_{set,im} = 0Nm$

Electric Propulsion Mode

- Diesel engine clutch open $Act_{Cl,de} = 0$
- Induction machine clutch closed $Act_{Cl,im} = 1$
- Diesel engine speed setpoint to stationary $\omega_{set,de} = \frac{400*2*\pi}{60} rad/s$
- Induction machine in speed control mode $C_{mode} = 1$
- Induction machine speed setpoint matches system setpoint $\omega_{set,im} = \omega_{set}$

2.5.3.2 Propulsion Mode Transition Control

In the scientific literature no standard control approach for propulsion mode transitions has been identified. Therefore, three transition approaches with an increasing degree of sophistication have been implemented:

Instant Approach
In the instant approach clutches are engaged and disengaged at the same point in time. No transition control is applied in this case and the propulsion mode state is instantly set from either diesel to electric or electric to diesel. This represents the most rudimentary way to approach a mode transition and serves as a baseline.

Staged Approach
In the staged approach the clutch for the new propulsion modes engine is first engaged, followed a number of seconds later by the disengagement of the clutch for the preceding propulsion mode. As a result there is effectively an overlap of the two propulsion modes where parallel speed control is active. It is the aim of this approach to asses the suitability of parallel speed control for handover of the drive torque between the drive engines during a mode transition. To enable this transition approach a separate state is defined as

an intermediate step between the two propulsion modes. The duration of the intermediate step is based on the time it takes for the clutches to apply full pressure and thus transmit the maximum drive torque, the duration of the transition is thus $5\ s$ for the applied pressure curve in fig.2.10. This intermediate state is defined by:

- Diesel engine clutch closed $Act_{Cl,de} = 1$
- Induction machine clutch closed $Act_{Cl,im} = 1$
- Diesel engine speed setpoint matches system setpoint $\omega_{set,de} = \omega_{set}$
- Induction machine in speed control mode $C_{mode} = 1$
- Induction machine speed setpoint matches system setpoint $\omega_{set,im} = \omega_{set}$

Torque Controlled Approach

For the torque controlled approach, in addition to an overlap in clutch engagement and disengagement, the torque control mode for the induction machine is used to ramp up or down the drive torque. It is the aim of this approach to force a handover of drive torque between the drive engines during a mode transition. To enable this transition approach, a separate state is defined as an intermediate step between the two propulsion modes for both directions of the transition. The duration of the intermediate step is based on the time it takes for the clutches to apply full pressure and thus transmit the maximum drive torque, the duration of the transition is thus $5\ s$ for the applied pressure curve in fig.2.10. The intermediate state for the diesel to electric propulsion transition is defined by:

- Diesel engine clutch closed $Act_{Cl,de} = 1$
- Induction machine clutch closed $Act_{Cl,im} = 1$
- Diesel engine speed setpoint matches system setpoint $\omega_{set,de} = \omega_{set}$
- Induction machine in torque control mode $C_{mode} = 2$
- Induction machine torque ramps up over the duration of this intermediate state from zero to the reference torque level M_{de} that is set at the moment the transition is initiated.

And the intermediate state for the electric to diesel propulsion transition is defined by:

- Diesel engine clutch closed $Act_{Cl,de} = 1$
- Induction machine clutch closed $Act_{Cl,im} = 1$
- Diesel engine speed setpoint matches system setpoint $\omega_{set,de} = \omega_{set}$
- Induction machine in torque control mode $C_{mode} = 2$
- Induction machine torque ramps down over the duration of this intermediate state to 0 from the reference torque level M_{im} that is set at the moment the transition is initiated.

2.6 Propulsion Modelling

In this section, the models for the ship propulsion are described. The model for the hull is described in subsection 2.6.1. The wave model is described in subsection 2.6.2 and finally the propeller model is described in subsection 2.6.3.

2.6.1 Hull Model

The torque of the propeller is dependent on the velocity of the ship. Therefore the relation between delivered power to the hull and speed has to be modelled. The hull model converts the thrust $T(t)$ generated by the propeller model into 1-D surge motion and thus ship speed $v_s(t)$. The model is adapted from [3]. As can be identified in the conceptual mode in fig.2.4 the hull model is also dependent on the state of the sea. Regarding the ship dynamics (2.6.1) the differential equation for the ship speed is a function of: the hull resistance $R_{hull}(t)$, thrust deduction factor t_{ded} and the displacement of the hull Δ_s.

$$\dot{v}_s(t) = \frac{T(t) - \frac{R_{hull}(t)}{1-t_{ded}}}{\Delta_s} \tag{2.6.1}$$

$$R_{hull}(t) = c_1 \cdot v_s^2 \tag{2.6.2}$$

$$c_1 = y \cdot c_0 \tag{2.6.3}$$

$$y = SM = y_1(fouling) \cdot y_2(hull) \cdot [\frac{\Delta_s}{\Delta_{nom}}]^{2/3} \cdot y_3(seastate) \cdot y_4(waterdepth) \tag{2.6.4}$$

The resistance largely determines the load on the propulsion system and this towing resistance of displacement type hulls is mainly dependent on the ship speed $v_s(t)$ and described by (2.6.2). The resistance factor c_1 is a function of the sea margin y and the nominal resistance factor c_0 which is considered constant (2.6.3). The sea margin y is a further function (2.6.4) of multiplying factors for fouling y_1, the hull shape y_2, the displacement $[\frac{\Delta_s}{\Delta_{nom}}]^{2/3}$, the state of the sea y_3 and the depth of the water y_4. The fouling resistance is constant over a large time horizon, it is therefore less relevant for transient analysis. The same is true for displacement and water depth. They do alter the resistance curve of the ship and are therefore relevant as baseline load cases for transient studies. The effect of sea state on ship resistance can also be regarded as constant over the duration of transient behaviour.

2.6.1.1 Hull Model Parameters

Regarding the hull resistance of the ship, an estimation has to be made as the actual towing data for the ship are unavailable. Specific resistance C_E is based on reference values for a $45500\ DWT$ Container Ship($C_E = 9 \cdot 9.5^{-3}$) and a $3750\ DWT$ Container Feeder($C_E = 14 \cdot 10^{-3}$) [3] and estimated at $C_E = 10 \cdot 10^{-3}$. Using (2.6.5) [3] C_E is transformed to the nominal resistance factor c_0 with $\rho_{sw} = 1.025 \cdot 10^3\ kg/m^3$ and $y_{nom} = 1$.

$$c_0 = \frac{c_E \cdot \rho_{sw}^{1/3} \cdot \Delta_{nom}^{2/3}}{y_{nom}} \tag{2.6.5}$$

Thrust deduction coefficient t_{ded} is based on reference data for a single shaft ship with similar power, DWT and design speed as the reference case from [3]. Nominal displacement Δ_{nom} is obtained from[35]. The displacement when loaded is estimated assuming a relatively light $5 \cdot 10^3\ kg$ load per TEU for the entire 1740 TEU [35] resulting in an additional $8700 \cdot 10^3\ kg$ displacement.

Table 2.9: Hull model parameters

thrust deduction coefficient t_{ded}	0.12
nominal resistance factor c_0	$6.71 \cdot 10^3\ kg/m$
fouling dependent multiplying factor y_1	1.06
hull form dependent multiplying factor y_2	1
loaded displacement Δ_s	$27250 \cdot 10^3\ kg$
nominal displacement Δ_{nom}	$18550 \cdot 10^3\ kg$
sea state dependent multiplying factor y_3	1.0 (state 0), 1.1 (state 3), 1.36 (state 5)
water depth dependent multiplying factor y_4	1.0 (deep water)

The fouling dependent factor is defined for a number of years of fouling $y_1 = 1.06$ [3] and remains constant over the course of the experiments. $y_2 = 1$ remains constant as it is combined with the displacement term that governs the hull shape multiplier. y_3 and y_4 vary between experiments and are dependent on the state of the sea. Values for sea state 0, 3 and 8 have been obtained from [3] and are interpolated for sea state 5. The initial speed of the ship v_0 varies between the experiment and lays between zero and the maximum ship speed.

2.6.2 Wave Model

The environmental disturbance is described by the sea state, having a constant influence on the hull resistance and having a dynamic effect on the wake of the propeller $v_w(t)$. The wave model is adapted from [36] and simplified to a constant wave frequency ω_{wave}. The wave model (2.6.6) is further dependent on the wave amplitude ζ, the depth of the propeller centre z and the wave number k (2.6.7).

$$v_w(t) = \zeta \cdot \omega_{wave} \cdot e^{k \cdot z} \cdot sin[\omega_{wave} \cdot t] \tag{2.6.6}$$

$$k = \frac{\omega_{wave}^2}{9.81} \tag{2.6.7}$$

2.6.2.1 Wave Model Parameters

Wave amplitudes for the considered sea states are obtained from UK Met Office [64]. The propeller depth is taken from the reference ship [35] and considered constant. The wave radial frequency is considered constant over the range of sea state and obtained from Moskowitz [65].

Table 2.10: Wave model parameters

wave amplitude ζ	$0\ m$ (state 0), $0.3\ m$ (state 3), $1.5\ m$ (state 5)
wave radial frequency ω_{wave}	$0.63\ rad/s$
depth of the propeller centre z	$8\ m$

2.6.3 Propeller Model

The propeller converts torque to thrust and is modelled for operation in the first quadrant as described in Woud and Stapersma [3]. Governing equations (2.6.8 - 2.6.12) describe the thrust torque relation of the propeller using the advance ratio $J(t)$ that is dependent on ship speed $v_s(t)$, wave disturbance $v_w(t)$, propeller speed n_p and the propeller diameter D. The thrust-torque relation is described using the typical $K_T(J(t))$, $K_Q(J(t))$ open water diagrams that are generated for the selected propeller using the polynomials in Oosterveld and Oossanen [66]. Further parameters are the relative rotative efficiency η_r, the wake factor w, and the density of seawater ρ_{sw}.

$$T(t) = K_T(J(t)) \cdot \rho_{sw} \cdot n_p^2(t) \cdot D_p^4 \tag{2.6.8}$$
$$Q(t) = K_Q(J(t)) \cdot \rho_{sw} \cdot n_p^2(t) \cdot D_p^5 \tag{2.6.9}$$
$$M_p(t) = \frac{-Q(t)}{\eta_R} \tag{2.6.10}$$
$$J(t) = \frac{v_a(t)}{n_p(t) \cdot D_p} \tag{2.6.11}$$
$$v_a(t) = v_s(t)[1 - w] + v_w(t) \tag{2.6.12}$$

2.6.3.1 Propeller Model Parameters

The propeller has been matched in accordance with the procedure described in Woud and Stapersma [3]. The propeller is matched at 15 knots using 85% of the available diesel engine power, following the developments in slow steaming and using the typical engine margin for merchant vessels [3]. The Wageningen B5-75 propeller with a P/D ratio of 0.7 has been selected from the matching procedure in fig.2.12. For the matching of the propeller, the design condition has been defined as: moderate fouling, sea state 3, deep water, loaded. The propeller diagram is generated using the polynomials from Oosterveld and Oossanen [66]. The moment of inertia of the propeller is determined from the geometry and multiplied by 1.25 to account for the entrained water [67]. The wake factor and relative rotative efficiency have been taken from a similar ship case in Woud and Stapersma [3].

Table 2.11: Parameters for the propeller model

density of sea water ρ_{sw}	$1025\ kg/m^3$
diameter of the propeller D_p	$5.8\ m$
relative rotative efficiency η_R	1
wake factor w	0.20
propeller mass moment of inertia J_{prop}	$2.20 \cdot 10^4\ kg \cdot m^2$

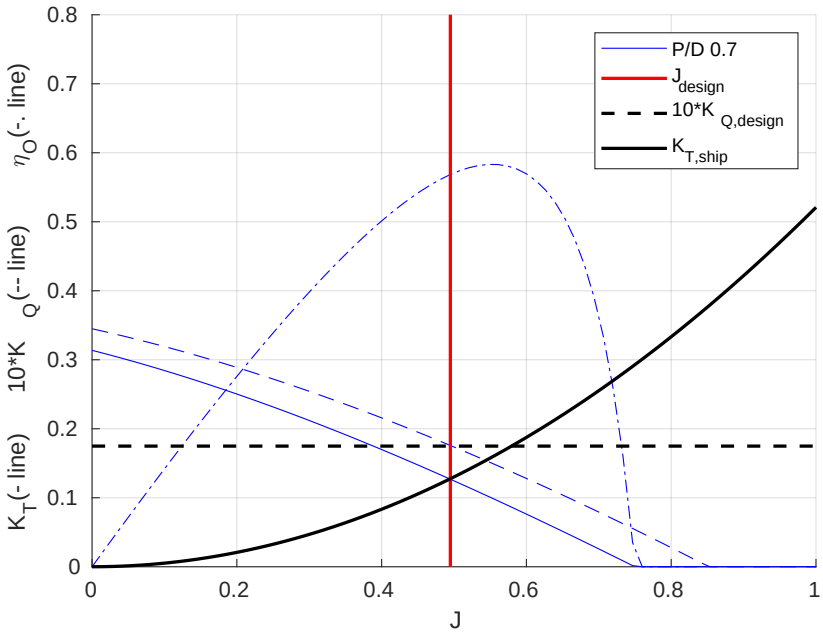

Figure 2.12: Matching diagram for the selected wageningen B5-75 propeller.

2.7 Implementation & Validation

The mathematical model has been established and the parameters selected. The implementation and verification of the system model is discussed in subsection 2.7.1. The validity of the system model is discussed in subsection 2.7.2.

2.7.1 Implementation

The system model has been implemented in Matlab Simulink, where first a model library containing all the implemented submodels has been setup. The submodels are then connected according to the system structure and coupling in the conceptual model fig.2.4. The Simulink implementation of the diesel engine and governor used in Geertsma, Negenborn, Visser, *et al.* [14] has been made available by dr.ir. R.D.Geertsma. The induction machine and drive has been implemented and provided by dr.ir. U.Shipurkar from MARIN as part of the v-ZEL model library. For the simulations in this thesis a computer with an Intel i7-12700K CPU coupled with 32 GB of GDDR4 RAM has been used.

2.7.1.1 Solver and Step size

As the system contains a multitude of high stiffness components, with the gear mesh stiffness being the highest, the stiff version of ode23 is selected. A number of test simulations have been executed where the parameters for the variable step ode23 solver have been varied to asses the numerical stability. As a result of the test simulations the following solver settings are selected:

- Minimum step size: $1 \cdot 10^{-7}\ s$
- Maximum step size: $1 \cdot 10^{-3}\ s$
- Relative tolerance: $1 \cdot 10^{-3}$
- Adaptive Zero-crossing control algorithm

The main criteria in this process has been observing how well the sinusoidal waveform of the vibrations are resolved in the output, where smooth sinusoidal signals indicate a sufficiently small step size. Using these solver settings a 30 s model simulation can be executed in 5-15 min.

2.7.1.2 Mesh Stiffness

As the analytical gear mesh stiffness is multiple orders of magnitude higher than the next stiffest component, this stiffness forces a small time step leading to excessive simulation times. As the mesh stiffness is used to study the occurrence of gear hammer, where the mesh force crosses zero, the choice has been made to reduce the mesh stiffness to be one order of magnitude higher that the next stiffest component (the shaftline). This approach enables investigating the occurrence of gear hammer but limits the quantitative conclusions that can be drawn on the severity of the gear hammer which is deemed a reasonable compromise.

2.7.1.3 Damping

The damping coefficients are estimated using (2.3.16) where Ψ is the relative power dissipation of a hysteresis cycle and f_{damp} is the approximate frequency of the hysteresis cycle. This frequency results from the vibration of the shaft and an average value for this frequency over a number of simulations is taken as a constant value for this parameter. The range of identified frequencies with a significant amplitude in the system varies within an order of magnitude, but is concentrated at the $6\ Hz$ average. As a result the magnitude of the damping in general can be expected to be only accurate regarding the order of magnitude. However, when the frequency of the vibration is close to $6\ Hz$, as is mostly the case for the observed vibrations during propulsion mode transitions, the damping closely matches the parameter for the damped energy in each oscillation Ψ.

2.7.1.4 Verification

Verification has been performed for each subsystem during the implementation. For the submodel verification, a framework with an dummy propeller load has been used in combination with ramp and step inputs. The subsystem parameters have been varied and the subsystem response is checked against analytical results. The implementation of the combined subsystems of the transmission has been been verified using the same methodology. To verify the implementation of the complete propulsion system model a number of 30s steady state simulations for diesel mode and electric mode have been performed, these runs are included in appendix B.2. The outcomes have been checked to match with the expected system behaviour following the methodology from Vrijdag, Stapersma, and Terwisga [68]. It is concluded that the the observed behaviour of the implemented model is in agreement with the mathematical models.

2.7.1.5 Initialisation

It is identified that the model initialises in about 5 seconds. In this period the twist angle in the flexible components has to be established resulting in an initial vibration. Effectively the system responds to a torque step response during the initialisation. Calculating the steady state twist angles and setting them as the initial conditions would stop the initial oscillatory behaviour. However, as the system initialises itself within 5s this is deemed unnecessary.

2.7.2 Validation

In Vrijdag, Stapersma, and Terwisga [68] validation is defined as: "The process of determining the degree to which a model is an accurate representation of the real world from the perspective of the intended uses of the model." In correspondence with this definition the validity of the hybrid propulsion system model is discussed in this subsection.

2.7.2.1 Validity of the Propulsion Models

For the propulsion models the trust torque relation of the propeller is most important. The model is based on the experimentally determined open water diagrams that are a well accepted modelling methodology for the torque thrust relation. The hull and wave models are not validated using experimental data. The used hull model is widely applied and combined with the grounding of the selected model parameters in reality, it is assumed that it is sufficiently valid. The wave model is considered an acceptable representation of wave disturbance given the application of measured values for the wave height and frequency.

2.7.2.2 Validity of the Transmission System Models

For the transmission system model the gearbox friction is validated in Geertsma [36]. The same friction model has been used for the shaftline, for which the corresponding parameter are based on estimations. The clutch thermal model has been calibrated and validated using data from a high fidelity finite element model in subsection 2.4.4. The remainder of the transmission system has not been validated using experimental data. The applied lumped-inertia technique is successfully used for torsional vibration analysis, application in dynamic propulsion system simulation is uncommon. This validity of this approach has to be further assessed in future research. However, it is assumed that the application of parameters based on manufacturer data in the transmission system models, does result in a reasonable representation of the low frequency torsional dynamics.

2.7.2.3 Validity of the Driver Models

The diesel engine model has been validated in Geertsma [36] for evaluation of the dynamic operation of the engine, in relation to its envelope, in propulsion control studies. The same case is made for the induction machine, the parameters have been adapted from Geertsma [36] and applied in a similar electric motor model. As their intended use corresponds with the use of these models in this thesis, the validity of these models is assumed.

2.7.2.4 Validity of the System Model

Combining a number of separately validated models does not lead to the conclusion that the model of the complete system is valid. This is equally true for the system model in this thesis. For full validation, comparison of the model with measurements from an actual hybrid propulsion system is needed. It is recommended that the model in this thesis is validated using measurements from a hybrid propulsion system in future research. Considering the thorough modelling of the system in this chapter, it is assumed that the accuracy of the system model is sufficient for evaluating the impact of clutch operation in propulsion mode transitions, in regards to the defined impact measures. However, validation of the complete system model in future research, using measurements from a hybrid propulsion system, is needed to verify this assumption.

2.8 Conclusions

In this chapter, first a hybrid propulsion system has been defined, then the modelling of the system has been described. By this process the four sub-research questions have been addressed. This section concludes the system modelling by describing how the sub-questions have been addressed.

Hybrid Propulsion System Case
First the sub-question: "*What is an appropriate hybrid maritime propulsion system case to investigate clutch operation in propulsion mode transitions?*" has been addressed in section 2.1. A hybrid propulsion has been defined by introducing multi disk wet friction clutches in the reference propulsion[14] system and ship[35], resulting in the following system:

- Hull of a 172 m container feeder
- Wageningen-B series fixed pitch propeller
- Diesel engine with 9.1 MW of power at 1000 rpm
- Electric motor with 3 MW of power at 600 rpm
- Multi disk wet friction clutches that enable selecting and combining the main drive engine
- Elastic couplings between the clutches and the engines
- Shaftline connecting the propeller and gearbox
- Dual engine gearbox that connect the two drive engines to the shaftline using the same gear ratio. As a result the electric motor can be used for low speed operation and the diesel engine is most suitable for the higher speed operation.

The defined hybrid propulsion system is able to operate in a number of single engine and parallel engine propulsion modes. The considered propulsion modes within the scope of this thesis are diesel engine propulsion and electric propulsion.

Characteristics and Dynamics of a Maritime Clutch
The second sub-question: "*What are the characteristics and dynamics of a typical clutch in a maritime propulsion system?*" has been addressed in section 2.4. It is identified that the dynamics of wet friction multi plate clutches are governed by the stribeck behaviour of the wet friction. It is concluded that the critical dependencies of wet friction dynamics in the engagement of wet friction clutches are:

- The applied pressure on the disks
- The relative velocity of the clutch halves
- The temperature of the oil between the friction interfaces

System Model
The sub-question: "*How to model the hybrid maritime propulsion system to enable evaluation of the impact of clutch operation in propulsion mode transitions?*" has been addressed in sections 2.2 - 2.7. In subsection 2.2.1 first the impact measures that are to be evaluated are defined:

- Operation of the induction machine relative to its torque-speed operating envelope
- Operation of the diesel engine relative to its torque-speed operating envelope
- Electric load profile of the induction machine
- Low frequency torsional vibrations
- Stress in the shaftline
- Temperature of the clutch
- Gear hammer in the gearbox
- Rotational speed of the propeller

In subsection 2.2.2 the concept for the system model has been described. To asses the basic vibratory behaviour of the transmission system, the system is divided in 8 lumped inertias connected by the nonrigid subsystems (shaftline, gearbox, elastic couplings). In this concept the inertias connected by the clutch can be in two states, rigidly connected or uncoupled. In the sections 2.3 - 2.6 the subsystems have been modelled and parameter values have been determined. The resulting model can be summarised as follows:

- Transmission System submodels:
  - The shaftline model, where the friction losses are modelled as a torque loss model and the contribution to the vibratory torsional dynamics is modelled as a parallel spring damper. The parameters are selected from design rules and estimations.
  - The gearbox model, where the friction losses are modelled as a torque loss model and the meshing of the gears is modelled as a parallel spring damper. The friction parameters are obtained from the reference propulsion system case and the geometric parameters are estimated.
  - The elastic coupling model, where the contribution to the vibratory torsional dynamics is modelled as a parallel spring damper. The corresponding parameters have been selected from public manufacturer data.
  - The clutch model, where switching the definition of the clutch torque at lock-up is selected for the state model. For modelling the wet friction the identified critical dependencies are considered. The wet friction is consequently modelled using the load sharing approach consisting of a hydrodynamic friction part and a contact friction part. The heat dynamics of the clutch are modelled using a lumped thermal mass. The geometric parameters are obtained from public manufactures data, the friction parameters are estimated and the clutch thermal model has been calibrated using the data of a detailed thermal finite element model from literature [53].
- Driver & Control submodels:
  - The model for the diesel engine and governor dynamics has been provided by dr.ir. R.D.Geertsma and further described in [36]. The mean value first principle model describes the dynamic performance and includes the thermal loading of the engine. The parameters for the diesel engine, PI controller and fuel limiters are obtained from the reference hybrid propulsion system.
  - The induction machine and drive models are part of the v-ZEL and are provided by dr.ir. U.Shipurkar from MARIN. The model captures the dynamics of the electric machine using the inverse-y equivalent circuit and is implemented in the dq-reference frame. The electric machine is driven using direct torque control with the option to select an outer speed control loop. The parameters are obtained from the reference hybrid propulsion system case.
  - The propulsion control model feeds control set-points to the primary controllers in the electric machine and diesel engine models. The propulsion model consists of a number of states containing the set-points for the propulsion modes.
- Propulsion submodels:
  - The hull model, where the 1-D surge motion of the ship is considered which is modelled as a function of the hull resistance and the propeller thrust. The parameters are obtained from the reference ship case and estimated.
  - The wave model adds a sinusoidal disturbance to the wake inflow speed of the propeller. Parameters for the wave model are based on the average wave height and frequency in a given sea-state.
  - The propeller is modelled for operation in the first quadrant using the $K_T(J(t))$, $K_Q(J(t))$ open water diagrams. The open water diagrams are generated for the matched propeller from the original polynomial series, further parameters are based on design estimations.

The implementation and the verification of the defined mathematical models has been discussed in subsection 2.7.1. The system model has been implemented in Matlab Simulink and suitable parameters for the variable step ode23 solver have been selected. Due to the high stiffness of the gear mesh forcing a small time step the choice has been made to reduce the mesh stiffness to be one order of magnitude higher then the next stiffest component(the shaftline). Verification of the mathematical implementation has been performed for each subsystem during the implementation. To verify the implementation of the complete propulsion system model, a number of steady state simulations has been performed. From analysing these simulations it is concluded that the the observed behaviour of the implemented model is in agreement with the mathematical models. It is also identified that the implemented model initialises in about 5 seconds.

Finally the validity of the system model has been discussed in subsection 2.7.2. It is concluded that, considering the thorough modelling of the system, it can be assumed that the accuracy of the system

model is sufficient for evaluating the impact of clutch operation in propulsion mode transitions, in regards to the defined impact measures. However, validation of the complete system model in future research, using measurements from a hybrid propulsion system, is needed to verify this assumption.

Propulsion Mode Transition Control Approach

The final sub-question: "*How to approach the propulsion mode transitions from a propulsion control point of view?*" has been addressed in subsection 2.5.3. In the scientific literature no standard control approach for propulsion mode transitions was identified. Three transition control approaches with an increasing degree of sophistication have been selected:

- The instant approach where clutches are engaged and disengaged at the same point in time. This represents the most rudimentary way to approach a propulsion mode transition ans serves as a baseline.
- The staged approach where the clutch for the new propulsion modes engine is first engaged followed five seconds later by the disengagement of the clutch for the preceding drive engine. It is the aim of this approach to asses the suitability of parallel speed control for handover of the drive torque between the drive engines during a propulsion mode transition.
- The torque controlled approach where, in addition to a 5 second overlap in clutch engagement and disengagement, the torque control mode for the induction machine is used to ramp up or down the drive torque. It is the aim of this approach to force a handover of drive torque between the drive engines during a propulsion mode transition.

These three propulsion control approaches for the mode transitions have been implemented in the propulsion control model. The approaches are evaluated in the following chapter 3 where the propulsion mode transitions are simulated.

Chapter 3

Propulsion Mode Transition Simulations

The main research question: "*What is the impact of clutch operation in propulsion mode transitions on hybrid maritime propulsion systems?*" is addressed in this chapter by performing simulations, using the hybrid propulsion system model described in chapter 2. In section 3.1 the setup of the simulation experiments is described. In sections 3.2 - 3.4 the results of the simulations are analysed. In section 3.5 the results of the propulsion mode transitions simulations are compared. In section 3.6 the simulation results are discussed. Section 3.7 concludes this chapter by summarising how the the main research question has been addressed in this chapter.

3.1 Setup of the Simulations

For the simulations in this chapter the implemented model of the hybrid propulsion system described in chapter 2 is used. In this section, the setup of the simulations is discussed by first describing the simulated propulsion mode transitions in subsection 3.1.1. The considered output of the simulations, from which the impact of clutch operation is evaluated, is described in subsection 3.1.2.

3.1.1 Propulsion Mode Transitions

The considered propulsion modes within the scope of this research are diesel propulsion (Diesel Mode) and electric propulsion (Electric Mode). For the transitions between these modes, three transition control approaches have been defined and implemented in the propulsion control model. These are further described in subsection 2.5.3 and can be summarised as follows:

- The instant approach where clutches are engaged and disengaged at the same point in time. This represents the most rudimentary way to approach a propulsion mode transition and serves as a baseline.
- The staged approach where the clutch for the new propulsion modes engine is first engaged followed five seconds later by the disengagement of the clutch for the preceding drive engine. It is the aim of this approach to asses the suitability of parallel speed control for handover of the drive torque between the drive engines during a propulsion mode transition.
- The torque controlled approach where, in addition to a 5 second overlap in clutch engagement and disengagement, the torque control mode for the induction machine is used to ramp up or down the drive torque. It is the aim of this approach to force a handover of drive torque between the drive engines during a propulsion mode transition.

3.1.1.1 Operational point for the transitions

For the propulsion mode transitions, a steady state operating point is selected. Below 600 rpm the diesel engine operates at a relatively low efficiency. The induction machine, at 600 rpm, would operate at its design speed and corresponding high efficiency. Steady state simulations have been performed at the 600 rpm operating point to confirm that this would be an appropriate case for a propulsion mode transition. In fig.3.1 the operation of both the diesel engine and the induction machine relative to their respective operating envelope is presented. It can be observed that both engines are able to propel the ship in this operating point, with a safe margin to the operating envelopes. The 600 rpm steady state operating point is thus selected as a case to transition between diesel engine and electric propulsion. From the steady state simulations it is concluded that the selected 600 rpm speed setpoint corresponds with a 10 kn steady state ship speed.

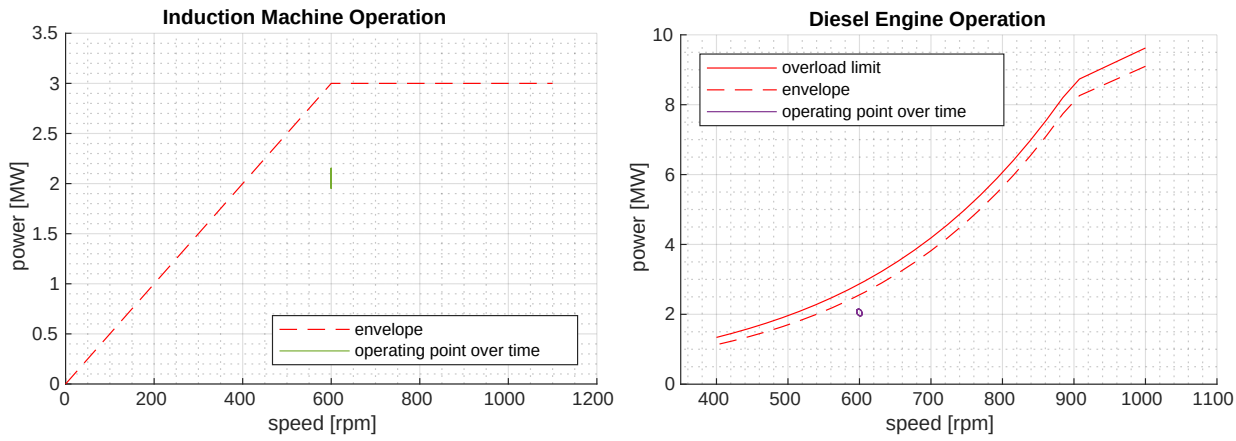

Figure 3.1: Diesel and Electric Propulsion at 600 rpm, steady state operation with ship speed of 10 kn

3.1.1.2 Simulated Propulsion Mode Transitions

The impact of clutch operation, using one of the three transitions approaches, is evaluated by running a number of simulations and analysing the results. These simulations are performed for the three approaches and for both directions of the transitions, from diesel to electric mode and from electric to diesel mode, resulting in a total of six simulations. The transitions are performed at the selected 600 rpm speed setpoint which corresponds with a 10 kn steady state ship speed. The time span of the simulations is 30 s where the mode transitions is initiated at 15 s. These times have been selected to leave ample margin to the 5s initialisation time of the model and to allow the impact of the propulsion mode transitions on the transient behaviour of the system to be fully evaluated. For the conditions a moderate sea state 3 is selected with the ship at the loaded displacement. A computer with an Intel i7-12700K CPU coupled with 32 GB of GDDR4 RAM has been used to run the propulsion mode transition simulations.

From analysing the simulation results it is concluded that the torque controlled transition approach is able to significantly limit the impact of clutch operation in a propulsion mode transition from electric to diesel propulsion. To asses if the torque controlled transition approach is also able to limit the impact in rough sea conditions, an additional simulation has been performed for this case with the sea state set to 5.

3.1.2 Impact Evaluation

In accordance with the defined impact measures in subsection 2.2.1 the impact of clutch operation is analysed by considering the following output of the simulation experiments:

- The mechanical power of the induction machine, the mechanical power of the diesel engine and the mechanical power draw of the propeller as a function of time.
- The rotational speeds of the diesel engine and induction machine as well as the propeller speed multiplied with the gear ratio and the shaft speed setpoint to enable assessment of their relative behaviour.
- The torque in the shaftline and propeller both multiplied by the gear ratio to enable a relative comparison with the diesel engine and induction machine torques.
- The transmitted torque through the clutches with the corresponding maximum holding torques.
- The operational point of the diesel engine over time. The operation is bounded by the engine envelope where running between the envelope and the overload limit is only allowed for a limited duration.
- The operational point of the induction machine over time with the operating envelope.
- The electric power draw by the induction machine power converter.
- The diesel engine governor setpoint relative to the fuel limiter.
- The Von Mises equivalent stress in the shaftline relative to the yield limit for the shaft material.
- The gear mesh force, where a crossing of zero indicates the occurrence of gear hammer.
- The temperature of the oil film between the clutch plates. The imposed limit is the temperature at which the oil starts burning, a limit that should be steered clear off under all circumstances.
- The running efficiency of the transmission system as measured by the power input from the engines from $t = 5\ s$ compared to the power delivered to the propeller. The function of this plot is to verify the results of the experiments as it provides insight in the conservation of energy in the transmission system.
- The ship speed as a function of time to indicate if the ship is accelerating, decelerating or keeping a constant speed, verifying that the initial speed in the experiment matches the approximate steady state in the operating point.

The results of the simulated propulsion mode transitions are discussed in the following sections 3.2 - 3.4 of this chapter. Not all the simulation outputs are relevant for the discussion of a specific mode transition results. Therefore the most relevant plots are presented in the discussion of the results. However, to enable assessment of all these metric for all the simulations, the complete simulation results are included in the appendix B.3.

3.2 Propulsion Mode Transitions using the Instant Approach

In this section the results of the propulsion mode transition simulations, where the instant approach is used, are discussed. In subsection 3.2.1 the electric to diesel transitions simulation results are discussed. In subsection 3.2.2 the electric to diesel transitions simulation results are discussed. Subsection 3.2.3 concludes this section by characterising the discussed simulation results for the instant approach.

3.2.1 Results Instant Electric to Diesel Transition

In this subsection the simulation results for the instant transition from electric to diesel propulsion are presented and discussed. In the instant transition, the clutches are engaged and disengaged at the same point in time. This approach represents the most basic and rudimentary way of performing the propulsion mode transition. No transition control is used in the switch between the states of the propulsion controller.

3.2.1.1 Clutch Operation

The instant transition approach is characterised by the simultaneous actuation of the clutches. In fig.3.2 the torque transmitted by the clutches and the maximum friction torque is presented for the electric to diesel transition. First the induction machine drives the propeller and transmits torque trough its respective clutch. Then at $t = 15\ s$ the clutch pressure is reduced to zero and correspondingly the maximum friction torque drops to zero. Equally at $t = 15\ s$ the clutch for the diesel engine is activated and pressure builds following the actuation curve.

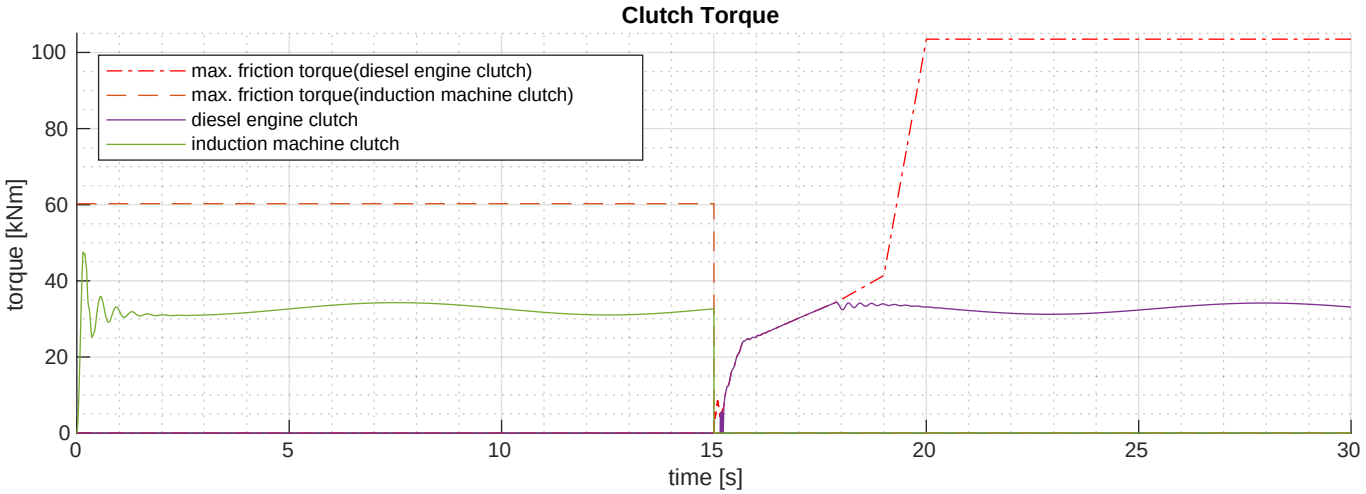

Figure 3.2: Clutch torque for the transition from electric to diesel mode using the instant transition approach in sea state 3.

The transmitted torque equals the maximum torque up to $t = 18\ s$ indicating a period of slipping in the clutch. During this period of slip the temperature of the clutch plates rises only slightly, as can be observed in fig.3.3. This relatively low rise in temperature can be explained by the magnitude of the slip and the friction torque during the slip. From the rotational speeds in fig.3.4 the slipping of the clutch can be observed from the difference between the diesel engine and propeller speed. Maximum slip is at the initial engagement with a speed difference of $200\ rpm$, a second peak is reached at $t \approx 15.5\ s$ with a slip of $100\ rpm$. Both these slip maxima occur at a point where the friction torque is still limited, thus limiting the generated heat flux into the clutch plates, explaining the limited rise in temperature of the clutch.

It must be observed in fig.3.4 that the slip maxima differ in their direction. In the initial slip the propeller speed is actually higher than the diesel engine speed. Whereas for the second maximum the diesel engine speed is higher than the propeller speed. This should be reflected in the friction torque for the initial maximum being negative, as energy is transferred from the propeller shaft to the diesel engine to speed it up. This can indeed be observed in fig.3.2, the friction torque right after the diesel engine clutch actuation does not follow the max. friction torque but emerges only after $1/4\ s$. This indicates that the friction torque

was negative for this period and followed the trajectory of the maximum friction torque for the reversed slip. The magnitude of this friction is a mirror image over the x-axis of the positive max friction torque.

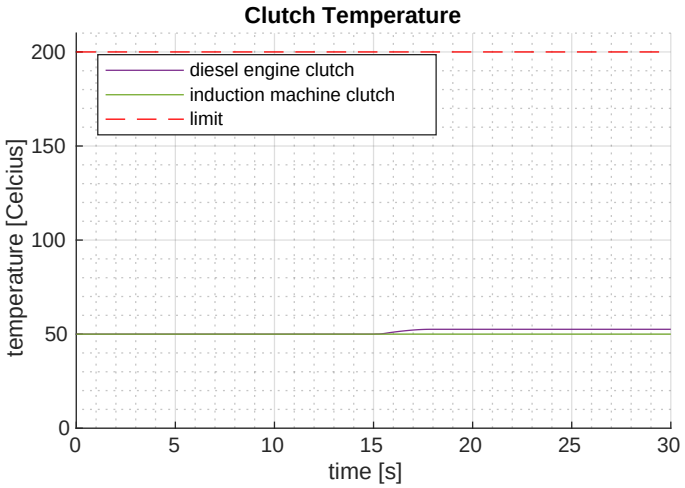

Figure 3.3: Clutch temperature for the transition from electric to diesel mode using the instant transition approach in sea state 3.

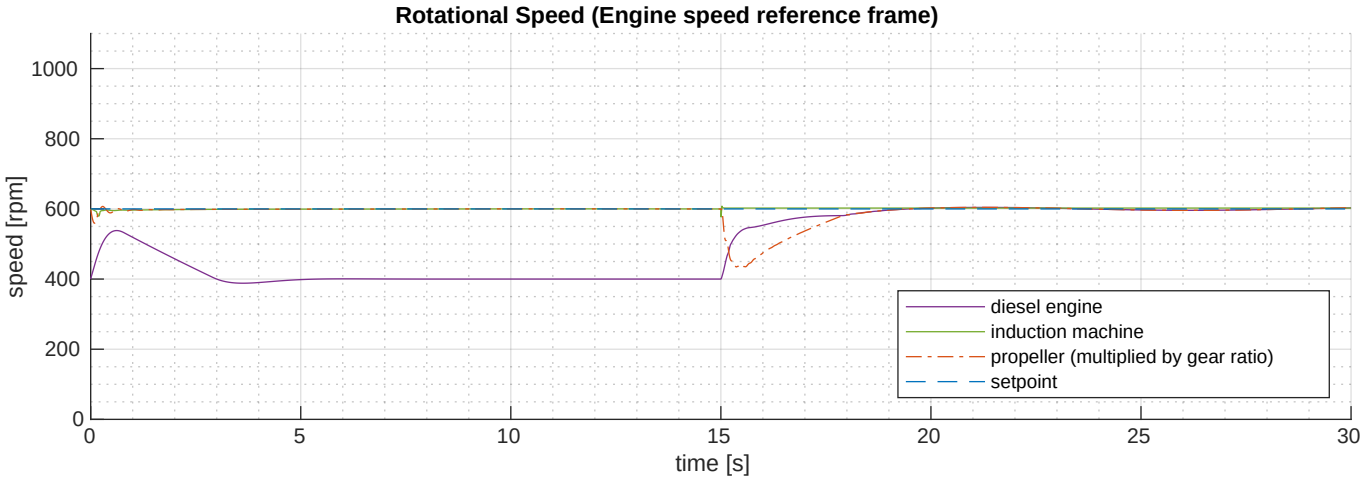

Figure 3.4: Rotational speed in the engine speed reference frame for the transition from electric to diesel mode using the instant transition approach in sea state 3.

3.2.1.2 Impact on Propulsion System Rotational Speeds

The drop in propeller speed observed in fig.3.4 can be traced back to the gap in torque transfer between the handover from one engine to the other in fig.3.2. The diesel engine's clutch is not able to transmit the steady state torque until about $3\ s$ after its activation, limited by the maximum friction torque of the clutch. This drop on propeller speed is undesirable given that maintaining shaft speed is the control goal of the speed controllers. The drop has limited impact in itself. The short duration of the drop in speed has no significant impact on the speed of the ship.

Further analysing the rotational speeds in fig.3.4 it is observed that the speed of the diesel engine does not drop below its minimum speed of $400\ rpm$. Moreover, diesel engine shows no drop of speed at all when the diesel engine clutch is activated. This can be explained by a combination of the negative initial slip, where the rotational energy in the propeller shaft speeds up the diesel engine, and a rapid response of the diesel engine speed controller.

3.2.1.3 Impact on Propulsion System Torque

The impact of the instant transition approach is most pronounced in the effect it has on the torques throughout the propulsion system. At the transition a significant vibration in the shaft line torque can be observed in fig.3.5. When the induction machine clutch is deactivated and the diesel engine clutch is activated the maximum torque to the propeller shaft is limited. This releases the energy from the torsional spring that the shaft line effectively is, resulting in the observed torsional oscillation. More specifically, due to the the gap in maximum torque transfer, that can be observed in fig.3.2, the twist angle first reduces rapidly before reestablishing itself when the steady state torque is once again reached.

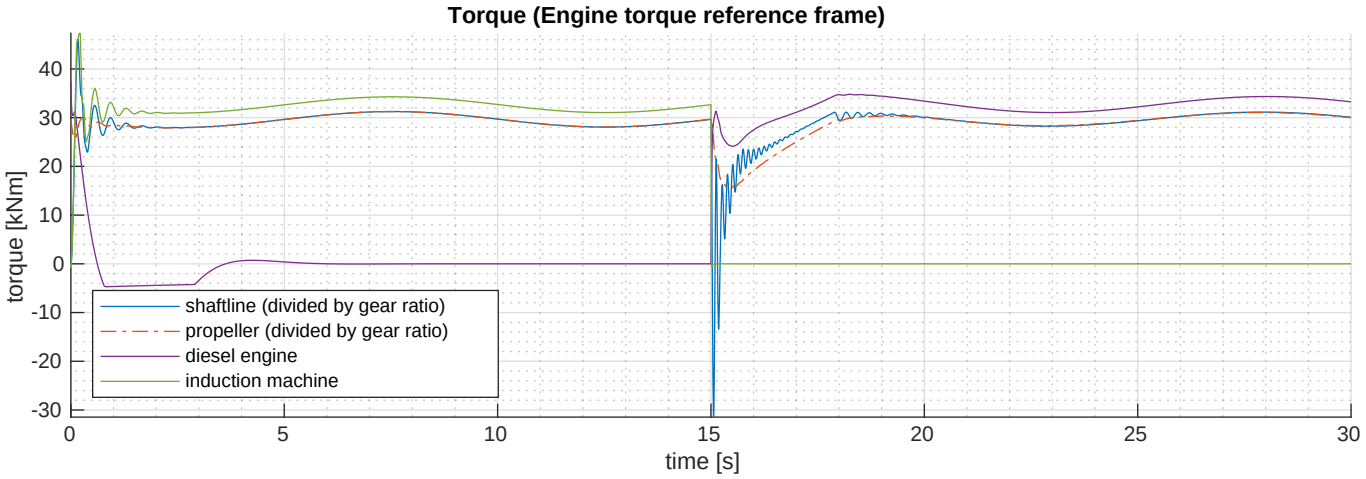

Figure 3.5: Torques in the engine torque reference frame for the transition from electric to diesel mode using the instant transition approach in sea state 3.

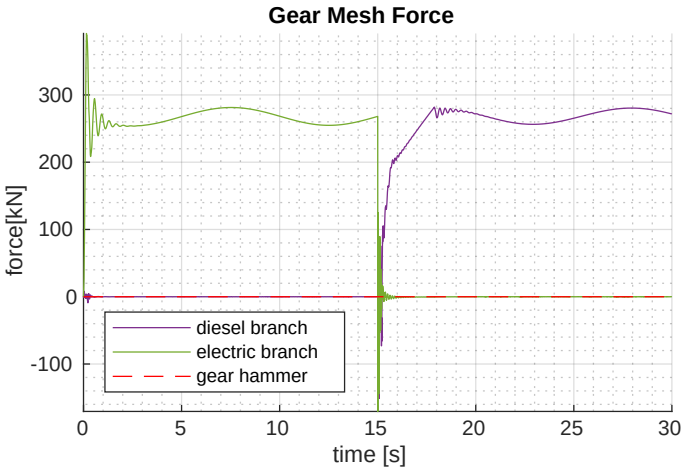

Figure 3.6: Gear mesh force for the transition from electric to diesel mode using the instant transition approach in sea state 3.

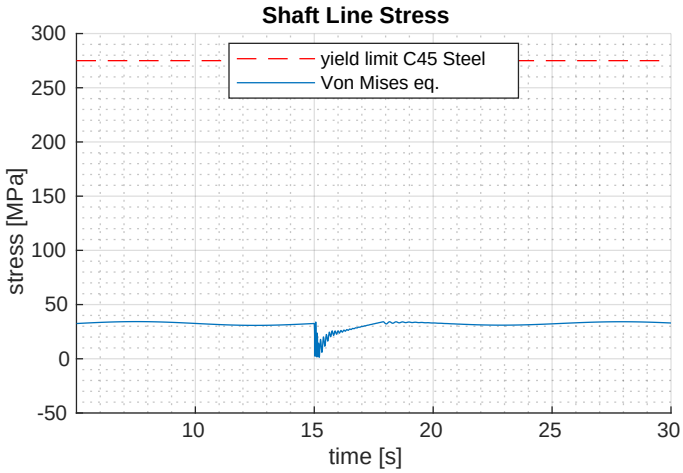

Figure 3.7: Shaft line stress for the transition from electric to diesel mode using the instant transition approach in sea state 3.

It can also be observed that the torque crosses zero, an indication of gear hammer. In fig.3.6 this can be confirmed by the zero crossing gear mesh force present in both branches of the gearbox. The electric motor branch is subject to the highest impact. This branch moves from a driving to a driven state, in this transition the gears hammer back and forth until damping out after about 1 second. The diesel engine branch starts in a driven state as discussed in earlier sections, and transitions to a driving state.

Finally the torque directly represents the stress in the shaft line. In fig.3.7 it can be observed that the stress does not come close to the yield limit of the shaft material. The vibration can be observed in the shaft line stress as well.

3.2.1.4 Concluding Summary of the Instant Electric to Diesel Transition Results

- As a result of the transferable torque limit of the diesel engine clutch there is a $3\ s$ gap where the transmission system is unable to deliver the required torque to the propeller.
- The slip of the clutch that is limiting the transfer of torque results in a $2℃$ rise of the clutch temperature.
- The gap in propulsion torque results in a 25% drop of the propeller speed.
- The gap in propulsion torque releases the spring energy in the shaft line and inducing a significant torsional vibration with a maximum peak-to-peak amplitude that is 160% of the steady state torque.
- The instant torque transfer reversal in the gears combined with the torsional vibration induced by the shaft line result in gear hammer in both gear mesh interfaces.
- Shaft line stress does not approach the yield limit but the stress oscillations might induce fatigue damage.

3.2.2 Results Instant Diesel to Electric Transition

In this subsection the simulation results for the operational diesel to electric transition with the instant actuation approach are presented and discussed. In the instant transition the clutches are engaged and disengaged at the same point in time. The transition is initiated at $15\ s$.

3.2.2.1 Clutch Operation

In fig.3.8 the torque transmitted by the clutches and the maximum friction torque is visualised. First the diesel engine drives the propeller and transmits torque through its respective clutch. Then at $t = 15\ s$ the clutch pressure is reduced to zero and correspondingly the maximum friction torque drops to zero. Equally at $t = 15\ s$ the clutch for the induction machine is activated and pressure builds following the actuation curve.

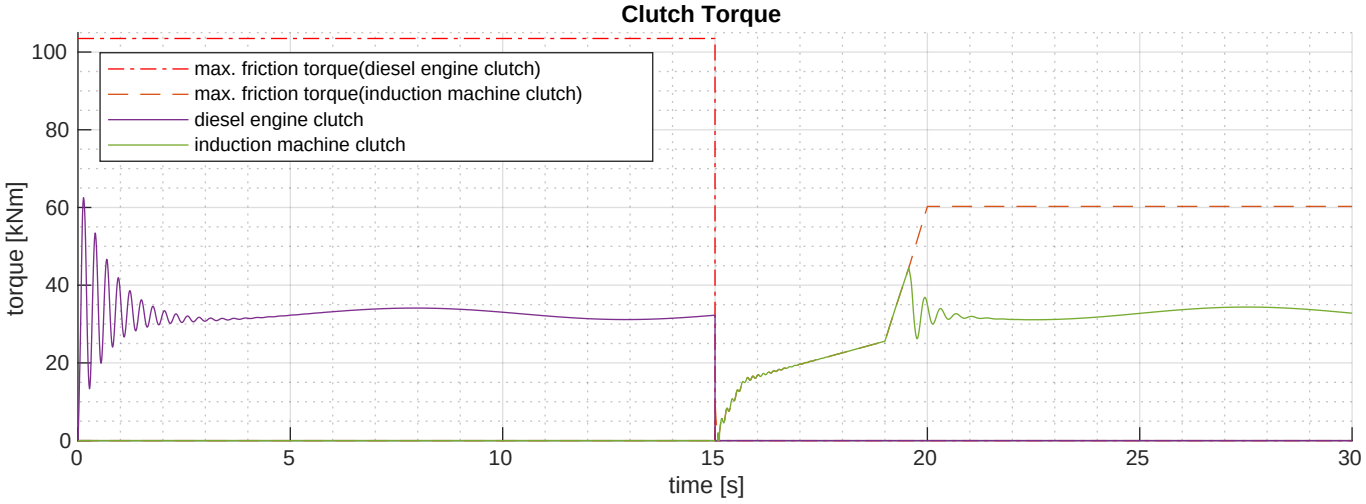

Figure 3.8: Clutch torque for the transition from diesel to electric mode using the instant transition approach in sea state 3.

When the torque matches maximum friction torque through the clutch this indicates a slipping clutch. The period of clutch slip lasts from $15\ s$ up to $19.5\ s$. It is confirmed by the speed graph of the propeller and induction machine in fig.3.10 that the clutch indeed slips during this period. During this period of slip the temperature of the clutch rises significantly from $50℃$ to $62℃$ as can be observed in fig.3.9. This significant rise can be attributed to the relatively large magnitude of the slip. The Induction machine speed

is maintained at the reference $600\ rpm$ by the induction machine controller. As the friction heat in the clutch is the product of the slip and friction torque this results in a significant heat flux into the clutch plates.

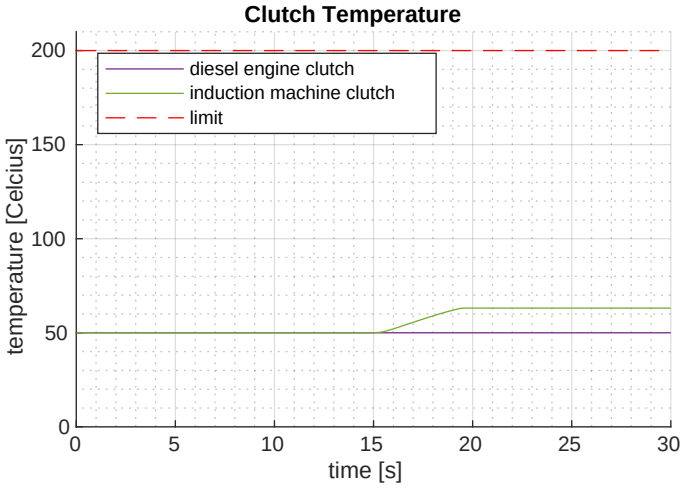

Figure 3.9: Clutch temperature for the transition from diesel to electric mode using the instant transition approach in sea state 3.

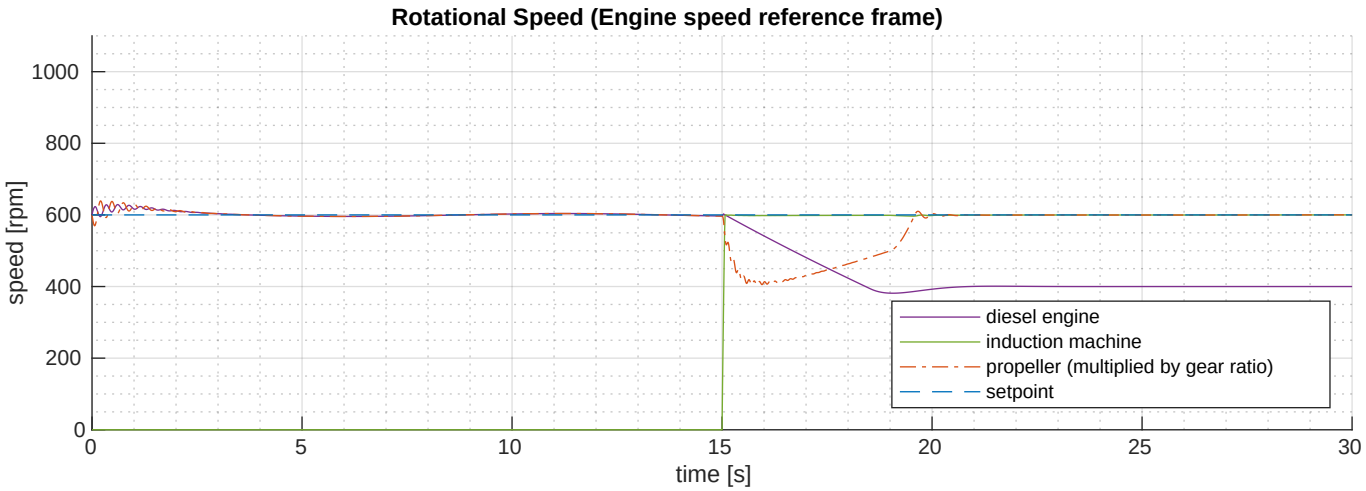

Figure 3.10: Rotational speed in the engine speed reference frame for the transition from diesel to electric mode using the instant transition approach in sea state 3.

3.2.2.2 Impact on Propulsion System Rotational Speeds

The period of slip of the clutch that can be observed in fig.3.8 also results in a period where the torque transmitted to the propeller is limited by the maximum friction torque of the clutch. The friction torque is significantly lower than the steady torque needed to sustain propeller rotation at the setpoint and therefore results in a 30% drop in propeller speed during the transition that can be observed in fig.3.10.

It can be observed that the speed of the inductions machine rapidly rises to the setpoint at the transition point. This is the result of the application of high peak torque by the induction machine drive as can be observed from the torque peak at $15\ s$ in fig.3.11.

3.2.2.3 Impact on Propulsion System Torque

The operation of the clutches results in two torsional vibrations in the transmission system as can be seen in fig.3.11. The first oscillation occurs at $15\ s$ when the clutches are actuated. At this time the clutches are able to transmit limited torque. This releases the wound up spring energy in the shaft line that initiates the large vibration. The second vibration is triggered as the clutch locks up at $19.5\ s$, the torque drops from the

friction torque to the steady state torque and settles after some oscillations. The second vibration damps out after only a small number of oscillations whereas the first oscillation damps out significantly slower. This can be attributed to the flexible coupling not being connected to the system in the first vibration as the clutch is slipping. These torque vibrations are not significantly transmitted through the clutch and therefore not damped out by the flexible coupling. When the clutch locks up the flexible coupling is able to dissipate the released spring energy and reduces the severity of the oscillation.

From the gear mesh force in fig.3.12 it can be observed that there is an indication of gear hammer in both branches of the gearbox. The diesel engine branch transitions from a driving gear to a driven gear. As a result of this occurring, almost instantaneous a large force is induced in the gear mesh. This results in the gear hammering back and forth until reaching a steady state. As the gear of the electric branch transitions from a driven gear to a driving gear, gear hammer can also be observed. This is damped out as the transmitted torque increases.

The torque vibrations in the shaft line are reflected in the shaft line stress of fig.3.13. The yield limit is not a constraint to the system but the stress variations might induce fatigue damage to the material.

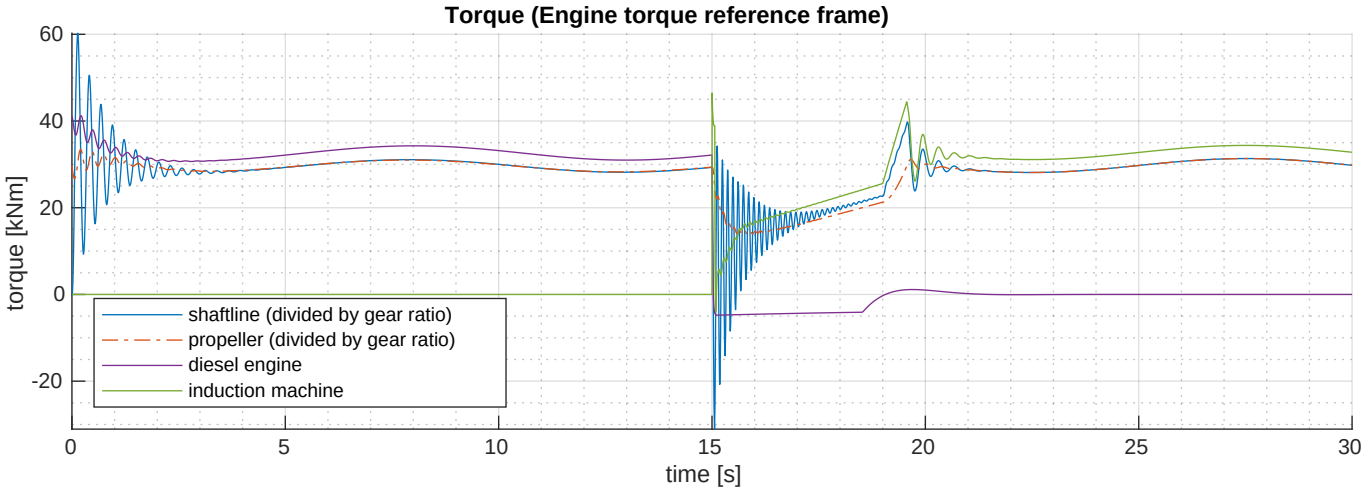

Figure 3.11: Torques in the engine torque reference frame for the transition from electric to diesel mode using the instant transition approach in sea state 3.

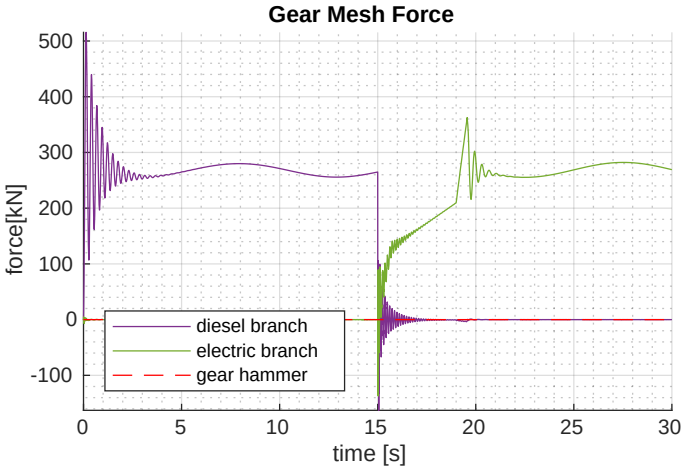

Figure 3.12: Gear mesh force for the transition from electric to diesel mode using the instant transition approach in sea state 3.

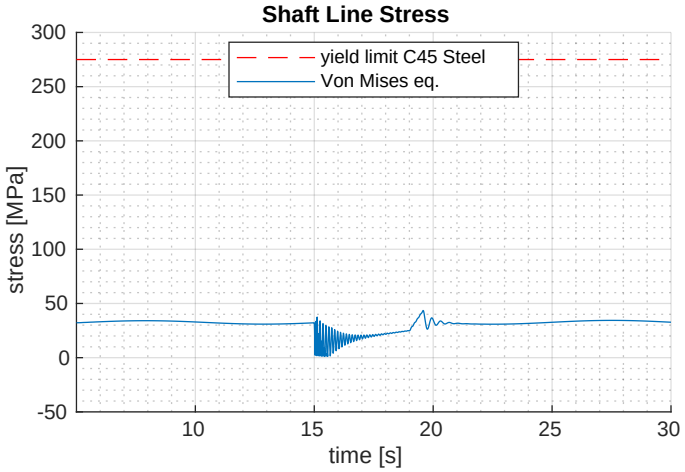

Figure 3.13: Shaftline stress for the transition from electric to diesel mode using the instant transition approach in sea state 3.

3.2.2.4 Concluding Summary of the Instant Diesel to Electric Transition Results

- As a result of the transferable torque limit of the induction machine clutch there is a $4\ s$ gap where the transmission system is unable to deliver the required torque to the propeller.
- The slip of the clutch that is limiting the transfer of torque results in a $12℃$ rise of the clutch temperature. The significant increase in clutch temperature is the result of the large magnitude of the slip that is maintained by the induction machine speed controller.
- The gap in propulsion torque results in a 30% drop of the propeller speed.
- The gap in propulsion torque releases the spring energy in the shaft line and inducing a significant torsional vibration with a maximum peak-to-peak amplitude 200% of the steady state torque.
- When the clutch locks up a second torsional vibration occurs with a maximum peak-to-peak amplitude that is 50% of the steady state torque.
- The second torsional vibration is damped out significantly quicker than the first as a result of the flexible coupling being able to contribute to the damping in the second instance.
- The instant torque reversal in the gears combined with the torsional vibration induced by the shaftline results in gear hammer in both gear mesh interfaces.
- Shaft line stress does not approach the yield limit but the stress oscillations might induce fatigue damage.

3.2.3 Impact of Clutch Operation in the Instant Transitions

By comparing the results of the diesel to electric and electric to diesel transitions the following characteristic is identified:

- During the transition there is a gap in drive torque to the propeller.
- The gap in drive torque is the result of a slipping clutch that limits the torque that can be transmitted.
- The period of slip results in a rise of the clutch temperature that is significant but is well within the envelope of the clutch.
- The gap in drive torque results in a significant drop of the propeller speed during the transition.
- The gap in drive torque releases the spring energy in the shaftline resulting in significant torsional vibrations.
- The torsional vibrations combined with a lack of drive torque result in gear hammer in both branches of the gearbox.
- The torsional vibrations correspond with a oscillating stress load on the shaftline that does not approach the yield limit but might induce fatigue in the shaft material.

It is identified that the main source of disturbance during the transition is the lack of drive torque during the transition. The lack of drive torque results from the transmittable torque trough the clutches. It can thus be concluded that the the instant approach results are characterised by a gap in transmittable drive torque, with significant impact on the propulsion system as a result.

3.3 Propulsion Mode Transitions using the Staged Approach

In this section the results of the propulsion mode transition simulations, where the staged approach is used, are discussed. In subsection 3.3.1 the electric to diesel transitions simulation results are discussed. In subsection 3.3.2 the diesel to electric transitions simulation results are discussed. Subsection 3.3.3 concludes this section by characterising the discussed simulation results for the staged propulsion mode transition approach.

3.3.1 Results Staged Electric to Diesel Transition

In this subsection the simulation results for the staged transition approach used in the electric to diesel transition are presented and discussed. In the staged transition, first the clutch for the new propulsion mode engine is engaged. This is followed a few seconds later by the disengagement of the clutch for the current engine.

3.3.1.1 Clutch Operation

In fig.3.14 the main characteristic of the staged transition can be observed in the overlap of the clutch friction envelopes. The clutch of the induction machine is depressurised after $5\ s$ when the diesel engine clutch reaches it peak torque capacity. From the clutch torques it becomes clear that as a result of this approach there is no longer a gap in the transferable torque, as is the aim of the staged approach.

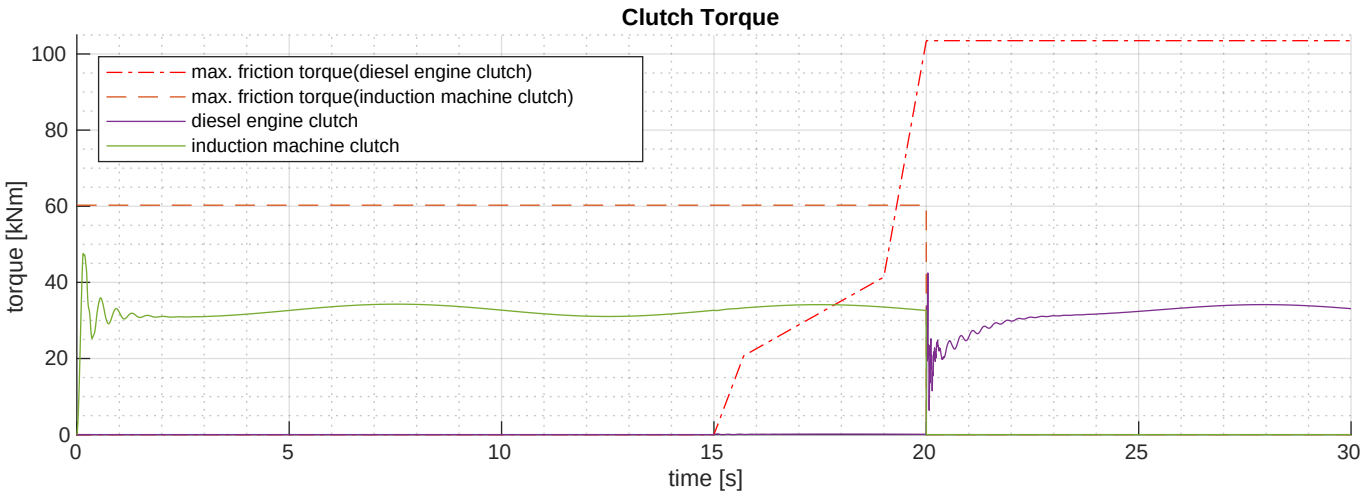

Figure 3.14: Clutch torque for the transition from electric to diesel mode using the staged transition approach in sea state 3.

The staged approach does however not lead to a gradual handover between the engines. The diesel engine only starts providing significant torque when the clutch of induction machine is disengaged. This suggest that, during the $5\ s$ that both clutches are engaged and both engines are in speed control mode, the rapid response of the induction machine controller prevents any large speed error from occurring and does not trigger the governor of the diesel engine. This is confirmed by fig.3.16 where the fuel rack setpoint resulting from the diesel engine speed governor is presented. The fuel setpoint only rises at $t = 20\ s$, when the induction machine clutch has been disengaged.

3.3.1.2 Impact on Propulsion System Rotational Speeds

In the staged transition approach the speed of the diesel engine is already matched to the speed of the induction machine before the clutch is engaged. As a result no significant period of clutch slip can be observed in fig.3.15 during the transition. There is however an approximate 15% drop in both the speed of the propeller and diesel engine after the clutch of the induction machine has disengaged. This as a result

of the torque provided by the diesel engine that is too low to sustain the reference speed. The lack of a gradual transition has been discussed in the previous section.

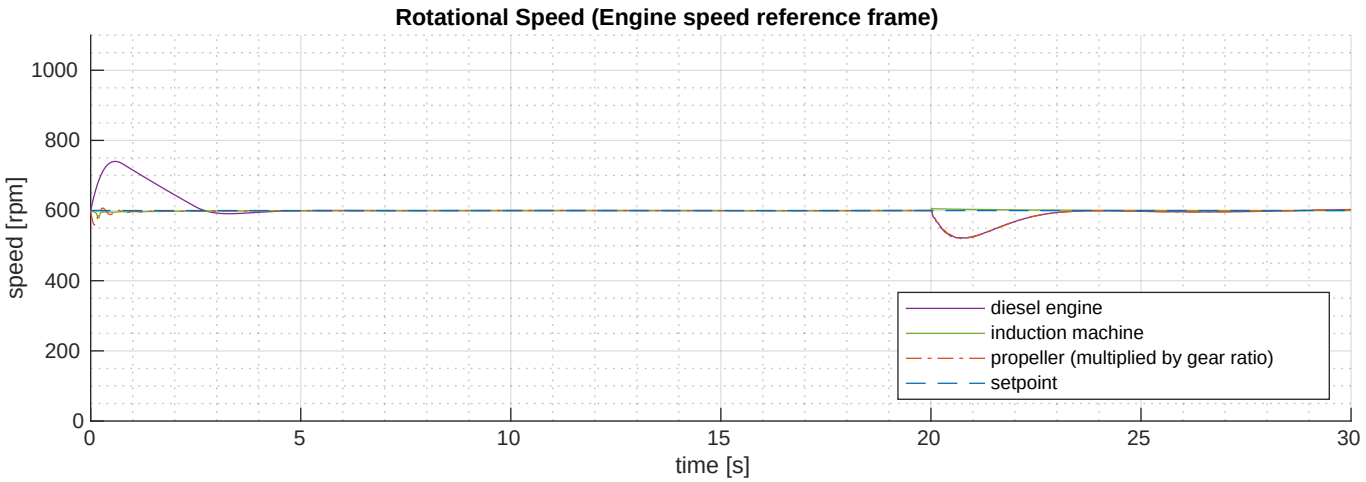

Figure 3.15: Rotational speed in the engine speed reference frame for the transition from electric to diesel mode using the staged transition approach in sea state 3.

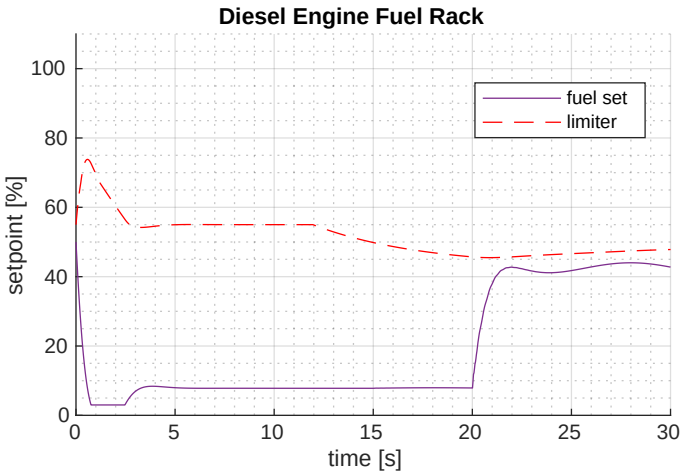

Figure 3.16: Diesel Engine fuel rack setpoint for the transition from electric to diesel mode using the staged transition approach in sea state 3.

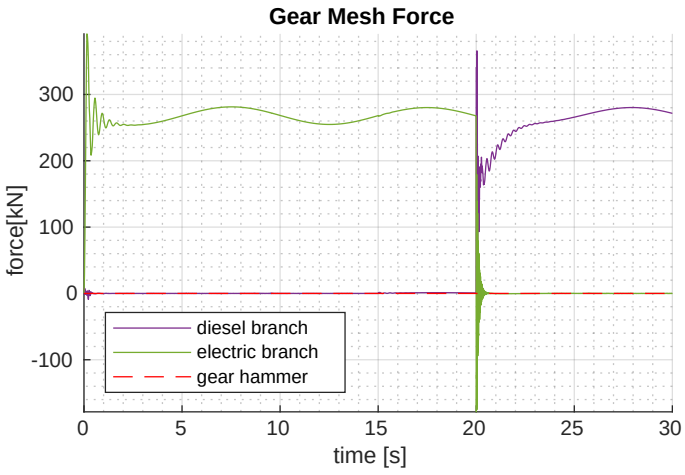

Figure 3.17: Gear mesh force for the transition from electric to diesel mode using the staged transition approach in sea state 3.

3.3.1.3 Impact on Propulsion System Torque

In fig.3.18 the torque gap causing the drop in propeller speed can be identified. The diesel engine torque reaches the steady state value only after $1\ s$. As no control handover takes place between the engines during the parallel phase, a torque gap results from the transition. The transition triggers a relatively minor torsional vibration in the shaft line.

When comparing the torque through the diesel engine clutch in fig.3.14 with the torque provided by the diesel engine in fig.3.18 it is observed that the torque through the clutch exceeds the torque provided by the diesel engine between $t = 20\ s$ and $t = 21\ s$. This matches with the observed deceleration of both the diesel engine and the propeller in fig.3.15 during the same period.

It is also observed that the induction machine provides negative torque at the point of clutch disengagement, this is overshoot of the torque controller that is set to zero from that point onward. As the the clutch is disconnected this has no impact on the speed of the propeller. It does result in gear hammer in the mesh of the electric branch, as can be observed in fig.3.17.

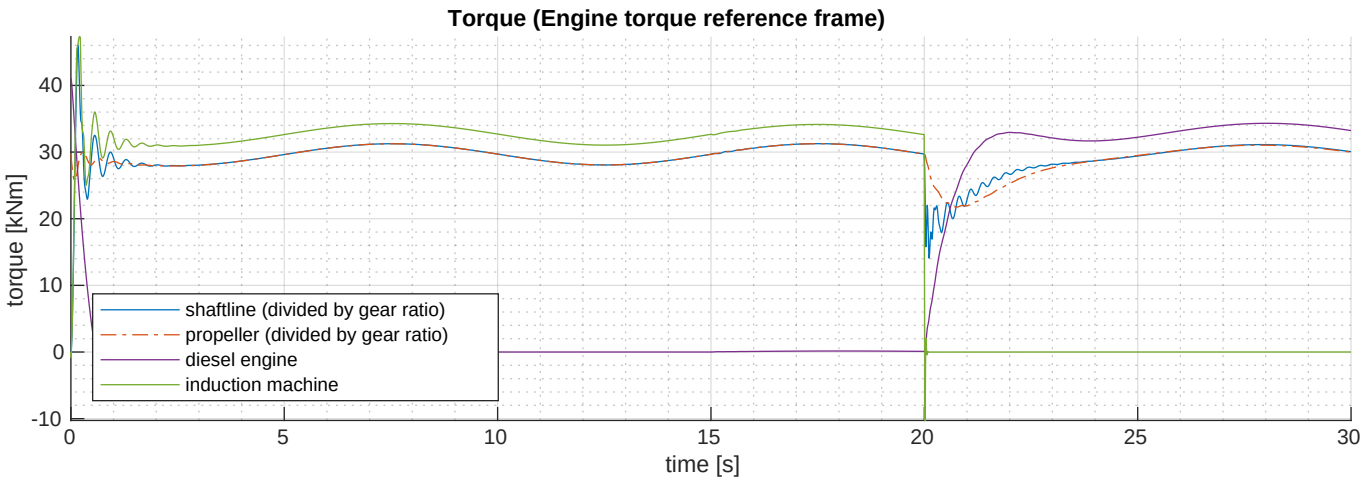

Figure 3.18: Torques in the engine torque reference frame for the transition from electric to diesel mode using the staged transition approach in sea state 3.

3.3.1.4 Concluding Summary of the Staged Electric to Diesel Transition Results

- During the parallel speed control phase the diesel engine does not start providing drive torque to the propeller. Only after the induction machine clutch is released does the diesel engine take over. This can be attributed to the relatively relaxed tuning of the diesel engine speed controller compared to the tuning of the induction machine drive speed controller.

- The response of the diesel engine speed controller to the instant load increase is relatively slow resulting in a 15% drop of the propeller speed.

- The gap in drive torque that results from the slow response of the diesel engine triggers a torsional vibration in the transmission system with a maximum peak-to-peak amplitude with a magnitude that is 25% of the steady state torque.

- As a result of overshoot of the induction machine torque controller, gear hammer can be identified in the electric gear mesh branch.

3.3.2 Results Staged Diesel to Electric Transition

In this subsection the simulation results for the staged transition approach applied to the transition from diesel to electric propulsion are presented and discussed. In the staged transition, first the clutch for the induction machine is engaged. This is followed five seconds later by the disengagement of the clutch for the diesel engine.

3.3.2.1 Clutch Operation

Overlap of the clutch engagement in fig. 3.19 does not lead to a gradual transition. Due to the fast response of the induction machine, the wave disturbance is taken over by the induction machine in the parallel speed control phase. This can be observed by the straight line in the diesel engine fuel rack plot of fig.3.20 and the power delivered to the induction machine during the parallel control phase in fig.3.21. The result of the disengagement of the diesel engine clutch is the occurrence of a torque step as the induction machine control responds to the handover. This torque step initiates a small torsional vibration. The fast response of the induction machine controller to the handover leads to a power peak in the electric power profile followed by a small oscillation in power as the controller is keeping the shaft line speed at the setpoint.

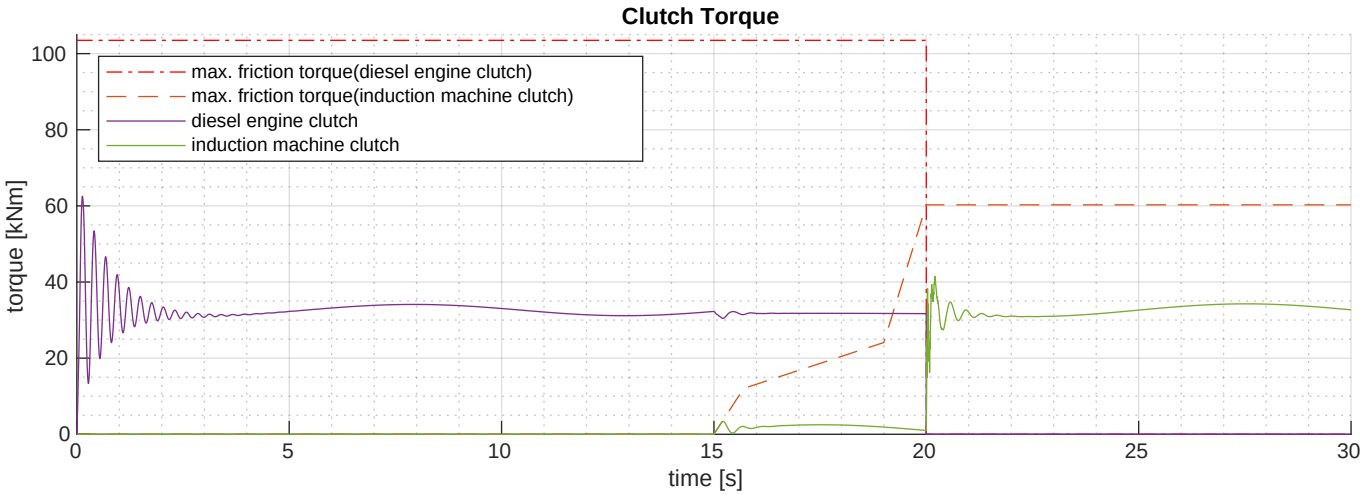

Figure 3.19: Clutch torque for the transition from diesel to electric mode using the staged transition approach in sea state 3.

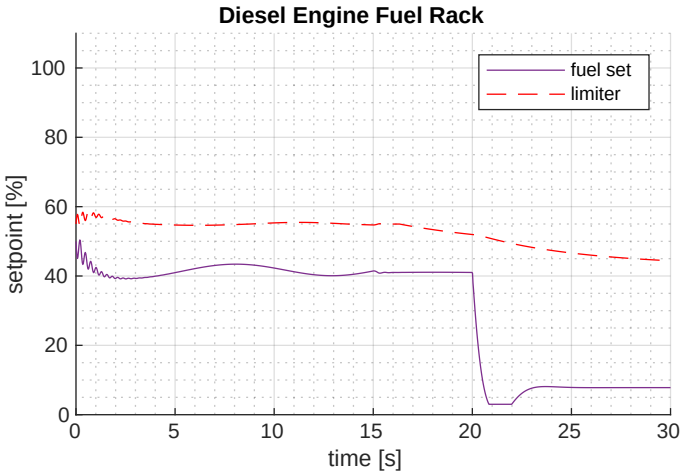

Figure 3.20: Diesel Engine fuel rack setpoint for the transition from diesel to electric mode using the staged transition approach in sea state 3.

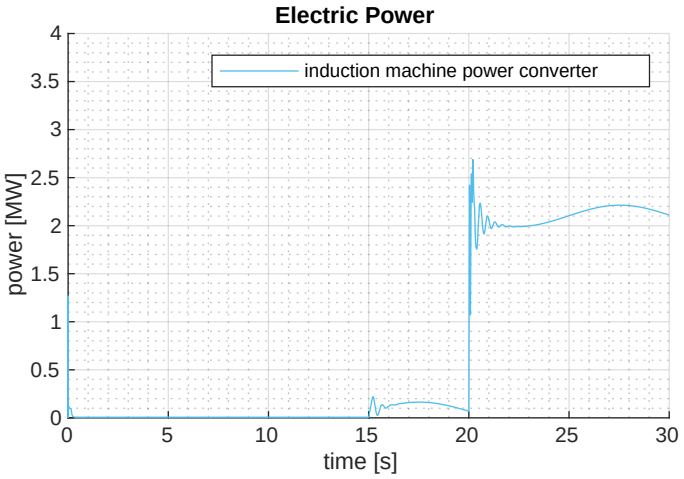

Figure 3.21: Induction machine drive power for the transition from diesel to electric mode using the staged transition approach in sea state 3.

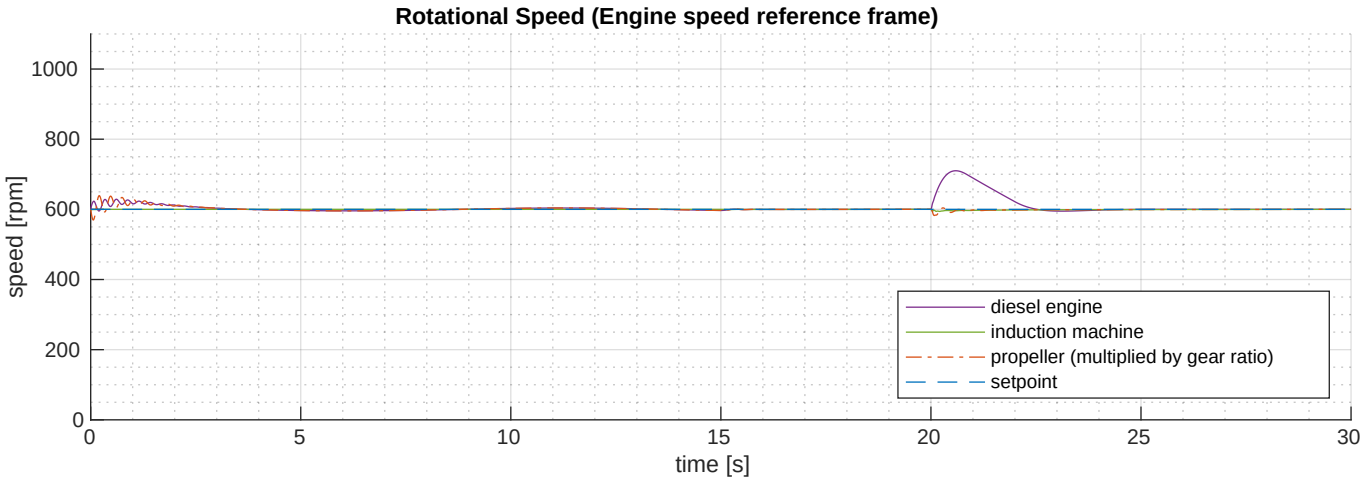

Figure 3.22: Rotational speed in the engine speed reference frame for the transition from diesel to electric mode using the staged transition approach in sea state 3.

3.3.2.2 Impact on Propulsion System Rotational Speeds

Even though the induction machine contributes little torque to the propeller at the time point where the diesel engine clutch is disengaged, it is able to provide the required torque fast enough to keep the speed of the propeller at the setpoint, as can be observed in fig.3.22. The diesel engine speed trace does show a significant response to the disengagement of the diesel engine clutch. The relaxed tuning of the engine makes it that it takes some time to readjust to the reduced load. The drop in load results in the observed increase in speed of the engine.

3.3.2.3 Impact on Propulsion System Torque

To make up for the lack of handover during the transition the induction machine applies almost a full torque step in fig.3.23 when the diesel engine clutch is disengaged. This triggers a torsional vibration in the transmission system. The amplitude of the vibration is limited and it quickly damps out. When the diesel engine clutch is disengaged the transition of the corresponding gear branch in fig.3.24 from driving to driven triggers gear hammer in the gear contact.

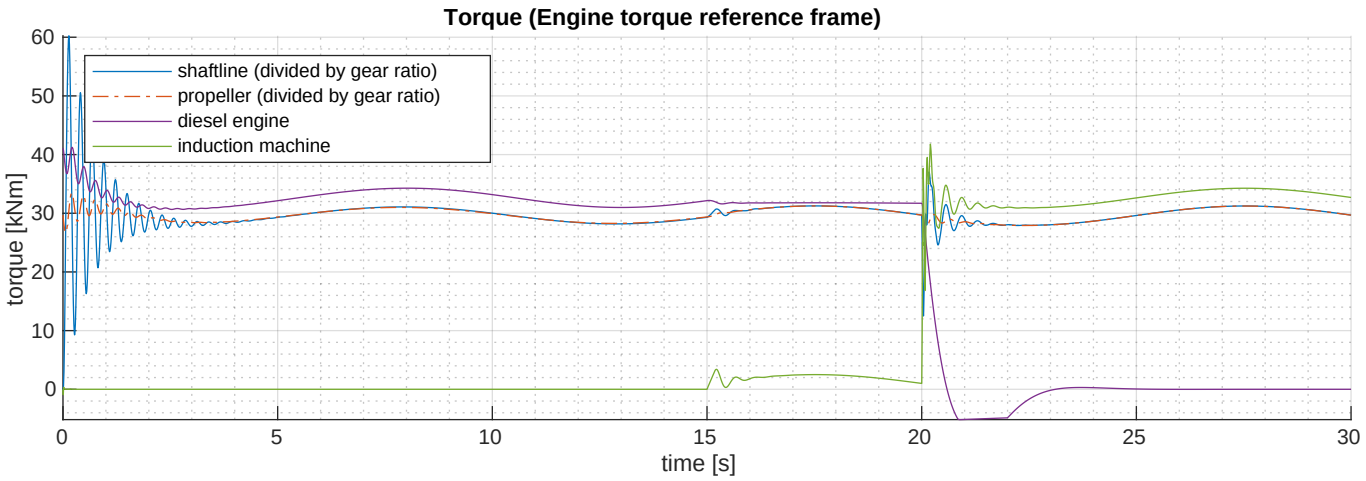

Figure 3.23: Torques in the engine torque reference frame for the transition from diesel to electric mode using the staged transition approach in sea state 3.

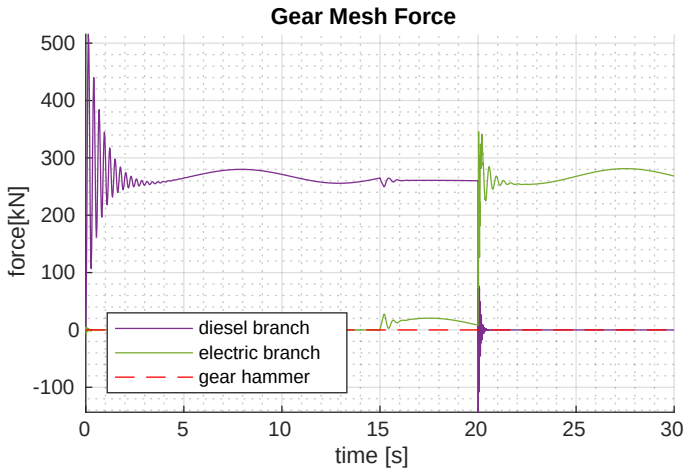

Figure 3.24: Gear mesh force for the transition from diesel to electric mode using the staged transition approach in sea state 3.

3.3.2.4 Concluding Summary of the Staged Diesel to Electric Transition Results

- During the parallel speed control phase the induction machine provides the torque corresponding with the wave disturbance. The diesel engine maintains steady state torque until the diesel engine clutch is disengaged.
- The speed controller of the induction machine quickly responds to the disengagement of the diesel engine clutch with a torque step. This triggers a torsional vibration in the transmission system with a maximum peak-to-peak amplitude with a magnitude corresponding with 50% of the steady state torque.
- The transitions induces a significant disturbance in the electric power.
- Due to the fast response of the induction machine the speed of the propeller only drops by 2% during the transition.
- As the gear of the diesel engine almost instantly transitions from driving to being driven, gear hammer is observed in the diesel engine gear mesh.

3.3.3 Impact of Clutch Operation in the Staged Transitions

By comparing the results of the diesel to electric and electric to diesel transitions the following characteristic has been formulated:

- No significant handover of drive torque during the parallel speed control phase. Only the deactivation of the clutch of the original engine triggers a significant response of the speed controller corresponding with the new mode.
- The relatively relaxed tuning of the diesel engine speed controller results in a significant drop of the propeller speed and triggers a moderate torsional vibration.
- The strict tuning of the induction machine speed controller results in a limited drop of the propeller speed at the cost of triggering an more severe torsional vibration.
- As the engine of the initial mode is still providing the drive torque when the clutch is disengaged, the corresponding gear rapidly transitions from driving to driven, resulting in gear hammer.

It is concluded that the impact of clutch operation in a propulsion mode transition where the staged approach is applied is characterised by a lack of drive torque handover during the parallel speed control phase.

3.4 Propulsion Mode Transitions using the Torque Controlled Approach

In this section the results of the propulsion mode transition simulations, where the torque controlled approach is used, are discussed. In subsection 3.4.1 the electric to diesel transition simulation results are discussed. In subsection 3.4.2 the diesel to electric transition simulation results are discussed. In subsection 3.4.3 the electric to diesel transition simulation results for a rough sea are discussed. Subsection 3.3.3 concludes this section by characterising the discussed simulation results for the torque controlled propulsion mode transition approach.

3.4.1 Results Torque Controlled Electric to Diesel Transition

In this subsection the simulation results for the torque controlled transition from electric to diesel mode are presented and discussed. In the torque controlled transition, in addition to a $5\ s$ overlap in clutch engagement and disengagement, the torque control mode for the induction machine is used to ramp down the torque.

3.4.1.1 Clutch Operation

The torque controlled transition is characterised by, in addition to the staged transition approach, the use of the induction machine in torque control mode to achieve a smooth transition. In figure 3.25 it becomes apparent that this results in a gradual handover of driving torque between the engines. As the torque of the induction machine ramps down, the speed governor of the diesel engine takes over. In fig. 3.27 this behaviour is confirmed as the fuel setpoint shows a gradual increase during the transition.

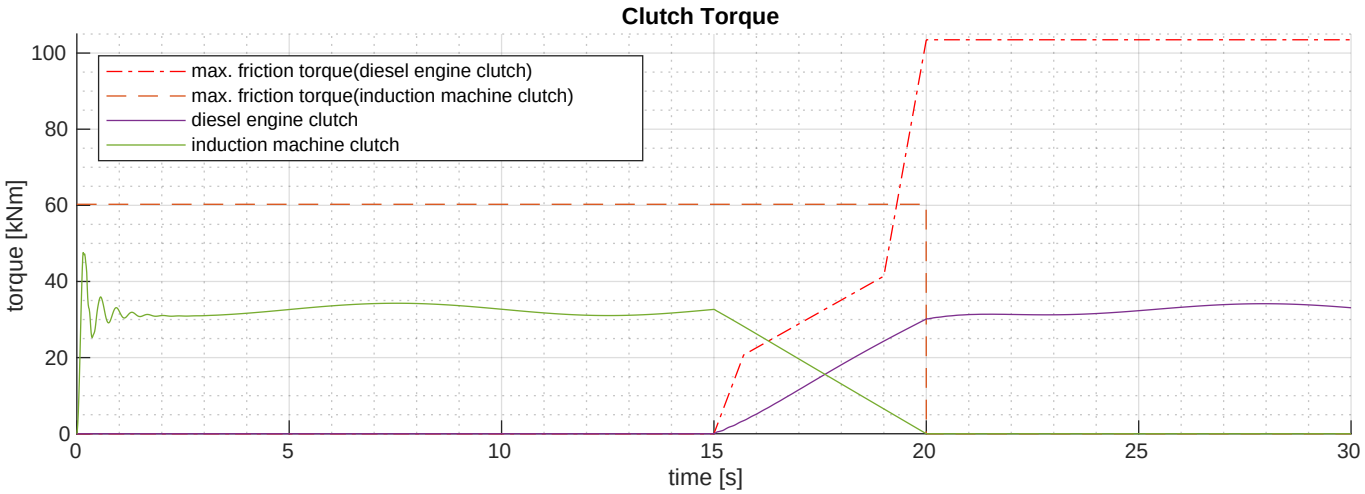

Figure 3.25: Clutch torque for the transition from electric to diesel mode using the torque controlled transition approach in sea state 3.

3.4.1.2 Impact on Propulsion System Rotational Speeds

As a result of the gradual handover of the torque it can be expected that there is a corresponding limited drop in propeller speed. This behaviour is indeed observed in fig.3.26, the speed of the propeller only drops by approximately 5% during the transition.

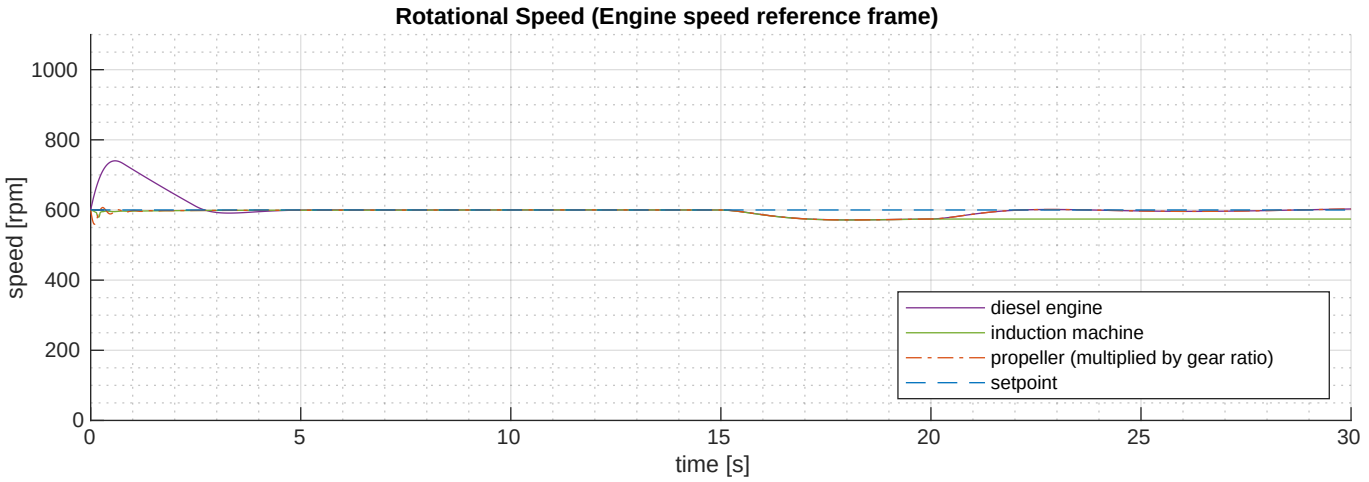

Figure 3.26: Rotational speed in the engine speed reference frame for the transition from electric to diesel mode using the torque controlled transition approach in sea state 3.

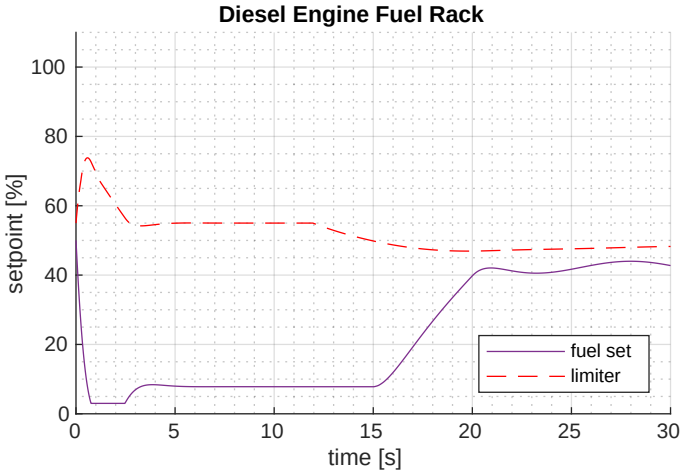

Figure 3.27: Diesel Engine fuel rack setpoint for the transition from electric to diesel mode using the torque controlled transition approach in sea state 3.

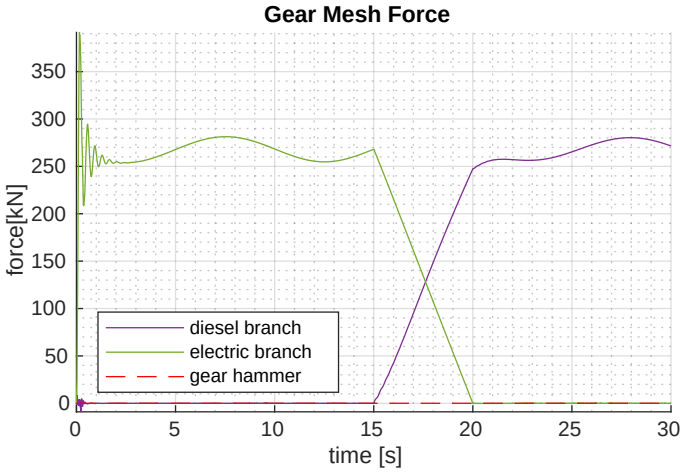

Figure 3.28: Gear mesh force for the transition from electric to diesel mode using the torque controlled transition approach in sea state 3.

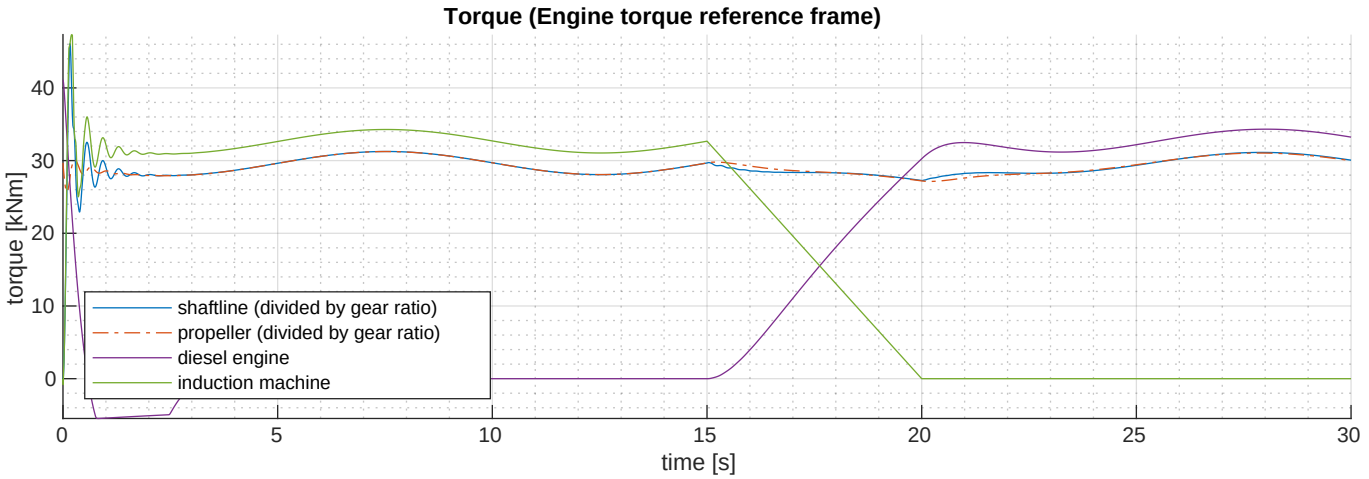

Figure 3.29: Torques in the engine torque reference frame for the transition from electric to diesel mode using the torque controlled transition approach in sea state 3.

3.4.1.3 Impact on Propulsion System Torque

In fig.3.29 the gradual transition from the induction machine to the diesel engine is further confirmed. There is no longer a gap in applied torque, as can be observed from the continuation of the shaft line torque at approximately the steady state level between $t = 15\ s$ and $t = 20\ s$. As a result of the handover of drive torque no torsional vibration is excited. This is the result of the angle of twist in the shaft line being sustained throughout the transition and the angle of twist in the flexible couplings being introduced gradually. This is a contrast with both the instant and staged approaches where the sudden application of torque excites significant torsional oscillations. The smooth transition is also able to eliminate hammering of the gears entirely. The mesh forces in fig.3.28 show a gradual in/decrease as a reflection of the gradual handover of the torque.

3.4.1.4 Concluding Summary of the Torque Controlled Electric to Diesel Transition Results

- As the induction machine torque ramps down the diesel engine speed controller takes over, resulting in a gradual handover of drive torque between the engines.
- As a result of the relatively relaxed tuning of the diesel engine the speed of the propeller drops 5% during the transition.
- As a result of the gradual handover of drive torque there are no torsional vibrations triggered in the transmission system.
- As a result of the gradual handover of drive torque there is no indication of gear hammer.

It is concluded that the torque controlled transition approach is able to significantly limit the impact of clutch operation in a propulsion mode transition from electric to diesel propulsion.

3.4.2 Results Torque Controlled Diesel to Electric Transition

In this subsection the simulation results for the torque controlled transition from diesel to electric are presented and discussed. In the torque controlled transition, in addition to a $5\ s$ overlap in clutch engagement and disengagement, the torque control mode for the induction machine is used to ramp up the torque. The speed controller of the diesel engine is then forced to respond by reducing the torque output.

3.4.2.1 Clutch Operation

In the period that both clutches are engaged the torque of the induction machine ramps up to the torque level of the diesel engine at $15\ s$. As a result the diesel engine torque should be gradually reduced as the speed controller responds. This matches with the observed behaviour in fig.3.30, the torque of the diesel engine reduces and the torque of the induction machine rises to the steady state level. From the diesel engine fuel rack and electric drive power it can be observed that the controllers hand over the provision of power during the parallel period. A significant torsional vibration can however be observed when the diesel engine clutch disengages, this results from the switch from torque control to speed control of the induction machine which will be discussed further on.

3.4.2.2 Impact on Propulsion System Rotational Speeds

In fig.3.30 it can also be observed that the induction machine torque is limited by the clutch friction around the $19\ s$ mark. The result of this is a brief period of slip that can be observed as a bump in the induction machine speed in fig.3.33. As the tuning of the diesel engine speed controller is relaxed the response to the torque ramp of the induction machine lags behind slightly. Therefore the torque during the parallel engaged clutches exceeds the required torque and the speed of the propeller increases as can be observed in fig.3.33. When the induction machine is set to speed control mode the speed is quickly restored to the setpoint.

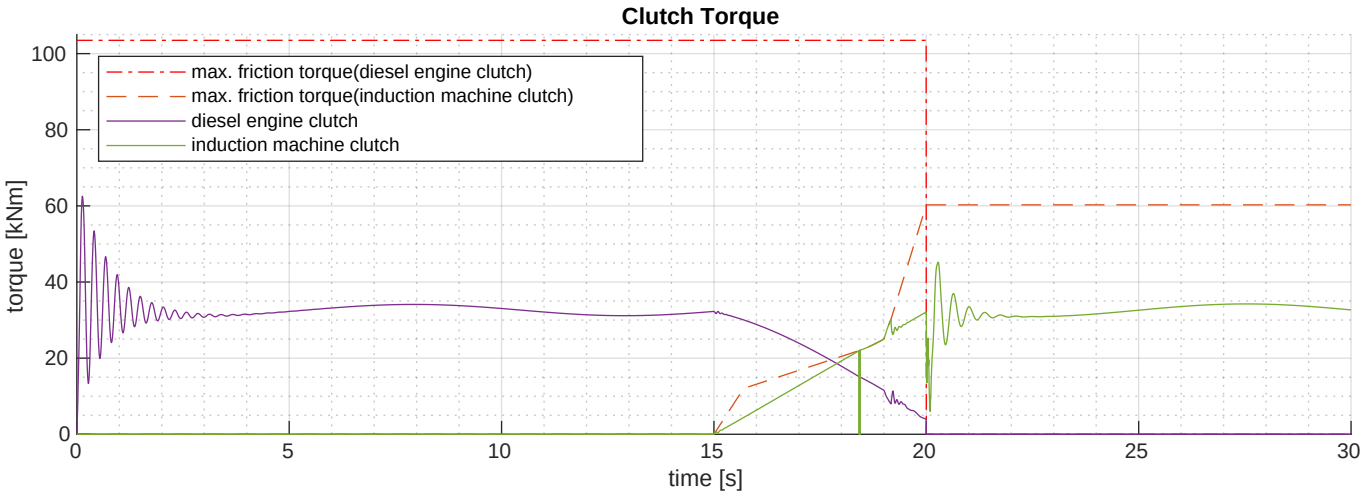

Figure 3.30: Clutch torque for the transition from diesel to electric mode using the torque controlled transition approach in sea state 3.

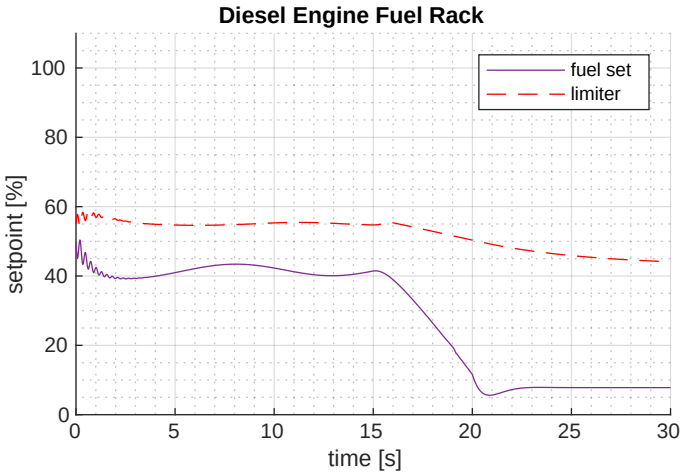

Figure 3.31: Diesel Engine fuel rack setpoint for the transition from diesel to electric mode using the torque controlled transition approach in sea state 3.

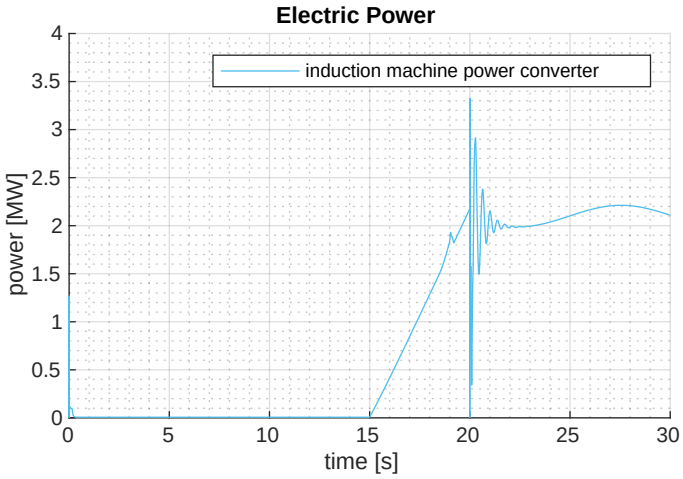

Figure 3.32: Induction machine drive power for the transition from diesel to electric mode using the torque controlled transition approach in sea state 3.

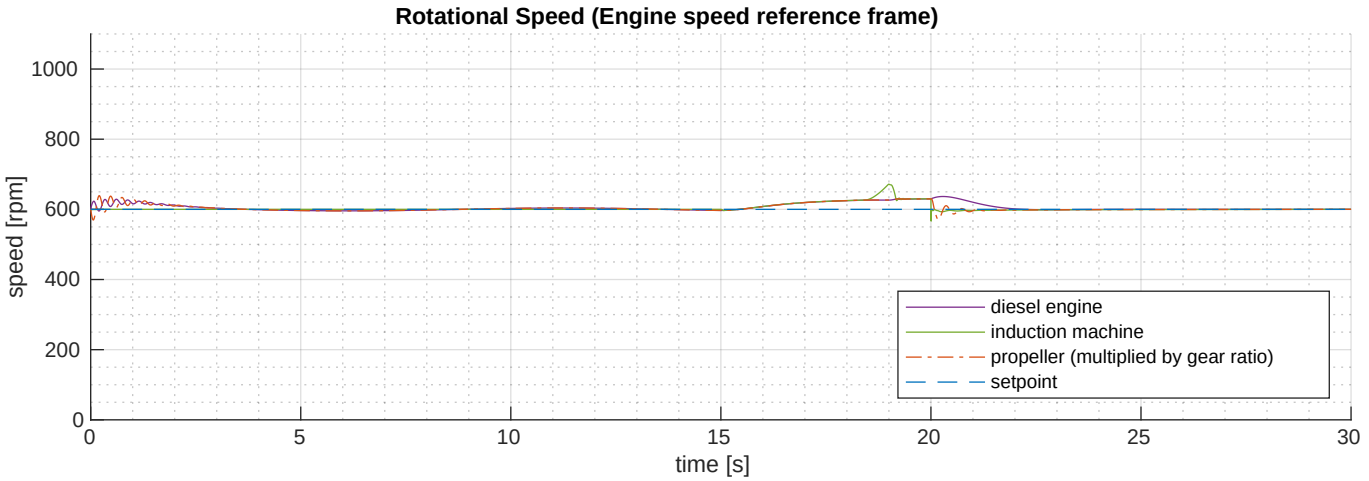

Figure 3.33: Rotational speed in the engine speed reference frame for the transition from diesel to electric mode using the torque controlled transition approach in sea state 3.

3.4.2.3 Impact on Propulsion System Torque

The disturbance of the torque in the slip period at $19\ s$ is insignificant and the torque signals smoothly transition during the parallel phase. The most notable observation from fig.3.30 is the significant torsional vibration at $20\ s$, when the diesel engine's clutch disengages. This is the result of the induction machine switching from torque control to speed control while there is a significant deviation of the shaft speed from its setpoint. The speed controller of the induction machine rapidly responds to this deviation with a large negative torque step, observable in fig.3.34. This negative torque step quickly restores the propeller speed to the setpoint, it also triggers the observed torsional vibration and applies a significantly disturbed power profile to the systems power system that is observable in fig.3.32.

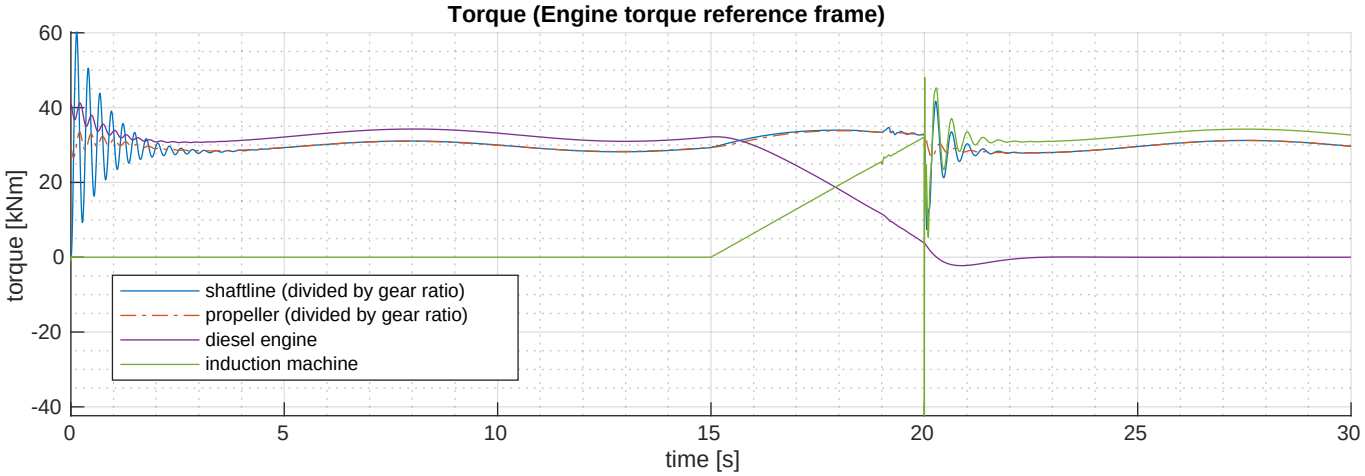

Figure 3.34: Torques in the engine torque reference frame for the transition from diesel to electric mode using the torque controlled transition approach in sea state 3.

As the diesel engine torque is not at zero when the diesel engine clutch disengages there is a minor occurrence of gear hammer observed in fig.3.35 for the diesel engine branch. The negative torque step of the induction machine does not lead to the occurrence of gear hammer as the torque does not cross zero at the gear mesh interface.

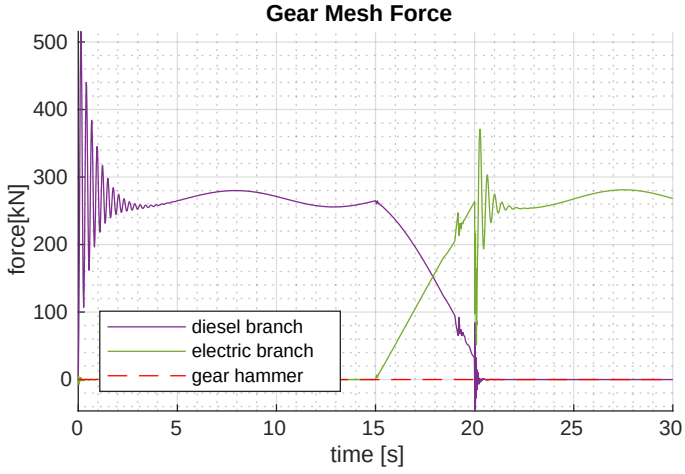

Figure 3.35: Gear mesh force for the transition from diesel to electric mode using the torque controlled transition approach in sea state 3.

3.4.2.4 Concluding Summary of the Torque Controlled Diesel to Electric Transition Results

- As the induction machine torque ramps up, the speed controller of the diesel engine responds with a gradual reduction in torque.
- During the handover the relaxed tuning of the diesel engine results in a 5% over-speed of the propeller. When the diesel engine clutch is disengaged and the induction machine control mode is set to speed control, the over-speed causes the induction machine speed controller to introduce a negative torque pulse to reduce the propeller speed. This causes a torsional vibration in the transmission system with a maximum peak-to-peak amplitude with a magnitude 115% of the steady state torque.
- A significantly disturbed power profile results from the induction machine switch from torque to speed control.
- The torque ramp up of the induction machine is temporary limited by the clutch friction. As a result the induction machine speeds up rapidly. Given that the limitation is only small, this causes little problems. A large limitation of transferable torque in a torque controlled mode might however be problematic, as during clutch slip the speed of the induction machine is uncontrolled.
- When the diesel engine clutch is disengaged gear hammer is identified in the diesel engine gear mesh.

The torque controlled transition approach is unsuccessful in limiting the impact of clutch operation in the diesel to electric transition. The main issue is the response of the induction machine to the switch from torque control to speed control.

3.4.3 Results Torque Controlled Electric to Diesel Transition in a Rough Sea

It is concluded that the torque controlled transition approach is able to significantly limit the impact of clutch operation in a propulsion mode transition from electric to diesel propulsion. To asses if the torque controlled transition approach is also able to limit the impact in rough sea conditions, an additional simulation is performed with the sea state set to 5.

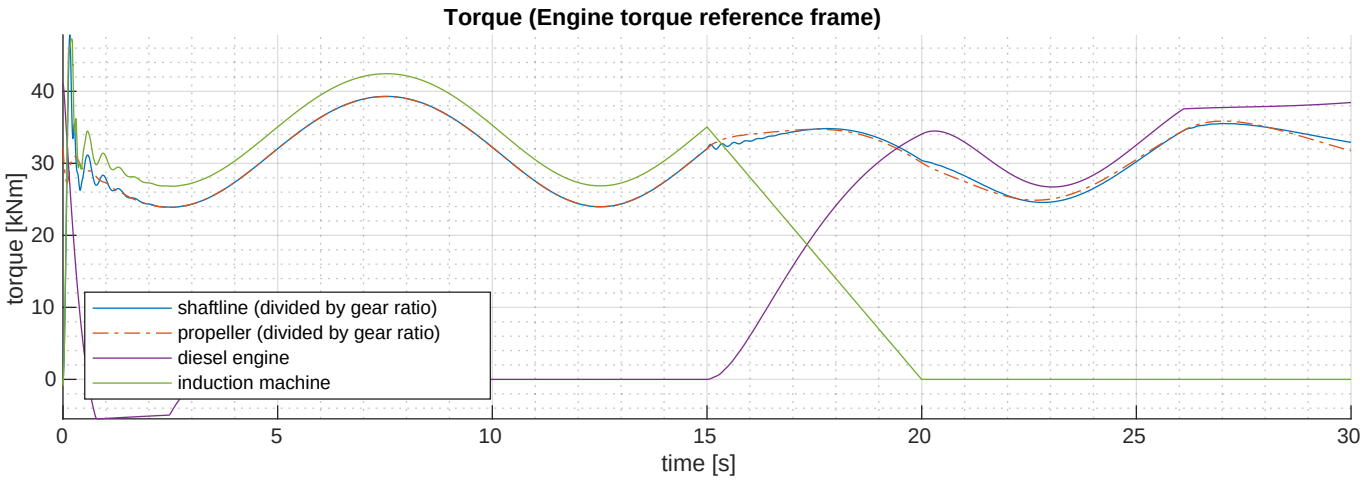

Figure 3.36: Torques in the engine torque reference frame for the transition from electric to diesel mode using the torque controlled transition approach in sea state 5.

From the propulsion system torques in fig.3.36 a similar smooth transition as in sea state 3 can be observed. A minor oscillation in the shaft line torque can be observed at $t = 15\ s$, the result of the increased wave disturbance as the diesel engine speed controller has to ramp up the fuel setpoint while the resistance of the propeller is increasing due to the wave. The magnitude of the vibration is insignificantly small compared to the observed oscillations in the instant and staged transition approaches.

The impact of the transition on the speed on the propeller is limited as can be observed in fig.3.37. The speed of the propeller drops by about 8% during the transition, this has to be attributed to the relaxed tuning of the diesel engine.

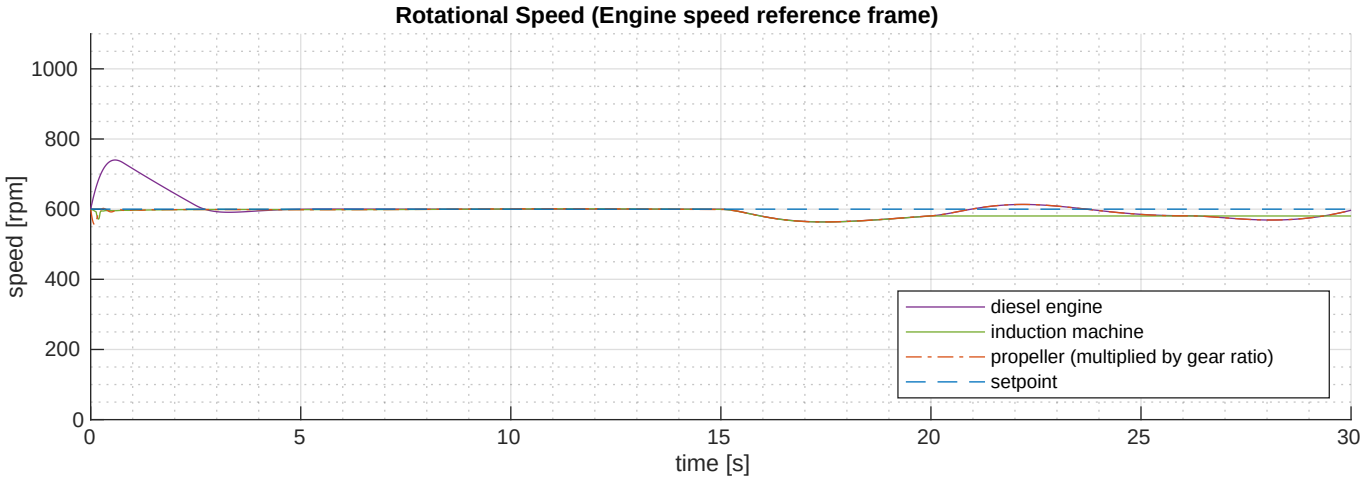

Figure 3.37: Rotational speed in the engine speed reference frame for the transition from electric to diesel mode using the torque controlled transition approach in sea state 5.

In fig.3.36 it can be observed that the diesel engine torque continues in a straight line from $t = 26\ s$ onward. This indicates the fuel flow limiters coming into action to prevent engine overload. In fig.3.38 it is observed that the operation of the diesel engine is indeed at the boundary of the envelope. A transition to diesel mode in these conditions is questionable. In fig.3.39 it can be observed that the induction machine operates within its operating window. It would thus be better to remain in electric mode or transition to a parallel control mode where the induction machine supports the diesel engine.

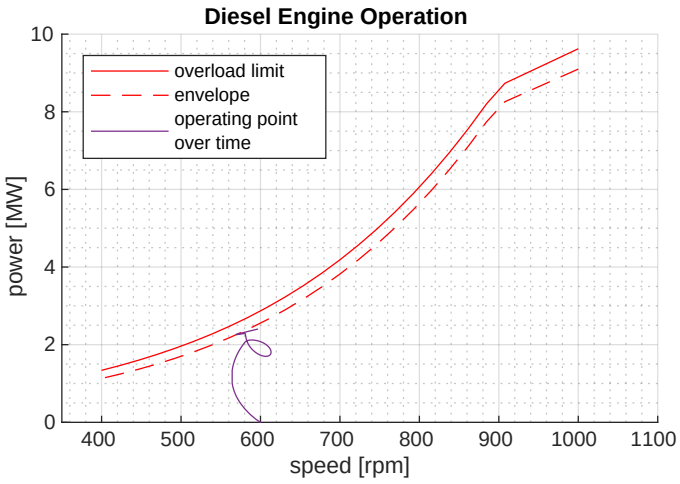

Figure 3.38: Operation of the diesel engine for the transition from electric to diesel mode using the torque controlled transition approach in sea state 5.

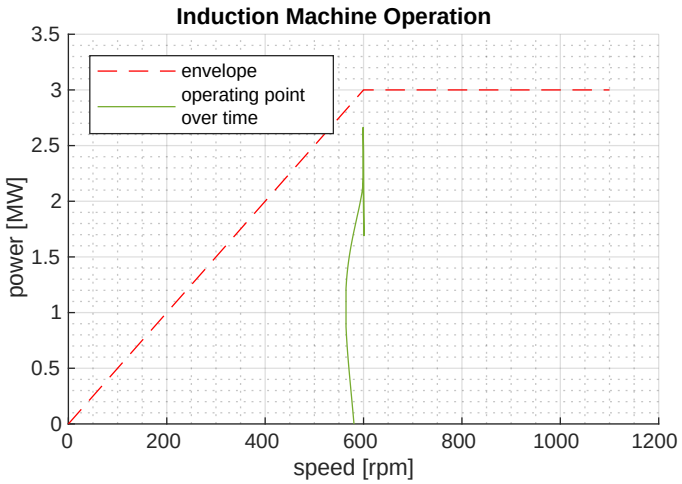

Figure 3.39: Operation of the induction machine for the transition from electric to diesel mode using the torque controlled transition approach in sea state 5.

3.4.3.1 Wave Disturbance

It can be concluded that the torque controlled transition approach successfully limits the impact of clutch operation in a transition from electric to diesel mode in a rough sea condition. However, it must be noted that the wave frequency of $0.1\ Hz$ that corresponds with a $5\ s$ half-wave period nicely matches with the $5\ s$ duration of the transition. Combined with the fact that the phase of the wave disturbance aligns with the timing of the transition, as it is initiated at $15\ s$ which is a multiple of the $5\ s$ half wave period. As a result the torque demand at $15\ s$ closely matches the torque demand at $20\ s$. An improvement of the test of the

transition approach would be to perform two additional simulations where the transition is timed to initiate either at the peak or the trough of the wave. This improvement does however not address the fact that a actual wave spectrum is seldom homogeneous and perfectly sinusoidal. It would thus be best to implement a wave disturbance model corresponding with a fully developed wave spectrum to be able to asses the performance of operational transition approaches in rough sea.

3.4.3.2 Conclusions for the Rough Sea Torque Controlled Electric to Diesel Transition Results

- The torque controlled transition approach successfully limits the impact of clutch operation in a transition from electric to diesel mode in a rough sea condition.
- The increased wave disturbance does result in a minor torsional vibration when the speed control is handed over from the induction machine to the diesel engine.
- The transition from electric to diesel in rough sea conditions is questionable as the diesel engine has to operate at the boundary of its envelope as a result. The Induction machine does operate within its envelope and remaining in electric mode or transitioning to a parallel propulsion mode would be most likely be a better option.
- It must be noted that the used wave disturbance model does not represent the best test for the rough sea condition and mode transitions in rough sea conditions should be further investigated in future research.

3.4.4 Impact of Clutch Operation in the Torque Controlled Transitions

By comparing the results of the diesel to electric and electric to diesel transitions the following characteristic is formulated:

- The torque ramp of the induction machine results in a gradual handover of drive torque.
- In the electric to diesel transition there is no occurrence of torsional vibration or gear hammer.
- The transition form torque control to speed control mode in the diesel to electric transition causes problems when the diesel engine clutch disengages and induction machine control switches from torque to speed control.
- The torque controlled transition approach successfully limits the impact of clutch operation in a transition from electric to diesel mode in a rough sea condition. It must be noted that the used wave disturbance model does not represent the best test for the rough sea condition. Also the transition from electric to diesel in rough sea conditions does not make sense as the diesel engine has to operate at the boundary of its envelope as a result.

It is concluded that the torque controlled transition approach successfully limits the impact of clutch operation in the electric to diesel transition. The torque controlled approach is unsuccessful in limiting the impact of clutch operation in the diesel to electric transition as the switch from torque control to speed control for the induction machine significantly disturbs the system. The transitions simulation indicate that the performance of the torque controlled transition in a rough sea is promising. However, this has to be further investigated in terms of wave disturbance and suitability of the propulsion modes.

3.5 Comparison of the Impact of Clutch Operation in the Simulations

In this section, the impact of clutch operation in the simulated propulsion mode transitions is compared. This comparison is based on the summarised simulation results in table.3.1 and the characterisation of the results of the transition approaches in subsection 3.2.3, 3.4.4, 3.3.3.

Table 3.1: Table summarising the key results of the operational transitions between electric(E) and diesel(D) mode at a speed of 10 knots(18.5 km/h), corresponding with a engine speed setpoint of 600 rpm, in sea state 3.

Transition	Approach	Clutch Slip	Clutch Temp.	Propeller Speed (max. deviation)	Torsional Vibration (max. p-to-p amplitude)	Gear Hammer
E to D	Instant	3 s	+ 2 °C	-25%	160 % of steady state	both gears
D to E	Instant	4.5 s	+ 12 °C	-30%	200 % of steady state	both gears
E to D	Staged	0 s	+ 0 °C	-15%	25 % of steady state	electric gear
D to E	Staged	0.25 s	+ 0 °C	-2%	50 % of steady state	diesel gear
E to D	T-Controlled	0 s	+ 0 °C	-5 %	not identified	not identified
D to E	T-Controlled	1 s	+ 1 °C	+5%	115 % of steady state	diesel gear

It is concluded in section 3.2.3 that the instant approach is characterised by a lack of drive torque during the transition. This lack of drive torque finds its origin in a slipping clutch and results in significant torsional vibrations a large drop in propeller speed, as can be asserted from table3.1.

The gap in drive torque characterising the instant approach can be prevented by overlapping the envelopes of the clutches as implemented in the staged approach. In section 3.3.3 it is concluded that the staged approach is characterised by a lack of drive torque handover during the parallel speed control phase. As a result of the poor handover during the parallel speed control phase the transmission system is significantly impacted when the clutch of the original mode deactivates. Even so, when comparing the magnitudes of the impact on the system in table 3.1 it must be concluded that the staged approach significantly outperforms the instant approach.

To aid the handover in the parallel phase the induction machine can be set to torque control mode and the torque can be ramped up or down depending on the transition, this is implemented in the torque controlled approach. In section 3.4.4 it is concluded that the torque controlled transition successfully limits the impact of clutch operation in the electric to diesel transition. The approach is unsuccessful in the diesel to electric transition as the switch from torque control to speed control for the induction machine significantly disturbs the system.

3.5.1 Conclusions

The impact of clutch operation in the simulated propulsion mode transitions is in general characterised by:

- Significant torsional vibrations
- Gear hammer
- A drop in propeller speed

The impact can be limited by implementing an appropriate propulsion control approach for the transition. A torque controlled handover of drive torque between drive engines is identified as a suitable approach. However, ramping up the induction machine torque and switching from torque control to speed control is found to introduce significant disturbances in the system. As a result the used implementation of the torque controlled approach does not perform well in the diesel to electric transition.

3.6 Discussion of the Propulsion Mode Transition Simulation Results

In this section, the results of the propulsion mode transition simulations are discussed from a more general perspective. In subsection 3.6.1 the impact on the hybrid propulsion system is discussed. In subsection 3.6.2 the operation of the clutch is discussed. In subsection 3.6.3 the influence of the primary controllers is discussed. In subsection 3.6.4 propulsion mode transitions are discussed.

3.6.1 Impact on the Hybrid Propulsion System

3.6.1.1 Impact on the Electric Power System

For the torque controlled diesel to electric transition in subsection 3.4.2 it is identified in fig.3.32 that a significantly disturbed power profile results from the induction machine switch from torque to speed control. A similar result is observed in subsection 3.3.2, where the staged diesel to electric transition induces a significant disturbance in the electric power, which can be assessed in fig.3.21. A pattern emerges where the response of the induction machine controller, to the sudden increase in load, introduces power peaks in the load profile. These power peaks have to potential to severely disrupt the stability of the ships power system. The power system is however out of scope for the current research. It is recommended to further investigate the impact of these load peaks on the power system of the ship in further research.

3.6.1.2 Impact on Transmission System Wear

In the results of the propulsion mode transition simulations, the von-mises equivalent stress does not approach the yield limit in any experiment. However, the stress in the shaftline has a significant amplitude and frequency, the possible fatigue damage this causes is currently not taken into consideration. Similarly it is concluded that propulsion mode transitions is in general characterised by the occurrence of gear hammer. The impact of gear hammer on the wear of the tooth surface is not considered in this thesis. This impact might be significant considering the magnitudes and frequency of the identified gear hammer. More research in this area is needed to provide more insight into possible impact on wear of the system components. The model developed in this thesis can be the basis for such research. This research direction could extend to the development of condition monitoring in regards to wear on the transmission system components.

3.6.1.3 Impact on Clutch Temperature

In the results of the propulsion mode transition simulations in table 3.1, a significant rise of the clutch temperature is observed in the diesel to electric transition where the instant transition approach is applied. This rise in temperature coincides with the relatively long duration of the slip period. This long slip results from the induction machine speed being maintained at the reference $600\ rpm$ while the drive torque, and thus the speed of the propeller, is limited by the clutch. This behaviour can be prevented by implementing more advanced approaches for the transition control, as shown in this thesis. The clutch slip and corresponding rise in clutch temperature is limited in the other simulations. A temperature rise of a couple of Celsius cannot be considered significant considering that the absolute limit for the oil is $200\ ^{\circ}C$. It is concluded that the temperature development of clutch during the propulsion mode transitions is not significant.

3.6.1.4 Impact on Engine Operation

In subsection 3.4.2, concerning the simulation results of the torque controlled diesel to electric transition. The torque ramp up of the induction machine is temporary limited by the clutch friction. As a result, the induction machine speeds up rapidly as a result of increasing the motor torque. Given that the limitation is only small this causes little problems. However, a large limitation of transferable torque in a torque controlled mode might be problematic. During clutch slip the speed of the induction machine is uncontrolled. This could lead to a sudden high speed of the induction machine, potentially damaging the transmission system

or engine. To prevent the unbounded increase of the engine speed when the drive torque is limited by a slipping clutch, it is advisable to include a speed limiter for engines operating in a torque control mode.

3.6.1.5 Impact on Torsional Vibrations

It is concluded in section 3.5 that the impact of clutch operation in the simulated propulsion mode transitions is, in general, characterised by significant torsional vibrations. These torsional vibrations further impact the system in terms of gear hammer, possible fatigue damage to the shaftline and disturbance of the power system as a result of the induction machine control response to the vibrations. It is not considered within the scope of this thesis how these torsional excitations interact with the steady state torsional vibrations in the system. This could be addressed in further research by including the torsional vibration characteristics of both the propeller and diesel engine in the system model. The fidelity of the transmission system inertias also has to be increased for detailed analysis of the torsional vibration characteristic.

3.6.2 Clutch Operation

3.6.2.1 Influence of the Clutch Pressure Profile

For the instant transition approach, it is concluded that the source of the impact of clutch operation is the limitation of drive torque. The transmitted torque is determined by the applied pressure on the clutch disks that follows a predefined profile. If the clutch pressure could be ramped up more rapidly, how then would this change the impact of the clutch operation during the mode transition? A faster ramp up of clutch pressure in the limit case would result in an instant application of full pressure. This scenario is not tested directly, however, the results of the staged transition approach give a good indication of what the effect would be. As there is a limited handover of drive torque in the staged transition it is comparable with the limit case of the instant approach where maximum clutch pressure is applied instantaneously when the clutches are actuated. A more rapid application of clutch pressure for the instant approach is expected to reduce the impact of the operation of the clutches in the transition. This could be further investigated by implementing a model of the clutch oil pressure system. With such a model the influence of the pressure curve, based on physical constraints of the actuation system, could be investigated.

3.6.2.2 Potential of a pressure controlled clutch disengagement

In the staged transition approach the sudden disengagement of the clutch results in gear hammer. A smooth disengagement, where the pressure of the clutch is ramped down, could probably alleviate this problem. Moreover, the limiting of drive torque by the clutch would force the speed controller of the engine of the new mode to take over. This would most probably result in a transition similar to the torque controlled transition approach. However, the use of the clutch as a torque controller would subject the clutch to more wear. Given these potential benefits, it is recommended for further research to investigate the implementation of a pressure controlled clutch disengagement.

3.6.2.3 Clutch Friction

In the used model, clutch friction is assumed zero when the applied pressure is zero. In reality the clutch always has some friction between the plates and between the plates and the housing, due to the oil being present. Manufacturers try to prevent this by introducing mechanisms that force separate the clutch plates when disengaged. The effect of the clutch friction losses are not expected to contribute significantly to the transient dynamics during clutch engagement. They might be significant for energy efficiency studies, as the constant losses might add up to significant values. Further research is needed to asses if the continuous energy losses in friction clutches are significant.

3.6.3 Influence of the Primary Controllers

3.6.3.1 Control Objective

It is identified that the tuning of the speed controller contributes significantly to the impact of the clutch operation in the investigated operational propulsion mode transitions. The relaxed tuning of the diesel engine is characterised by greater deviations of the propeller speed and more limited torsional vibrations in the transmission system. The tuning of the induction machine is characterised by a strict adherence to the speed setpoint at the cost of inducing significant torsional vibrations in the system. The motivation behind the relaxed tuning of the diesel engine is to reduce thermal load on the engine. It is observed that the high torque, that is needed for the strict response of the induction machine, is reflected in the electric power demand of the converted. The high degree of electric power variation in a short time interval severely loads the electric power system. Similar as for the diesel engine, tuning the induction machine speed controller for a more relaxed response might therefore be beneficial. This would also reduce the peak torque loads and induced vibrations in the propulsion system.

This leads to the question: What should the ultimate control goal be? In general, a trade-off between constant speed (preferred from a maritime point of view), constant torque (preferred from a mechanical point of view) and constant power (preferred from an electrical point of view) has to be made, but this trade-off is not static. Rapid ship manoeuvring might be required, preferring propeller speed control, in other cases the state of charge of batteries might limit the power availability which shifts the control approach preference to power control. Finally, from condition monitoring it might be concluded that when the propulsion system components are at or near a fatigue failure, the propulsion system could benefit from torque control that limits the torque fluctuations in the system until the component can be fixed or replaced. Model based control with a cost function based on the system state that balances these control objectives might be a way to approach this trade-off.

3.6.3.2 Influence of Speed Control on Clutch Slip

For the instant approach in table. 2.5 it can be identified that the rise of the clutch temperature in the diesel to electric transition is significantly greater than for the electric to diesel transition. This is the result of the speed control tuning. The electric machine is maintained at the speed setpoint for the entire duration of the slip, which results in a relatively high slip. The diesel engine speed control is relatively relaxed, slip magnitude is lower and therefore the heat flux into the clutches is lower. The speed controllers indirectly control the speed of the propeller as their direct feedback is the speed of the respective engines. As a result, the induction machine speed is maintained at the setpoint during the slip. If the speed controllers would receive the speed feedback of the propeller. Then as the clutch is slipping, the propeller and engine speeds would differ. This would most likely result in a runaway of the engine speed as the speed controller aims to increase propeller speed but is limited by the slipping clutch. This would result in an even higher increase in clutch temperature and would dissipate energy without necessity. A solution could however be the implementation of anti wind-up in the speed controller.

3.6.3.3 Potential for Diesel Engine Torque Control

It is concluded that using the induction machine in torque control mode to control the diesel to electric transition is unsuccessful in limiting the impact of clutch operation. A solution to this problem could be to use the diesel engine in torque control mode for the transition. Then, the induction machine could be in speed control mode for the entirety of the transition and the problem when switching from torque to speed control could be prevented. Diesel engine torque control could even be implemented without needing any torque sensors in the system. The position of the fuel rack from the start of the transition could be ramped down. However, it must be avoided to stall the diesel engine in this process. It would be worthwhile to implement torque control for the diesel engine. This can then be used in a torque controlled handover of drive torque from the diesel engine to the electric motor in a propulsion mode transition.

3.6.4 Propulsion Mode Transitions

3.6.4.1 Emergency Operations

In [17] acceleration and crash-stop manoeuvres for ship propulsion systems are investigated. Transitioning between operational modes for emergency operations has not be considered within the scope of this research. Emergency manoeuvres could be investigated by extending the propeller and hull models for four quadrant operation. This would enable reversing the ship and thus enable the emergency performance to be evaluated. Specifically the case where the ship has to be reversed quickly is relevant for further research. It is expected that this case subjects the propulsion system to peak loads and disturbances.

3.6.4.2 Parallel Control Modes

In subsection 3.4.3 the results for an electric to diesel transition in rough sea are discussed. It is concluded that transition from electric to diesel in rough sea conditions is questionable, as the diesel engine has to operate at the boundary of its envelope as a result. It is also observed that the induction machine does operate within its envelope, and that remaining in electric mode or transitioning to a parallel propulsion mode would be most likely be a better option. Parallel propulsion modes have not been considered within the scope of this research, however the advantages of such modes are shown in [14], [5]. It would therefore be worthwhile to further extend the research in this thesis and apply the developed model for investigating transitions concerning parallel propulsion modes.

For further research in this direction, it is advised to consider the use of controllable pitch propeller. Controllable pitch propellers unlock the full potential of hybrid propulsion systems, when the electric machine can both be used as motor and generator [36]. The propeller should then be matched considering the combined maximum electric and diesel power [69].

3.6.4.3 Environmental Conditions

In subsection 3.4.3 the results for an electric to diesel transition in rough sea are discussed. It is concluded that the used wave disturbance model does not represent rough sea condition to a satisfactory degree, and that mode transitions in rough sea conditions should be further investigated in future research. The current wave model only disturbs the wake of the propeller with a single harmonic disturbance and the hull resistance remains constant. Improvements to this model for future research could be made by introducing time series data of wave disturbances having a full wave spectrum, as suggested by prof. Stapersma in a discussion on the topic. In extension, the wave model can be further improved by considering the dynamic fluctuations of both the propeller wake and hull resistance.

3.7 Conclusions

The main research question: "*What is the impact of clutch operation in propulsion mode transitions on hybrid maritime propulsion systems?*" has been addressed in this chapter. The implemented model of the hybrid propulsion system is used to simulate and evaluate the impact of clutch operation in propulsion mode transitions. Sailing at 10 knots in sea state 3, corresponding with a 600 rpm engine speed setpoint, is selected in section 3.1 as an appropriate operation point for the operational transitions between diesel and electric propulsion. The instant approach, staged approach and torque controlled approach have been applied to the transition. The results of the simulations have been analysed and compared in sections 3.2-3.5 leading to the following conclusions:

- The instant approach results are characterised by a gap in transmittable drive torque, with significant impact on the propulsion system as a result.
- The staged approach results are characterised by a lack of drive torque handover during the parallel phase, with significant impact on the propulsion system as a result.
- The torque controlled approach results are characterised by a smooth handover of drive torque with a limited impact on the propulsion system as a result. The torque controlled approach is unsuccessful in limiting the impact of clutch operation in the diesel to electric transition as the switch from torque control to speed control for the induction machine significantly disturbs the system.
- The effectiveness of the torque controlled transitions approach in a rough sea has been investigated and it is concluded that the torque controlled transition approach successfully limits the impact of clutch operation for the electric to diesel transition in the rough sea condition.
- In general, the impact of clutch operation in the operational transitions between diesel and electric propulsion is characterised by significant torsional vibrations, gear hammer and a drop in propeller speed.
- The impact can be limited by implementing an appropriate propulsion control approach for the transition. A torque controlled handover of drive torque between engines is identified as a suitable approach.

In section 3.6 the results of the propulsion mode transition simulations have been discussed from a more general perspective, resulting in the following conclusions and recommendations:

- It is recommended to investigate the impact of the power peaks, that are introduced by the induction machine as a result of the mode transition, on the power system of the ship in further research.
- The stress in the shaftline has a significant amplitude and frequency, possibly causing fatigue damage. The wear of the tooth surface might be significant considering the magnitudes and frequency of the identified gear hammer. Further research is needed to provide more insight into possible impact on wear and fatigue of the system components. The modelling work in this thesis could be the basis for such research.
- It is concluded that the temperature development of clutch during the propulsion mode transitions is not significant.
- To prevent the unbounded increase of the engine speed when the drive torque is limited by a slipping clutch, it is advisable to include a speed limiter for engines operating in a torque control mode.
- In future research it could be investigated how the torsional excitation from clutch engagement interact with the steady state torsional vibrations in the system. This could be done by including the torsional vibration characteristics of the propeller and diesel engine in the propulsion system model and increasing the fidelity of the transmission system inertias.

- It is identified that a more rapid application of clutch pressure has the potential of reducing the impact. This could be investigated in further research by implementing a model of the oil pressure system to enable an exploration of the operational envelope of the clutch.
- The implementation of a pressure controlled clutch disengagement has potential benefits and is recommended for investigation in further research.
- The effect of the clutch losses might be significant regarding energy efficiency. Further research is needed to asses if the continuous energy losses in friction clutches are significant.
- The impact of speed control tuning for both the diesel and electric motors is significant. A more relaxed tuning of the electric speed controller might be beneficial for reducing the impact on the system. A strict tracking of the shaft speed setpoint would have to be sacrificed.
- There is potential for implementation of diesel engine torque control for the diesel to electric transition. A similar limitation of the impact as, in the torque controlled electric to diesel transition, is expected.
- Quick reversal of the ship in emergency operations is expected to subject the propulsion system to peak loads and disturbances. In further research this could be investigated by extending the propeller and hull models for four quadrant operation.
- Considering the relevance of parallel propulsion modes, it is recommended to investigate mode transitions concerning parallel propulsion modes. The developed propulsion system model in this thesis could be used for this research.
- The wave model should be improved to better evaluate the mode transitions in rough sea conditions.

Chapter 4

Conclusions & Recommendations

4.1 Conclusions

The main research question: "*What is the impact of clutch operation in propulsion mode transitions on hybrid maritime propulsion systems?*" has been addressed in chapter 3 by performing simulations, using the hybrid propulsion system model described in chapter 2. The simulation results have been analysed and discussed, from which it is concluded that:

- Torsional vibrations, gear hammer and a drop in propeller speed characterise the significant impact of clutch operation on hybrid propulsion systems in propulsion mode transitions.
- The impact of clutch operation can be limited by implementing an appropriate propulsion control approach for the transition. A torque controlled handover of drive torque between engines is identified as a suitable approach.
- It is concluded that the temperature development of the clutch during the propulsion mode transitions is not significant.

Scientific Contribution
It is shown in this thesis that there can be a significant impact on the propulsion system, resulting from the operation of clutches in propulsion mode transitions. Therefore, the impact of clutch operation in propulsion mode transitions has to be taken into consideration when designing hybrid propulsion systems. The model described in this thesis can be used to predict the impact of clutch operation in the early stages of the design process. Furthermore, it has been shown that the model in this thesis can be used to develop and evaluate propulsion mode transition control approaches. The research in this thesis is thus considered a relevant contribution to the model based (control) design of hybrid maritime propulsion systems.

Sub-Research Questions
To enable investigation of the impact of clutch operation in propulsion mode transitions, a number of sub-research questions have been addressed. First the sub-question: "*What is an appropriate hybrid maritime propulsion system case to investigate clutch operation in propulsion mode transitions?*" has been addressed in section 2.1. A hybrid propulsion has been defined by introducing multi disk wet friction clutches in the reference propulsion[14] system and ship[35]. The defined hybrid propulsion system is able to operate in a number of single engine and parallel engine propulsion modes. The considered propulsion modes within the scope of this thesis are diesel engine propulsion and electric propulsion.

The second sub-question: "*What are the characteristics and dynamics of a typical clutch in a maritime propulsion system?*" has been addressed in section 2.4. It is identified that the dynamics of wet friction multi plate clutches are governed by the stribeck behaviour of the wet friction. It is concluded that the critical dependencies of wet friction dynamics in the engagement of wet friction clutches are: the applied pressure on the disks, the relative velocity of the clutch halves and the temperature of the oil between the friction interfaces.

The sub-question: "*How to model the hybrid maritime propulsion system to enable evaluation of the impact of clutch operation in propulsion mode transitions?*" has been addressed in sections 2.2 - 2.7. The following impacts are considered for the system model:

- Operation of the induction machine relative to its torque-speed operating envelope
- Operation of the diesel engine relative to its torque-speed operating envelope
- Electric load profile of the induction machine
- Low frequency torsional vibrations
- Stress in the shaftline
- Temperature of the clutch
- Gear hammer in the gearbox
- Rotational speed of the propeller

The system has been modelled in correspondence with the impact measures and parameter values have been determined for the hybrid propulsion system case. To asses the basic vibratory behaviour of the transmission system, the system is divided in 8 lumped inertias connected by the nonrigid subsystems (shaftline, gearbox, elastic couplings). It is concluded that, considering the thorough modelling of the system, it can be assumed that the accuracy of the system model is sufficient for evaluating the impact of clutch operation in propulsion mode transitions in regards to the defined impact measures.

The final sub-question: "*How to approach the propulsion mode transitions from a propulsion control point of view?*" has been addressed in subsection 2.5.3. In the scientific literature no standard control approach for propulsion mode transitions was identified. Therefore, three transition control approaches with an increasing degree of sophistication have been implemented: the instant approach, the staged approach and the torque controlled approach.

4.2 Recommendations for Further Research

- It has been assumed that the accuracy of the system model is sufficient for evaluating the impact of clutch operation in propulsion mode transitions in regards to the defined impact measures. However, validation of the complete system model in future research, using measurements from a hybrid propulsion system, is needed to verify this assumption.
- Investigating the claimed advantages of the synchronous clutch type, specifically when implemented in hybrid propulsion systems of merchant ships, is recommended for further research.
- It is recommended to investigate the impact of the power peaks, that are introduced by the induction machine as a result of the mode transition, on the power system of the ship in further research. The model in this thesis could be extended with the electrical models of the MARIN v-ZEL library to conduct this research.
- The stress in the shaftline has a significant amplitude and frequency, possibly causing fatigue damage. The wear of the tooth surface might be significant considering the magnitudes and frequency of the identified gear hammer. Further research is needed to provide more insight into possible impact on wear and fatigue of the system components. The modelling work in this thesis could be the basis for such research.
- In future research, it could be investigated how the torsional excitation from clutch engagement interact with the steady state torsional vibrations in the system. This could be done by including the torsional vibration characteristics of the propeller and diesel engine in the propulsion system model, and increasing the fidelity of the transmission system inertias.
- It is identified that a more rapid application of clutch pressure has the potential of reducing the impact. This could be investigated in further research by implementing a model of the oil pressure system to enable an exploration of the operational envelope of the clutch.
- The implementation of a pressure controlled clutch disengagement has potential benefits and is recommended for investigation in further research.
- Quick reversal of the ship in emergency operations is expected to subject the propulsion system to peak loads and disturbances. In further research this could be investigated by extending the propeller and hull models for four quadrant operation.
- Considering the relevance of parallel propulsion modes, it is recommended to investigate mode transitions concerning parallel propulsion modes. The developed propulsion system model in this thesis could be used for this research.
- The wave model should be improved to better evaluate the mode transitions in rough sea conditions.

Bibliography

[1] L. Mocerino, F. Quaranta, and E. Rizzuto, "Climate changes and maritime transportation: A state of the art," *Technology and Science for the Ships of the Future*, pp. 1005–1013, 2018, Publisher: IOS Press. DOI: 10.3233/978-1-61499-870-9-1005.

[2] M. Krijgsman, "New zero emissions lab for pioneering research," vol. MARIN Report 125, p. 1, Dec. 15, 2018.

[3] H. K. Woud and D. Stapersma, *Design of propulsion and electric power generation systems*. Institute of Marine Engineering Science and Technology, 2019, ISBN: 978-1-85609-849-6.

[4] R. D. Geertsma, R. R. Negenborn, K. Visser, and J. J. Hopman, "Design and control of hybrid power and propulsion systems for smart ships: A review of developments," *Applied Energy*, vol. 194, pp. 30–54, May 15, 2017, ISSN: 0306-2619. DOI: 10.1016/j.apenergy.2017.02.060.

[5] C. Sui, "Energy effectiveness and operational safety of low-powered ocean-going cargo ship in various (heavy) operating conditions," OCLC: 9110919630, Ph.D. dissertation, 2021.

[6] O. B. Inal, J.-F. Charpentier, and C. Deniz, "Hybrid power and propulsion systems for ships: Current status and future challenges," *Renewable and Sustainable Energy Reviews*, vol. 156, p. 111 965, Mar. 1, 2022, ISSN: 1364-0321. DOI: 10.1016/j.rser.2021.111965.

[7] Wartsila. "Wärtsilä 32 methanol engine," Wartsila.com. (2022), [Online]. Available: https://www.wartsila.com/marine/products/engines-and-generating-sets/wartsila-32-methanol-engine (visited on 07/22/2022).

[8] B. Vollmer and F. Hartmann, "Applications of advanced marine electric and hybrid drives," *MTZ industrial*, vol. 6, no. 1, pp. 46–51, Mar. 1, 2016, ISSN: 2194-8690. DOI: 10.1007/s40353-015-0526-5.

[9] W. P. Symington, A. Belle, H. D. Nguyen, and J. R. Binns, "Emerging technologies in marine electric propulsion," *Proceedings of the Institution of Mechanical Engineers, Part M: Journal of Engineering for the Maritime Environment*, vol. 230, no. 1, pp. 187–198, Feb. 1, 2016, Publisher: SAGE Publications, ISSN: 1475-0902. DOI: 10.1177/1475090214558470.

[10] R. H. Marvin, D. J. Broomfield, B. T. Helenbrook, and K. D. Visser, "Optimum design of a lightweight 10mw propulsion motor," in *2017 IEEE Electric Ship Technologies Symposium (ESTS)*, Aug. 2017, pp. 424–431. DOI: 10.1109/ESTS.2017.8069317.

[11] W. Li, T. W. Ching, K. T. Chau, and C. H. T. Lee, "A superconducting vernier motor for electric ship propulsion," *IEEE Transactions on Applied Superconductivity*, vol. 28, no. 3, pp. 1–6, Apr. 2018, ISSN: 1558-2515. DOI: 10.1109/TASC.2017.2787136.

[12] ABB. "Azipod electric propulsion | ABB marine & ports," Marine. (2021), [Online]. Available: https://new.abb.com/marine/systems-and-solutions/azipod (visited on 12/17/2021).

[13] B. Gan, B. Zhang, and G. Feng, "Design and analysis of modular permanent magnet fault-tolerant motor for ship direct-drive propulsion," *IEEJ Transactions on Electrical and Electronic Engineering*, vol. 16, no. 9, pp. 1260–1278, 2021, ISSN: 1931-4981. DOI: 10.1002/tee.23424.

[14] R. D. Geertsma, R. R. Negenborn, K. Visser, and J. J. Hopman, "Parallel control for hybrid propulsion of multifunction ships," *IFAC-PapersOnLine*, 20th IFAC World Congress, vol. 50, no. 1, pp. 2296–2303, Jul. 1, 2017, ISSN: 2405-8963. DOI: 10.1016/j.ifacol.2017.08.229.

[15] T. M. Bui, T. Q. Dinh, J. Marco, and C. Watts, "An energy management strategy for DC hybrid electric propulsion system of marine vessels," in *2018 5th International Conference on Control, Decision and Information Technologies (CoDIT)*, Thessaloniki: IEEE, Apr. 2018, pp. 80–85, ISBN: 978-1-5386-5065-3. DOI: 10.1109/CoDIT.2018.8394785.

[16] G. Papalambrou, S. Samokhin, S. Topaloglou, N. Planakis, N. Kyrtatos, and K. Zenger, "Model predictive control for hybrid diesel-electric marine propulsion," *IFAC-PapersOnLine*, 20th IFAC World Congress, vol. 50, no. 1, pp. 11 064–11 069, Jul. 1, 2017, ISSN: 2405-8963. DOI: 10.1016/j.ifacol.2017.08.2488.

[17] K. R. Deleroi, "Simulation study of acceleration and crash-stop manoeuvers for ship machinery systems," Ph.D. dissertation, Feb. 1995.

[18] H. Engja, "Modelling and simulation of propulsion dynamics due to clutching," in *Proceedings of the ISME sixth international symposium on marine engineering*, Tokyo, Japan, Oct. 23, 2000.

[19] M. Montazeri-Gh and S. A. Miran Fashandi, "Modeling and simulation of a two-shaft gas turbine propulsion system containing a frictional platetype clutch," *Proceedings of the Institution of Mechanical Engineers, Part M: Journal of Engineering for the Maritime Environment*, vol. 233, no. 2, pp. 502–514, May 1, 2019, ISSN: 1475-0902. DOI: 10.1177/1475090218765378.

[20] D. Jiang, "The study on dynamic parameters of CODOG in the mode switching process," in *2008 IEEE/ASME International Conference on Mechtronic and Embedded Systems and Applications*, Oct. 2008, pp. 500–504. DOI: 10.1109/MESA.2008.4735647.

[21] J. M. Apsley, A. Gonzalez-Villasenor, M. Barnes, *et al.*, "Propulsion drive models for full electric marine propulsion systems," *IEEE Transactions on Industry Applications*, vol. 45, no. 2, pp. 676–684, Mar. 2009, ISSN: 1939-9367. DOI: 10.1109/TIA.2009.2013569.

[22] M. Figari and M. Altosole, "Dynamic behaviour and stability of marine propulsion systems," *Proceedings of the Institution of Mechanical Engineers, Part M: Journal of Engineering for the Maritime Environment*, vol. 221, no. 4, pp. 187–205, Dec. 1, 2007, ISSN: 1475-0902. DOI: 10.1243/14750902JEME58.

[23] M. Viviani, M. Altosole, M. Cerruti, A. Menna, and G. Dubbioso, "Marine propulsion system dynamics during ship manoeuvres," *6th International Conference on high-performance marine vehicles (Hiper 2008)*, vol. 18, no. 19, p. 14, 2008.

[24] M. Altosole, G. Dubbioso, M. Figari, and M. Viviani, "Simulation of the dynamic behaviour of a codlag propulsion plant," in *Warship 2010: Advanced Technologies in Naval Design and Construction*, RINA, Jun. 9, 2010, pp. 115–122, ISBN: 978-1-905040-71-1. DOI: 10.3940/rina.ws.2010.13.

[25] S. Skjong, B. Taskar, Eilif Pedersen, and Sverre Steen, "Simulation of a hybrid marine Propulsion-System in waves," presented at the CIMAC Congress, Helsinki, 2016.

[26] H. Bartlett, R. Whalley, and S. S. I. Rizvi, "Hybrid modelling, simulation and torque control of a marine propulsion system," *Proceedings of the Institution of Mechanical Engineers, Part I: Journal of Systems and Control Engineering*, vol. 213, no. 1, pp. 1–10, Feb. 1, 1999, ISSN: 0959-6518. DOI: 10.1243/0959651991540331.

[27] A. A. Ayu, J. K. Kambrath, Y.-J. Yoon, Y. Wang, Y. Liu, and X. Liu, "Sensor placement analysis for torsional vibration suppression on marine electric propulsion," in *2017 Asian Conference on Energy, Power and Transportation Electrification*, Oct. 2017, pp. 1–6. DOI: 10.1109/ACEPT.2017.8168607.

[28] Y. Guo, W. Li, S. Yu, *et al.*, "Diesel engine torsional vibration control coupling with speed control system," *Mechanical Systems and Signal Processing*, vol. 94, pp. 1–13, Sep. 15, 2017, ISSN: 0888-3270. DOI: 10.1016/j.ymssp.2017.01.017.

[29] N. Xiao, R. Zhou, and X. Xu, "Vibration of diesel-electric hybrid propulsion system with nonlinear component," *Journal of Vibration and Control*, vol. 24, no. 22, pp. 5353–5365, Nov. 1, 2018, ISSN: 1077-5463. DOI: 10.1177/1077546317753010.

[30] J. Gong, G. Liu, L. Liu, and L. Yang, "Review article: Research on coupled vibration of multi-engine multi-gearbox marine gearing," *Mechanical Sciences*, vol. 12, no. 1, pp. 393–404, Apr. 7, 2021, ISSN: 2191-9151. DOI: 10.5194/ms-12-393-2021.

[31] J. C. Dermentzoglou and C. Papadopoulos, “Dynamics of shaft machine systems including planetary gear boxes for hybrid ship propulsion,” in *2016 XXII International Conference on Electrical Machines*, Sep. 2016, pp. 2941–2947. DOI: 10.1109/ICELMACH.2016.7732942.

[32] J. C. Dermentzoglou and J. M. Prousalidis, “Emulation of a system with a power split device for hybrid propulsion of ships,” in *2018 XIII International Conference on Electrical Machines*, ISSN: 2381-4802, Sep. 2018, pp. 2529–2534. DOI: 10.1109/ICELMACH.2018.8507133.

[33] M. Godjevac, J. Drijver, L. de Vries, and D. Stapersma, “Evaluation of losses in maritime gearboxes,” *Proceedings of the Institution of Mechanical Engineers, Part M: Journal of Engineering for the Maritime Environment*, vol. 230, no. 4, pp. 623–638, Nov. 1, 2016, ISSN: 1475-0902. DOI: 10.1177/1475090215613814.

[34] T. Cepowski, “Regression formulas for the estimation of engine total power for tankers, container ships and bulk carriers on the basis of cargo capacity and design speed,” *Polish Maritime Research*, vol. nr 1, 2019, ISSN: 1233-2585.

[35] DAMEN, *Product sheet CONTAINER FEEDER 1700*, Jul. 2017. [Online]. Available: https://products.damen.com/en/ranges/container-feeder/container-feeder-1700 (visited on 05/17/2022).

[36] R. D. Geertsma, “Autonomous control for adaptive ships: With hybrid propulsion and power generation,” Ph.D. dissertation, 2019.

[37] M. L. Hendry and N. Bellamy, “Advantages and experience of using SSS (synchro-self-shifting) clutches in hybrid propulsion such as CODELOG or CODELAG naval marine systems,” in *Volume 1*, American Society of Mechanical Engineers, Jun. 17, 2019, V001T25A006, ISBN: 978-0-7918-5854-7. DOI: 10.1115/GT2019-91873.

[38] SSS Clutch Company, *SSS notes reference: NR2167 - SSS clutch operating principle*, 2015.

[39] G. Kuiper, “The wageningen propeller series,” *MARIN Publication 91-001 Published on the occasion of its 60th anniversary, MARIN Wageningen, The Netherlands*, 1992.

[40] Ortlinghaus, *Product sheet ortlinghaus marine technology*, May 2019. [Online]. Available: https://www.ortlinghaus.com/ (visited on 02/09/2022).

[41] Vulkan Couplings, *TECHNICAL DATA RATO r/r+*, Sep. 2021. [Online]. Available: https://www.vulkan.com/en-us/couplings/products/highly-flexible-couplings/rato-r-r+ (visited on 01/06/2022).

[42] K. Jonsson, “Modelling of torsional vibrations in marine powertrains,” *SAE Technical Paper*, Feb. 1, 1996, ISSN: 0148-7191, 2688-3627. DOI: 10.4271/960776.

[43] C. W. Bert, “Material damping: An introductory review of mathematic measures and experimental technique,” *Journal of Sound and Vibration*, vol. 29, no. 2, pp. 129–153, Jul. 22, 1973, ISSN: 0022-460X. DOI: 10.1016/S0022-460X(73)80131-2.

[44] A. v. Beek, *Advanced engineering design: lifetime performance and reliability*, Ed. 2009. Delft: TU, 2009, 520 pp., ISBN: 978-90-810406-1-7.

[45] Lloyd’s Register, “Rules and regulations for the classification of ships,” Jul. 2021, p. 1811.

[46] Roy L. Harrington et al., *Marine Engineering*. The Society of Naval Architects and Marine Engineers, 1992.

[47] X. Xu and R. P. Zhou, “Research on torsional vibration of the propulsion shafting gear system based on an extended lumped parameter model,” *Applied Mechanics and Materials*, vol. 37-38, pp. 1120–1124, 2010, ISSN: 1662-7482. DOI: 10.4028/www.scientific.net/AMM.37-38.1120.

[48] S. Wang and R. Zhu, “An improved mesh stiffness model for double-helical gear pair with spalling defects considering time-varying friction coefficient under mixed EHL,” *Engineering Failure Analysis*, vol. 121, p. 105 174, Mar. 1, 2021, ISSN: 1350-6307. DOI: 10.1016/j.engfailanal.2020.105174.

[49] N. Rogkas, G. Vasileiou, E. Tsolakis, V. Spitas, and P. Zalimidis, “Fast modelling and simulation of the dynamic behaviour of a wet multidisc clutch during the engagement phase,” *MATEC Web of Conferences*, vol. 287, p. 01 018, 2019, ISSN: 2261-236X. DOI: 10.1051/matecconf/201928701018.

[50] M. Bak, "Torque capacity of multidisc wet clutch with reference to friction occurrence on its spline connections," *Scientific Reports*, vol. 11, no. 1, p. 21 305, Oct. 29, 2021, ISSN: 2045-2322. DOI: 10.1038/s41598-021-00786-6.

[51] S. Iqbal, F. Al-Bender, A. P. Ompusunggu, B. Pluymers, and W. Desmet, "Modeling and analysis of wet friction clutch engagement dynamics," *Mechanical Systems and Signal Processing*, vol. 60-61, pp. 420–436, Aug. 1, 2015, ISSN: 0888-3270. DOI: 10.1016/j.ymssp.2014.12.024.

[52] C. L. Davis, F. Sadeghi, and C. M. Krousgrill, "A simplified approach to modeling thermal effects in wet clutch engagement: Analytical and experimental comparison," *Journal of Tribology*, vol. 122, no. 1, pp. 110–118, Jan. 7, 1999, ISSN: 0742-4787. DOI: 10.1115/1.555370.

[53] T. Lin, Z.-r. Tan, Z.-y. He, H. Cao, and H.-s. Lv, "Analysis of influencing factors on transient temperature field of wet clutch friction plate used in marine gearbox," *Industrial Lubrication and Tribology*, vol. 70, no. 2, pp. 241–249, Jan. 1, 2018, ISSN: 0036-8792. DOI: 10.1108/ILT-08-2016-0181.

[54] P. Marklund and R. Larsson, "Wet clutch friction characteristics obtained from simplified pin on disc test," *Tribology International*, Nordtrib 2006, vol. 41, no. 9, pp. 824–830, Sep. 1, 2008, ISSN: 0301-679X. DOI: 10.1016/j.triboint.2007.11.014.

[55] H. Kitabayashi, C. Li, and H. Hiraki, "Analysis of the various factors affecting drag torque in multiple-plate wet clutches," *SAE Technical Paper*, No. 2003-01-1973 2003. DOI: 10.4271/2003-01-1973.

[56] M. Mansouri, M. Holgerson, M. M. Khonsari, and W. Aung, "Thermal and dynamic characterization of wet clutch engagement with provision for drive torque," *Journal of Tribology*, vol. 123, no. 2, pp. 313–323, Jun. 16, 2000, ISSN: 0742-4787. DOI: 10.1115/1.1329856.

[57] RENK, *Double marine gearboxes type NDS(h)(q)(l)*, Sep. 2017. [Online]. Available: https://www.renk-group.com/en/products-and-service/products/marine-propulsion-units/dual-engine-gear-units/nds/ (visited on 06/01/2022).

[58] Reintjes, *Reintjes gearbox product sheet DLG 1113 110131*, Sep. 2015. [Online]. Available: https://www.reintjes-gears.de/en/powertrain-marine (visited on 06/01/2022).

[59] TEXACO, *Texamatic 7045e product sheet*, Dec. 18, 2013.

[60] R. D. Geertsma, R. R. Negenborn, K. Visser, M. A. Loonstijn, and J. J. Hopman, "Pitch control for ships with diesel mechanical and hybrid propulsion: Modelling, validation and performance quantification," *Applied Energy*, vol. 206, 2017, ISSN: 0306-2619. DOI: 10.1016/j.apenergy.2017.09.103.

[61] M. Hoeijmakers, *Modelling of AC Machines*. 2004.

[62] L. Harnefors and H.-P. Nee, "Model-based current control of AC machines using the internal model control method," *IEEE Transactions on Industry Applications*, vol. 34, no. 1, pp. 133–141, Feb. 1998, ISSN: 00939994. DOI: 10.1109/28.658735.

[63] J. Umland and M. Safiuddin, "Magnitude and symmetric optimum criterion for the design of linear control systems: What is it and how does it compare with the others?" *IEEE Transactions on Industry Applications*, vol. 26, no. 3, pp. 489–497, Jun. 1990, ISSN: 00939994. DOI: 10.1109/28.55967.

[64] UK Met Office. "Beaufort wind force scale," Met Office. (2022), [Online]. Available: https://www.metoffice.gov.uk/weather/guides/coast-and-sea/beaufort-scale (visited on 05/19/2022).

[65] L. Moskowitz, "Estimates of the power spectrums for fully developed seas for wind speeds of 20 to 40 knots," *Journal of Geophysical Research (1896-1977)*, vol. 69, no. 24, pp. 5161–5179, 1964, ISSN: 2156-2202. DOI: 10.1029/JZ069i024p05161.

[66] M. Oosterveld and P. van Oossanen, "Further computer-analyzed data of the wageningen b-screw series," *International Shipbuilding Progress*, vol. 22, no. 251, pp. 251–262, Jul. 1, 1975, ISSN: 15662829, 0020868X. DOI: 10.3233/ISP-1975-2225102.

[67] D. MacPherson, R. Puleo, and B. Packard, "Estimation of entrained water added mass properties for vibration analysis," *SNAME New England Section*, p. 11, 2007.

[68] A. Vrijdag, D. Stapersma, and T. van Terwisga, "Systematic modelling, verification, calibration and validation of a ship propulsion simulation model," *Journal of Marine Engineering & Technology*, vol. 8, no. 3, pp. 3–20, Jan. 2009, ISSN: 2046-4177, 2056-8487. DOI: 10.1080/20464177.2009.11020223.

[69] D. Stapersma, “Main propulsion arrangement and power generation concepts,” in *Encyclopedia of Maritime and Offshore Engineering*, J. Carlton, P. Jukes, and Y. S. Choo, Eds., Chichester, UK: John Wiley & Sons, Ltd, Apr. 20, 2017, pp. 1–40, ISBN: 978-1-118-47635-2 978-1-118-47640-6.

Appendix A

Scientific Research Paper

A Simulation Study on the Impact of Clutch Operation in Propulsion Mode Transitions on Hybrid Maritime Propulsion Systems

Authors G.J. van den Bogerd, Dr.ir. U. Shipurkar (MARIN), Dr.ir. H. Polinder (TU-Delft)

August 14, 2022

Abstract

Over the coming decades the worldwide fleet of ships will have to change to reduce emissions. Hybridisation of the propulsion system is a stepping stone to full electrification, which is required to reduce emissions of the maritime sector to zero. In hybrid propulsion systems, clutches are used to switch between drive engines when transitioning between operational modes. The operation of clutches is indicated to generate significant disturbances in propulsion systems, however, this impact is overlooked in hybrid propulsion simulation studies in the scientific literature. The identified research gap is addressed in this paper by simulating propulsion mode transition in a hybrid propulsion system and analysing the impact of clutch operation, using of a model developed for this purpose.

A hybrid propulsion is defined by introducing multi disk wet friction clutches in a reference propulsion system consisting of a 9.1 MW diesel engine in parallel with a 3 MW electric motor. A broad scope of impact measures, that includes the electric load on the power system and the temperature development of the clutch, is defined and the system is thoroughly modelled to enable evaluation of these measures. The Transmission system is modelled with a higher fidelity than typically applied in propulsion system simulation studies to enable assessment of the basic vibratory behaviour of the transmission system. The considered propulsion modes transitions are between diesel and electric propulsion. To enable these transitions, three transition control approaches with an increasing degree of sophistication are implemented.

The developed model is used to perform simulations, from which it is concluded that torsional vibrations, gear hammer and a drop in propeller speed characterise the significant impact of clutch operation on hybrid propulsion systems in propulsion mode transitions. It is also concluded that the impact of clutch operation can be limited by implementing an appropriate propulsion control approach for the transition. A torque controlled handover of drive torque between engines is identified as a suitable approach. However, the induction machine switching from torque to speed control introduces power peaks in the load profile that have the potential to severely disrupt the stability of the ships power system. It is finally concluded that the temperature development of the clutch during the propulsion mode transitions is not significant.

It is shown in this paper that there can be a significant impact on the propulsion system as a result of the operation of clutches in propulsion mode transitions. Therefore, this impact has to be taken into consideration when designing hybrid propulsion systems. The model described in this paper can be used to predict the impact of clutch operation in the early stages of the design process. Furthermore, the model can be used to develop and evaluate propulsion mode transition control approaches.

1 Introduction

Over the coming decades the worldwide fleet of ships will have to change radically to reduce emissions [1]. Hybridisation of the propulsion system is identified as both attainable given current energy storage technology and a stepping stone to full electric propulsion, that will be required to reduce emissions of the maritime sector to zero [2].

In a hybrid system, propulsion can be provided by the diesel engine and electric motor combined or separately. The electric motor enables efficient operation at part-load conditions and can be used to supplement the diesel engine in acceleration manoeuvres to reduce emissions [3] or adverse weather conditions [4]. In hybrid propulsion systems switching between drive engines when transitioning between operational modes is identified as a challenge [2]. Clutches enables this switching and the operation of clutches is indicated to generate significant disturbances in propulsion systems [5], [6], however this impact is overlooked in hybrid propulsion simulation studies in the scientific literature. The identified research gap is addressed in this paper by simulating propulsion mode transition in a hybrid propulsion system and analysing the impact of clutch operation, using of a model developed for this purpose.

This paper is structured as follows: in section 2 a hybrid propulsion system is defined and the modelling of the system is described. In section 3 the results of the performed simulations are presented and analysed. In section 4 the results are discussed and in section 5 the conclusions can be found. In section 6 recommendations for further research are made. Appendix A contains the model parameters that have been used for the simulations.

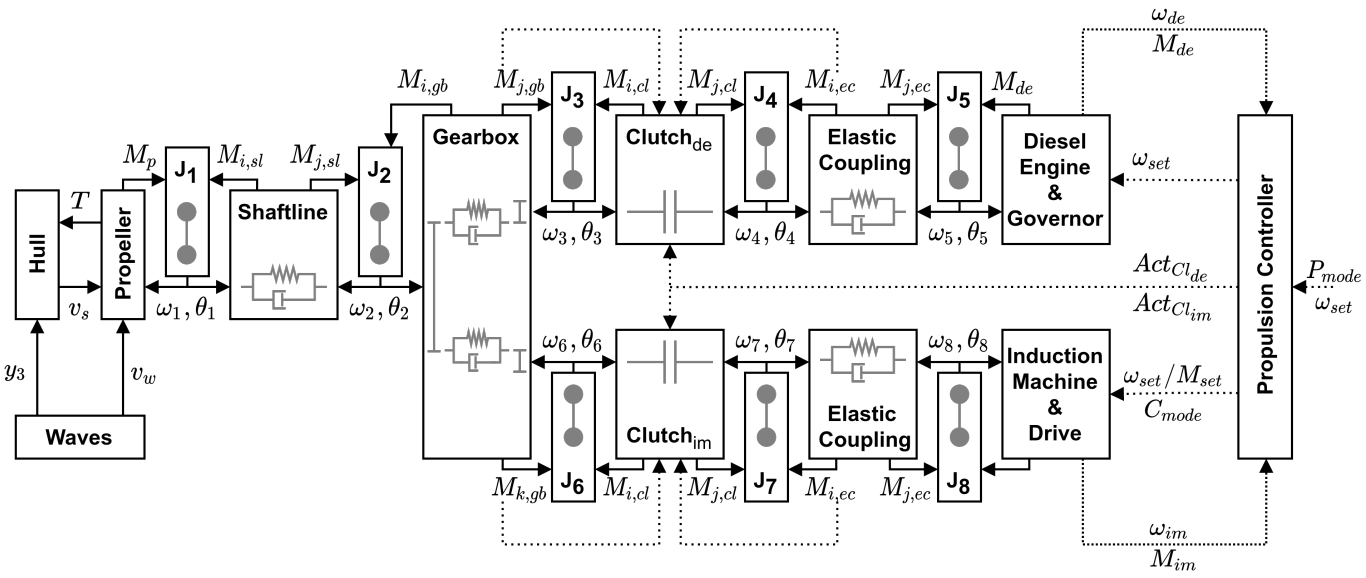

Figure 1: Schematic representation and model coupling of the propulsion system model.

2 System Modelling

A hybrid propulsion has been defined by introducing multi disk wet friction clutches [7] in the reference propulsion system from Geertsma, Negenborn, Visser, *et al.* [3] and matching the propulsion with a reference ship [8], resulting in the following system:

- Hull of a 172 m container feeder
- Wageningen-B series fixed pitch propeller
- Diesel engine with 9.1 MW of power at 1000 rpm
- Electric motor with 3 MW of power at 600 rpm
- Multi disk wet friction clutches that enable selecting and combining the main drive engine
- Elastic couplings between the clutches and the engines
- Shaftline connecting the propeller and gearbox
- Dual engine gearbox that connect the two drive engines to the shaftline using the same gear ratio. As a result the electric motor can be used for low speed operation and the diesel engine is most suitable for the higher speed operation.

The defined hybrid propulsion system is able to operate in a number of single engine and parallel engine propulsion modes. The considered propulsion modes within the scope of this paper are diesel and electric propulsion.

2.1 Impact Measures

Before the system can be modelled at an appropriate fidelity level the impact measures are defined. In Deleroi [6] the impact of clutch operation on the engines is identified. In Engja [5] it is concluded that large transient loads may occur in the transmission system when performing clutch operations. it is concluded that clutch operation is expected to have both an impact on the transmission system components themselves, as well as the operation of the engines. In Deleroi [6] the operation of the clutch is identified as being limited by the developed heat during clutch operation. From experience at MARIN it was identified that hammering of the gears in the gearbox could be a significant impact of the operation of clutches. When gears hammer back and forth, the tooth surface is work-hardened by the impact force making the surface both harder and more brittle, increasing the risk of damage to the gear teeth surface. The typical control goal for ship propulsion systems is identified in Geertsma, Negenborn, Visser, *et al.* [9] as maintaining the speed of the propeller at the desired setpoint. Considering this broad spectrum of potential impacts, the following measures are defined:

- Operation of the induction machine relative to its torque-speed operating envelope
- Operation of the diesel engine relative to its torque-speed operating envelope
- Electric load profile of the induction machine
- Low frequency torsional vibrations
- Stress in the shaftline
- Temperature of the clutch
- Gear hammer in the gearbox
- Rotational speed of the propeller

2.2 System Model

Considering the defined hybrid propulsion system and the impact measures a conceptual model for the system is defined. To asses the basic vibratory behaviour of the transmission system, the system is divided in 8 lumped inertias connected by the nonrigid subsystems (shaftline, gearbox, elastic couplings) inspired by previous work in Engja [5]. In this concept the inertias connected by the clutch can be in two states: rigidly connected or uncoupled. The multi inertia concept is integrated in the model concept in fig.1 where a schematic representation and the coupling of the submodels is given. The submodels are further described in sub-subsections 2.2.1 - 2.2.11 and appendix A contains the model parameters.

2.2.1 Rotational Dynamics

The rotational dynamics are governed by (2.1 - 2.3) where $J_{i,x}$ and $J_{i,y}$ represent the inertia contributions of the connecting sub-system x and y respectively. $M_{i,x}$ and $M_{i,y}$ represent the applied torque from the connected subsystems to the lumped inertia element. The state variables ω_i in rad/s and θ_i in rad describe the rotation of the inertia element. The parameters for the lumped inertias in table 2 have been obtained by combining the inertia contributions of the connecting submodels.

$$\dot{\omega_i}(t) = \ddot{\theta_i}(t) = \frac{J_i}{M_i(t)} \tag{2.1}$$

$$J_i = J_{i,x} + J_{i,y} \tag{2.2}$$

$$M_i(t) = M_{i,x}(t) + M_{i,y}(t) \tag{2.3}$$

2.2.2 Shaftline Model

The shaftline model is divided into two submodels, the material model describing the shaft flexibility and the friction model that describes the losses from shaft bearings, that are added (2.4) ,(2.5) to form the complete model of the shaftline.

$$M_{i,sl}(t) = M_{i,sl_f}(t) + M_{sl}(t) \tag{2.4}$$

$$M_{j,sl}(t) = M_{j,sl_f}(t) - M_{sl}(t) \tag{2.5}$$

$$M_{sl}(t) = k_{i,j}[\theta_j(t) - \theta_i(t)] + c_{i,j}[\omega_j(t) - \omega_i(t)] \tag{2.6}$$

$$M_{i,sl_f}(t) = sign[-\omega_i(t)] \cdot \frac{1}{2} \cdot M_{sl_{nom}}[1 - \eta_{sl}] \cdot [a_{loss} + b_{loss}\frac{|\omega_i(t)|}{\omega_{sl_{nom}}} + c_{loss}\frac{|M_{sl}(t)|}{M_{sl_{nom}}}] \tag{2.7}$$

$$M_{j,sl_f}(t) = sign[-\omega_j(t)] \cdot \frac{1}{2} \cdot M_{sl_{nom}}[1 - \eta_{sl}] \cdot [a_{loss} + b_{loss}\frac{|\omega_j(t)|}{\omega_{sl_{nom}}} + c_{loss}\frac{|M_{sl}(t)|}{M_{sl_{nom}}}] \tag{2.8}$$

In the material model (2.6) the shaft flexibility is modelled as a parallel spring damper [10]. The friction in the shaft line (2.7), (2.8) is modelled, using the torque loss model from Godjevac, Drijver, Vries, *et al.* [11]. The torque loss model parameterisation is based on a division of the nominal shaft line losses between a dimensionless constant loss parameter a_{loss}, velocity dependent loss parameter b_{loss} and torque dependent loss parameter c_{loss}. The parameters in table 3 for the shaftline model are selected from design rules and estimations.

2.2.3 Gearbox Model

The gearbox model is split into two submodels, one describing gear mesh and the other the friction losses. The contributions of these models are combined (2.9-2.12), where r_i, r_j and r_k are the radius's of the respective gears and the friction is applied at the main drive gear i. The gear meshes $F_{i,j}(t)$ and $F_{i,k}(t)$ that transfer force between gears i, j, k are modelled (2.14)(2.15) as a parallel spring damper acting along the gear line of action. Gearbox friction $M_{i,gb_{loss}}(t)$ is modelled the same as the shaftline friction as a torque loss model [11] and applied in [3]. The friction torque is applied at the propeller side gear i of the gearbox. The parameters for the gearbox model in table 4 are determined as in Xu and Zhou [12] for the stiffness, [13] is used for the friction and gear geometry is estimated.

$$M_{i,gb}(t) = M_{i,gb_{loss}}(t) + M_{gb}(t) \tag{2.9}$$

$$M_{gb}(t) = r_i \cdot F_{i,j}(t) + r_i \cdot F_{i,k}(t) \tag{2.10}$$

$$M_{j,gb}(t) = r_j \cdot -F_{i,j}(t) \tag{2.11}$$

$$M_{k,gb}(t) = r_k \cdot -F_{i,k}(t) \tag{2.12}$$

$$\tag{2.13}$$

$$F_{i,j}(t) = k_{i,j}[r_j\theta_j(t) - r_i\theta_i(t)] + c_{i,j}[r_j\omega_j(t) - r_i\omega_i(t)] \tag{2.14}$$

$$F_{i,k}(t) = k_{i,k}[r_k\theta_k(t) - r_i\theta_i(t)] + c_{i,k}[r_k\omega_k(t) - r_i\omega_i(t)] \tag{2.15}$$

$$M_{i,gb_{loss}}(t) = sign[-\omega_i(t)] \cdot M_{gb,loss_{nom}}[a_{gb} + b_{gb}\frac{|\omega_i(t)|}{\omega_{gb_{nom}}} + c_{gb}\frac{|M_{gb}(t)|}{M_{gb_{nom}}}] \tag{2.16}$$

2.2.4 Elastic Coupling Model

The torques $M_{i,ec}(t)$ and $M_{j,ec}(t)$ are defined by (2.17), (2.18) and connect to the lumped inertias as visualised in fig.1. The flexible coupling is modelled as a parallel spring damper (2.19) with constant stiffness $k_{i,j}$ and damping $c_{i,j}$ coefficients. Frequency dependent material characteristics are not taken into consideration. The parameters for the elastic couplings in table 5 have been obtained from the manufacturer data [14].

$$M_{i,ec}(t) = M_{ec}(t) \tag{2.17}$$

$$M_{j,ec}(t) = -M_{ec}(t) \tag{2.18}$$

$$M_{ec}(t) = k_{i,j}[\theta_j(t) - \theta_i(t)] + c_{i,j}[\omega_j(t) - \omega_i(t)] \tag{2.19}$$

2.2.5 Clutch Model

The model of the clutch is divided in three submodels: the state model, wet friction model and the thermal model.

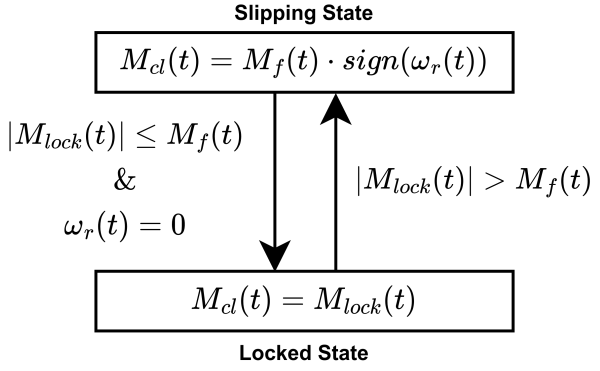

Figure 2: Clutch state definitions and transition conditions.

The state model in fig.2 defines the behaviour of the clutch in the open and closed condition. Switching the definition of the clutch torque $M_{cl}(t)$, at lock-up is selected for the clutch state model [5]. In the locked state the torque through the clutch is defined by (2.20) to keep both inertias synchronised.

$$M_{lock}(t) = \frac{J_i M_{j,y}(t) - J_j M_{i,x}(t)}{J_i + J_j} \tag{2.20}$$

The wet friction model describes the friction between the clutch plates. The load sharing approach [15] is applied (2.21) and entails that the friction is split in a hydrodynamic part $M_{visc}(t)$ and contact friction part $M_{cont}(t)$. The friction is a function of the pressure on the disk stack $P(t)$, when there is no pressure applied the friction is considered zero (2.22).

$$P(t) > 0 \rightarrow M_f(t) = M_{cont}(t) + M_{visc}(t) \tag{2.21}$$

$$P(t) = 0 \rightarrow M_f(t) = 0 \tag{2.22}$$

Regarding the clutch geometry, the effective torque radius of the friction at the interface r_e is described by (2.24) assuming a constant pressure distribution between the disks. The area of a friction interface A_{fi} is defined by (2.25).

$$\omega_r(t) = \omega_j(t) - \omega_i(t) \tag{2.23}$$

$$r_e = \frac{2}{3}\frac{r_o^3 - r_i^3}{r_o^2 - r_i^2} \tag{2.24}$$

$$A_{fi} = \pi[r_o^2 - r_i^2] \tag{2.25}$$

The contact friction is simplified to a constant friction coefficient μ as in Lin, Tan, He, *et al.* [16]. The resulting friction torque $M_{cont}(t)$ is a function (2.26) of applied pressure $P(t)$, the number of friction interfaces N, the effective torque radius r_e and the area of a friction interface A_{fi}.

$$M_{cont}(t) = N \cdot \mu \cdot r_e \cdot A_{fi} \cdot P(t) \tag{2.26}$$

The hydrodynamic shear torque $M_{visc}(t)$ is modelled as a function (2.27) of the relative velocity $\omega_r(t)$, the number of friction interfaces N, the effective torque radius r_e, the area of a friction interface A_{fi}, oil film viscosity $\eta(t)$ and thickness $h(t)$ [17]. The film thickness $h(t)$ is assumed to be dependent on the applied pressure $P(t)$ and rapidly decreases from the initial thickness h_0 to the final thickness h_c corresponding with asperity contact governed by (2.28). The oil viscosity $\eta(t)$ is dependent (2.29) on the temperature $T_{oil}(t)$, dynamic viscosity shape function parameter κ and the base viscosity η_0.

$$M_{visc}(t) = \frac{N \cdot \eta(t) \cdot A_{fi} \cdot r_e^2}{h(t)} \cdot |\omega_r| \tag{2.27}$$

$$h(t) = \frac{h_0}{P(t) + 1} + h_c \tag{2.28}$$

$$\eta(t) = \eta_0 \cdot e^{-\kappa T_{oil}(t)} \tag{2.29}$$

The thermal model describes the temperature of the clutch plates. Heat $\dot{Q}_f(t)$ generated in the clutch results (2.30) from the relative sliding velocity $\omega_r(t)$ (2.23) and friction force $M_f(t)$ [16]. The friction interface is modelled as a homogeneous thermal mass m_{fi} of which the temperature is determined by (2.31). T_{oil_0} is the initial oil temperature in the clutch, c_{fi} is the specific heat of the thermal mass. The thermal mass m_{fi} is described by (2.32). The lumped thermal mass is calibrated using the thermal FE results from Lin, Tan, He, *et al.* [16] by tuning parameter d_{fi}.

$$\dot{Q}_f(t) = |\omega_r(t)| \cdot M_f(t) \tag{2.30}$$

$$T_{fi}(t) = T_{oil}(t) = \frac{Q_f(t)}{m_{fi} \cdot c_{fi}} + T_{oil_0} \tag{2.31}$$

$$m_{fi} = N \cdot A_{fi} \cdot d_{fi} \cdot \rho_{fi} \tag{2.32}$$

There are two clutches in the propulsion system. Table 6 contains the shared parameters, table 7 and table 8 contain the individual geometric parameters that are derived from public manufacturer data [7]. The engagement pressure map describing $P(t)$ is defined in fig.9 and based on [16].

2.2.6 Diesel Engine & Governor Model

The model for the diesel engine and governor dynamics is provided by dr.ir. R.D.Geertsma and further described in Geertsma [13]. The mean value first principle model describes the dynamic performance and includes the thermal loading of the engine. The governor contains a PI speed controller with an anti windup loop, also charge air inlet pressure and speed dependent fuel limiters are implemented. Parameters for the diesel engine, PI controller and fuel limiters are obtained from the reference for the hybrid propulsion system (table 3.3, 3.4, 5.1 and 5.2 in [13]).

2.2.7 Induction Machine & Drive Model

The induction machine and drive models have been provided for this research and are part of the MARIN v-ZEL. The dynamic model of the induction machine is implemented in the dq-reference frame, based on the inverse-y equivalent circuit and ignores transient reactances and saturation effects [18]. Induction machine parameters for a 10 pole induction machine at 3.15 kV with synchronous speed of 600 rpm and a nominal power of 3 MW, are obtained from the reference for the hybrid propulsion system (table 5.3 in Geertsma [13]).

The electric machine is driven using direct torque control with an outer speed control loop. The torque PI control loop parameters are determined using Internal Mode Control [19]. The outer speed PI control loop is tuned using the symmetric optimum criteria [20].

2.2.8 Propulsion Control Model

For the control architecture two control levels are defined. The primary control level containing the torque and speed control loops of the engines and the clutch activation. The primary control level is integrated in the diesel and electric motor models, and in the clutch model. The second

control level is implemented in the propulsion controller that regulates the propulsion modes and mode transitions and feeds control set points and control modes to the primary control level. The propulsion controller functions by selecting a state for the propulsion control outputs based on the propulsion mode setpoint P_{mode} in fig.1. The electric and diesel propulsion modes are considered within the scope of this research. For these propulsion modes the following propulsion controller states are defined:

Diesel Propulsion Mode

- Diesel engine clutch closed
- Induction machine clutch open
- Diesel engine speed setpoint matches system setpoint
- Induction machine in torque control mode
- Induction machine torque setpoint at zero

Electric Propulsion Mode

- Diesel engine clutch open
- Induction machine clutch closed
- Diesel engine speed setpoint to stationary
- Induction machine in speed control mode
- Induction machine speed setpoint matches system setpoint

The propulsion control model can be used for controlling the propulsion mode transitions. In the scientific literature no standard control approach for propulsion mode transitions has been identified. Therefore, three transition approaches with an increasing degree of sophistication have been implemented.

Instant Transition Control Approach
In the instant approach clutches are engaged and disengaged at the same point in time. No transition control is applied in this case and the propulsion mode state is instantly set from either diesel to electric or electric to diesel. This represents the most rudimentary way to approach a mode transition and serves as a baseline.

Staged Transition Control Approach
In the staged approach the clutch for the new propulsion modes engine is first engaged, followed a number of seconds later by the disengagement of the clutch for the preceding propulsion mode. As a result there is effectively an overlap of the two propulsion modes where parallel speed control is active. It is the aim of this approach to asses the suitability of parallel speed control for handover of the drive torque between the drive engines during a mode transition. To enable this transition approach a separate state is defined as an intermediate step between the two propulsion modes. This intermediate state is active for 5 s during the mode transition and defined by:

- Diesel engine clutch closed
- Induction machine clutch closed
- Diesel engine speed setpoint matches system setpoint
- Induction machine in speed control mode
- Induction machine speed setpoint matches system setpoint

Torque Controlled Transition Control Approach
For the torque controlled approach, in addition to an overlap in clutch engagement and disengagement, the torque control mode for the induction machine is used to ramp up or down the drive torque. It is the aim of this approach to force a handover of drive torque between the drive engines during a mode transition. To enable this transition approach, a separate state is defined as an intermediate step between the two propulsion modes for both directions of the transition. This intermediate state is active for 5 s during the mode transition and defined by:

- Diesel engine clutch closed
- Induction machine clutch closed
- Diesel engine speed setpoint matches system setpoint
- Induction machine in torque control mode
- (for diesel to electric) Induction machine torque ramps up over the duration of this intermediate state from zero to the reference torque level M_{de} that is set at the moment the transition is initiated.
- (for electric to diesel) Induction machine torque ramps down over the duration of this intermediate state to 0 from the reference torque level M_{im} that is set at the moment the transition is initiated.

2.2.9 Hull Model

The hull model converts the thrust $T(t)$ generated by the propeller model into 1-D surge motion and thus ship speed $v_s(t)$. The model is obtained from Woud and Stapersma [21]. Regarding the ship dynamics (2.33) the differential equation for the ship speed is a function of: the hull resistance $R_{hull}(t)$, thrust deduction factor t_{ded} and the displacement of the hull Δ_s. The resistance largely determines the load on the propulsion system and this towing resistance of displacement type hulls is mainly dependent on the ship speed $v_s(t)$ and described by (2.34). The resistance factor c_1 is a function of the sea margin y and the nominal resistance factor c_0 which is considered constant (2.35). The sea margin y is a further function (2.36) of constant multiplying. The parameters in table 9 are estimated for the reference ship case [8].

$$\dot{v}_s(t) = \frac{T(t) - \frac{R_{hull}(t)}{1-t_{ded}}}{\Delta_s} \tag{2.33}$$

$$R_{hull}(t) = c_1 \cdot v_s^2 \tag{2.34}$$

$$c_1 = y \cdot c_0 \tag{2.35}$$

$$y = SM = y_1(fouling) \cdot y_2(hull) \cdot [\frac{\Delta_s}{\Delta_{nom}}]^{2/3} \cdot y_3(seastate) \cdot y_4(waterdepth) \tag{2.36}$$

2.2.10 Wave Model

The environmental disturbance is described by the sea state, having a constant influence on the hull resistance

y_3 in (2.36) and having a dynamic effect on the wake of the propeller $v_w(t)$. The wave model is obtained from [13] and simplified to a constant wave frequency ω_{wave}. The wave model (2.37) is further dependent on the wave amplitude ζ, the depth of the propeller centre z and the wave number k (2.38). Parameters for the wave model in table 10 are based on the average wave height and frequency in a given sea-state.

$$v_w(t) = \zeta \cdot \omega_{wave} \cdot e^{k \cdot z} \cdot sin[\omega_{wave} \cdot t] \tag{2.37}$$

$$k = \frac{\omega_{wave}^2}{9.81} \tag{2.38}$$

2.2.11 Propeller Model

The propeller converts torque to thrust and is modelled for operation in the first quadrant as described in Woud and Stapersma [21]. Governing equations (2.39 - 2.43) describe the thrust torque relation of the propeller using the advance ratio $J(t)$ that is dependent on ship speed $v_s(t)$, wave disturbance $v_w(t)$, propeller speed n_p and the propeller diameter D. The thrust-torque relation is described using the typical $K_T(J(t))$, $K_Q(J(t))$ open water diagrams that are generated for the selected propeller using the polynomials in Oosterveld and Oossanen [22].

$$T(t) = K_T(J(t)) \cdot \rho_{sw} \cdot n_p^2(t) \cdot D_p^4 \tag{2.39}$$

$$Q(t) = K_Q(J(t)) \cdot \rho_{sw} \cdot n_p^2(t) \cdot D_p^5 \tag{2.40}$$

$$M_p(t) = \frac{-Q(t)}{\eta_R} \tag{2.41}$$

$$J(t) = \frac{v_a(t)}{n_p(t) \cdot D_p} \tag{2.42}$$

$$v_a(t) = v_s(t)[1 - w] + v_w(t) \tag{2.43}$$

The propeller has been matched to the ship for a 15 kn speed using 85% of the available diesel engine power, in accordance with the procedure described in [21]. The Wageningen B5-75 propeller with a P/D ratio of 0.7 has been selected from the matching procedure and combined with table 11 this completes the parameters for the model.

2.3 Implementation

The system model has been implemented in Matlab Simulink and suitable parameters for the variable step ode23 solver have been selected:

- Minimum step size: $1 \cdot 10^{-7}$ s
- Maximum step size: $1 \cdot 10^{-3}$ s
- Relative tolerance: $1 \cdot 10^{-3}$
- Adaptive Zero-crossing control algorithm

Due to the high stiffness of the gear mesh forcing a small time step the choice has been made to reduce the mesh stiffness to be one order of magnitude higher then the next stiffest component(the shaftline).

2.4 Validation

In Vrijdag, Stapersma, and Terwisga [23] validation is defined as: "The process of determining the degree to which a model is an accurate representation of the real world from the perspective of the intended uses of the model." In correspondence with this definition the validity of the hybrid propulsion system model is discussed in this subsection.

2.4.1 Validity of the Propulsion Models

The propeller model is based on the experimentally determined open water diagrams that are a well accepted modelling methodology for the torque thrust relation. The hull and wave models are not validated using experimental data. The used hull model is widely applied and it can be assumed to be sufficiently valid given its small direct impact on the transient dynamics. The wave model is considered an acceptable representation of wave disturbance given the application of measured values for the wave height and frequency.

2.4.2 Validity of the Transmission Models

For the transmission system model the gearbox friction is validated in [13]. The same friction model has been used for the shaftline, for which the corresponding parameter are based on estimations. The clutch thermal model has been calibrated and validated using data from a high fidelity finite element model [16]. The remainder of the transmission system has not been validated using experimental data. The applied lumped-inertia technique is successfully used for torsional vibration analysis, application in dynamic propulsion system simulation is uncommon. This validity of this approach has to be further assessed in future research. However, it is assumed that the application of parameters based on manufacturer data in the transmission system models, does result in a reasonable representation of the low frequency torsional dynamics.

2.4.3 Validity of the Driver Models

The diesel engine model has been validated in [13]. The induction machine parameters have been adapted from [13] and applied in a similar electric motor model. As their intended use corresponds with the use of these models in this thesis, the validity of these models is assumed.

2.4.4 Validity of the Complete System Model

Combining a number of separately validated models does not lead to the automatic conclusion that the model of the complete system is valid. Considering the thorough modelling of the system in this chapter, it is assumed that the accuracy of the system model is sufficient for evaluating the impact of clutch operation in propulsion mode transitions, in regards to the defined impact measures. However, validation of the complete system model in future research, using measurements from a hybrid propulsion system, is needed to verify this assumption.

3 Results

The considered propulsion modes within the scope of this research are diesel propulsion (Diesel Mode) and electric propulsion (Electric Mode). For the transitions between these modes, three transition control approaches have been defined and implemented in the propulsion control model as described in sub-subsection 2.2.8.

Below 600 rpm the diesel engine operates at a relatively low efficiency [13] while the induction machine, at 600 rpm, would operate at it's design speed and corresponding high efficiency. Consequently, the 600 rpm steady state operating point is selected as a representative case to transition between diesel engine and electric propulsion, the selected setpoint corresponds with a 10 kn steady state ship speed. For the conditions a moderate sea state 3 is selected with the ship at the loaded displacement.

3.1 Simulations

Simulations have been performed using the model described in section 2, using the three propulsion mode transition control approaches, for both directions of the transition. The results of the six simulations are summarised in table 1. To enable evaluation of the propulsion mode transition approaches, all the torque plots resulting from the diesel to electric transitions are presented (fig.3, fig.4, fig.5). The torque plot for the torque controlled electric to diesel transition is included (fig.6) to compare the results in regards to the direction of the transition. The plot for the electric load is included, for the staged diesel to electric mode transition (fig.7) and for the torque controlled diesel to electric mode transition (fig.8), to enable assessment of the impact on the power system resulting from these transitions.

The time span of the simulations is 30 s where the mode transitions is initiated at 15 s. A computer with an Intel i7-12700K CPU coupled with 32 GB of GDDR4 RAM has been used to run the propulsion mode transition simulations. It is identified that the model initialises in approximately 5 seconds. In this period the twist angle in the flexible components has to be established resulting in an initial torsional vibration.

Table 1: Table summarising the key results of the operational transitions between electric(E) and diesel(D) mode at a speed of 10 knots(18.5 km/h), corresponding with a engine speed setpoint of 600 rpm, in sea state 3.

Transition	**Approach**	**Clutch Slip**	**Clutch Temp.**	**Propeller Speed (max. deviation)**	**Torsional Vibration (max. p-to-p amplitude)**	**Gear Hammer**
E to D	Instant	3 s	+ 2 °C	-25%	160 % of steady state	both gears
D to E	Instant	4.5 s	+ 12 °C	-30%	200 % of steady state	both gears
E to D	Staged	0 s	+ 0 °C	-15%	25 % of steady state	electric gear
D to E	Staged	0.25 s	+ 0 °C	-2%	50 % of steady state	diesel gear
E to D	T-Controlled	0 s	+ 0 °C	-5 %	not identified	not identified
D to E	T-Controlled	1 s	+ 1 °C	+5%	115 % of steady state	diesel gear

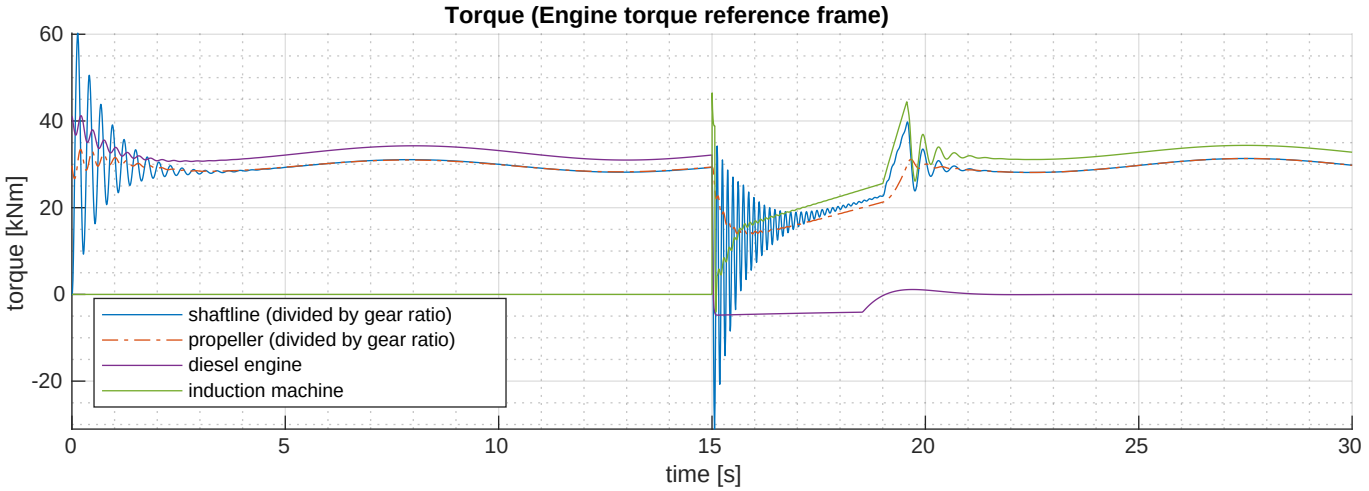

Figure 3: Torques in the engine torque reference frame for the transition from electric to diesel mode using the instant transition approach in sea state 3.

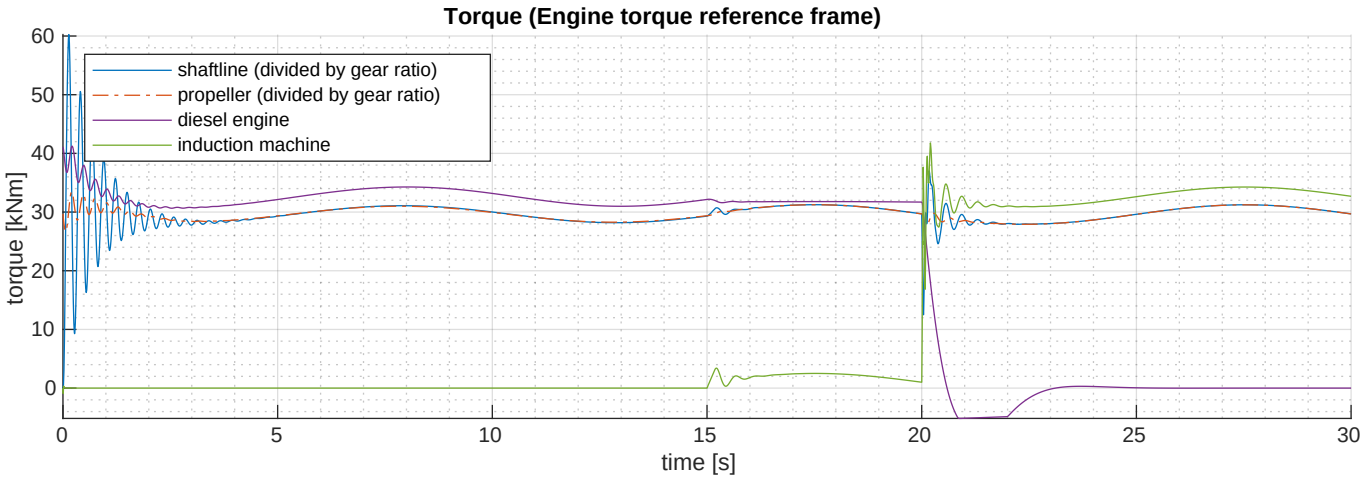

Figure 4: Torques in the engine torque reference frame for the transition from diesel to electric mode using the staged transition approach in sea state 3.

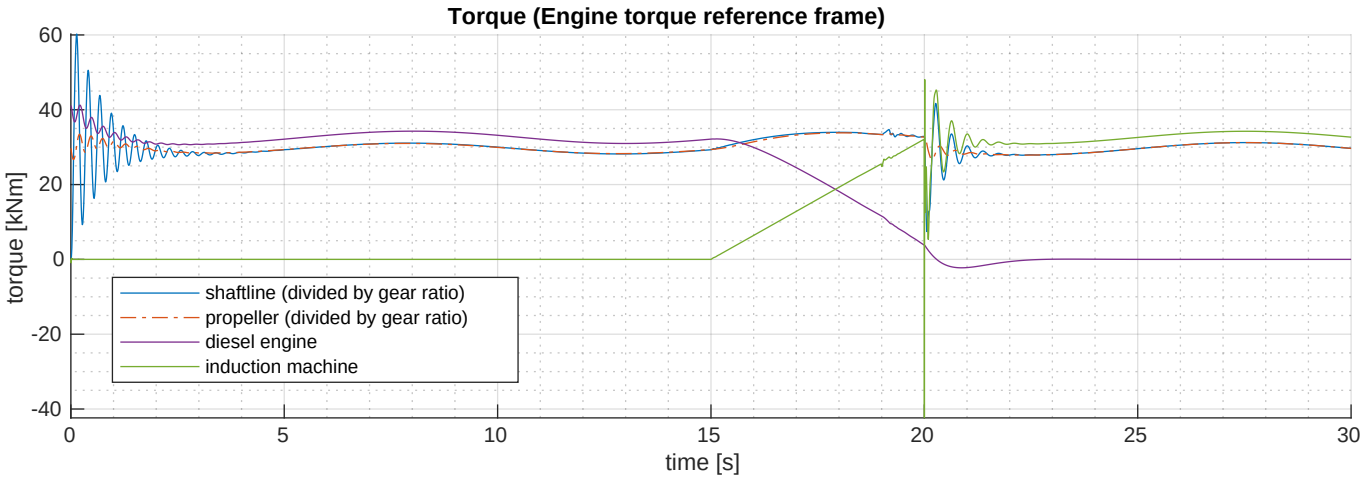

Figure 5: Torques in the engine torque reference frame for the transition from diesel to electric mode using the torque controlled transition approach in sea state 3.

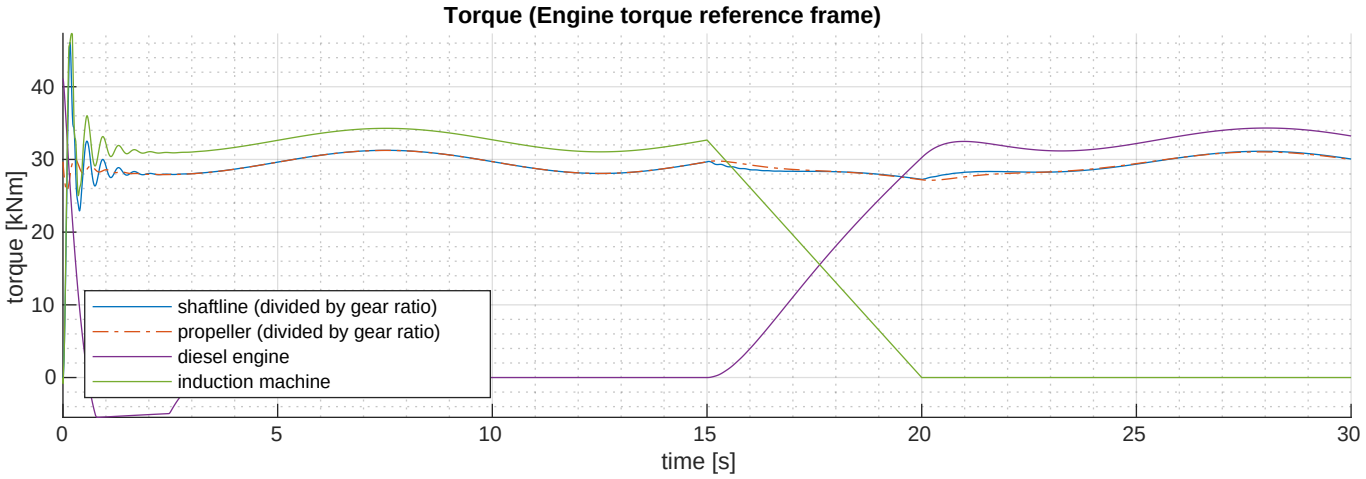

Figure 6: Torques in the engine torque reference frame for the transition from electric to diesel mode using the torque controlled transition approach in sea state 3.

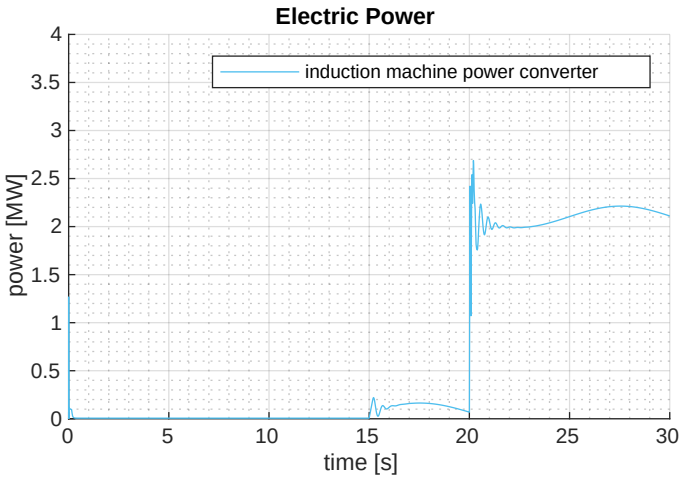

Figure 7: Induction machine drive power for the transition from diesel to electric mode using the staged transition approach in sea state 3.

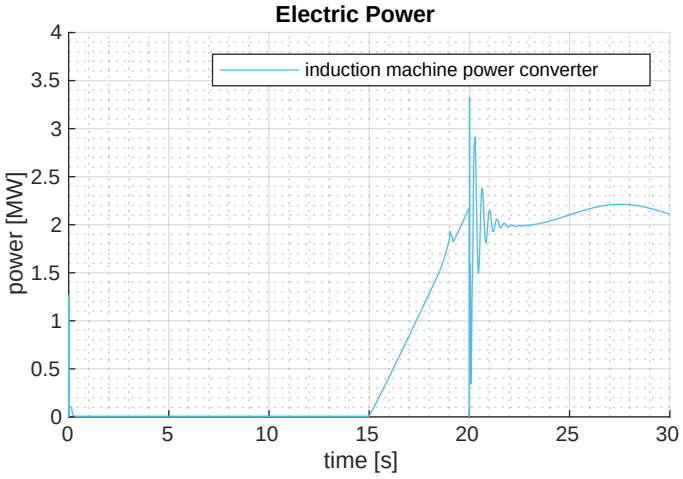

Figure 8: Induction machine drive power for the transition from diesel to electric mode using the torque controlled transition approach in sea state 3.

3.2 Analysis of the Results

The instant approach in fig.3 is characterised by a lack of drive torque during the transition. This lack of drive torque finds its origin in a slipping clutch and results in significant torsional vibrations a large drop in propeller speed, as can be asserted from table 1.

The gap in drive torque characterising the instant approach can be prevented by overlapping the envelopes of the clutches as implemented in the staged approach. However, it is observed that the staged approach in fig.4 is characterised by a lack of drive torque handover during the parallel speed control phase. As a result the transmission system is significantly impacted when the clutch of the original mode deactivates. The response of the induction machine speed controller to the lack of handover is reflected in the electric load on the power system, fig.7. When comparing the magnitudes of the impact on the system in table 1 it must be observed that the staged approach significantly outperforms the instant approach.

To aid the handover in the parallel phase the induction machine is set to torque control mode and used to force a handover of drive torque between the engines. In fig.6 and table 1 it can be observed that this approach successfully limits the impact in the electric to diesel transition. The approach is unsuccessful in the diesel to electric transition in fig.5 as the switch from torque control to speed control for the induction machine significantly disturbs the system. This is reflected in fig.8 concerning the electric load on the power system during the transition.

4 Discussion

The impact of clutch operation in the simulated propulsion mode transitions, summarised in table. 1, is in general characterised by:

- Significant torsional vibrations
- Gear hammer
- A drop in propeller speed

By using the torque controlled approach, the impact is limited in the electric to diesel transition. However, ramping up the induction machine torque and switching from torque control to speed control is found to introduce significant disturbances in the system. As a result the used implementation of the torque controlled approach does not perform well in the diesel to electric transition. There is potential in implementation of diesel engine torque control for the diesel to electric transition. When using diesel engine torque control for the transition, a similar limitation of the impact as in the torque controlled electric to diesel transition is expected.

4.1 Impact on the Electric Power System

For the torque controlled diesel to electric transition it is identified that a significantly disturbed power profile results from the induction machine switch from torque to speed control, fig.8. A similar impact is observed in the staged diesel to electric transition, fig.7. A pattern emerges where the response of the induction machine controller, to the sudden increase in load, introduces power peaks in the load profile. These power peaks have to potential to severely disrupt the stability of the ships power system.

4.2 Impact on Clutch Temperature

In the results of the propulsion mode transition simulations in table 1, a significant rise of the clutch temperature is observed in the diesel to electric transition where the instant transition approach is applied. This rise in temperature coincides with the relatively long duration of the slip period. This long period of slip can be prevented by implementing more advanced approaches for the transition control, as can be observed form table 1. The rise in clutch temperature is insignificant in the other simulations considering that the absolute limit for the oil is 200 $^{\circ}C$.

4.3 Impact on System Condition

The torsional vibrations in the shaftline have a significant amplitude and frequency, especially when using a rudimentary approach for the propulsion mode transition control as in fig.3. This has the risk of possibly causing fatigue damage. The wear of the tooth surface could also be significant considering the magnitudes and frequency of the identified gear hammer.

5 Conclusions

The identified research gap regarding the impact of clutch operation in propulsion mode transitions has been addressed in this paper by performing simulations, using a developed hybrid propulsion system model, from which it is concluded that:

- Torsional vibrations, gear hammer and a drop in propeller speed characterise the significant impact of clutch operation on hybrid propulsion systems in propulsion mode transitions.
- The impact of clutch operation can be limited by implementing an appropriate propulsion control approach for the transition. A torque controlled handover of drive torque between engines is identified as a suitable approach.
- The induction machine switching from torque to speed control introduces power peaks in the load profile. These power peaks have the potential to severely disrupt the stability of the ships power system.
- It is concluded that the temperature development of the clutch during the propulsion mode transitions is not significant.

It is shown in this paper that there can be a significant impact on the propulsion system, resulting from the operation of clutches in propulsion mode transitions. Therefore, the impact of clutch operation in propulsion mode transitions has to be taken into consideration when designing hybrid propulsion systems. The model described in this paper can be used to predict the impact of clutch operation in the early stages of the design process. Furthermore, it has been shown that the model in this paper can be used to develop and evaluate propulsion mode transition control approaches. The research described in this paper is thus considered a relevant contribution to the model based (control) design of hybrid maritime propulsion systems.

6 Recommendations

- Validation of the complete system model using measurements from a hybrid propulsion system is needed to increase the confidence in the results of the simulations.
- There is potential in implementation of diesel engine torque control for the diesel to electric transitions. A similar limitation of the impact as, in the torque controlled electric to diesel transition, is expected.
- It is recommenced to investigate the impact of the power peaks, that are introduced by the induction machine as a result of the mode transition, on the power system of the ship.
- Further research is needed to provide more insight into possible impact on wear and fatigue of the system components. The model described in this paper could be the basis for such research.

References

[1] L. Mocerino, F. Quaranta, and E. Rizzuto, "Climate Changes and Maritime Transportation: A State of the Art," *Technology and Science for the Ships of the Future*, pp. 1005–1013, 2018, Publisher: IOS Press. DOI: 10.3233/978-1-61499-870-9-1005.

[2] O. B. Inal, J.-F. Charpentier, and C. Deniz, "Hybrid power and propulsion systems for ships: Current status and future challenges," en, *Renewable and Sustainable Energy Reviews*, vol. 156, p. 111 965, Mar. 2022, ISSN: 1364-0321. DOI: 10.1016/j.rser.2021.111965.

[3] R. D. Geertsma, R. R. Negenborn, K. Visser, and J. J. Hopman, "Parallel Control for Hybrid Propulsion of Multifunction Ships," en, *IFAC-PapersOnLine*, 20th IFAC World Congress, vol. 50, no. 1, pp. 2296–2303, Jul. 2017, ISSN: 2405-8963. DOI: 10.1016/j.ifacol.2017.08.229.

[4] C. Sui, "Energy Effectiveness and Operational Safety of Low-Powered Ocean-going Cargo Ship in Various (Heavy) Operating Conditions," en, OCLC: 9110919630, Ph.D. dissertation, 2021.

[5] H. Engja, "Modelling and simulation of propulsion dynamics due to clutching," in *Proceedings of the ISME sixth international symposium on marine engineering*, Tokyo, Japan, Oct. 2000.

[6] K. R. Deleroi, "Simulation study of Acceleration and crash-stop manoeuvers for ship machinery systems," en, Ph.D. dissertation, Feb. 1995.

[7] Ortlinghaus, *Product Sheet Ortlinghaus Marine Technology*, May 2019. [Online]. Available: https://www.ortlinghaus.com/ (visited on 02/09/2022).

[8] DAMEN, *Product Sheet CONTAINER FEEDER 1700*, en, Jul. 2017. [Online]. Available: https://products.damen.com/en/ranges/container-feeder/container-feeder-1700 (visited on 05/17/2022).

[9] R. D. Geertsma, R. R. Negenborn, K. Visser, and J. J. Hopman, "Design and control of hybrid power and propulsion systems for smart ships: A review of developments," en, *Applied Energy*, vol. 194, pp. 30–54, May 2017, ISSN: 0306-2619. DOI: 10.1016/j.apenergy.2017.02.060.

[10] C. W. Bert, "Material damping: An introductory review of mathematic measures and experimental technique," en, *Journal of Sound and Vibration*, vol. 29, no. 2, pp. 129–153, Jul. 1973, ISSN: 0022-460X. DOI: 10.1016/S0022-460X(73)80131-2.

[11] M. Godjevac, J. Drijver, L. de Vries, and D. Stapersma, "Evaluation of losses in maritime gearboxes," en, *Proceedings of the Institution of Mechanical Engineers, Part M: Journal of Engineering for the Maritime Environment*, vol. 230, no. 4, pp. 623–638, Nov. 2016, ISSN: 1475-0902. DOI: 10.1177/1475090215613814.

[12] X. Xu and R. P. Zhou, "Research on Torsional Vibration of the Propulsion Shafting Gear System Based on an Extended Lumped Parameter Model," en, *Applied Mechanics and Materials*, vol. 37-38, pp. 1120–1124, 2010, ISSN: 1662-7482. DOI: 10.4028/www.scientific.net/AMM.37-38.1120.

[13] R. D. Geertsma, "Autonomous control for adaptive ships: With hybrid propulsion and power generation," en, Ph.D. dissertation, 2019.

[14] Vulkan Couplings, *TECHNICAL DATA RATO R/R+*, Sep. 2021. [Online]. Available: https://www.vulkan.com/en-us/couplings/products/highly-flexible-couplings/rato-r-r+ (visited on 01/06/2022).

[15] C. L. Davis, F. Sadeghi, and C. M. Krousgrill, "A Simplified Approach to Modeling Thermal Effects in Wet Clutch Engagement: Analytical and Experimental Comparison," *Journal of Tribology*, vol. 122, no. 1, pp. 110–118, Jan. 1999, ISSN: 0742-4787. DOI: 10.1115/1.555370.

[16] T. Lin, Z.-r. Tan, Z.-y. He, H. Cao, and H.-s. Lv, "Analysis of influencing factors on transient temperature field of wet clutch friction plate used in marine gearbox," *Industrial Lubrication and Tribology*, vol. 70, no. 2, pp. 241–249, Jan. 2018, ISSN: 0036-8792. DOI: 10.1108/ILT-08-2016-0181.

[17] S. Iqbal, F. Al-Bender, A. P. Ompusunggu, B. Pluymers, and W. Desmet, "Modeling and analysis of wet friction clutch engagement dynamics," en, *Mechanical Systems and Signal Processing*, vol. 60-61, pp. 420–436, Aug. 2015, ISSN: 0888-3270. DOI: 10.1016/j.ymssp.2014.12.024.

[18] M. Hoeijmakers, *Modelling of AC Machines*. 2004.

[19] L. Harnefors and H.-P. Nee, "Model-based current control of AC machines using the internal model control method," en, *IEEE Transactions on Industry Applications*, vol. 34, no. 1, pp. 133–141, Feb. 1998, ISSN: 00939994. DOI: 10.1109/28.658735.

[20] J. Umland and M. Safiuddin, "Magnitude and symmetric optimum criterion for the design of linear control systems: What is it and how does it compare with the others?" en, *IEEE Transactions on Industry Applications*, vol. 26, no. 3, pp. 489–497, Jun. 1990, ISSN: 00939994. DOI: 10.1109/28.55967.

[21] H. K. Woud and D. Stapersma, *Design of propulsion and electric power generation systems*, English. Institute of Marine Engineering Science and Technology, 2019, ISBN: 978-1-85609-849-6.

[22] M. Oosterveld and P. van Oossanen, "Further computer-analyzed data of the Wageningen B-screw series," *International Shipbuilding Progress*, vol. 22, no. 251, pp. 251–262, Jul. 1975, ISSN: 15662829, 0020868X. DOI: 10.3233/ISP-1975-2225102.

[23] A. Vrijdag, D. Stapersma, and T. van Terwisga, "Systematic modelling, verification, calibration and validation of a ship propulsion simulation model," en, *Journal of Marine Engineering & Technology*, vol. 8, no. 3, pp. 3–20, Jan. 2009, ISSN: 2046-4177, 2056-8487. DOI: 10.1080/20464177.2009.11020223.

A Model Parameters

Table 2: Rotational dynamics model parameters

System Inertia	
J_1	22239 $kg \cdot m^2$
J_2	3213 $kg \cdot m^2$
J_3	16 $kg \cdot m^2$
J_4	44 $kg \cdot m^2$
J_5	663 $kg \cdot m^2$
J_6	10 $kg \cdot m^2$
J_7	16 $kg \cdot m^2$
J_8	31 $kg \cdot m^2$
Total	26232 $kg \cdot m^2$

Table 3: Shaftline model parameters

length of the shaftline l_{sl}	20 m
radius of the solid shaftline r_{sl}	0.199 m
shear modulus of the shaft material G_{sl}	$8.3 \cdot 10^{10}$ Pa
material damping coefficient $c_{i,j}$	$2.158 \cdot 10^{3}$ $Nm \cdot s/rad$
material stiffness coefficient $k_{i,j}$	$1.022 \cdot 10^{7}$ Nm/rad
shaft line mass moment of inertia $J_{i,sl}$ and $J_{j,sl}$	215 $kg \cdot m^2$
shaft line efficiency η_{sl} at nominal torque and speed	0.99
nominal shaftline torque $M_{sl_{nom}}$	$896 \cdot 10^{3}$ Nm
nominal shaftline speed $\omega_{sl_{nom}}$	13.51 rad/s
shaft line constant loss parameter a_{loss}	0.1
shaft line velocity dependent loss parameter b_{loss}	0.4
shaft line torque dependent loss parameter c_{loss}	0.5

Table 4: Gearbox model parameters

gear ratio i	7.75
gear radius r_i	0.944 m
gear radius r_j and r_k	0.122 m
gear mesh damping coefficient $c_{i,j}$ and $c_{i,k}$ in $Nm \cdot s/rad$	$1.06 \cdot 10^{4}$ $Nm \cdot s/rad$
gear mesh stiffness coefficient $k_{i,j}$ and $k_{i,k}$ in Nm/rad	$1.48 \cdot 10^{8}$ Nm/rad
gear mass moment of inertia J_i, gb	$3.00 \cdot 10^{3}$ $kg \cdot m^2$
gear mass moment of inertia $J_{j,gb}$ and $J_{k,gb}$	0.831 $kg \cdot m^2$
nominal gearbox torque loss $M_{gb,loss_{nom}}$	$3.58 \cdot 10^{4}$ Nm
nominal propeller shaft torque $M_{gb_{nom}}$	$8.96 \cdot 10^{5}$ Nm
nominal propeller shaft speed $\omega_{gb_{nom}}$	13.51 rad/s
dimensionless gearbox constant loss parameter a_{gb}	0.0269
dimensionless gearbox velocity dependent loss parameter b_{gb}	0.7254
dimensionless gearbox torque dependent loss parameter c_{gb}	0.2454

Table 5: Elastic coupling model parameters

	DE elastic coupling	IM elastic coupling
damping coefficient $c_{i,j}$	$2.297 \cdot 10^{3}$ $Nm \cdot s/rad$	$2.232 \cdot 10^{3}$ $Nm \cdot s/rad$
stiffness coefficient $k_{i,j}$	$6.40 \cdot 10^{5}$ Nm/rad	$3.90 \cdot 10^{5}$ Nm/rad
mass moment of inertia $J_{i,ec}$	29.1 $kg \cdot m^2$	7.2 $kg \cdot m^2$
mass moment of inertia J_{j_ec}	42.9 $kg \cdot m^2$	13.6 $kg \cdot m^2$

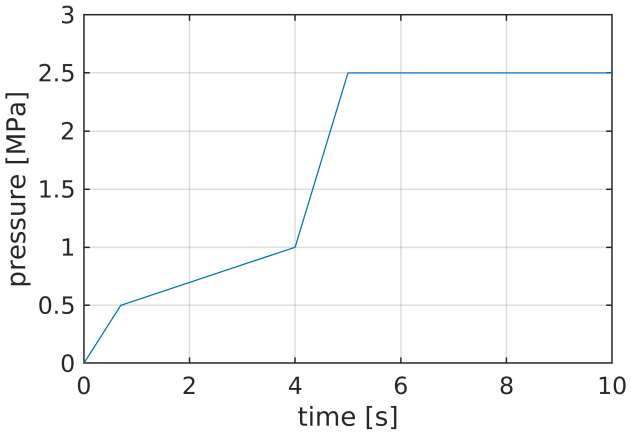

Figure 9: Clutch actuation pressure curve $P(t)$

Table 6: Parameter shared by the models for the diesel engine and induction machine clutches

coefficient of friction μ	0.10
contact oil film thickness at the friction interface h_c	$6 \cdot 10^{-6}\ m$
initial oil film thickness at the friction interface h_0	$2.0 \cdot 10^{-3}\ m$
base viscosity η_0	$0.0703\ Pa \cdot s$
dynamic viscosity shape function parameter κ	0.0203
initial oil temperature T_{oil_0}	$50\ °C$
specific heat of the thermal mass c_{fi}	$450\ J/kg \cdot K$
thickness of the lumped thermal mass d_{fi}	$0.020\ m$
density of the thermal mass material ρ_{fi}	$8000\ kg/m^3$

Table 7: Parameters for the diesel engine clutch model

mass moment of inertia $J_{i,cl}$ and J_{j_cl}	$15\ kg \cdot m^2$
outer radius of the clutch disks r_o	$0.232\ m$
inner radius of the clutch disks r_i	$0.162\ m$
number of friction interfaces N	24

Table 8: Parameters for the induction machine clutch model

mass moment of inertia $J_{i,cl}$ and J_{j_cl}	$9\ kg \cdot m^2$
outer radius of the clutch disks r_o	$0.206\ m$
inner radius of the clutch disks r_i	$0.144\ m$
number of friction interfaces N	20

Table 9: Hull model parameters

thrust deduction coefficient t_{ded}	0.12
nominal resistance factor c_0	$6.71 \cdot 10^3\ kg/m$
fouling dependent multiplying factor y_1	1.06
hull form dependent multiplying factor y_2	1
loaded displacement Δ_s	$27250 \cdot 10^3\ kg$
nominal displacement Δ_{nom}	$18550 \cdot 10^3\ kg$
sea state dependent multiplying factor y_3	1.0 (state 0), 1.1 (state 3), 1.36 (state 5)
water depth dependent multiplying factor y_4	1.0 (deep water)

Table 10: Wave model parameters

wave amplitude ζ	$0\ m$ (state 0), $0.3\ m$ (state 3), $1.5\ m$ (state 5)
wave radial frequency ω_{wave}	$0.63\ rad/s$
depth of the propeller centre z	$8\ m$

Table 11: Parameters for the propeller model

density of sea water ρ_{sw}	$1025\ kg/m^3$
diameter of the propeller D_p	$5.8\ m$
relative rotative efficiency η_R	1
wake factor w	0.20
propeller mass moment of inertia J_{prop}	$2.20 \cdot 10^4\ kg \cdot m^2$

Appendix B

Complete Simulation Results

This appendix contains the complete results of the simulations. In section B.1 a description of the simulation outputs is given. Section B.2 contains the results for the steady state propulsion mode simulations and section B.3 contains the results for the propulsion mode transition simulations.

B.1 Simulation Output Description

Each experiment outputs two figures each spanning a full A4 page. Conceptually the first figure summarises the dynamic behaviour of the propulsion system as a whole, the second figure contains the performance indicators with their respective limits.

First figure description

- The mechanical power of the induction machine, the mechanical power of the diesel engine and the mechanical power draw of the propeller as a function of time.
- The rotational speeds of the diesel engine and induction machine as well as the propeller speed multiplied with the gear ratio and the shaft speed setpoint to enable assessment of their relative behaviour.
- The torque in the shaftline and propeller both multiplied by the gear ratio to enable a relative comparison with the diesel engine and induction machine torques.
- The transmitted torque through the clutches with the corresponding maximum holding torques.

Second figure description

- The operational point of the diesel engine over time. The operation is bounded by the engine envelope where running between the envelope and the overload limit is only allowed for a limited amount of time.
- The operational point of the induction machine over time with the operating envelope.
- The electric power draw by the induction machine power converter.
- The diesel engine governor setpoint relative to the fuel limiter.
- The Von Mises equivalent stress in the shaftline relative to the yield limit for the shaft material.
- The gear mesh force, where a crossing of zero (marked with red dotted line) indicates the occurrence of gear hammer.
- The temperature of the oil film between the clutch plates. The imposed limit is the temperature at which the oil starts burning, a limit that should be steered clear off under all circumstances.
- The running efficiency of the transmission system as measured by the power input from the engines from $t = 5\ s$ compared to the power delivered to the propeller. The function of this plot is to verify the results of the experiments as it provides insight in the conservation of energy in the transmission system.
- The ship speed as a function of time to indicate if the ship is accelerating, decelerating or keeping a constant speed. Verifying that the initial speed in the experiment matches the approximate steady state in the operating point.

B.2 Steady State Propulsion Mode Simulation Results

- Diesel mode in the design condition: 15 kn, sea state 3, 1000 rpm. (fig.B.1, fig.B.2)
- Diesel mode at medium speed: 10 kn, sea state 3, 600 rpm. (fig.B.3, fig.B.4)
- Electric mode at medium speed: 10 kn, sea state 3, 600 rpm. (fig.B.5, fig.B.6)

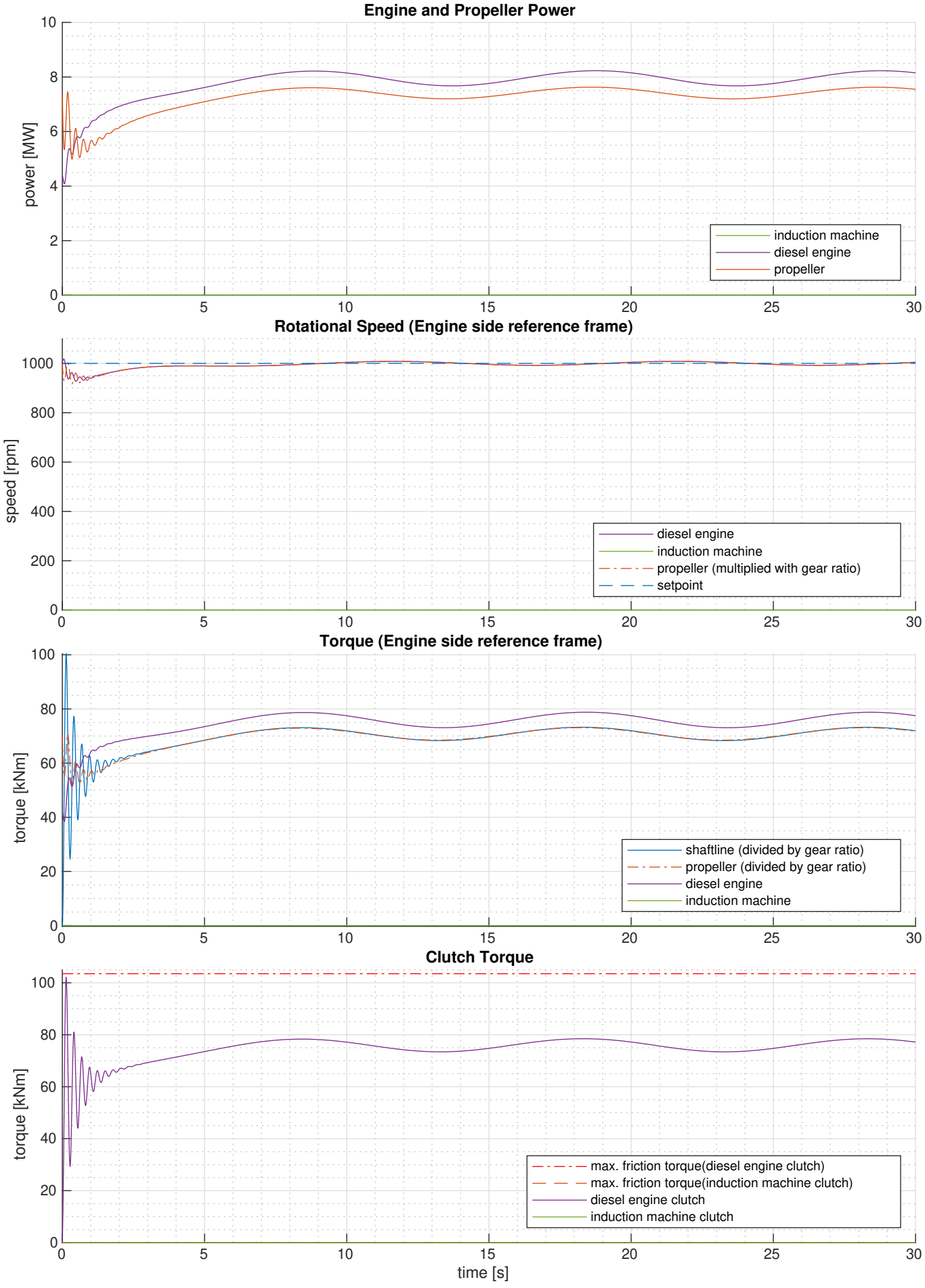

Figure B.1: Diesel propulsion mode in the design condition: 15 kn, sea state 3, 1000 rpm. [figure 1 of 2]

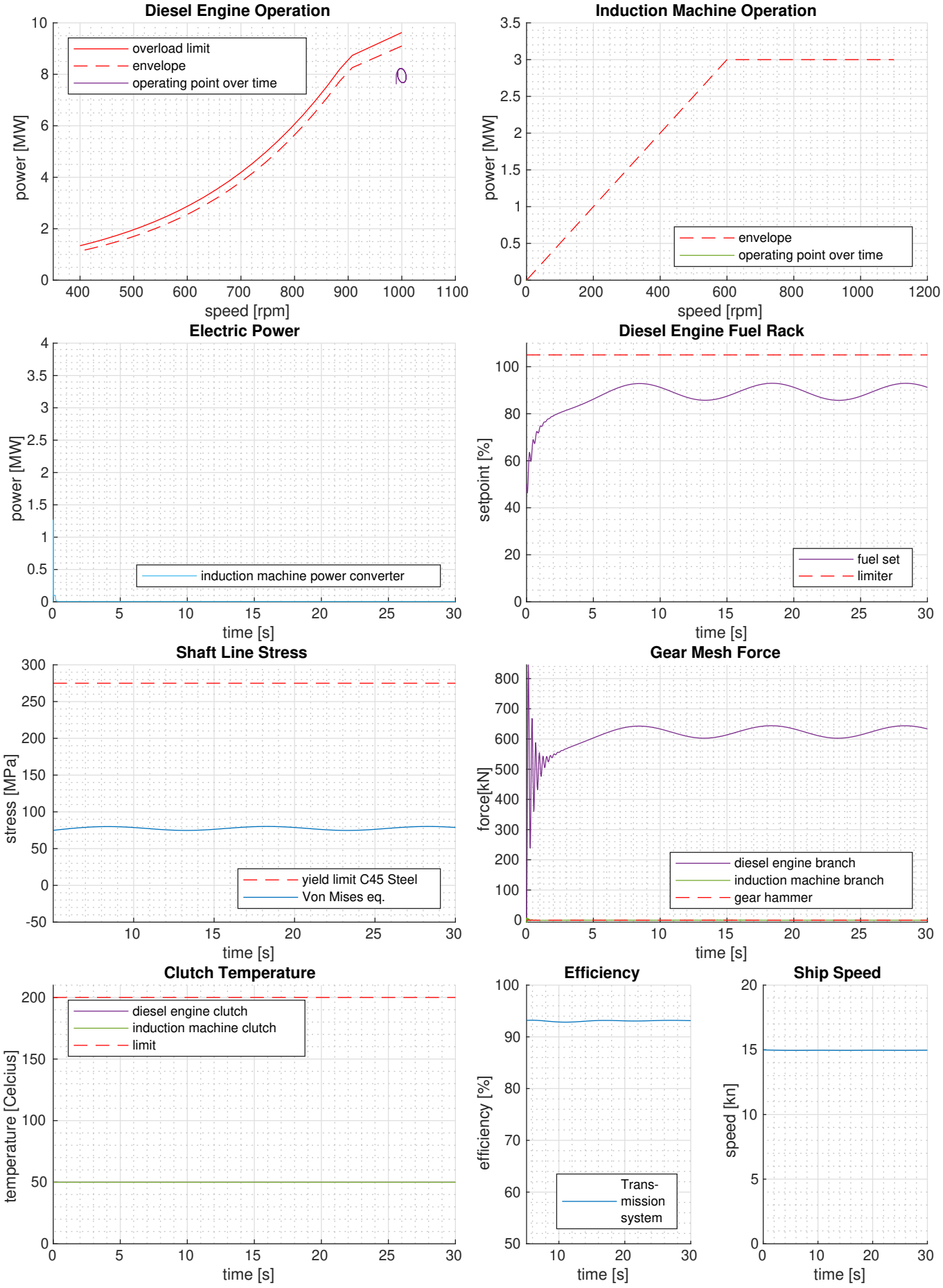

Figure B.2: Diesel propulsion mode in the design condition: 15 kn, sea state 3, 1000 rpm. [figure 2 of 2]

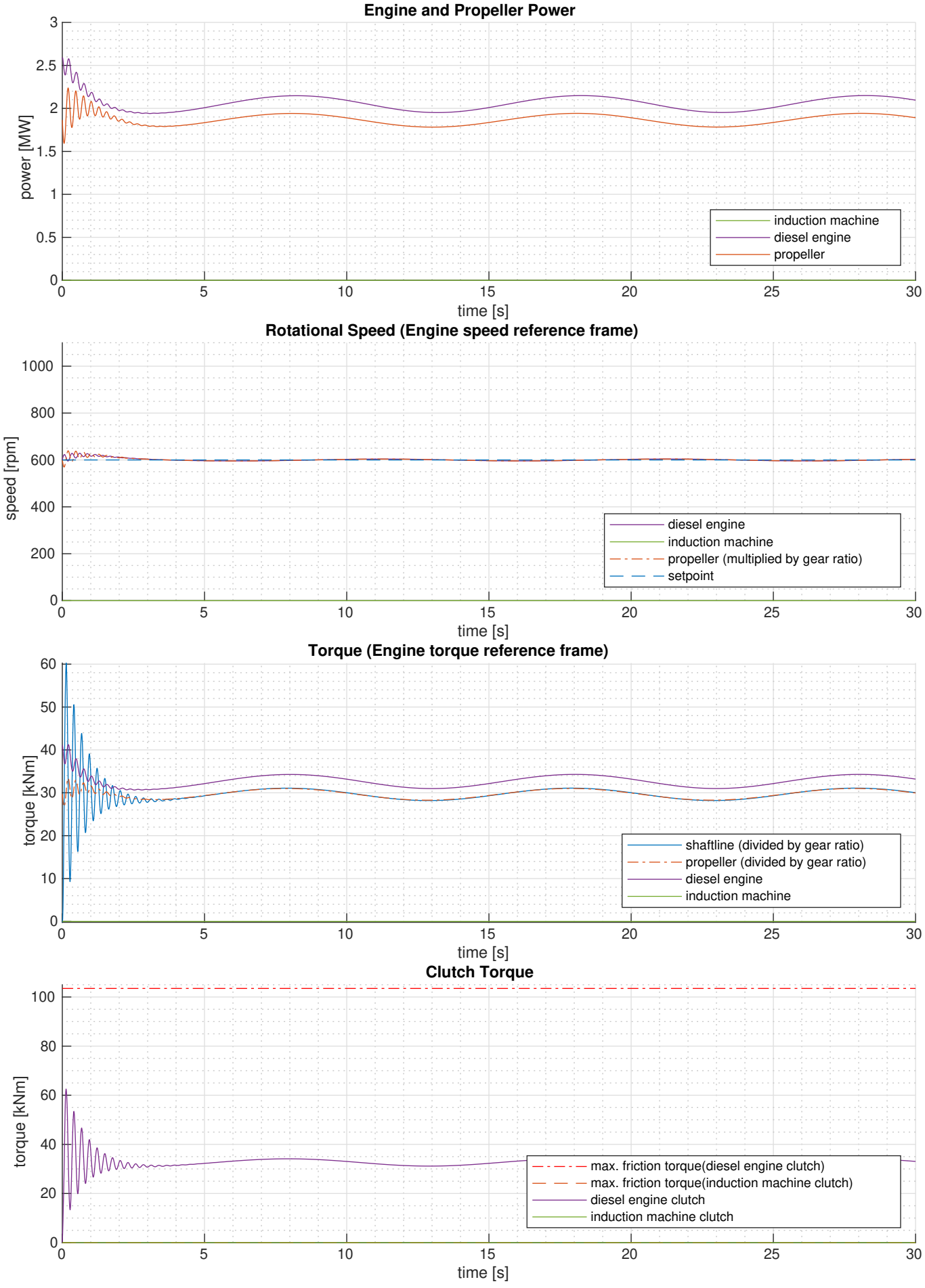

Figure B.3: Diesel mode at medium speed: 10 kn, sea state 3, 600 rpm. [figure 1 of 2]

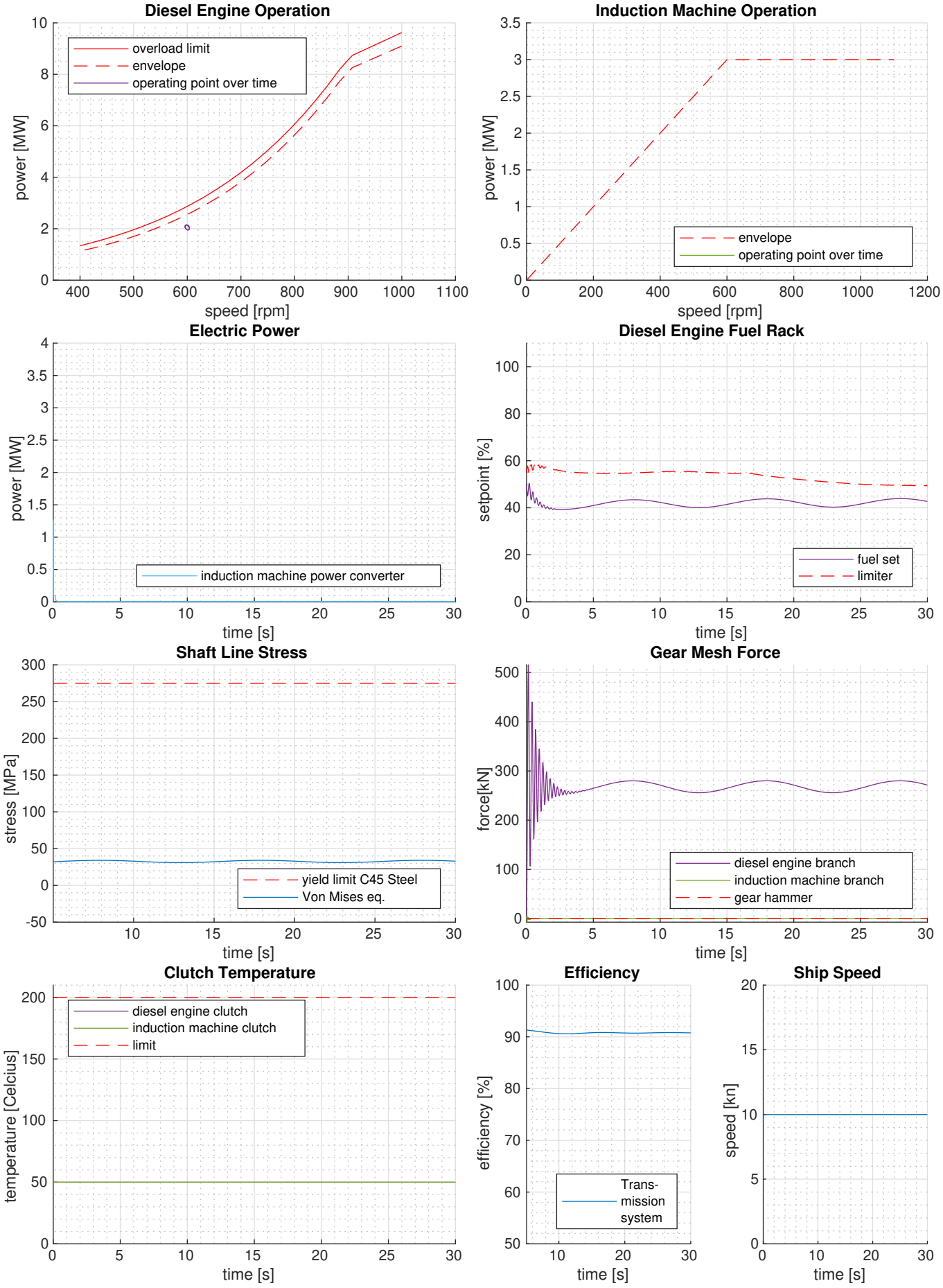

Figure B.4: Diesel mode at medium speed: 10 kn, sea state 3, 600 rpm. [figure 2 of 2]

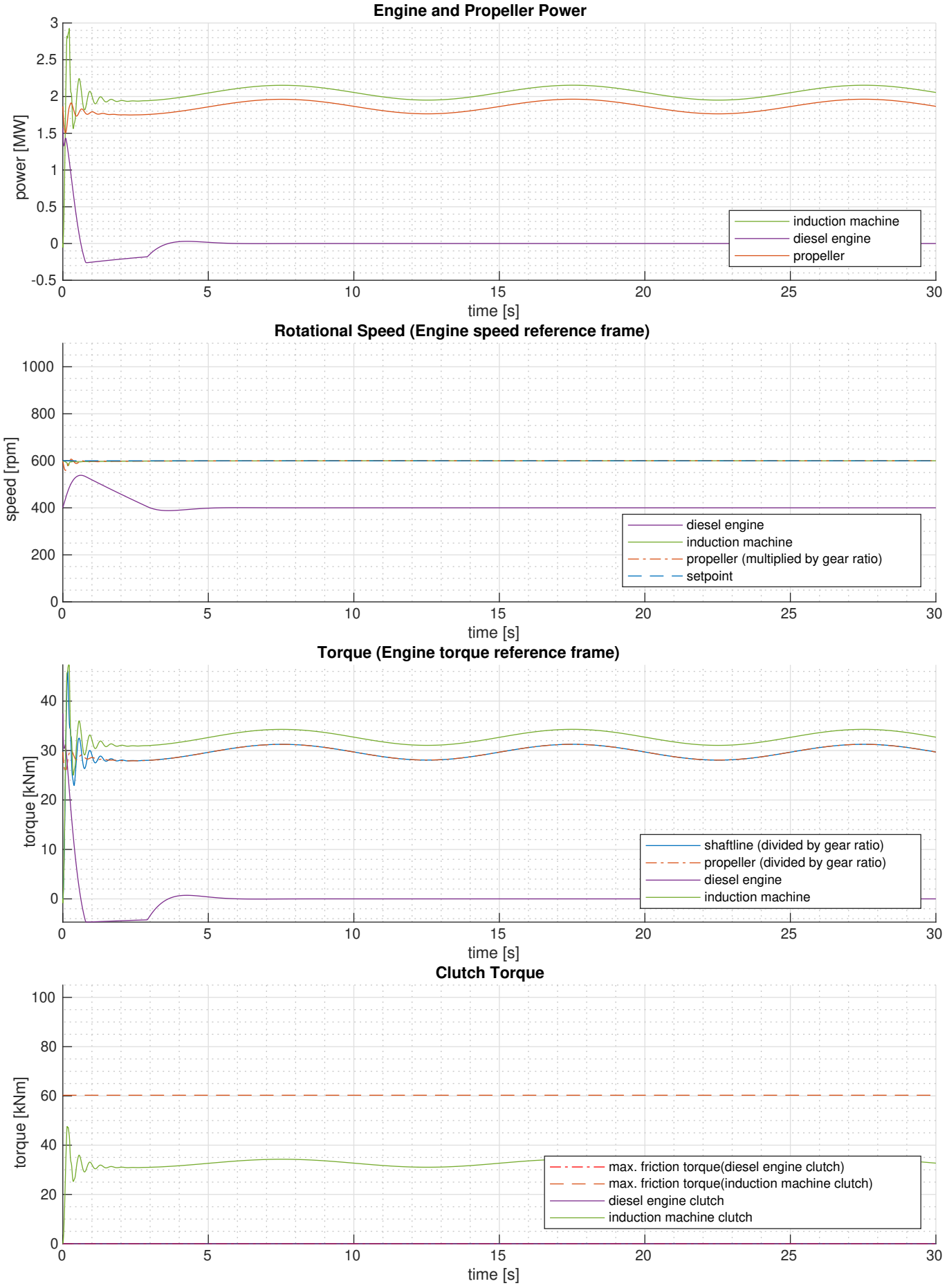

Figure B.5: Electric mode at medium speed: 10 kn, sea state 3, 600 rpm. [figure 1 of 2]

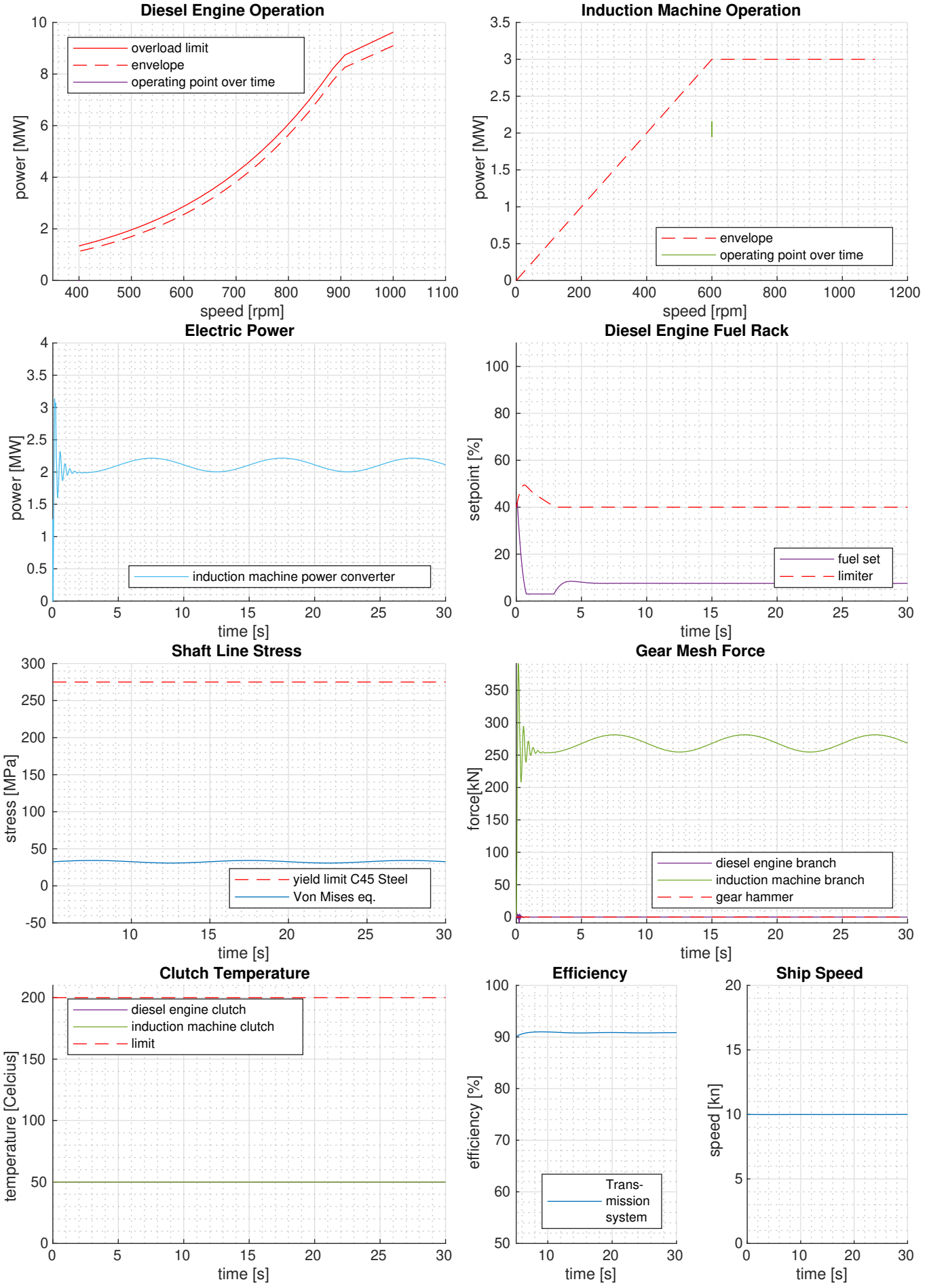

Figure B.6: Electric mode at medium speed: 10 kn, sea state 3, 600 rpm. [figure 2 of 2]

B.3 Propulsion Mode Transitions Simulation Results

- Electric to diesel propulsion mode transition using the instant approach in sea state 3. (fig.B.7, fig.B.8)
- Diesel to electric propulsion mode transition using the instant approach in sea state 3. (fig.B.9, fig.B.10)
- Electric to diesel propulsion mode transition using the staged approach in sea state 3. (fig.B.11, fig.B.12)
- Diesel to electric propulsion mode transition using the staged approach in sea state 3. (fig.B.13, fig.B.14)
- Electric to diesel propulsion mode transition using the torque controlled approach in sea state 3. (fig.B.15, fig.B.16)
- Diesel to electric propulsion mode transition using the torque controlled approach in sea state 3. (fig.B.17, fig.B.18)
- Electric to diesel propulsion mode transition using the torque controlled approach in sea state 5. (fig.B.19, fig.B.20)

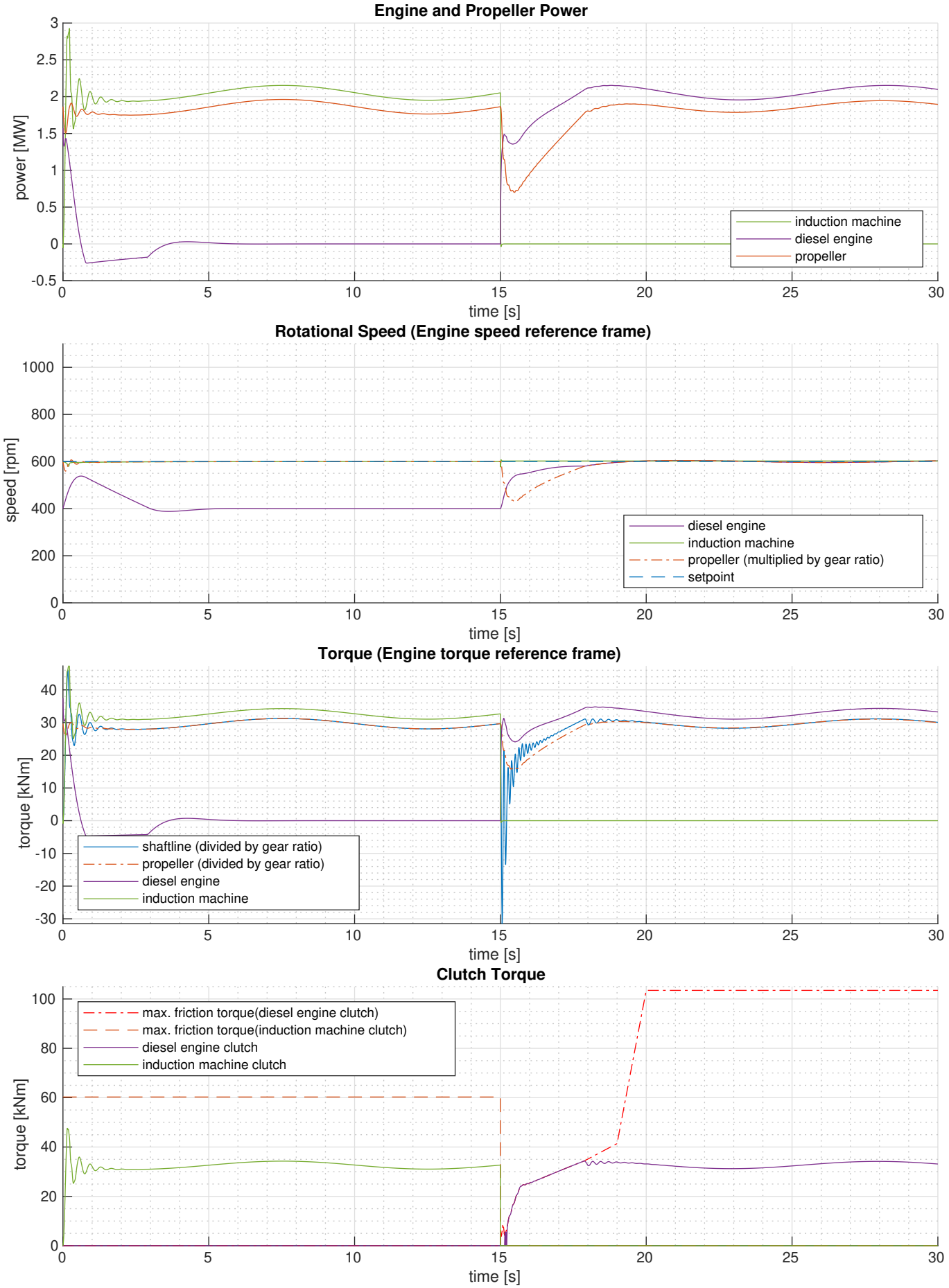

Figure B.7: Simulation results for the electric to diesel propulsion mode transition using the instant approach in sea state 3. [figure 1 of 2]

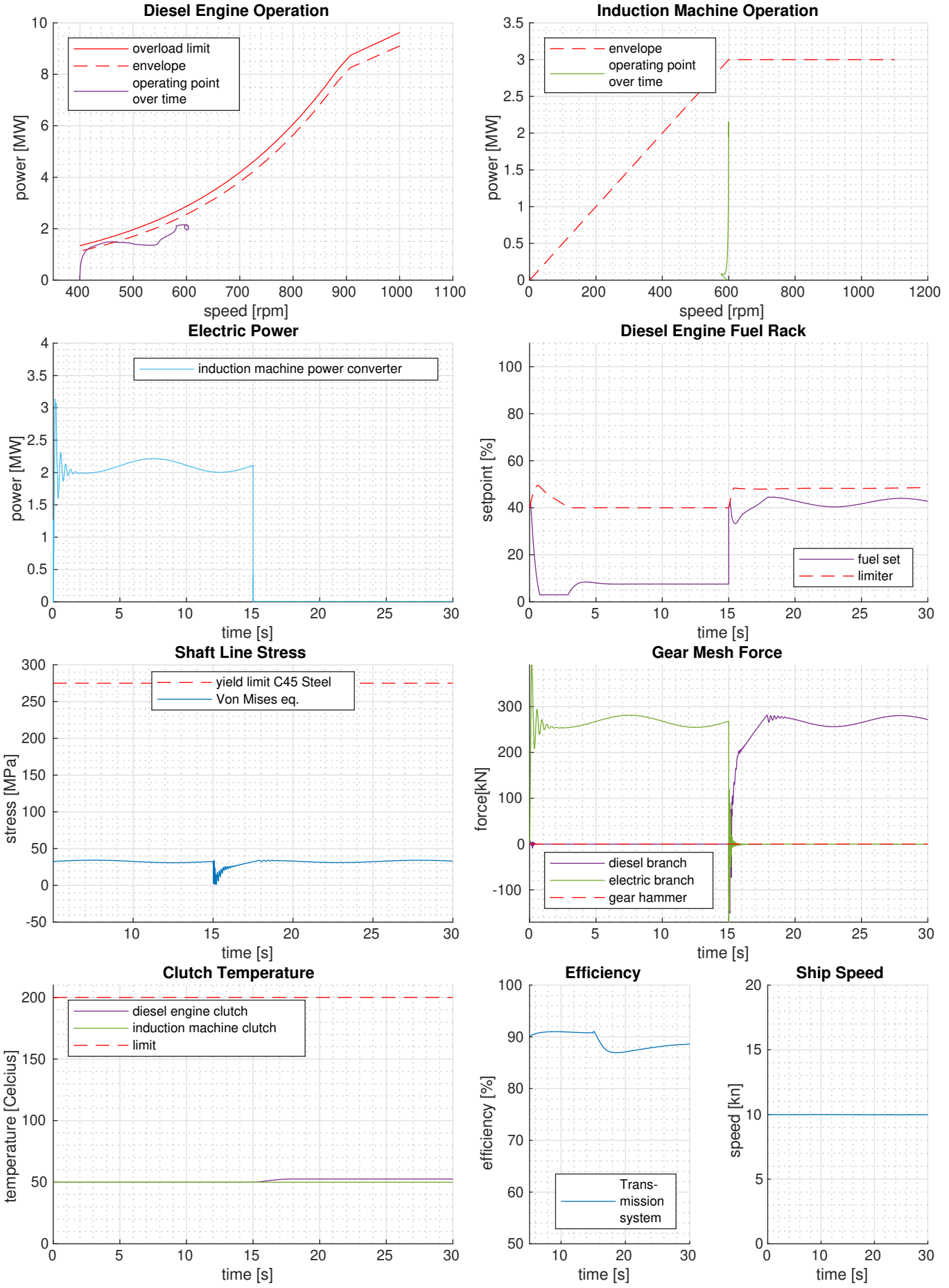

Figure B.8: Simulation results for the electric to diesel propulsion mode transition using the instant approach in sea state 3. [figure 2 of 2]

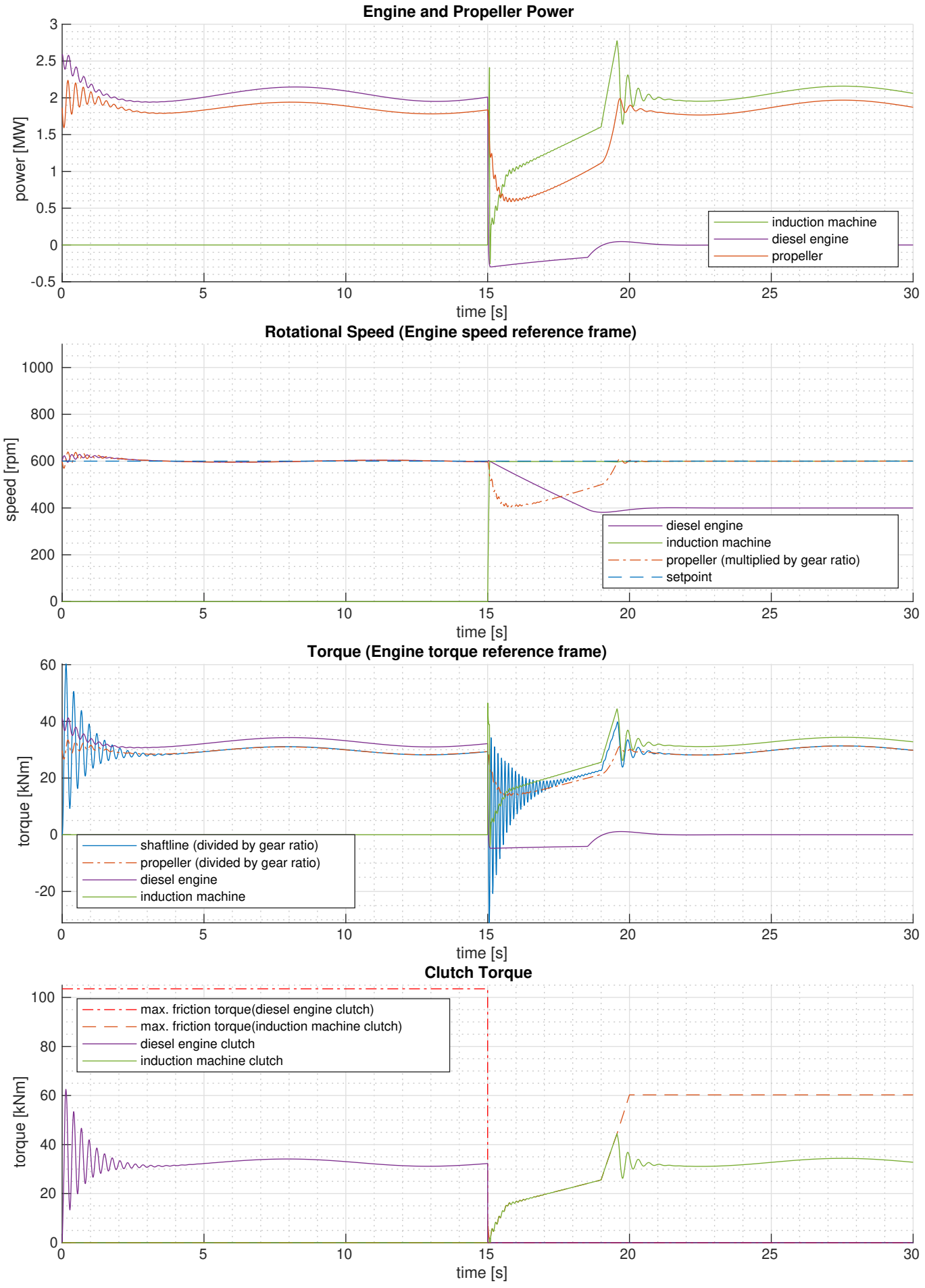

Figure B.9: Simulation results for the diesel to electric propulsion mode transition using the instant approach in sea state 3. [figure 1 of 2]

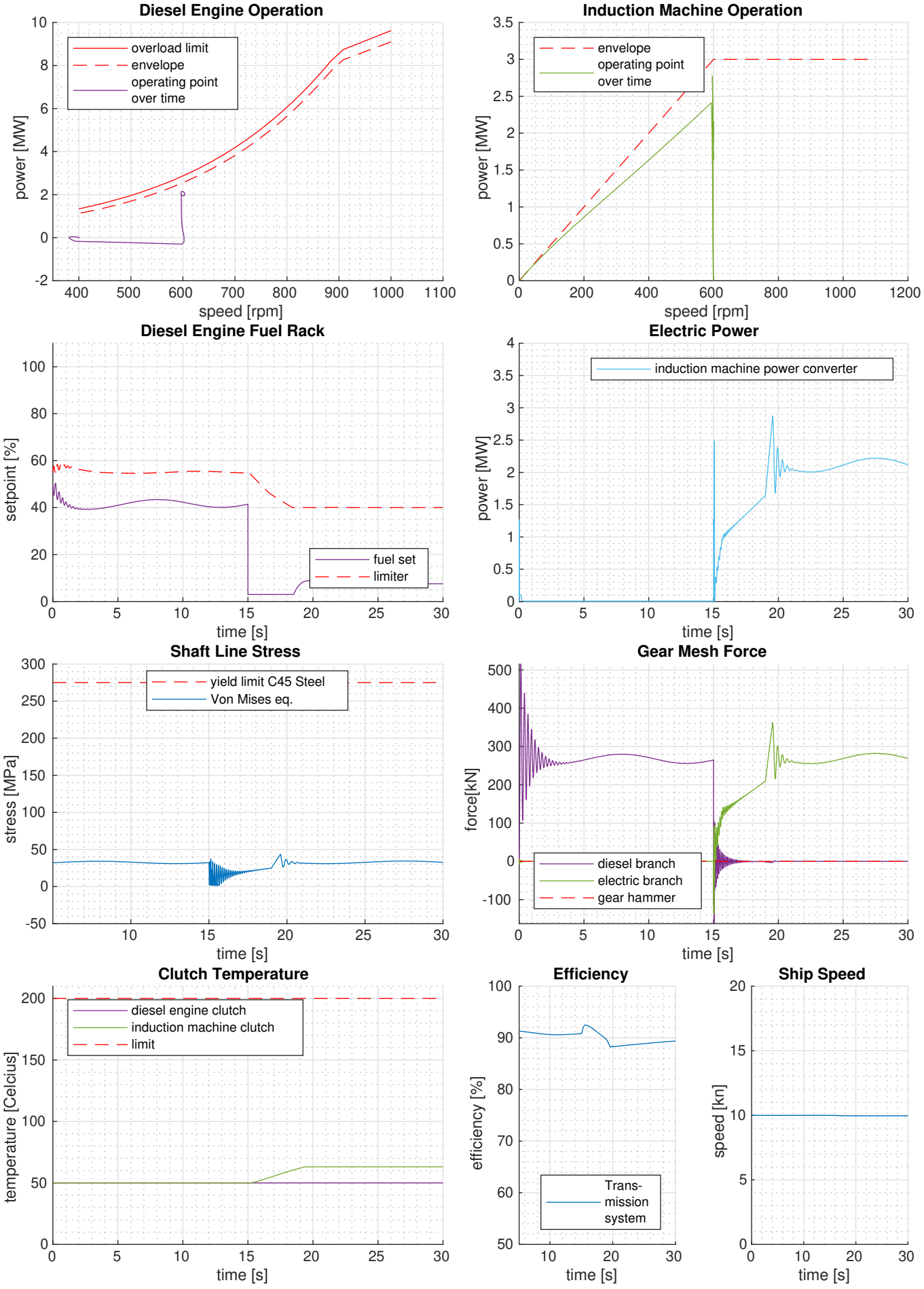

Figure B.10: Simulation results for the diesel to electric propulsion mode transition using the instant approach in sea state 3. [figure 2 of 2]

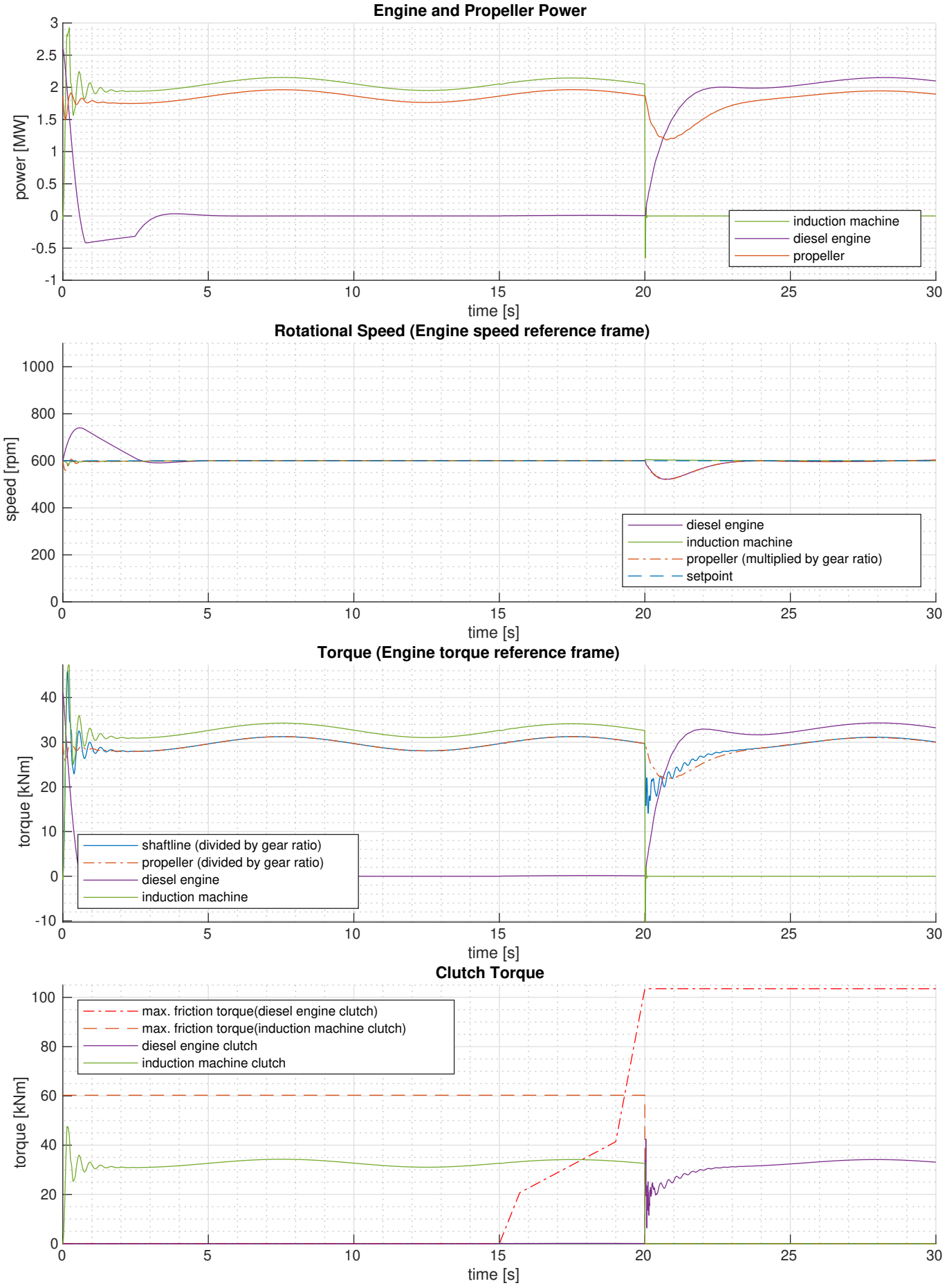

Figure B.11: Simulation results for the electric to diesel propulsion mode transition using the staged approach in sea state 3. [figure 1 of 2]

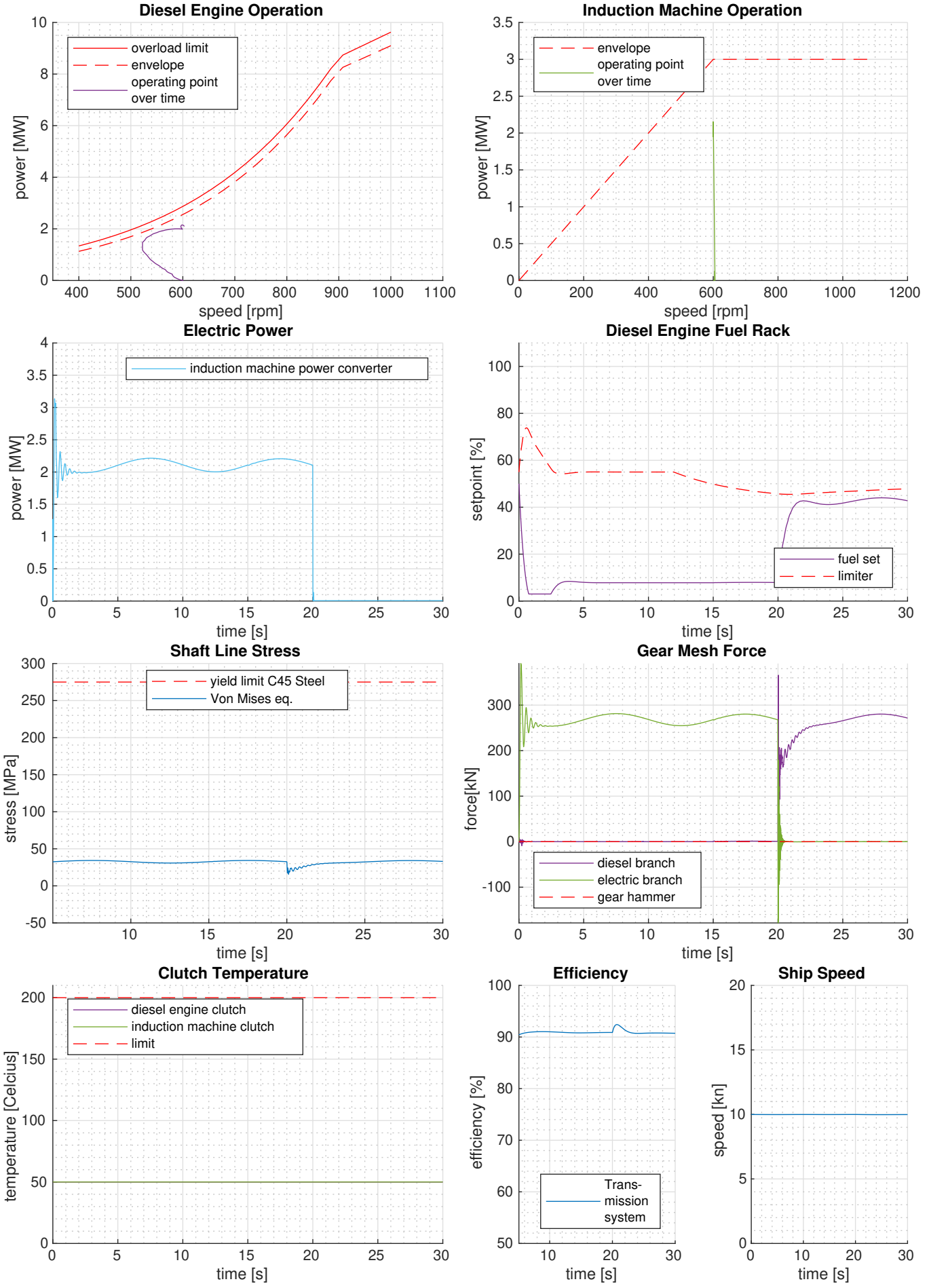

Figure B.12: Simulation results for the electric to diesel propulsion mode transition using the staged approach in sea state 3. [figure 2 of 2]

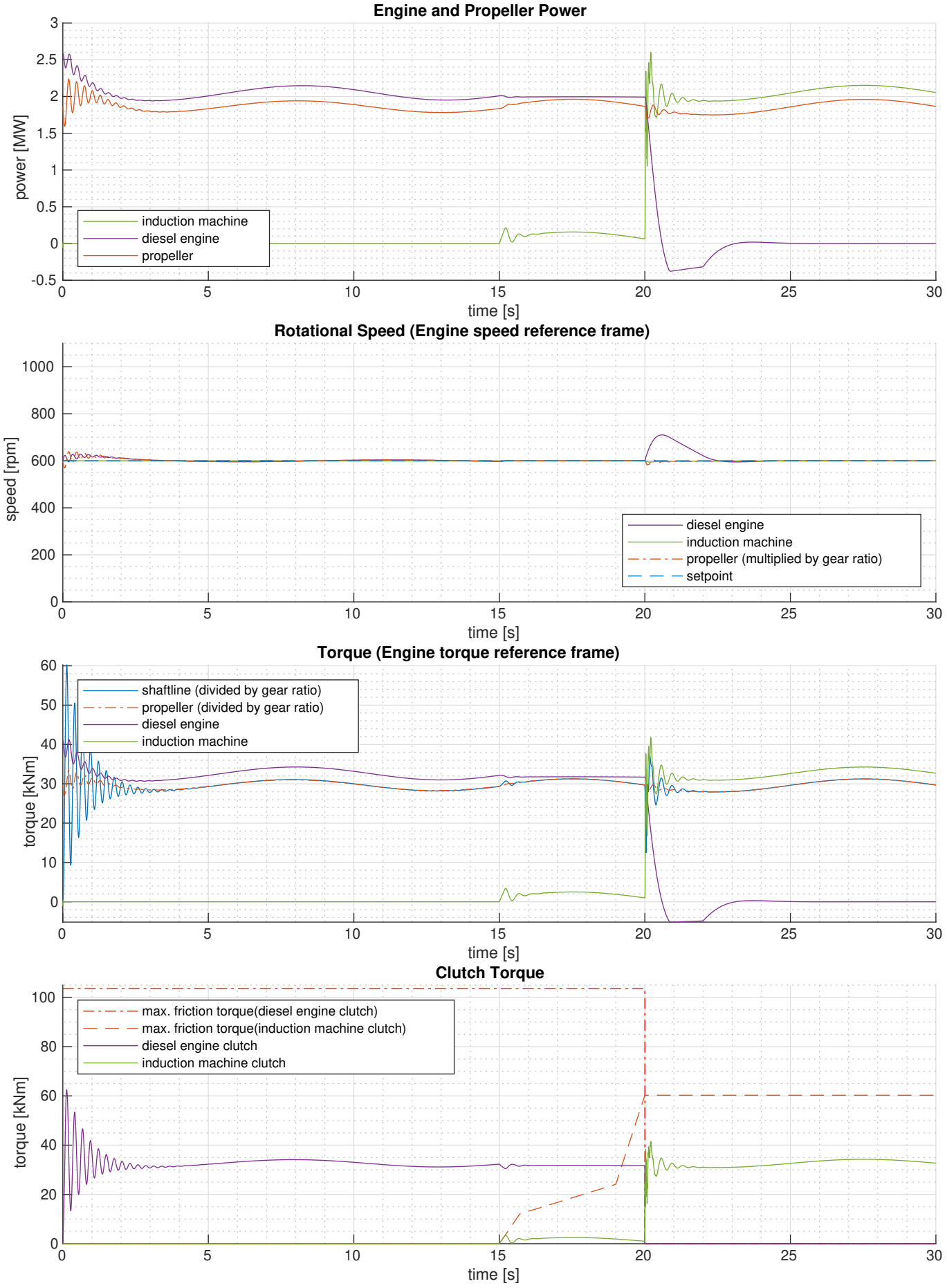

Figure B.13: Simulation results for the diesel to electric propulsion mode transition using the staged approach in sea state 3. [figure 1 of 2]

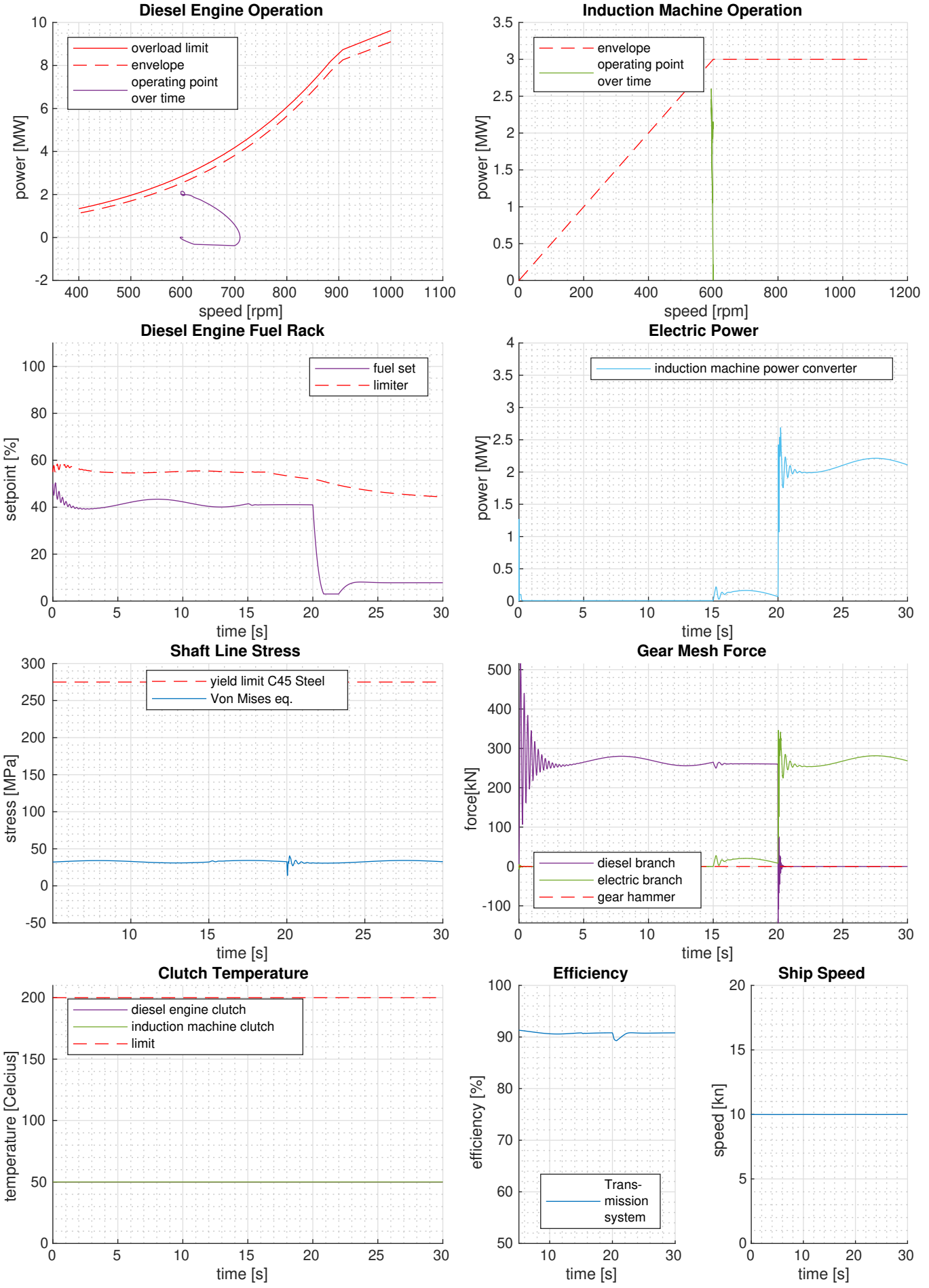

Figure B.14: Simulation results for the diesel to electric propulsion mode transition using the staged approach in sea state 3. [figure 2 of 2]

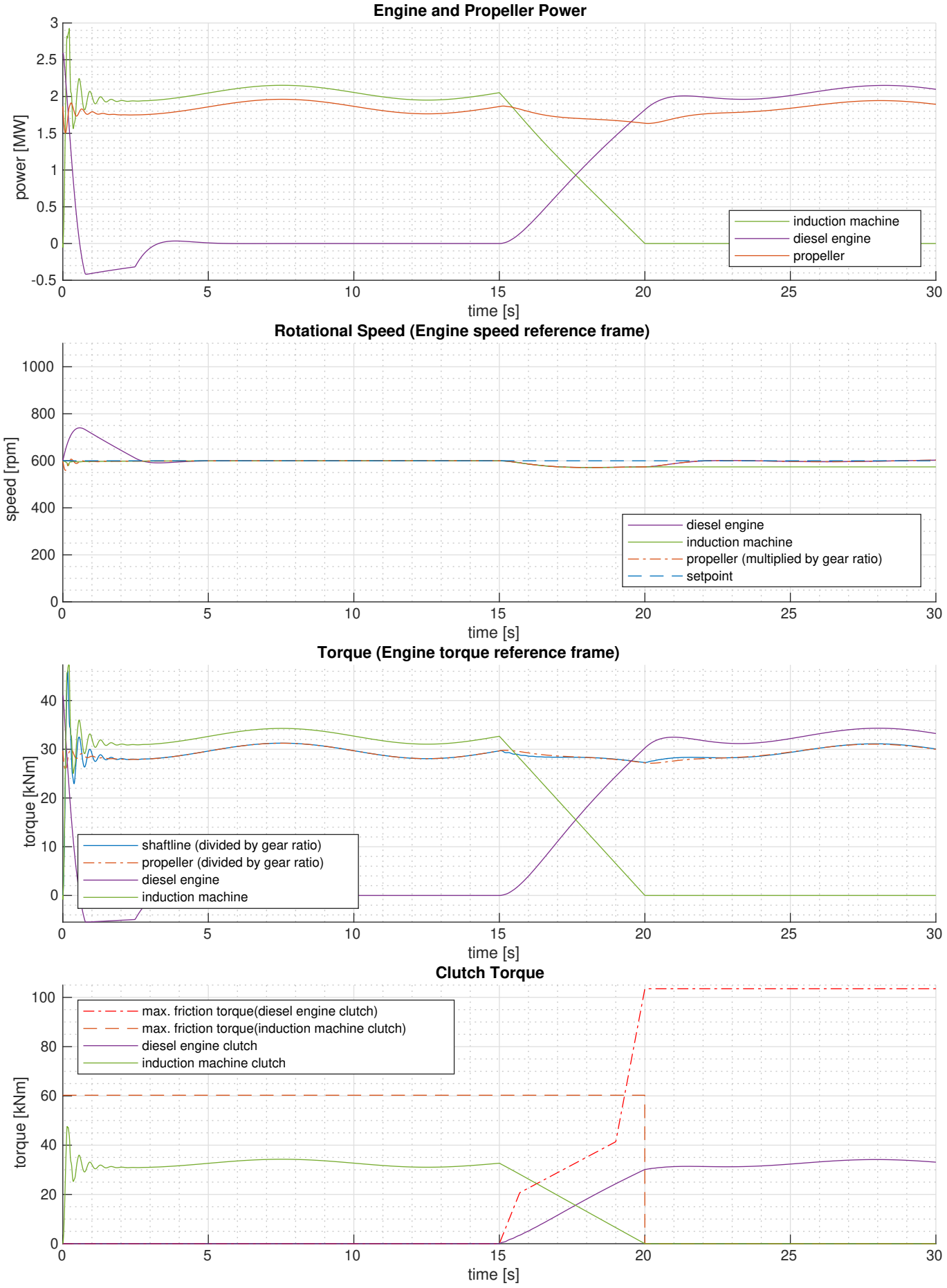

Figure B.15: Simulation results for the electric to diesel propulsion mode transition using the torque controlled approach in sea state 3. [figure 1 of 2]

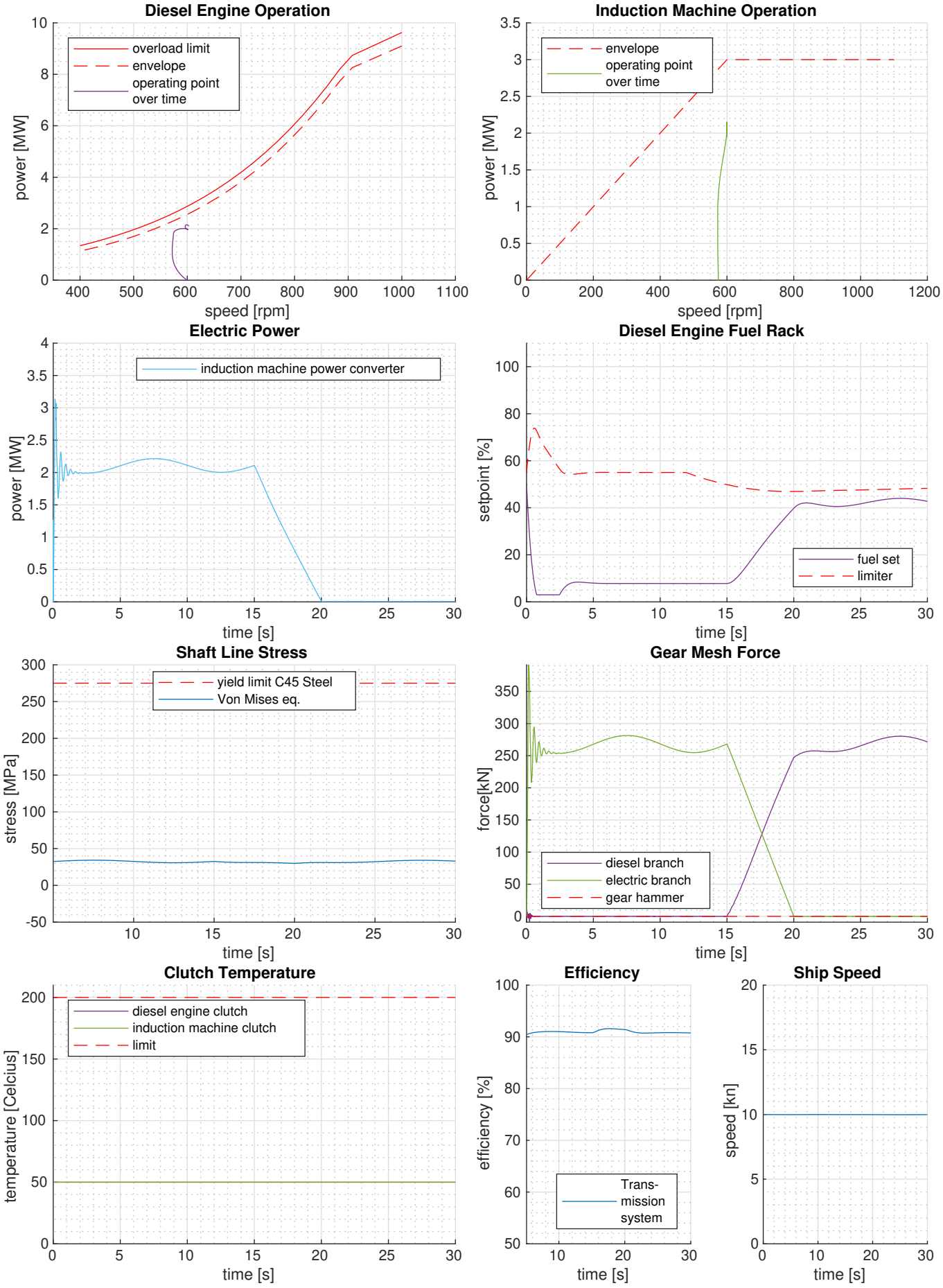

Figure B.16: Simulation results for the electric to diesel propulsion mode transition using the torque controlled approach in sea state 3. [figure 2 of 2]

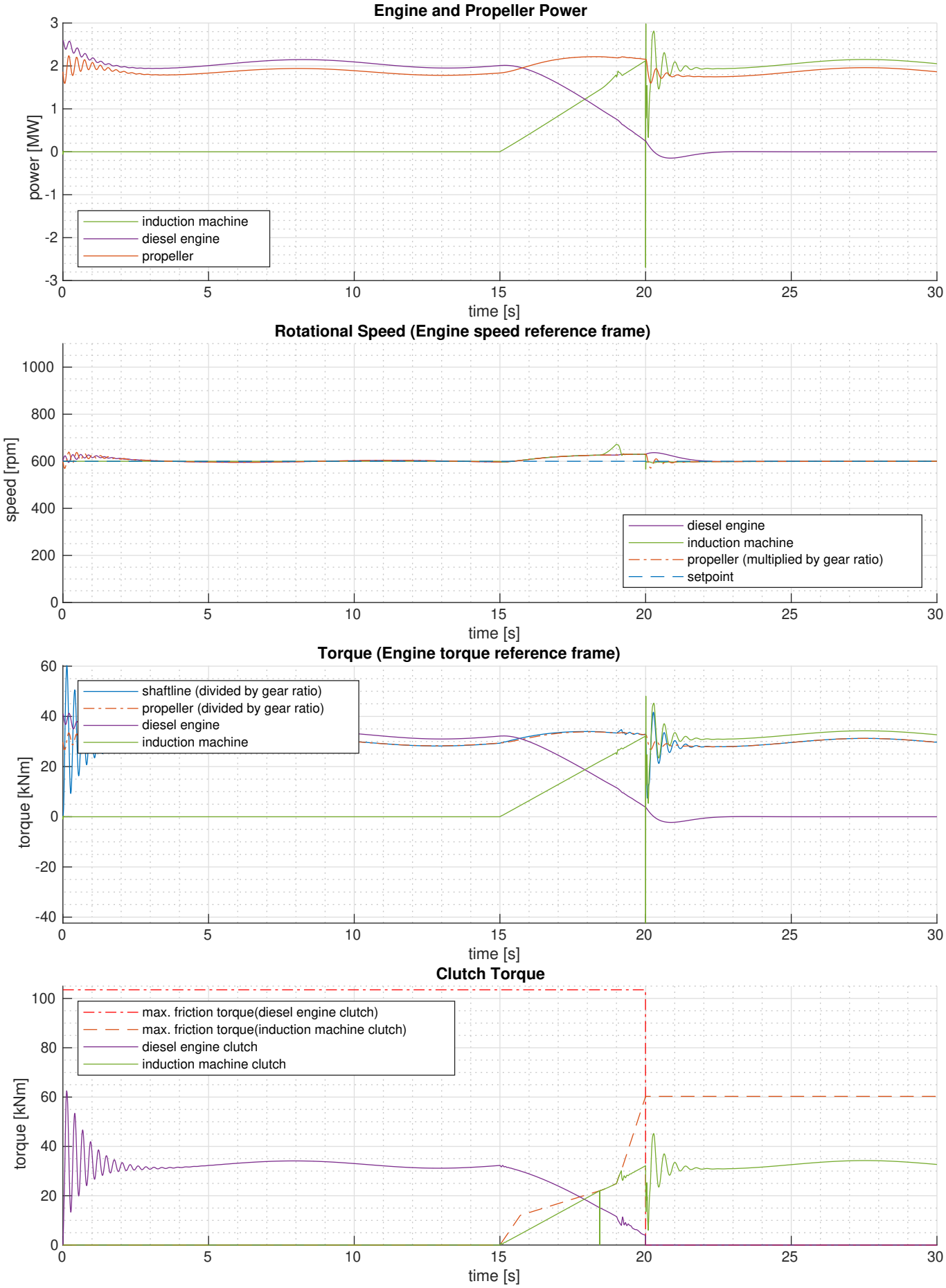

Figure B.17: Simulation results for the diesel to electric propulsion mode transition using the torque controlled approach in sea state 3. [figure 1 of 2]

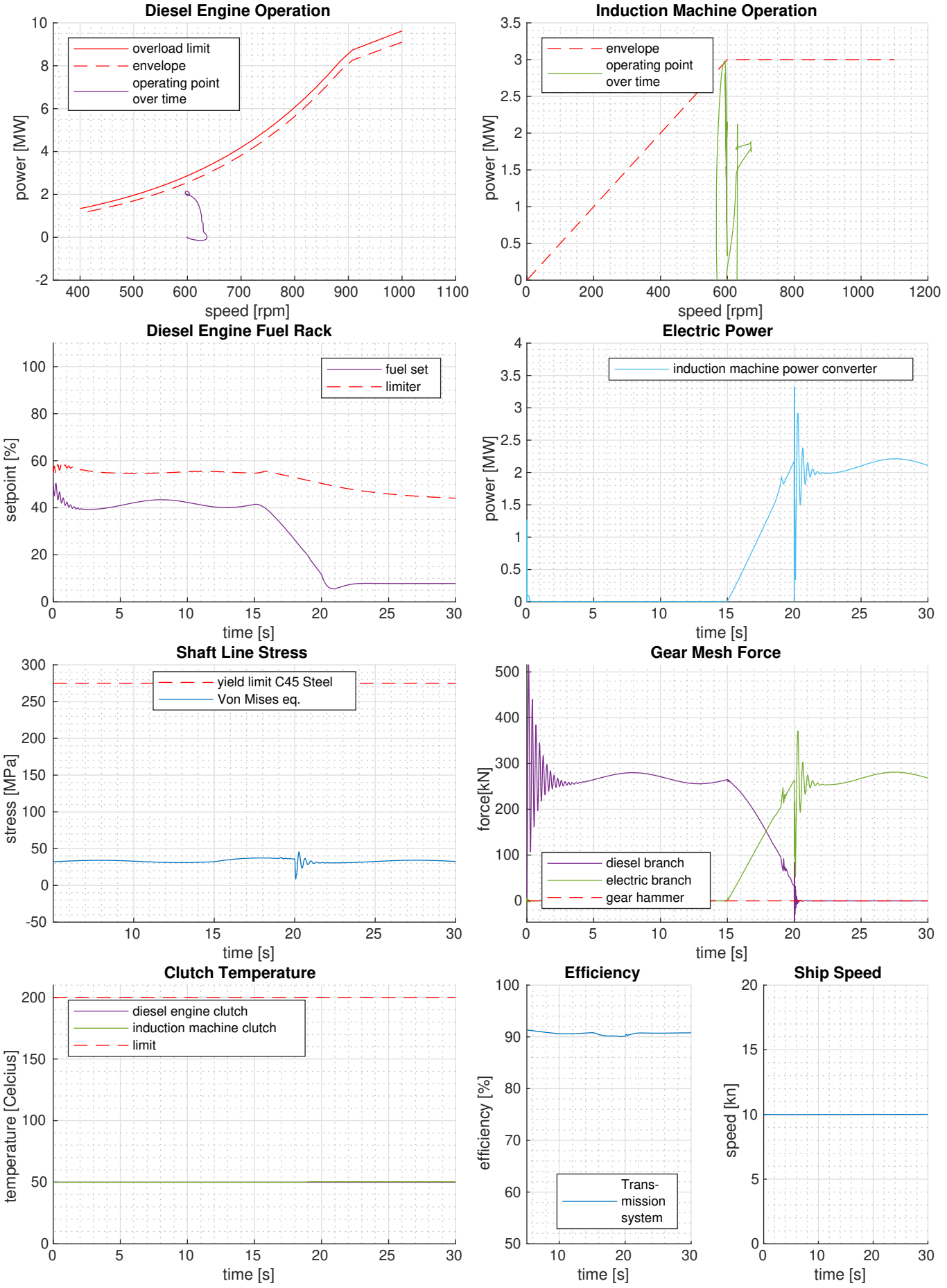

Figure B.18: Simulation results for the diesel to electric propulsion mode transition using the torque controlled approach in sea state 3. [figure 2 of 2]

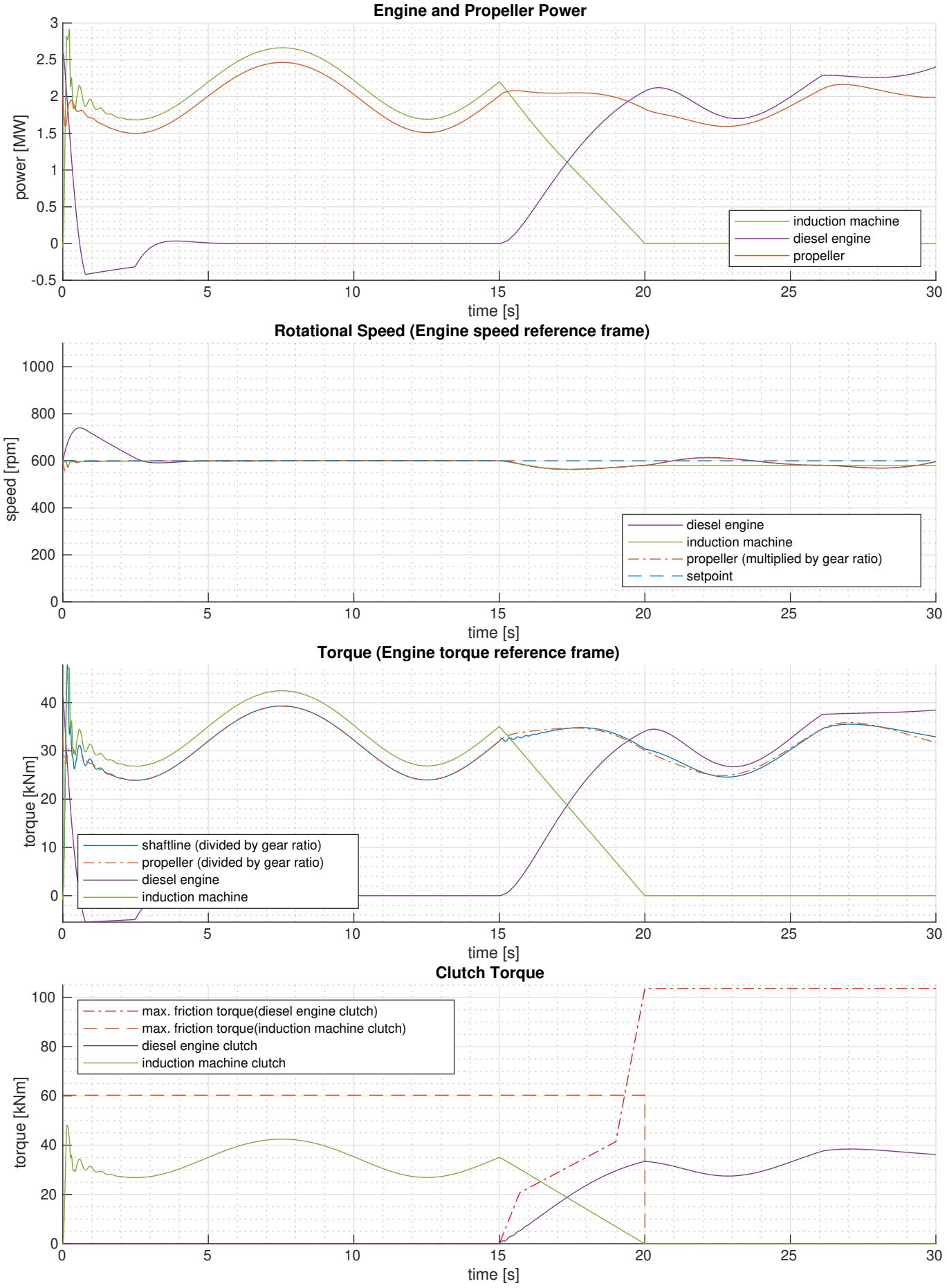

Figure B.19: Simulation results for the electric to diesel propulsion mode transition using the torque controlled approach in sea state 5. [figure 1 of 2]

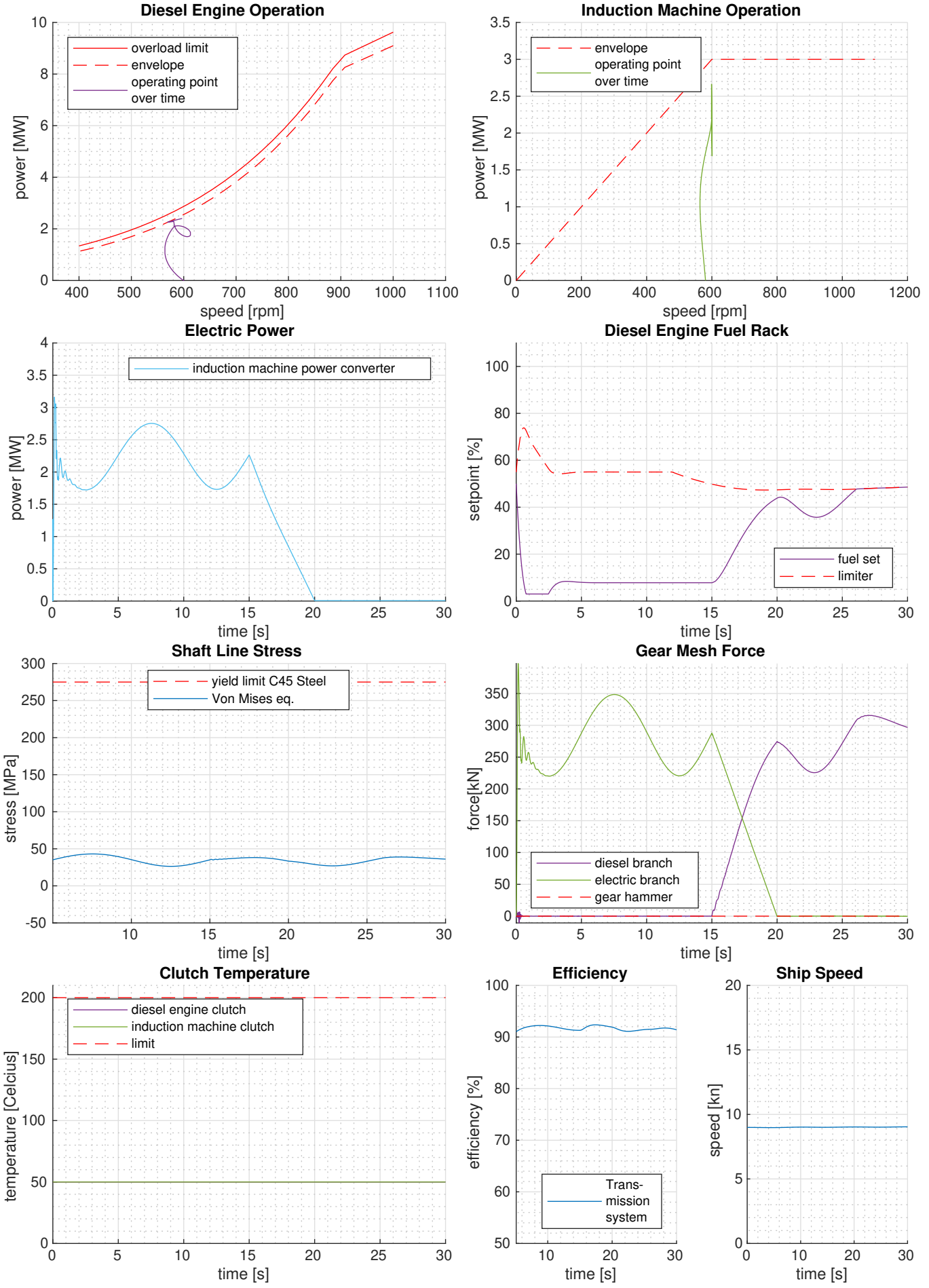

Figure B.20: Simulation results for the electric to diesel propulsion mode transition using the torque controlled approach in sea state 5. [figure 2 of 2]